



University
of Glasgow

Easton, Alistair Scott. (2010) *The role of lipo-oligosaccharide ganglioside mimicry on the interaction of Guillain-Barré syndrome associated strains of Campylobacter jejuni with the immune system.* PhD thesis.

<http://theses.gla.ac.uk/2019/>

Copyright and moral rights for this thesis are retained by the author

A copy can be downloaded for personal non-commercial research or study, without prior permission or charge

This thesis cannot be reproduced or quoted extensively from without first obtaining permission in writing from the Author

The content must not be changed in any way or sold commercially in any format or medium without the formal permission of the Author

When referring to this work, full bibliographic details including the author, title, awarding institution and date of the thesis must be given

**The role of lipo-oligosaccharide ganglioside mimicry on
the interaction of Guillain-Barré syndrome associated
strains of *Campylobacter jejuni* with the immune system**

Dr Alistair Scott Easton MBChB (Hons) BSc (Hons)

Thesis submitted for the degree of Doctor of Philosophy

The University of Glasgow

Faculty of Medicine

May 2010

(C) Alistair Scott Easton 28/07/2010

Abstract

The post infectious paralytic autoimmune disease, Guillain-Barré syndrome (GBS), has been associated with the generation of cross-reactive auto-antibodies after *Campylobacter jejuni* infection. These auto-antibodies interact with both the ganglioside mimicking *C. jejuni* lipo-oligosaccharides (LOS) and endogenous gangliosides. This study sought to investigate novel interactions of the ganglioside mimicking LOS with immune system ganglioside specific receptors. In addition, studies investigated if such receptor recognition affects antigen trafficking or the immunostimulatory potency of the LOS, which could participate in auto-antibody generation. Results presented in this thesis demonstrate for the first time that certain members of the siglec receptor family are capable of recognising LOS from a GBS associated strain of *C. jejuni*. This interaction did not definitively result in enhanced, or altered, potency of ganglioside mimicking LOS in stimulating immune cells. Interestingly, ganglioside mimicry was shown to enhance phagocytosis of *C. jejuni*, however, *in vivo* differences in bacterial trafficking were not observed.

Dedication and Acknowledgements

This thesis is dedicated to all of my teachers, in the broadest sense, who have educated, cajoled or inspired me throughout my life. Special thanks go to my supervisors; Dr Carl Goodyear, Professor Hugh Willison and Professor Allan Mowat for their guidance, advice and support. In addition, thanks go to the Pathological Society of Great Britain and Ireland who sponsored my fellowship and to Professor Barry Gusterson for his unrelenting enthusiasm and help.

I would like to acknowledge the help and reagents provided by groups in Rotterdam and Dundee with whom I collaborated. I am deeply grateful to Jim Guthrie and the staff at the Southern General Hospital Bacteriology Department for their efforts and patience. In addition, a special acknowledgment goes to Dr Ruth Huizinga whom I worked closely with in the final experiments and who generated and analysed the majority of the data in the *in vivo* co-localisation studies.

“The sweetest and most inoffensive path of life leads through the avenues of science and learning; and whoever can either remove any obstruction in this way, or open up any new prospect, ought, so far, to be esteemed a benefactor to mankind”

David Hume

Contents

1	Introduction	16
1.1	Guillain-Barré syndrome (GBS)	16
1.2	Pathophysiology of GBS	17
1.3	Models of GBS	19
1.4	Immunobiology of GBS	20
1.5	<i>C. jejuni</i> pathogenesis	22
1.6	<i>C. jejuni</i> LOS signalling in the immune system	24
1.7	Gangliosides in the immune system	27
1.8	Immune responses to carbohydrate antigens	30
1.9	Tolerance to carbohydrate antigens	35
1.10	Hypothesis	38
2	Materials and Methods (see Appendix 1 for buffers and media)	40
2.1	Analysis software	40
2.1.1	Statistical analysis	40
2.1.2	Acquisition and analysis of FACS data	40
2.1.3	Analysis of immunohistology and immunocytology	40
2.2	Preparation of Lipo-oligosaccharide (LOS)	41
2.2.1	<i>C. jejuni</i> strains	41
2.2.2	Growth and heat inactivation of <i>C. jejuni</i>	41
2.2.3	Crude hot phenol extraction of LOS	41
2.2.4	Quantification of LOS by dry weight	42
2.2.5	Purification of LOS	42
2.2.6	Purification of commercially bought LPS	43
2.2.7	Determination of LOS purity by silver stain	43
2.2.8	Determination of LOS purity by spectrophotometry	43
2.2.9	Determination of LOS epitopes by Western blot	44
2.2.10	Generation of GM1 mimicking LOS from GM1/GD1a mimicking LOS	44
2.2.11	Determination of LOS purity by alcian blue stain	45
2.2.12	Quantification of LOS by thiobarbituric acid assay	45

2.3	Binding of cellular receptors and humoral factors to <i>C. jejuni</i> and LOS	46
2.3.1	Binding of Sialoadhesin, Siglec E and Siglec F to LOS and gangliosides	46
2.3.2	Binding of Sialoadhesin, Siglec E and Siglec F to <i>C. jejuni</i>	47
2.3.3	Visualisation of siglec binding to <i>C. jejuni</i>	47
2.3.4	Binding of Sialoadhesin to <i>C. jejuni</i> following neuraminidase treatment	48
2.3.5	Binding of purified human Factor H to <i>C. jejuni</i> by ELISA	48
2.3.6	Binding of purified human Factor H to <i>C. jejuni</i> by FACS.....	49
2.3.7	Visualisation of Factor H binding to <i>C. jejuni</i>	49
2.3.8	Deposition of C3c and C9 on <i>C. jejuni</i> using ELISA	49
2.3.9	Binding of natural IgM and IgG to <i>C. jejuni</i> or LOS.....	50
2.4	Harvesting and labelling of cells for <i>in vitro</i> experiments.....	50
2.4.1	Mouse strains	50
2.4.2	Harvesting of splenocytes	51
2.4.3	Purification of splenic B cells	51
2.4.4	Carboxyfluorescein diacetate succinimidyl ester (CFSE) labelling of splenocytes and B cells	52
2.4.5	Generation of M-CSF containing supernatant	52
2.4.6	Generation of GM-CSF containing supernatant	52
2.4.7	Harvesting of bone marrow	53
2.4.8	Generation of bone marrow derived macrophages	53
2.4.9	Generation of bone marrow derived dendritic cells.....	54
2.5	<i>In vitro</i> stimulation of splenocytes, B cells, dendritic cells and macrophages .	54
2.5.1	Stimulation of splenocytes and purified B cells	54
2.5.2	Stimulation of bone marrow derived dendritic cells with LOS	55
2.5.3	Quantification of bacteria	56
2.5.4	Stimulation of bone marrow derived dendritic cells with whole <i>C. jejuni</i>	56
2.5.5	Blocking of siglec receptors on bone marrow derived dendritic cells.....	57
2.5.6	Stimulation of bone marrow derived macrophages with LOS.....	57
2.5.7	Stimulation of bone marrow derived macrophages with whole <i>C. jejuni</i> .	57
2.5.8	Stimulation of bone marrow derived dendritic cells and macrophages with exogenous gangliosides and LOS	58

2.5.9	Quantification of dead cells by trypan blue exclusion assay	59
2.6	Analysis of stimulated cells	59
2.6.1	Preparation and staining of B cells and splenocytes for FACS analysis ..	59
2.6.2	IgG immunoglobulin ELISA	60
2.6.3	IgM Immunoglobulin ELISA	60
2.6.4	Interleukin-10 ELISA	61
2.6.5	Interferon Gamma (IFN- γ) ELISA	61
2.6.6	Interleukin-12 ELISA	61
2.6.7	Tumour Necrosis Factor Alpha (TNF- α) ELISA.....	61
2.7	Immunisation of mice with LOS.....	62
2.7.1	Injection of mice with LOS.....	62
2.7.2	Immunohistochemical staining of spleen following LOS injection	62
2.8	Harvesting and fluorophore labelling of <i>C. jejuni</i>	63
2.8.1	CFSE labelling of bacteria.....	63
2.8.2	Quantification of the fluorescence of labelled bacteria	63
2.8.3	Confirmation CFSE remains bound to bacteria	64
2.9	Phagocytosis and cell association of intact bacteria	64
2.9.1	Association of <i>C. jejuni</i> with splenic B cells in the presence or absence of fresh serum.....	64
2.9.2	Identification of Sialoadhesin receptor on bone marrow derived macrophages	65
2.9.3	Bone marrow derived macrophage phagocytosis of <i>C. jejuni</i>	65
2.9.4	Inhibition of bone marrow derived macrophage phagocytosis.....	66
2.9.5	Injection and tracking of labelled <i>C. jejuni</i>	67
2.9.6	Immunohistology of splenic sections.....	67
2.9.7	FACS analysis of spleen following bacterial injections	68
3	Isolation and purification of <i>C. jejuni</i> LOS	71
3.1	Introduction.....	71
3.2	Results.....	77
3.2.1	Hot phenol extraction of <i>C. Jejuni</i> LOS and assessment of purity	77
3.2.2	Purification of hot phenol extracted LOS	79

3.2.3	Assessment of purity and determination of the nature of the precipitate .	81
3.2.4	Control of macro-molecular structures	85
3.2.5	Generation of a control strain of LOS and confirmation of ganglioside mimicking epitopes	87
3.2.6	Isolation and purification of GB11 wild type, GB11 CSTII knock out, GB2 wild type and GB2 CSTII knock out LOS	89
3.2.7	Detection of capsular polysaccharide contamination	91
3.2.8	Confirmation of GM1 and GD1a epitopes on GB11 and GB2 wild type LOS	93
3.2.9	Determination of LOS concentration by thiobarbituric acid assay.....	95
3.2.10	Assessment of the validity of the thiobarbituric acid assay	97
3.3	Discussion	99
4 Interaction of ganglioside mimicking LOS and whole <i>C. jejuni</i> with ganglioside specific cellular receptors and complement components		105
4.1	Introduction.....	105
4.2	Results.....	108
4.2.1	Sialoadhesin binding to <i>C. jejuni</i>	108
4.2.2	Visualisation of Sialoadhesin binding to <i>C. jejuni</i>	110
4.2.3	Confirmation of Sialoadhesin binding to the GD1a epitope.....	112
4.2.4	Siglec F binding to gangliosides, LOS and <i>C. jejuni</i>	114
4.2.5	Visualisation of Siglec F binding to <i>C. jejuni</i>	116
4.2.6	Siglec E binding to gangliosides, LOS and <i>C. jejuni</i>	118
4.2.7	Visualisation of Siglec E binding to <i>C. jejuni</i>	120
4.2.8	Siglec E binding to LOS, gangliosides and ganglioside complexes	122
4.2.9	Purified human complement Factor H binding to <i>C. jejuni</i>	124
4.2.10	Human C3c and C9 complement deposition on <i>C. jejuni</i>	130
4.2.11	Natural IgM and IgG binding to <i>C. jejuni</i> LOS	132
4.2.12	Natural IgM and IgG binding to whole <i>C. jejuni</i>	134
4.3	Discussion	135
5 Immunostimulatory effects and potency of purified <i>C. jejuni</i> LOS		143
5.1	Introduction.....	143

5.2	Results.....	148
5.2.1	<i>In vivo</i> mobilisation of Marginal Zone B cells	148
5.2.2	B cell activation by ganglioside mimicking and non-mimicking <i>C. jejuni</i> LOS in a purified B cell culture.....	150
5.2.3	B cell activation by ganglioside mimicking and non-mimicking LOS in a mixed splenocyte culture	155
5.2.4	Comparison of LOS potency at stimulating antibody secretion	158
5.2.5	Comparison of LOS potency at stimulating cytokine secretion	161
5.2.6	Potency of ganglioside mimicking and non-ganglioside mimicking LOS at stimulating myeloid antigen presenting cells.....	165
5.2.7	Potency of whole <i>C. jejuni</i> at stimulating myeloid antigen presenting cells	172
5.2.8	Effect of exogenous gangliosides on knock out LOS potency	174
5.2.9	Effect of siglec blockade on LOS potency	176
5.2.10	Upregulation of co-stimulatory molecule CD40 following LOS stimulation.....	178
5.2.11	Effect of LOS on cell death	180
5.2.12	LOS stimulation of dendritic cells from C3H/HeJ LPS hyporesponsive mice and TLR2 ^{-/-} mice	182
5.3	Discussion.....	183
6 <i>In vitro</i> and <i>in vivo</i> tracking of ganglioside mimicking and non-mimicking <i>C. jejuni</i>		195
6.1	Introduction.....	195
6.2	Results.....	197
6.2.1	Fluorophore labelling of <i>C. jejuni</i>	197
6.2.2	Confirmation that CFSE is retained by the <i>C. jejuni</i>	199
6.2.3	Development of a convenient and reliable method for quantification of <i>C.</i> <i>jejuni</i>	201
6.2.4	Effect of complement opsonisation of <i>C. jejuni</i> on B cell association <i>in</i> <i>vitro</i>	203

6.2.5	Identification of the Sialoadhesin receptor on bone marrow derived macrophages	206
6.2.6	Bone marrow derived macrophage phagocytosis of <i>C. jejuni</i>	208
6.2.7	Microscopy of phagocytosed <i>C. jejuni</i>	210
6.2.8	Phagocytosis following incubation with Sialoadhesin blocking antibodies.	212
6.2.9	<i>In vivo</i> tracking of i.v. injected <i>C. jejuni</i> to metallophilic macrophages	214
6.2.10	<i>In vivo</i> tracking of i.v. injected <i>C. jejuni</i> to marginal zone macrophages	218
6.2.11	Quantification of <i>C. jejuni</i> association with macrophage populations ...	222
6.2.12	Analysis of <i>C. jejuni</i> association with different splenic cell populations using FACS.....	226
6.3	Discussion.....	227
7	Conclusion	233
7.1.1	LOS purification	235
7.1.2	Binding of LOS to ganglioside specific receptors	238
7.1.3	Effect of ganglioside mimicry on LOS potency	243
7.1.4	Uptake of ganglioside mimicking <i>C. jejuni</i>	248
7.1.5	Future experiments.....	253
8	Bibliography	254
	Appendix 1 – Buffers and media	280
	Complete RPMI (cRPMI).....	280
	Supplemented cRPMI.....	280
	FACS Buffer	280
	Complete RPMI for phagocytosis experiments	280
	0.1 M Sodium Carbonate buffer for Ig ELISAs	280
	Appendix 2 – Structure and expression of siglecs	281
	Appendix 3 – Binding specificities of siglecs	283
	Appendix 4 – Structures of siglec-human-Fc fusion proteins	284

List of Figures

Figure 1: Structure of <i>E. coli</i> LPS and <i>C. jejuni</i> LOS.....	70
Figure 2: Structures of HS O:19 and HS O:3 <i>C. jejuni</i> LOS.....	72
Figure 3(A): Structures of GB2 and GB11 wild type <i>C. jejuni</i> LOS.....	74
Figure 3(B): Structures of GB2 and GB11 CSTII knock out <i>C. jejuni</i> LOS.....	75
Figure 4: Silver stain analysis of hot phenol extracted LOS.	76
Figure 5: Photograph of LOS solution following enzyme treatment.....	78
Figure 6: Silver stain analysis of LOS precipitate.	80
Figure 7: Western blot analysis of ganglioside mimicking LOS epitopes.....	82
Figure 8: Silver stain analysis of LOS following micelle dispersal.....	84
Figure 9: Western blot analysis of LOS epitopes following neuraminidase treatment. ...	86
Figure 10: Silver stain analysis of enzyme purified LOS.	88
Figure 11: Alcian blue and silver stain analysis of purified LOS and whole cell lysate. .	90
Figure 12: Western blot analysis of gangliosides mimicry by GB11 and GB2 LOS.	92
Figure 13: LOS concentration determined by thiobarbituric acid assay.....	94
Figure 14: Thiobarbituric acid assay of GM1 and sialic acid.....	96
Figure 15: Thiobarbituric acid assay of KDO and sialic acid.....	98
Figure 16: Diagram of LOS macromolecular structures.....	101
Figure 17: Sialoadhesin binding to whole <i>C. jejuni</i>	107
Figure 18: Immunocytometry of Sialoadhesin binding to <i>C. jejuni</i>	109
Figure 19: Sialoadhesin binding to <i>C. jejuni</i> following neuraminidase treatment.	111
Figure 20: Siglec F binding to gangliosides, LOS and <i>C. jejuni</i>	113
Figure 21: Immunocytometry of Siglec F binding to <i>C. jejuni</i>	115
Figure 22: Siglec E binding to gangliosides, LOS and <i>C. jejuni</i>	117
Figure 23: Immunocytometry of Siglec E binding to <i>C. jejuni</i>	119
Figure 24: Siglec E binding to LOS, gangliosides and complexed gangliosides.	121
Figure 25: Factor H binding to <i>C. jejuni</i>	123
Figure 26: FACS of Factor H binding to <i>C. jejuni</i>	125
Figure 27: Immunocytometry of Factor H binding to <i>C. jejuni</i>	126

Figure 28: Factor H binding following incubation with serum.	127
Figure 29: Complement C3c and C9 deposition on <i>C. jejuni</i>	129
Figure 30: Anti-LOS natural IgM and IgG antibody.	131
Figure 31: Anti- <i>C. jejuni</i> natural IgM and IgG.	133
Figure 32: <i>In vivo</i> mobilisation of marginal zone B cells by LPS.	147
Figure 33: Example FACS plots of labelled B cells.	149
Figure 34: B cell responses to <i>C. jejuni</i> LOS in a purified B cell population.	151
Figure 35: B cell responses to <i>C. jejuni</i> LOS in a mixed splenocyte population.	154
Figure 36: Immunoglobulin production by LOS stimulated B cells and splenocytes. ...	157
Figure 37: Cytokine production by LOS stimulated B cells and splenocytes.	160
Figure 38: Cytokine production by rough v smooth LPS stimulated mixed splenocytes.	162
Figure 39: Bone marrow derived dendritic cell and macrophage purity assessed by FACS.	164
Figure 40: Cytokine production by LOS stimulated dendritic cells and macrophages. .	166
Figure 41: Dendritic cell IL10 production in response to alternative <i>C. jejuni</i> LOS strains.	169
Figure 42: Whole <i>C. jejuni</i> stimulation of dendritic cells and macrophages.	171
Figure 43: LOS and ganglioside stimulation of dendritic cells and macrophages.	173
Figure 44: IL10 production by dendritic cells following blocking of siglec receptors. .	175
Figure 45: Upregulation of co-stimulator CD40 by LOS and whole <i>C. jejuni</i> stimulated dendritic cells and macrophages.	177
Figure 46: Dendritic cell and macrophage death following LOS stimulation.	179
Figure 47: C3H/HeJ and TLR2 ^{-/-} dendritic cell IL10 production following LOS stimulation.....	181
Figure 48: Analysis of CFSE labelled <i>C. jejuni</i>	196
Figure 49: Confirmation of durable CFSE binding.	198
Figure 50: Quantification of <i>C. jejuni</i> by optical density.	200
Figure 51: Association of opsonised <i>C. jejuni</i> with B cells.	202
Figure 52: Immunocytometry of Sialoadhesin on bone marrow derived macrophages.	205
Figure 53: Macrophage phagocytosis of <i>C. jejuni</i> analysed by FACS.	207

Figure 54: Immunocytochemistry of phagocytosed <i>C. jejuni</i> .	209
Figure 55: Inhibition of phagocytosis by Sialoadhesin blockade.	211
Figure 56: <i>In vivo</i> association of wild type <i>C. jejuni</i> with metallophilic macrophages.	216
Figure 57: <i>In vivo</i> association of knock out <i>C. jejuni</i> with metallophilic macrophages.	217
Figure 58: <i>In vivo</i> association of wild type <i>C. jejuni</i> with marginal zone macrophages.	219
Figure 59: <i>In vivo</i> association of knock out <i>C. jejuni</i> with marginal zone macrophages.	220
Figure 60: Analysis of <i>C. jejuni</i> and macrophage <i>in vivo</i> co-localisation.	221
Figure 61: FACS analysis of <i>C. jejuni</i> co-localisation with splenocytes <i>in vivo</i> .	224

List of Abbreviations

AIDP	Acute Inflammatory Demyelinating Polyradiculopathy
AMAN	Acute Motor Axonal Neuropathy
AMSAN	Acute Motor and Sensory Axonal Neuropathy
BCR	B cell receptor
BSA	Bovine serum albumin
CD	Cluster of differentiation
CFSE	Carboxyfluorescein succinimidyl ester
CgtA	N-acetylgalactosaminyl-transferase
CgtB	Galactosyltransferase
cRPMI	Complete RPMI
CpG	Cytosine-phosphate-guanine
CSTII	Sialyltransferase II
DAPI	4,6-diamidino-2-phenylindole
EDTA	Ethylenediaminetetraacetic acid
ELISA	Enzyme-linked immunosorbant assay
FACS	Fluorescence activated cell sorting
fH	(complement) Factor H
FO	Follicular Origin
GA1	Asialo-GM1
GA2	Asialo-GM2
GA3	Lactosyl ceramide
GBS	Guillain-Barré syndrome
GM-CSF	Granulocyte-macrophage colony stimulating factor

HBSS	Hanks buffered salt solution
HRP	Horseradish peroxidase
IFN	Interferon
Ig	Immunoglobulin
IL	Interleukin
IVIg	Intravenous immunoglobulin
KDO	3 deoxy-D-manno-oct-2-ulosonic acid
LOS	Lipo-oligosaccharide
LPS	Lipopolysaccharide
mAb	Monoclonal antibody
M-CSF	Macrophage colony stimulating factor
MFI	Mean fluorescence intensity
MFS	Miller-Fisher syndrome
MHC	Major histocompatibility complex
MZ	Marginal Zone
NF- κ B	Nuclear factor κ B
NK	Natural Killer
NNP	4-hydroxy-3, 5-dinitrophenyl
PAGE	Polyacrylamide gel electrophoresis
PBS	Phosphate buffered saline
PVDF	Polyvinylidene fluoride
SDS	Sodium dodecyl sulphate
Siglec	Sialic acid binding immunoglobulin like lectin
TD	Thymus dependent

Th	T helper
TI	Thymus independent
TIR	Toll/IL1 receptor
TLR	Toll like receptor
TNF α	Tumour Necrosis Factor α
TRAM	TRIF Related Adaptor Molecule
TRIF	TIR-Domain-containing Adaptor-inducing Interferon β

1 Introduction

1.1 Guillain-Barré syndrome (GBS)

Guillain-Barré syndrome is an autoimmune inflammatory disease of the peripheral nervous system characterised by an acute progressive flaccid paralysis followed by a variable recovery¹. GBS represents a spectrum of clinical and pathological entities with a number of subtypes being recognised. These include Acute Inflammatory Demyelinating Polyradiculopathy (AIDP)², Acute Motor Axonal Neuropathy (AMAN)³⁻⁵, Acute Motor and Sensory Axonal Neuropathy (AMSAN)⁶ and Miller Fisher syndrome (MFS)⁷. Since the widespread eradication of polio, GBS has become the foremost cause of acute flaccid paralysis in the world with an incidence of between 0.6 and 4 cases per 100,000 per year⁸.

The disease subtype is determined by the clinical manifestations supplemented by laboratory investigations¹. AIDP typically presents with muscle weakness which spreads proximally and can lead to respiratory paralysis. Numbness and paraesthesia are frequently present. AIDP is complicated by an autonomic neuropathy in 15% of cases, leading to life threatening dysfunction of the cardiovascular, alimentary and urinary systems. The disease reaches its nadir at two weeks and after a variable period of time recovery begins. This can take weeks to months with up to 16% of patients suffering recurring episodes^{7,9-11}. The axonal forms, AMAN and AMSAN, cause a pure motor impairment or motor and sensory impairment respectively. These axonal subtypes progress more rapidly, are more severe and more often require ventilation. Autonomic complications are mild and less common^{6,9,10}. MFS is a triad of acute ophthalmoplegia, ataxia and areflexia⁷. The GBS subtypes show regional variations in incidence. AIDP is the most common subtype worldwide and constitutes 90% of cases in Western countries. The axonal forms (AMAN, AMSAN and MFS) constitute 5% of cases in North America and Europe and 30-47% of cases in China, Japan and South/Central America^{4,5,11,12}.

The most severe and life threatening complication of GBS is paralysis of the respiratory muscles which, in 25% of cases, leads to a requirement for artificial ventilation¹³. Ten to 20% of patients suffer permanent disability, one third need to make substantial changes to their lifestyle¹⁴ and 4 to 15% of cases result in mortality within 1 year^{15,16}.

GBS patients represent a clinical challenge due to the multitude of systems affected by the disease. Respiratory function must be closely monitored for early signs of failure. Autonomic dysfunction can cause arrhythmias and blood pressure crises as well as gastrointestinal and bladder paralysis. Deep vein thrombosis is a risk in non-ambulatory patients¹. Other than supportive measures, the mainstay of treatment is immunotherapy, either plasmapheresis or intravenous immunoglobulin (IVIg). Both are equally effective at reducing disability, reducing mortality and reducing the number of patients requiring artificial ventilation¹⁷. However, even with immunotherapy intervention, 14% of patients still require ventilation⁸. The current immunotherapy regimes are inadequate due their restricted efficacy, expense, inherent risks and lack of availability, particularly in developing countries. There is a pressing need for a better understanding of the pathogenesis of GBS to allow development of novel targeted treatments and better prognostic indicators that will allow clinicians to predict who will require intensive treatment and who will benefit most from which intervention.

1.2 Pathophysiology of GBS

The pathophysiology of GBS is incompletely understood. AIDP is frequently associated with multifocal lymphocytic infiltrations² in which both $\alpha\beta$ and $\gamma\delta$ T cells have been identified¹⁸. AIDP is also characterised by a macrophage infiltrate around peripheral nerves. At this site the macrophages penetrate the Schwann cell basal lamina and ingest and digest the myelin, leading to demyelination of the axons^{3,19,20}. The distribution of this infiltrate correlates with the neurological deficits. T cell mediated pathology is

considered central in AIDP and the disease bears similarities to the animal model, experimental autoimmune neuritis^{2,21,22}.

AMAN and AMSAN show substantially different pathology from AIDP. Macrophages are associated with the nodes of Ranvier and axons rather than Schwann cells, and the macrophages are often observed beneath the intact myelin sheath in contact with the axons^{3,6,23,24}. The axonal forms of GBS produce lesions with a relative lack of lymphocyte infiltrate and, in contrast to AIDP, are believed to be antibody mediated diseases²⁰. The primary pathological event is thought to be targeting of the nodes of Ranvier and nerve terminals by auto-antibodies leading to complement activation. Activated complement components have been identified around the axons²⁵, resulting in damage between the axon and Schwann cell, leaving the myelin sheath initially intact. Antibody mediated cellular cytotoxicity may also play a role. The molecular targets of these auto-reactive antibodies have been identified as a class of sialylated glycosphingolipids called gangliosides^{2,24,26,27}. Gangliosides comprise a membrane bound lipid tail (ceramide) and an external sialylated carbohydrate side chain. While gangliosides are found throughout the body, they are concentrated in the nervous system²⁸. Ganglioside nomenclature describes the number of sialic acid residues and migration on thin layer chromatography e.g. GM1 describes Ganglioside, Mono sialic acid and 1 is the position of the migration band.

Antibodies specific for a number of different gangliosides have been identified in the various axonal form of GBS²⁸⁻³¹ and are found in up to 50% of patients²⁰. For example, anti-GM1 antibodies have been detected in 10 to 42% of AMAN patients^{29,32-34} while Anti-GQ1b IgG antibodies are strongly associated with MFS³⁵. This picture is complicated by the finding that some GBS patients produce autoantibodies that are reactive with ganglioside complexes (e.g. GD1a and GD1b) but not the individual ganglioside in isolation³⁶. This reflects the capacity of gangliosides to form hetero-complexes with other gangliosides.

Approximately two thirds of all subtypes of GBS patients experience an infectious episode in the six weeks prior to GBS onset³⁷. The infection is often gastroenteritis or a flu-like illness^{2,8,38}. The organisms most commonly associated with GBS are *Campylobacter jejuni* (4-66%), cytomegalovirus (5-15%), Epstein-Barr virus (2-10%) and *mycoplasma pneumonia* (1-5%)²⁸.

A mechanistic connection between an antecedent *C. jejuni* infection and GBS was established when it was found that the lipo-oligosaccharide (LOS) synthesised by GBS associated strains of *C. jejuni* often have inner core sugars which perfectly mimic gangliosides in their structure³⁹. Thus molecular mimicry between pathogen and self was proposed as the underlying aetiology. In support of this hypothesis, anti-ganglioside antibodies from the sera of GBS and MFS patients cross react with LOS purified from ganglioside mimicking strains of *C. jejuni*^{27,40}. It has since been shown that a number of strains of *C. jejuni* mimic a range of gangliosides, including mixtures of gangliosides, as part of their LOS molecule^{41,42}.

1.3 Models of GBS

The role of anti-ganglioside autoantibodies and the molecular mimicry hypothesis are supported by a number of animal and human studies which have revealed the importance of gangliosides, ganglioside mimics and genetic factors found in the pathogen and host. Immunisation of rabbits with gangliosides GD1b or GM1 induces acute neuropathies which are histologically similar to acute ataxic neuropathy (GD1b) and AMAN (GM1)⁴³⁻⁴⁵. In addition, humans injected with animal gangliosides occasionally develop the AMAN subtype of GBS and this correlates with the production of anti-GM1 antibodies. These antibodies are not present in ganglioside recipients who do not develop GBS⁴⁶. The injection of anti-ganglioside antibodies alone into mice is insufficient to cause GBS. It is thought that this may be due to an intact blood nerve barrier protecting nerves, due to insufficient ganglioside expression or due to weak murine complement activity. In

support of this, it has been shown that mouse monoclonal antibodies to GD1a, or serum from a patient with AMAN (in conjunction with a fresh source of human complement), can cause conduction block in motor axons in mice genetically engineered to over-express GD1a⁴⁷.

Important studies directly confirming the link between ganglioside mimicking *C. jejuni* LOS with anti-ganglioside antibodies have been conducted. Rabbits immunised with ganglioside mimicking LOS have been shown to produce antibody responses which are cross reactive between gangliosides and their biochemically defined LOS mimics⁴⁸⁻⁵⁰.

As gangliosides are a widely expressed self-antigen, it is expected that there is a high degree of immune system tolerance preventing self-reactivity. The role of tolerance has been investigated using GalNAc-Transferase knockout mice in which the ganglioside synthesising biochemical pathway has been disrupted. These mice lack all complex gangliosides synthesised beyond the GalNAcT step, and instead over-accumulate the simple gangliosides such as GM3 and GD3⁵¹. When normal mice are immunised with gangliosides or ganglioside mimicking LOS, they produce a weak antibody response. However, when complex ganglioside-naïve mice are immunised with complex gangliosides, or ganglioside mimicking LOS, they produce a robust antibody response with isotype class switching to T cell dependent IgG isotypes and immunological memory⁵². This confirms that failure of tolerance is an important factor in GBS pathogenesis.

1.4 Immunobiology of GBS

Analysis of GBS patient sera reveals intriguing insights into the induction of autoimmunity and the requirements for tissue damage. There are several reasons for believing antibody isotype class switching to IgG is an important factor in GBS pathogenesis. IgG1 and IgG3 are associated with AMAN and IgG1, IgG3 and IgG2 are

associated with MFS^{53,54}. The predominant isotype appears to be related to the triggering infection, for example, IgG1 responses are associated with *C. jejuni*⁵⁵. Antibody isotype is also a prognostic indicator as IgG1 is associated with an increased duration of disease⁵⁶.

Class switch recombination to IgG1 and IgG3 is thought to be a T cell dependent process characteristic of a Th1 dominated response, although the requirements for class switch recombination are poorly defined in humans⁵⁷. Interestingly, these isotypes are more often associated with responses against protein antigens, whereas IgG2 is normally associated with responses to glycolipids such as gangliosides or LOS^{58,59}. In *C. jejuni* enteritis not associated with GBS, IgG2 is the antibody isotype seen in response to the glycolipid LOS⁶⁰. This suggests that ganglioside mimicking strains may sometimes induce idiosyncratic immune responses in GBS. In contrast to IgG anti-ganglioside antibodies, poly-reactive IgM anti-ganglioside antibodies of low affinity are present in normal human serum as part of the “natural” antibody repertoire associated with responses to bacteria⁶¹ and these are not pathogenic.

A rabbit model of GBS shows that affinity maturation and the appearance of high affinity antibodies coincides with disease onset⁶². Affinity maturation of high affinity antibodies is generally thought to be a T dependent phenomenon. The importance of affinity maturation is highlighted by occasional case reports of humans with low affinity IgG anti-ganglioside antibodies who remain disease free⁶³.

These studies suggest that isotype class switching and affinity maturation are important in most instances of GBS. Different subclasses of IgG possess substantially different effector functions with the GBS associated isotypes, IgG1 and IgG3, being more effective at fixing complement and binding Fcγ receptors⁶⁴. Class switching to IgG has been associated with onset of autoimmunity in mouse models of various autoimmune diseases⁶⁵. Models studying anti-erythrocyte specific mouse IgG antibodies show that

high affinity IgG is essential for pathogenic complement activity although binding to Fc γ receptor bearing effector cells could compensate for low affinity binding to the target^{66,67} (mouse IgG2a is the most effective isotype at complement activation and Fc γ receptor binding). These studies demonstrate that both class switching and affinity maturation can contribute to pathogenicity.

GBS is an uncommon outcome following *C. jejuni* enteritis and occurs in approximately one in every thousand cases⁶⁸. This may be due to factors associated with the host or pathogen. There is very limited, and inconclusive, evidence to support genetic influences leading to an increased susceptibility to GBS. A small study showed a 2.6 fold increased risk in siblings developing GBS and repeated episodes of GBS occasionally occur in the same patient (although this may represent immunological memory)⁶⁹. A TNF α 2 allele has been linked to increased risk of GBS in Japanese patients^{69,70}. Other studies of immune receptor polymorphisms (Fc γ RIIIb and mannose binding lectin) show links to disease severity rather than occurrence⁷¹⁻⁷³. In contrast to the majority of autoimmune diseases, there is a lack of conclusive evidence linking GBS to particular MHC class I or II alleles^{72,74}. In addition, there is no evidence of an association of GBS with polymorphisms in the glycolipid antigen presenting molecules CD1A or CD1E⁷⁵ and a study of 242 GBS patients found no association of GBS with polymorphisms in the LPS receptor molecules CD14 and TLR4 (Toll Like Receptor 4)⁷¹.

1.5 *C. jejuni* pathogenesis

C. jejuni is a genetically variable, gram negative, spiral shaped, motile bacterium with unipolar or bipolar flagellum^{20,76}. It is a leading cause of food poisoning world-wide⁷⁷. While it is often a common commensal of birds and mammals, in humans it causes gastroenteritis with bloody or watery diarrhoea⁷⁶. A large number of strains of *C. jejuni* are recognised and these are typed either by the heat-stable antigenic system of Penner (over 70 serotypes), the heat-labile antigen of Loir (over 100 serotypes) or by direct DNA

comparisons⁷⁸. The Penner serotype O:19 and GD1a mimicking strains appear to be over-represented in GBS cases^{79,80,81}. *C. jejuni* strains express ganglioside mimics either alone or in differing ratios (for example GM1 and GD1a at a 1:1 ratio, GM1 and GD1a at a 9:1 ratio, GM2 alone etc). Although *C. jejuni* is a gut mucosal pathogen, it occasionally causes systemic infections with systemic immune responses^{82,83}. IgA antibodies against GM1 are found in 17% of *C. jejuni* associated GBS cases and these antibodies belong to the IgA1 subclass which is more commonly found in systemic responses (rather than the secretory subclass seen in mucosal responses)⁸⁴.

Following colonisation of the small bowel, *C. jejuni* transits to the colon which is the main target organ of disease⁸⁵. *C. jejuni* adheres to epithelial cells using a number of adhesins^{86,87} and can disrupt tight junctions⁸⁸⁻⁹⁰. *C. jejuni* is able to invade⁹¹ epithelial cells and macrophages where it replicates intracellularly^{92,93}. These interactions trigger a number of inflammatory signalling pathways, such as NF-κB (Nuclear Factor κB)^{94,95}. The sensing of *C. jejuni* by innate pattern recognition receptors is poorly understood although it appears that *C. jejuni* has evolved to limit immune activation in humans. For example, *C. jejuni* flagellin lacks the sites necessary to activate the flagellin receptor TLR5^{96,97}, while the low CpG (Cytosine-phosphate-Guanine) content of *C. jejuni* DNA results in reduced ability to stimulate the unmethylated-CpG-dinucleotide-receptor TLR9⁹⁸. However, *C. jejuni* derived LOS triggers cytokine release from dendritic cells⁹⁹ suggesting LOS is the principal immunostimulatory element of *C. jejuni*.

The role of *C. jejuni* LOS genes in GBS has been studied. Biosynthesis of ganglioside mimicking LOS requires specific enzymes; sialyltransferase (CSTII); N-acetylgalactosaminyl-transferase (CgtA) and galactosyltransferase (CgtB)¹⁰⁰. Genes responsible for LOS biosynthesis cluster into specific LOS biosynthesis gene loci. Specific loci are associated with GBS and with the presence of ganglioside mimicking LOS¹⁰¹. Mutant strains of GBS associated *C. jejuni* which are incapable of LOS sialylation (CSTII knock out) have been generated and studied. These knock out strains produce non-sialylated LOS structures such as asialo-GM3 (lactosyl ceramide), asialo-

GM2 (GA2) and asialo-GM1 (GA1). Unlike the wild type variant, the LOS molecules in the CSTII knock out strains do not cross react with GBS patient sera nor do they generate anti-ganglioside antibodies when injected into susceptible mouse strains¹⁰¹. This study demonstrates the importance of *C. jejuni* LOS biosynthesis genes in GBS.

1.6 *C. jejuni* LOS signalling in the immune system

Lipopolysaccharide (LPS) is a glycolipid molecule which is a vital component of the outer membrane of gram negative bacteria and also functions as one of the main targets of the mammalian innate immune system¹⁰². LPS is generally divided into three covalently linked parts; the Lipid A, the carbohydrate O-side chain and the core sugars^{103,104}. While LPS has an extended O-side chain, LOS has a truncated structure consisting of the core sugars alone (see figure 1 for a diagrammatic representation of *Escherichia coli* smooth mutant LPS and *C. jejuni* rough mutant LOS). Immune sensing of LPS results in activation of a wide range of cells such as macrophages, dendritic cells and specific classes of B and T lymphocytes¹⁰⁵⁻¹¹⁰. The immunostimulatory properties of LPS reside in the Lipid A tail¹¹¹. The structure of Lipid A varies between, and within, strains of gram negative bacteria and this imparts species specific properties and potency on LPS molecules¹⁰². *E. coli* LPS is considered the most potent LPS. The *C. jejuni* Lipid A backbone has a unique structure amongst gram negative bacteria. Despite this, *C. jejuni* retains its endotoxic activity although it is somewhat less potent than other forms of LPS^{102,112}.

Toll Like Receptors (TLRs) are sensing receptors of the innate immune system capable of recognising conserved Pathogen Associated Molecular Patterns (PAMPs) expressed by bacteria, viruses and fungi^{113,114}. These receptors form the first line of pathogen recognition and trigger a broad range of activation events including secretion of cytokines and functional maturation of immune cells^{114,115}. TLR4 was demonstrated to be the principal receptor mediating recognition of bacterial LPS when it was shown that the LPS

hypo-responsive mouse strains, C3H/HeJ and C57BL/10ScCr, have mutations affecting the Tlr4 gene¹¹⁶. TLR4 recognition of LPS involves a number of associated molecules and is partly dependent on the specific structure of the LPS being recognised. LPS Binding Protein (LBP) is a serum protein which binds to, and delivers, LPS to CD14^{117,118}. CD14 is expressed by myeloid cells and is found in serum in a soluble form. CD14 transfers LPS to a complex consisting of TLR4 and MD-2¹¹⁹ and this in turn causes TLR4 oligomerisation which brings TLR4 intracellular Toll-interleukin-1 receptor (TIR) domains together and facilitates signal transduction¹²⁰.

There are five adaptor proteins involved in TLR4 signalling: MyD88 (myeloid differentiation primary response gene 88), Mal (MyD88 adapter like), TRIF (TIR domain-containing adaptor inducing IFN- β), TRAM (TRIF related adaptor molecule), and SARM (sterile α and HEAT-Armadillo motifs-containing protein)¹²¹. TLR4 is unique amongst TLRs in its use of all of these adaptor molecules while other TLRs employ only some. Signalling via TLR4 is divided into two pathways; the MyD88 dependent pathway and the MyD88 independent (TRIF dependent) pathway. While both pathways cross over at the level of NF- κ B, the MyD88 dependent pathway is generally considered to trigger pro-inflammatory cytokine production, while the TRIF dependent pathway induces Type I interferons and interferon inducible genes¹²². Studies of CD14 mutated mouse strains have shown that “rough mutant” LPS, such as the truncated LOS found in *C. jejuni*, are capable of signalling via the TLR4-MyD88 pathway in the absence of CD14, whereas “smooth mutants”, such as *E. coli* LPS, cannot¹²³.

Negative regulators of TLR4 signalling are numerous and act at multiple levels in the signalling cascade¹²². For example, the plasma membrane expressed receptor RP105 (radioprotective 105) is believed to function on myeloid cells to inhibit LPS association with TLR4. Consistent with this, RP105 deficient mice show higher levels of serum TNF- α following LPS challenge¹²⁴. TRIAD3A (triad-domain containing protein 3 variant A) and SOCS-1 (suppressor of cytokine signalling 1) are both intracellular proteins which inhibit the TLR4 signalling cascade at multiple points. TRIAD3A over-

expression promotes degradation of TLR4 and TRIF, as well as downregulation of NF- κ B activation¹²⁵. SOCS-1 promotes degradation of TIRAP and there is increased pro-inflammatory cytokine secretion in LPS stimulated SOCS-1 deficient macrophages¹²⁶.

LPS stimulation of B cells causes polyclonal proliferation and differentiation. LPS is not considered a good initiator of class switching or memory¹⁰⁹. B cells are distinct from macrophages and dendritic cells in their requirements for LPS stimulation. Firstly, B cells are considered less sensitive than myelomonocytes to LPS stimulation. Secondly, a novel set of receptor molecules, RP105/MD1, which are structurally similar to TLR4/MD2 but lacking TIR domains, are important for LPS responses. B cells lacking RP105 are hyporesponsive to LPS in terms of proliferation and antibody production¹²⁷. However, co-stimulator up-regulation is not impaired in the absence of RP105¹²⁸. Although TLR4 and MD2 are expressed at extremely low levels on naïve B cells, in their absence, B cells do not respond to LPS at all. RP105/MD1 is expressed elsewhere by the immune system and in contrast to the apparent stimulatory function on B cells, they serve to inhibit TLR4 signalling¹²⁹. It is clear from these studies that the molecular pathways of B cell activation by LPS are complex and there is potential for unique or aberrant signals by unusual Lipid A structures (such as *C. jejuni*) or rough versus smooth mutants.

LPS causes polyclonal activation of B cells in an antigen independent manner through TLR4 signalling. However, by linking the hapten 4-hydroxy-3, 5-dinitrophenyl (NNP) to LPS and measuring anti-NNP antibody production following *in vitro* stimulation of splenocytes with LPS-NNP, it was shown that antigen specific activation of B cells by LPS occurs at substantially lower concentrations than polyclonal activation¹³⁰. It is thought that in these circumstances the B cell receptor (BCR) can concentrate the LPS near the B cell surface which potentially allows cross-linking of the BCR and TLR4. The BCR essentially substitutes for CD14, which is not expressed by B cells, in the function of concentrating LPS to the TLR4 complex.

LPS is frequently used as an *in vitro* B cell mitogen at concentrations of between 10 and 30µg/ml. Polyclonal activation begins at about 0.1µg/ml. However, concentrations as low as 2ng/ml LPS-NNP are sufficient to stimulate NNP antigen specific B cells¹³⁰. The Marginal Zone (MZ) B cell subset is more sensitive to LPS than Follicular Origin (FO) B cells and responds at lower concentrations with more rapid kinetics¹³¹. A serum LPS concentration of 10ng/ml is associated with an extremely high mortality in humans¹³². It is clear that *in vivo* polyclonal activation of B cells by LPS is an uncommon event except in severe sepsis. B cell sensitivity to LPS serves to select out antigen specific clones useful in the immune response against the LPS bearing pathogen. This concept can explain the selection and emergence of ganglioside specific B cells in GBS without polyclonal activation (which is not a feature of GBS). In addition, if unique or aberrant signalling occurs via *C. jejuni* LOS then it may be restricted to, or amplified on, ganglioside specific B cells due to the concentrating effect of the BCR. Cross-talk between the B cell receptor and TLR4 has been shown to occur during LPS stimulation¹³³ indicating that both signalling pathways can be modulated by each other, or perhaps any additional signal, for example, if the ganglioside mimic is able to deliver a signal.

1.7 Gangliosides in the immune system

GBS-associated *C. jejuni* LOS mimics gangliosides which are glycolipid molecules expressed widely in the body including on immune cells. Although their exact function remains enigmatic, they are associated with various immune-modulating functions¹³⁴.

Gangliosides exhibit immunomodulatory activity towards a number of different immune cell populations and, generally speaking, their effects tend to be inhibitory¹³⁵⁻¹³⁸. The mechanisms by which exogenous, or tumour derived, gangliosides mediate receptor non-specific effects are poorly understood. Gangliosides have been shown to negatively regulate the transcription factor NF-κB by inhibiting its activation and nuclear translocation in macrophages^{138,139} and T cells¹⁴⁰. Certain gangliosides, including GM1

and GD1a, have been shown to reversibly inhibit activation of monocytes which were stimulated through a number of TLR receptors, including TLR4, and this inhibition coincided with upregulation of the inhibitory molecule IRAK-M (IL-1 receptor associated kinase-M)¹⁴¹. In a separate study, it was shown that the carbohydrate moiety is necessary for the immunosuppressive activity of GD2 ganglioside. However, it was the length of the acyl chains in the ceramide moiety that appeared to determine the strength of the effect¹⁴². This is an important consideration as *C. jejuni* LOS only mimics the carbohydrate portion and not the ceramide portion of gangliosides. It is thought that non-receptor specific ganglioside effects rely on insertion of gangliosides into lipid rafts.

An alternative mechanism of ganglioside immune-modulation is via receptor specific interactions such as the sialic acid binding immunoglobulin like lectins (siglecs). Siglecs are a family of receptors which bind sialylated glycoconjugates and are expressed differentially on various immune system cells¹⁴³ (see Appendix 2 for siglec structure and cellular expression; see Appendix 3 for known siglec binding profiles). Siglecs are divided into two categories on the basis of sequence similarity. Sialoadhesin (Siglec 1), CD22 (Siglec 2), Myelin Associated Glycoprotein (Siglec 4) and Siglec 15 form one group while CD33 (Siglec 3), Siglec 5 to 11 and Siglec 14 make up the second group (termed the CD33 related siglecs)¹⁴⁴. The murine CD33 related siglecs comprise CD33, Siglec E, Siglec F, Siglec G and Siglec H while the non-CD33 related siglecs are named the same as for humans¹⁴⁴. Most of the CD33 related siglecs have two conserved cytoplasmic Immunoreceptor Tyrosine-Based Inhibitory Motifs (ITIMs) or ITIM-like motifs¹⁴⁴. Classically ITIMs function to inhibit signalling through Immunoreceptor Tyrosine-Based Activation Motifs (ITAMs) which form the signalling motifs of several types of activating receptors¹⁴⁵. There are significant variations in siglec receptors in their expression on haemopoietic cells, their sialic acid binding specificity and in their signalling motifs. Some siglecs, for example Siglec 13, Siglec 14, Siglec 15, and Siglec H, associate with adaptor proteins such as DAP12 which itself has an activating ITAM motif¹⁴⁶, while other siglecs such as Sialoadhesin have no signaling motif, although the receptor appears to enhance phagocytosis while inhibiting dendritic cell antigen presentation¹⁴⁷. Numerous studies have demonstrated the immunomodulatory function of

siglecs and these effects include inhibiting proliferation and activation, promoting apoptosis and promoting pro-inflammatory cytokine secretion¹⁴⁴. Certain members of the siglec family are capable of binding gangliosides and in one instance binding to ganglioside mimicking LOS has been shown. Siglec 7 (expressed on human NK cells and monocytes) mediates sialic acid dependent binding to LOS extracted from GM1/GT1a or GM3 mimicking strains of *C. jejuni*¹⁴⁸. The functional consequence of this remains to be investigated.

The ganglioside GM1 is one of the few endogenous ligands known to be presented by the CD1 class of MHC I-like antigen presenting molecules. CD1 presents glycolipid antigens to specific classes of T cells which are potent sources of immune polarising cytokines¹⁴⁹. However, there is no conclusive evidence to suggest that ganglioside mimicking LOS can substitute for gangliosides in the binding pocket of CD1 molecules.

Rough and smooth O-antigen side chains alter the interaction of LPS with the TLR4/MD2 receptor complex¹²³. Few studies have addressed whether the side chain is capable of signalling independently, or co-operatively, with the Lipid A through interactions with non-TLR4 receptors. However, it has been shown that LPS O-side chains bearing mannose are capable of mediating enhanced adjuvant activity through co-operative signalling via the mannose receptor on myeloid cells¹⁵⁰⁻¹⁵². A possible direct link between gangliosides and TLR4 signalling has been revealed using Neu1 (neuraminidase 1) deficient mice and neuraminidase inhibitors such as Tamiflu. For full TLR4 signalling to occur, endogenous α 2-3 linked sialic acid residues associated with the TLR4 must be cleaved, otherwise there is a deficiency in inflammatory cytokine production^{153,154}. LOS which mimics gangliosides GM1 and GD1a expresses α 2-3 linked sialic acid residues. It is theoretically possible that these can substitute for the endogenous sialic acid and affect TLR4 signalling.

There are clearly a number of ways in which gangliosides can alter immune function and it is possible that ganglioside mimicking LOS can substitute for gangliosides in these properties. For example, they could deliver a second signal in addition to Lipid A/TLR4 and also alter how the bacteria are taken up and processed by immune cells. Either of these events might have a substantial effect on the immune response to ganglioside mimicking *C. jejuni* or the maintenance of self-tolerance by the responding cells.

1.8 Immune responses to carbohydrate antigens

Thymus independent (TI) antigens are molecules capable of directly stimulating B cell antibody responses without the requirement of conventional, MHCII restricted, T cell help¹⁵⁵. Although not an exclusive rule, generally speaking, carbohydrate and glycolipid molecules, such as LOS and gangliosides, tend to be TI antigens, while proteins and peptides tend to be thymus dependent (TD) antigens. TI antigens are sub-classified into TI-1, which stimulate all sensitive B cells through innate receptor signalling such as TLR4, and are capable of causing polyclonal activation, and TI-2, which have repeating epitopes which cross link B cell receptors delivering an antigen specific signal which drives activation¹⁵⁶. LPS, and presumably *C. jejuni* LOS, signals through the innate LPS receptor TLR4 and are therefore TI-1 antigens. Although gangliosides do not express multiple epitopes on the same molecule, they behave as TI-2 antigens¹⁵⁷ presumably due to aggregates of molecules providing repeating epitopes, for example in micelles or cell membranes. Ganglioside mimicking LOS might also be considered a TI-2 antigen, as well as a TI-1 antigen, for this same reason. Immune responses to TI antigens are substantially different than responses to conventional TD antigens and involve specific sub-populations of B and T cells. TI responses provide prompt and specific humoral responses to common bacterial products such as capsular polysaccharides and LPS¹⁵⁶.

There is no conclusive evidence that GBS represents a pure TI immune response or that *C. jejuni* LOS alone is sufficient to induce GBS. Natural infection with *C. jejuni* results

in exposure to a range of antigens including proteins and bacterial DNA/RNA. Models of GBS use adjuvants such as Freund's and Keyhole Limpet Haemocyanin which introduce protein antigens and thus engage T cell help. In addition, the pathogenic antibody isotypes often seen in GBS are considered to be "T dependent". However, the ganglioside target in GBS, like LOS, is a non-protein molecule and is not presented for T cell help by conventional means. The immune response associated with GBS is often transient and no clear evidence of a lasting B cell memory has been shown. These are features more in keeping with TI responses. The lack of an MHC association with GBS⁷², which is virtually unique amongst auto-immune diseases, raises important questions about the exact role of T cells, or more specifically, protein antigens.

The naïve murine B cell compartment consists of two broad subsets, B1 (comprising B1a and B1b) and B2 (comprising MZ and FO B cells). Each subset shows distinct anatomical localisation. B1 B cells are found primarily in the peritoneal and pleural cavities¹⁵⁸ while the B2 subsets are located in secondary lymphoid organs such as the spleen and lymph nodes. Within the secondary lymphoid organs, MZ B cells are located near the marginal sinus where they are able to interact with particulate blood borne antigens such as encapsulated bacteria¹³¹. The traditional view is that B1 B cells and MZ B cells contribute to TI immune responses to glycolipid antigens and have a limited capacity for affinity maturation and class switch recombination^{131,158}. FO B cells participate in TD immune responses to protein antigens and produce highly specific affinity matured antibodies, with class switch recombination. They are classically not thought to play a major role in TI responses. However, the roles of B cell subsets are not as clearly delineated as this model suggests.

B1 B cells are thought to bridge the gap between innate and adaptive immunity. They are long lived cells with a BCR repertoire which is skewed towards polyreactivity with common bacterial and self antigens, particularly carbohydrate antigens. Being exquisitely sensitive to LPS, they are believed to be important in TI-1 immune responses. B1 B cells, alongside MZ B cells, are considered to be the source of natural IgM. B1 B

cells undergo class switch recombination to IgG3 and IgA although they do not usually undergo affinity maturation to any great extent^{158,159}. Animal and human studies of GBS indicate that isotype class switching and possibly affinity maturation are key events in pathogenesis. Although B1 B cells are probably responsible for the natural anti-ganglioside IgM (not usually associated with GBS), their restricted capacity for affinity maturation and class switch recombination makes them an unlikely candidate as the source of the high affinity IgG autoantibodies seen in GBS.

MZ B cells are essential for TI-2 responses¹⁵⁵. MZ B cells (reviewed¹⁶⁰) are highly enriched in the marginal zone of the spleen. This region contains a number of specialised immune cells such as marginal dendritic cells and marginal zone metallophilic macrophages. The latter population expresses siglec receptors and are postulated to play a role in capturing carbohydrate antigens to present to B cells¹⁶¹. MZ B cells share properties with B1 B cells that make them important in TI responses¹⁶²; they are highly sensitive to LPS (expressing higher levels of RP105/MD1 than FO B cells) and they respond rapidly following activation and produce large quantities of antibody^{158,163}. The preferred isotypes of murine MZ B cells are IgM and IgG3¹⁵⁸ although they are capable of class switching to all IgG isotypes including those associated with GBS^{160,164}.

Marginal zone B cells participate in both TI and TD immune responses¹⁶⁵. When stimulated with TD antigens, MZ B cells are able to form early antibody secreting cells as well as later germinal centres with associated affinity maturation and class switch recombination¹⁶⁶. MZ B cells also selectively participate in extrafollicular immune responses to TI-2 antigens which do not involve germinal centres. Although an initial interaction with T cells is seen, the plasmablasts depend on accessory help from a specialised population of CD11c⁺ dendritic cells which provide survival signals and promote isotype class switching in a T-independent manner. Both class switch recombination and affinity maturation occur to a lesser degree than that found in germinal centres^{165,167}. MZ B cells, unlike FO B cells, are potent activators of naïve CD4 T cells early in the immune response. They express higher levels of MHCII, higher

levels of co-stimulatory molecules and are capable of polarising T cells towards a Th1 phenotype¹⁶⁸. In addition, MZ B cells express the antigen presenting molecule CD1c which allows presentation of glycolipid antigens to specific subsets of T cells^{160,169}. However, the transient nature of GBS and the lack of any evidence supporting the existence of B cell memory following GBS would suggest that T cells are not involved in the conventional sense.

Models of GBS and other autoimmune diseases suggest that isotype class switching and affinity maturation are important events leading to pathogenesis. The factors which control these during B cell responses to TI antigens are less well understood than to TD antigens. This is made more complicated by the fact that substantial differences exist between human and mice in the generation of the MZ B cell pool. For example, genetic studies of MZ B cells in humans before and after immunisation with polysaccharide antigens have shown that MZ B cells which participate in the response had already undergone somatic mutation prior to vaccination suggesting humans have a pre-diversified repertoire. Isotype switching however takes place during the evolution of the response^{160,170,171}. Whatever factors govern this pre-diversification may have a substantial bearing on GBS. The factors that govern isotype class switching are also poorly understood. The antigen itself appears to have some bearing on the nature of the response and the resulting IgG isotype. For example, an antigen engineered to be expressed internally in *E. coli* triggered a TD response, while the same antigen expressed on the surface triggered a TI response¹⁷². In addition, a polysaccharide antigen and a protein antigen which mimics the polysaccharide antigen (an idiotype antibody) both triggered TI type responses (IgM and IgG3)¹⁷³⁻¹⁷⁵, indicating the shape and not the chemistry of the antigen was important. Other factors common to both TD and TI responses appear important in class switching to the highly pathogenic IgG2a isotype, for example co-operative signalling through complement receptors and IFN- γ . IFN- γ may be derived from conventional T cells, innate lymphocytes (such as Natural Killer (NK) cells) or other accessory cells¹⁵⁵.

T cells are able to recognise glycolipid molecules when they are presented on a novel family of MHC I like antigen presentation molecules termed CD1 (reviewed¹⁷⁶). Humans express five CD1 molecules (CD1a to CD1e) on antigen presenting cells. These are sub-classified into families. CD1a to CD1c comprises one family and CD1d and CD1e comprises two additional families. Mice only express CD1d. There is a degree of lipid binding specificity between CD1 molecules although some molecules, such as sulphatide, show promiscuity in being able to bind to several CD1 types.

T cells capable of engaging CD1 fall into two broad categories: those that engage CD1a to CD1d, which behave in a similar manner to conventional peptide specific T cells, and those that engage CD1d alone. The majority of this latter group (termed iNKT cells) have semi-invariant T cell receptors and behave in an innate manner in that they are capable of rapidly producing large quantities of cytokines including IL-4 and IFN- γ .

There has been considerable progress made in the identification of ligands for CD1, and these include both pathogen and self molecules (reviewed¹⁷⁶). The majority of bacterial antigens are cell wall components, particularly those derived from *Mycobacterium tuberculosis*. Bacterial lipopeptides have also been found to bind to CD1. Intriguingly, gangliosides are prominent amongst the known self-ligands, particularly of CD1b. Ganglioside specific T cells have been isolated from multiple sclerosis patients. In order to bind to CD1, the fatty tail of the ligand must conform to the hydrophobic binding pockets of the CD1 molecule while the carbohydrate portion must sit in, or extend from, the binding groove. There is no evidence that LPS lipid A, and presumably LOS lipid A, is capable of binding to CD1. Binding would not be predicted by the nature of the acyl chains on the Lipid A tail. Therefore it is unlikely that *C. jejuni* LOS, with its ganglioside mimic, can be presented directly to T cells (unless there is some, as yet unknown, processing pathway that substantially alters its Lipid A tail).

There are alternative routes by which LPS molecules might activate the T cell arm of the immune system. Studies using *Salmonella typhimurium* LPS (rough mutant) have shown that dendritic cells activated by LPS secrete IL-12 which in turn activates iNKT cells. Surprisingly this was in a CD1d dependent manner, indicating that some sort of self antigen, or alteration of self antigen, was being sensed alongside the IL-12 (as LPS cannot itself be presented on CD1d). In addition, there is evidence that iNKT cells can be activated directly by TLR ligands¹¹⁰.

The role of T cells in GBS is largely unexplored although studies show no association with CD1⁷⁵ or MHC haplotypes. In addition, a mouse model generating anti-ganglioside antibodies showed no role for the murine glycolipid antigen presenting molecule CD1d¹⁷⁷. However, this does not rule out non-antigen specific T cell help, as discussed above, in providing the cytokines necessary for pathogenic class switching.

1.9 Tolerance to carbohydrate antigens

Humoral tolerance to carbohydrate antigens probably follows similar mechanisms to tolerance to protein antigens. A number of complex factors determine tolerance and some of the principal mechanisms are receptor editing or deletion during ontogeny, antigen ignorance, anergy and suppression.

These processes may have specific differences when they relate to carbohydrate antigens and GBS. For example, MZ B cells and B1 B cells which take part in anti-carbohydrate responses also contribute to the natural immune antibody repertoire which contains anti-ganglioside specificities even in healthy people^{61,63}. Rather than negative selection of auto-reactive clones, the B cells which contribute to the natural repertoire are positively selected against self-antigen and possibly commensal flora in the gut¹⁷⁸⁻¹⁸¹. It appears that the affinity of the self-reactive BCR determines the fate of the B cell. For example, mice have been genetically engineered to express an anti- α Gal (carbohydrate) antibody.

In an α Gal negative background, these B cells escape into the periphery and produce IgM antibodies of a sufficient affinity to reject α Gal expressing grafts. However, in an α Gal expressing background, the anti- α Gal (auto-reactive) B cells are located in the marginal zone (presumably becoming MZ B cells), but have edited their receptors to produce lower affinity, non-pathogenic, anti- α Gal IgM antibodies¹⁸². In genetically engineered anti-red blood cell autoantibody transgenic mice, the conventional B cells get clonally deleted but auto-reactive B1 B cells persist in the peritoneal cavity usually without causing disease. Anaemia develops when the B1 B cells are activated by oral administration of LPS¹⁸³ or injections of cytokines IL-10 or IL-5¹⁸⁴.

It is clear that the presence of anti-ganglioside antibodies is not in fact the mystery of GBS, but rather what activation events take place that allow them to become pathogenic. Animal models and human studies suggest isotype switching and affinity maturation (either one or both) are important events. As low affinity anti-ganglioside specificities are already in place there are additional mechanisms of tolerance in these B cell populations which must be bypassed if they are to be responsible for the autoimmunity seen in GBS. For example, cross linking of the BCR in B1 B cells does not lead to activation, as it does in conventional B cells, but instead induces apoptosis¹⁸⁵. Additional stimulation in the form of LPS or cytokines is also required^{183,186}. In addition, despite repeated immunisation, B1 cell anti-carbohydrate responses will only show limited isotypes (IgM, IgA and IgG3 in mice), no typical memory responses and limited or no affinity maturation¹⁸⁷⁻¹⁹⁰. These combined factors will serve to protect the host from autoimmunity even when LPS type stimulation is present alongside ganglioside mimicry, such as with ganglioside mimicking LOS. MZ B cells present a different problem as they are more like conventional FO B cells in their capabilities to class switch and affinity mature. Previously described studies have demonstrated that MZ B cell receptors are edited to remove those with high affinity for self-antigens. In addition, extensive cross linking of the BCR renders both immature and mature B cells anergic¹⁵⁶ and therefore epitope density and presumably whether the antigen is soluble or particulate may be important in determining tolerance to TI-2 antigens. Those MZ B cells that enter the germinal centre to participate in responses might be subject to the same T cell help and

regulatory mechanisms as FO B cells responding to conventional peptide antigens, while those MZ B cells that participate in extra-follicular responses show less affinity maturation and isotype switching¹⁶⁷, presumably due to a lack of T cell help.

Antigen ignorance may play an important role in GBS. While gangliosides are expressed throughout the body, specific gangliosides are concentrated in certain regions. For example, GM1 is concentrated in peripheral motor nerve myelin¹⁹¹ and GQ1b is concentrated in the oculomotor nerve¹⁹². Antibodies to GM1 are associated with motor deficits and antibodies to GQ1b are associated with ophthalmoplegia²⁷. Complexes of mixed gangliosides provide unique epitopes from single gangliosides³⁶ and the nerves are partially protected from the immune system by a blood nerve barrier. Therefore, due to localised expression levels, the unique configurations of complexes and the blood nerve barrier, it is possible that B cell receptors are not exposed to all of the possible arrangements of gangliosides during their development and so are not adequately tolerised. In addition, it is possible that low levels of low affinity anti-ganglioside antibodies can safely exist due the protection afforded by the blood nerve barrier.

Substantial differences exist between the human and murine immune systems. Some of these may impact on responses to TI-1 and TI-2 antigens, such as LOS and gangliosides, in GBS. Murine B1 B cells have been recognised for some time and their function and phenotype have been studied extensively^{188,193-195}. However, human B1 B cells remain a controversial entity whose existence is disputed, although B cells with an appropriate phenotype (CD5 positive) have been identified in human peritoneal washings¹⁹⁶. An additional important difference is that the LPS/LOS receptor TLR4 is expressed by murine, but not human, B cells^{107,108,127,197}. This difference in TLR4 expression is no doubt responsible for a major difference in function between human and murine MZ B cells, that is, murine MZ B cells respond to TI-1 antigens whilst human MZ B cells do not¹⁹⁸. However, there are more similarities than differences as both murine and human MZ B cells express high levels of CD21 and IgM. In addition, both human and murine MZ B cells respond vigorously to TI-2 antigens, respond to TD antigens and are efficient

antigen presenting cells¹⁹⁸. No such comparison can be made between human and murine B1 B cells as the principal murine B1 marker, CD5, is expressed on a wider range of B cell populations in humans. While such differences can be related directly to GBS, there are many more general differences between human and murine immunity¹⁷⁰. This means that findings in murine models of GBS must always be taken in context and interpreted appropriately.

1.10 Hypothesis

The over-arching hypothesis is that ganglioside mimicking *C. jejuni* interact with the immune system in a unique way by virtue of their ganglioside mimicry, and this contributes to the events that lead to a break in tolerance. More specifically, the aim of this study is to address the following hypotheses:

1. LOS derived from a GBS associated strain of *C. jejuni* is able to bind to cellular or humoral ganglioside specific receptors through the ganglioside mimicking core sugars.
2. Binding of LOS to these ganglioside specific receptors alters the potency or polarising properties of ganglioside mimicking LOS compared to non-mimicking LOS.
3. Binding of ganglioside mimics to these ganglioside receptors alters trafficking of the *C. jejuni* within the immune system.

In essence, it is possible that ganglioside mimicking LOS can deliver three signals. First, the Lipid A can be sensed by TLR4; second, the ganglioside mimic can interact with ganglioside specific BCR; and third, putatively, the ganglioside mimic can interact with endogenous ganglioside specific receptors or can mediate *cis* interactions with endogenous gangliosides. The importance of gangliosides goes beyond receptor specific

interactions as they also play an important role in humoral immunity through interactions with natural antibody and complement components such as Factor H (fH)¹⁹⁹⁻²⁰¹. GBS is a heterogeneous condition and it is clear that there is no single underlying aetiology. Therefore it is unlikely there is a single pathway that leads to breaking of tolerance and autoimmunity.

If all, or some, of these hypotheses are proven correct it will alter our understanding of how GBS associated strains of *C. jejuni* interact with the immune system and might shed light on the events leading to pathogenesis. In addition, if it can be established in principle that the ganglioside mimic is not simply a passive target of the BCR, but instead actively manipulates the immune system, this would provide an interesting new paradigm for any autoimmune disease in which molecular mimicry of a self signalling molecule can be shown to be a preceding event.

2 Materials and Methods (see Appendix 1 for buffers and media)

2.1 Analysis software

2.1.1 Statistical analysis

Data were analysed using GraphPad Prism 4 (GraphPad Software Inc). Figure illustrations follow the standard format (* = $p < 0.05$, ** = $p < 0.01$ and *** = $p < 0.001$). Data were analysed using 1way ANOVA, 2way ANOVA with Bonferroni's posttest or students T test where appropriate (detailed in text). Graphs all show mean and standard error of the mean (SEM).

2.1.2 Acquisition and analysis of FACS data

FACS acquisition was done on a FACSCalibur machine (BD Biosciences) and analysis was done using FlowJo software (Treestar Inc)

2.1.3 Analysis of immunohistology and immunocytology

Immunohistology and immunocytology were visualised using an Apotome/Zeiss microscope or Laser Scanning Confocal microscope and the images analysed using AxioVision Rel 4.7 software with co-localisation module.

2.2 Preparation of Lipo-oligosaccharide (LOS)

2.2.1 *C. jejuni* strains

The strains of *C. jejuni* used were Penner serotype O:19 (HS O:19) in which the LOS structure mimics gangliosides GM1 and GD1a at 50:50 ratio²⁰²; Penner serotype O:3 (HS O:3) in which the LOS does not mimic gangliosides²⁰³; *C. jejuni* strains GB2 and GB11 in which the LOS structure mimics gangliosides GM1 and GD1a at 50:50 ratio; and the isogenic sialyltransferase gene (CSTII) knock-out strains, GB2 CSTII knock out and GB11 CSTII knock out, in which the LOS does not mimic gangliosides due to the failure of addition of sialic acid to the carbohydrate side chain¹⁰¹. GB19 LOS (GD1c mimic) and its CSTII knock out isogenic counterpart¹⁰¹ were also provided as pre-purified LOS. The GB2, GB11 and GB19 strains and their CSTII knock out counterparts were kind gifts from B. Jacobs and M. Kuijf, Erasmus University, Netherlands.

2.2.2 Growth and heat inactivation of *C. jejuni*

For LOS purification *C. jejuni* were grown for 48 hours at 37°C in a microaerobic environment on Columbia Agar and Horse Blood plates (E & O Laboratories, Scotland. Container P090). The bacteria were harvested into PBS (phosphate buffered saline) and heat inactivated at 60°C for 1 hour. For siglec binding experiments bacteria were harvested into 8% formalin/PBS and left for 1 hour to inactivate.

2.2.3 Crude hot phenol extraction of LOS

Heat inactivated bacteria were centrifuged at 6000rpm for 10 minutes (Sorval ultracentrifuge, Rotor SS34) and the supernatant discarded. The pellet was resuspended at 10g/ml in dH₂O (distilled water) and blended to a paste, on ice, using an Ultra Turrax

homogeniser. An equal volume of 85% liquid phenol (Sigma, UK) was added and the cells were blended on ice for 5 minutes. The mix was placed in a water bath at 65°C and blended for 1 minute at 2 minute intervals for 10 minutes. The mix was centrifuged at 2500rpm for 20 minutes at < 10°C. The aqueous (top) layer was removed and stored. An equal volume of dH₂O was added to the remaining sample and blended for five minutes on ice repeating the procedure. The combined aqueous layers were dialysed for 3 days at 4°C against 5 litres of dH₂O (whole volume changed twice daily) using 3.5 kDa MWCO (molecular weight cut-off) Snakeskin pleated dialysis tubing (Pierce Laboratories, UK). The crude LOS extract was lyophilised (Christ Alpha 1-2 LD lyophiliser).

2.2.4 Quantification of LOS by dry weight

LPS and LOS were lyophilised in pre-weighed conical flasks and the dry weight was determined using accurate scales (Ohaus Explorer Pro).

2.2.5 Purification of LOS

The LOS was resuspended to 10mg/ml in dH₂O. 200 µg/ml DNase I (Merck, UK) and 50 µg/ml RNase A (Merck, UK) were added and incubated at 37°C for 2 hours. 1mg/ml of Proteinase K (Merck, UK) was added and the LOS was incubated for a further 3 hours at 65°C to allow auto-digestion of the Proteinase K. The LOS was dialysed against 5 litres dH₂O for 48 hours (whole volume changed twice daily) at 4°C then lyophilised and resuspended to 2mg/ml in sterile dH₂O.

2.2.6 Purification of commercially bought LPS

Smooth mutant *E. coli* 0111:B4 LPS (Sigma, UK), rough mutant *S. typhimurium* LPS SL1181 (RE mutant) (Sigma, UK) and smooth mutant *S. typhimurium* LPS (RA mutant) (Sigma, UK) were subjected to the DNase, RNase and Proteinase K purification protocol to remove contaminants.

2.2.7 Determination of LOS purity by silver stain

SDS (sodium dodecyl sulphate) PAGE (Polyacrylamide Gel Electrophoresis) of LOS was carried out using a Novex 10-20% Tricine gel according to the manufacturer's instructions. Briefly, 5µg of LOS was added to 5µl Tricine SDS sample buffer and 1µl Nupage reducing agent (All Invitrogen, UK). The sample was heated to 85°C for 2 minutes and 10µl was then loaded into the wells. The gel was run in Tricine SDS running buffer (Invitrogen, UK) at 125 V constant for 90 minutes. A silver stain of the gel was performed using a SilverXpress silver stain kit (Invitrogen, UK) following the manufacturer's instructions.

2.2.8 Determination of LOS purity by spectrophotometry

2mg/ml LOS was titrated with 4µM EDTA (ethylenediaminetetraacetic acid) /dH₂O and 1% triton X to disperse micelles and clarify the solution for spectrophotometry. DNA, RNA and protein content was determined by spectrophotometry (Eppendorf biophotometer AG 22337) (Fisherbrand semi-micro cuvettes).

2.2.9 Determination of LOS epitopes by Western blot

LOS was subjected to SDS-PAGE and transferred onto an Invitralon PVDF (Polyvinylidene Fluoride) membrane (0.45µm pore size, Invitrogen, UK) following the manufacturer's instructions. The PVDF membrane was either stained immediately or dried and stored overnight at 4°C then reactivated with methanol. The membrane was blocked using 3% w/v Marvel (powdered milk)/PBS for 1 hour then washed three times for 5 minutes in PBS with 0.5% Tween 20. The GM1 epitope was detected using cholera toxin conjugated to HRP (horse radish peroxidase) (Sigma, UK) diluted in a 1:7000 solution in 0.2% Marvel/PBS while the GD1a epitope was detected using the MOG-35 monoclonal antibody²⁰⁴ (159µl diluted in 10ml PBS with 0.5% Tween 20) used in conjunction with an anti-mouse IgG HRP conjugated antibody (Southern Biotech, USA) diluted 1:2000 in PBS with 0.5% Tween 20. All incubation steps lasted 1 hour and the membrane was washed between steps three times in 0.5% PBS/Tween for 5 minutes. The membrane was developed using Super Signal West Pico (Pierce, USA) following the manufacturer's instructions.

2.2.10 Generation of GM1 mimicking LOS from GM1/GD1a mimicking LOS

LOS was resuspended to 1mg/ml in dH₂O and 0.3 units/mg of cholera neuraminidase (Calbiochem, UK) was added. Samples were incubated at 37°C for 2 hours. Proteinase K was then added for 3 hours at 65°C to remove the neuraminidase and allow for auto-digestion of the Proteinase K. The LOS was dialysed, lyophilised and resuspended as before.

2.2.11 Determination of LOS purity by alcian blue stain

A positive control for capsular polysaccharide was generated by lysing 200µl of heat inactivated *C. jejuni* (OD600 of 3.5) using 200µl of 200mg/ml Cell Lytic Express (Sigma, UK) according to the manufacturer's instructions. The sample was incubated for 20 minutes then centrifuged at 16,000g for 15 minutes and the supernatant kept for analysis. SDS-PAGE of LOS and the lysed bacteria supernatant was carried out. The gel was transferred to a PVDF membrane (Invitralon, 0.45µm, Invitrogen, UK) following the manufacturer's instructions. The PVDF membrane was dyed with 0.5% alcian blue in 7% acetic acid for 2 minutes then washed in PBS until clean.

2.2.12 Quantification of LOS by thiobarbituric acid assay

A 3 deoxy-D-manno-oct-2-ulosonic acid (KDO) standard curve was generated from 0, 0.5, 2.5, 5 and 7.5µl of 0.5mM KDO (Sigma, UK) dried overnight in eppendorf tubes. 10µg of each LOS was also dried overnight. 250µl of pH4.4, 0.1M, sodium acetate (Sigma, UK) was added to each tube and the solution heated at 100°C for 1 hour. 125µl of 40mM periodic acid in 0.125M sulphuric acid (H₂SO₄) was added and the solution was vortexed briefly then left to stand for 30 minutes at room temperature. 250µl of 0.2M sodium arsenite (Sigma, UK) in 0.5M hydrochloric acid was added and mixed thoroughly. 250µl of fresh 2-thiobarbituric acid (Sigma, UK) (60mg/10ml dH₂O) was added and the tubes heated to 100°C for 15 minutes. 500µl of DMSO was added into the hot tubes and mixed. The optical density (OD) of the solution was determined at 549nm.

2.3 Binding of cellular receptors and humoral factors to *C. jejuni* and LOS

2.3.1 Binding of Sialoadhesin, Siglec E and Siglec F to LOS and gangliosides

Purified GB11 wild type, GB11 CSTII knock out, HS O:19 and HS O:3 LOS were adsorbed onto 96 well half area ELISA plates by dissolving in methanol at 5µg/ml and adding 50µl per well before allowing the methanol to evaporate in a fume hood. The plates were washed twice with PBS then blocked with 100µl per well of 3% BSA (bovine serum albumin)/PBS for 1 hour. The plates were washed once with PBS then specific siglecs were added to each well. The siglec reagents were murine Siglec-human-Fc fusion proteins kindly supplied by Prof P. Crocker, University of Dundee (see Appendix 4 for siglec-human-Fc fusion protein structures). Sialoadhesin and Siglec F were made up at 1µg/ml in blocking buffer while Siglec E was used at 0.5µg/ml. The siglecs were combined with 3 times the volume of anti-human IgG-HRP (Southern Biotech, USA) and left for 1 hour at room temperature to form complexes. 50µl of siglec, diluted in blocking buffer, was added per well and incubated for 1 hour. The plates were washed 5 times then developed using Sure Blue TMB solution (Insight Biotechnology, UK) and read at 450nm using a Labsystems Multiscan Ascent plate reader. When siglec binding to gangliosides GM1 and GD1a (Sigma, UK) and O-side chain sugar molecules, asialo-GM1, asialo-GM2 (both Sigma, UK) and lactosyl ceramide (Merck, UK) was assessed, the gangliosides were adsorbed onto the plate at 2µg/ml. For complex ganglioside/O-side chain ELISAs (mixed ganglioside and sugar targets), the sugar molecules were dissolved together in methanol and sonicated for 5 minutes to generate micelles containing the different epitopes.

2.3.2 Binding of Sialoadhesin, Siglec E and Siglec F to *C. jejuni*

C. jejuni were grown and harvested into 8% formalin/PBS and left for 1 hour at room temperature to inactivate. The bacteria were washed 3 times in 20ml PBS by centrifugation at 12,000 g for 10 minutes (Beckman Coulter Allegra 64R, rotor F0630). They were then diluted in PBS to an OD600 of 1 and frozen at -80°C following the addition of glycerol to a final concentration of 10%. *C. jejuni* strains GB11 wild type, GB11 CSTII knock out, HS O:19 and HS O:3 were defrosted, centrifuged at 13,000g for 1 minute and resuspended to an OD600 of 0.1 in PBS. 50µl of bacteria were put in each well of a 96 well half area ELISA plate (Costar, UK) and allowed to adsorb onto the surface overnight at 4°C. The plate was washed twice with PBS and then blocked using 100µl per well of 3% BSA/PBS for 1 hour. The plate was washed once before the desired siglec was added at a diluting concentration (siglecs were made up as detailed earlier) and incubated for 1 hour. 50µl was added per well. The plate was washed 5 times with PBS before being developed using 50µl of Sure Blue TMB substrate solution per well and stopped using 25µl 4N H₂SO₄.

2.3.3 Visualisation of siglec binding to *C. jejuni*

70µl of formalin fixed HS O:19 and HS O:3 *C. jejuni* with an OD600 of 0.5 were centrifuged onto a microscope slide (VWR Superfrost Plus) using a cytopsin (600g, 5 minutes). The bacteria were labelled using Sialoadhesin, Siglec E and Siglec F adapting the above ELISA protocol except using a FITC labelled anti-human IgG (BD Biosciences, UK) instead of the HRP labelled antibody. The slides were mounted using Vectashield DAPI containing mounting media (Vector, USA) and visualised using an Apotome/Zeiss microscope.

2.3.4 Binding of Sialoadhesin to *C. jejuni* following neuraminidase treatment

Formalin fixed HS O:19 and HS O:3 were defrosted, centrifuged at 13,000g for 1 minute and resuspended to an OD600 of 0.1 in PBS. 50µl of bacteria were put in each well of a 96 well half area ELISA plate (Costar, UK) and allowed to adsorb overnight at 4°C. The plate was washed twice with PBS. Selected wells were treated with 50µl of 0.004 U/ml of neuraminidase from *vibrio cholerae* (Merck) in HBSS (Hanks buffered salt solution) for 1 hour at 37°C while control wells were incubated with HBSS alone. The plate was washed twice with PBS and then blocked using 100µl per well of 3% BSA/PBS for 1 hour. The ELISA was carried out as before. Increased GM1 expression was confirmed using the anti-GM1 mouse mAb DG2. 50µl of Ab (0.5mg/ml) diluted 1:200 in blocking buffer was added per well and incubated for 1 hour at room temperature. This was washed three times and an anti-mouse IgG HRP secondary (southern biotech) was added (1mg/ml diluted 1 in 500) and incubated for 1 hour. Following five washes the plate was developed with Sure Blue.

2.3.5 Binding of purified human Factor H to *C. jejuni* by ELISA

Formalin fixed *C. jejuni* were adsorbed onto ELISA plates, washed and blocked as before. The wells were incubated with 60µg/ml of purified human Factor H (fH) (Sigma, UK) for 1 hour at 37°C. The plate was washed twice with PBS and then incubated with a mouse monoclonal anti-human fH antibody (OX-23 clone, 1mg/ml, Serotec, UK) used at a 1:250 dilution. Following two washes the plate was incubated with an anti-mouse IgG HRP secondary antibody (1:500 dilution)(Southern Biotech) to detect fH binding to the bacteria. The plate was developed using Sure Blue substrate.

2.3.6 Binding of purified human Factor H to *C. jejuni* by FACS

Heat inactivated *C. jejuni* were washed and resuspended to an OD600 of 3.6 in sterile filtered HBSS. 90µl of bacteria were incubated with 5µg of purified human fH in 10µl of PBS for 30 minutes at 37°C then washed with 400µl HBSS. The bacteria were resuspended then incubated with 50µl of the anti-fH monoclonal antibody (1:100 dilution) for 30 minutes. After another wash they were incubated with 50µl of anti-mouse IgG FITC (1:100 dilution) (Southern Biotech) for 30 minutes. Following two final washes they were resuspended to 250µl in HBSS and acquired using a FACSCalibur FACS machine.

2.3.7 Visualisation of Factor H binding to *C. jejuni*

70µl of formalin fixed *C. jejuni* (OD600 of 0.5) were adsorbed onto a microscope slide by centrifugation (600g, 5 minutes), allowed to dry and marked using a pap pen. The bacteria were incubated with 5µg of purified human fH in 30µl of HBSS for 30 minutes at 37°C. Following a single wash the bacteria were incubated with the anti-fH mAb (30µl, 1:100 dilution) for 30 minutes. The slides were washed and the bacteria incubated with anti-mouse IgG FITC (1:100 dilution) for 30 minutes. The slides were washed and mounted with DAPI containing mounting media. The slides were visualised using an Apotome/Zeiss microscope.

2.3.8 Deposition of C3c and C9 on *C. jejuni* using ELISA

Formalin inactivated *C. jejuni* were adsorbed onto ELISA plates as before. The plates were blocked using 100µl of 3% BSA/PBS. Human serum (donated by individuals self-reporting no previous infection or exposure to *C. jejuni*) was diluted in PBS (dilutions detailed in results). Following two washes, 50µl of the diluted sera was added per well

and the plates incubated at 37°C for 20 minutes. The plates were washed 3 times after which 50µl of detection antibody was added: sheep anti-C3c or sheep anti-C9 (both Dako, Denmark) all diluted 1:500 in blocking buffer, and incubated for 1 hour. Following three washes anti-sheep IgG HRP (Santa Cruz Biotechnology, USA), diluted 1:500 in blocking buffer, was added. The plates were washed 5 times and developed using Sure Blue TMB solution.

2.3.9 Binding of natural IgM and IgG to *C. jejuni* or LOS

Formalin inactivated *C. jejuni* or LOS was adsorbed onto ELISA plates as before. Human sera was prepared as before and incubated for 1 hour at room temperature. Following 3 washes, IgM and IgG was detected using anti-human IgM HRP and anti-human IgG HRP (Southern Biotech, USA) diluted 1:1000 in blocking buffer. Following 1 hour incubation and five washes, the plates were developed using Sure Blue TMB solution.

2.4 Harvesting and labelling of cells for *in vitro* experiments

2.4.1 Mouse strains

Unless otherwise stated, the mice used were C57BL/6 wild type strains aged between 6 and 14 weeks old taken from the in-house colony of Dr C Goodyear or Prof H Willison. C3H/HeJ and C3H/HeN mice were female, aged 8 to 12 weeks and purchased from Harlan (UK). TLR2^{-/-} mice were female, aged 14 weeks and kindly supplied by Dr C Michels, University of Glasgow, UK.

2.4.2 Harvesting of splenocytes

Mice were sacrificed by suffocation with CO₂ and the spleens removed and placed in 3ml sterile cRPMI (complete RPMI). A cell strainer (Falcon, 70µm) was used to produce a single cell suspension of splenocytes which was washed in 10ml cRPMI by centrifugation at 500g for 5 minutes (Eppendorf Centrifuge 5408) with the supernatant being discarded. The pellet was resuspended in 2ml of ACK lysis buffer (BioWhittaker, UK) per spleen and gently mixed for 2 minutes before being washed with 10ml cRPMI and resuspended to 10ml in cRPMI. Any cell debris was removed using a sterile pipette and the cell concentration was determined using a haemocytometer. The splenocytes were then resuspended to 1x10⁷/ml in cRPMI and kept on ice. For experiments involving overnight culture the cRPMI was supplemented with 500µl 2-mercaptoethanol and 5ml non-essential amino acids per 500ml of media.

2.4.3 Purification of splenic B cells

Spleens were harvested as above and B cells were purified by negative selection using the EasySep magnetic B cell negative selection kit (Stemcell Technologies, USA) according to the manufacturer's instructions. Purity was assessed by flow cytometry (BD, FACSCalibur). Briefly, Fc receptors were blocked by incubating cells with Fc block (anti-mouse CD16/32, BD, UK), diluted 1:200 per million cells in 50µl FACS buffer for 10 minutes at 4°C. Cells were then stained with fluorophore labelled antibody (diluted 1:200 per million cells) in 50µl FACS buffer and incubated for 15 minutes at 4°C. The cells were washed in 500µl FACS buffer then resuspended in 250µl FACS buffer. Purity was assessed by comparing the percentage of B220⁺ cells (anti-mouse B220 APC, Southern Biotech, USA) before and after purification and typically showed >90% B220⁺ cells (example FACS plot in results).

2.4.4 Carboxyfluorescein diacetate succinimidyl ester (CFSE) labelling of splenocytes and B cells

Splenocytes, including erythrocytes, were harvested and resuspended to 1×10^7 nucleated cells/ml in RPMI (without added serum) at 37°C. 5mM stock CFSE (Invitrogen, UK) was diluted in RPMI so that 1µM CFSE was added to the cells. This was incubated at 37°C for 10 minutes with shaking. The cells were washed four times with 10ml of ice cold cRPMI (with added serum to mop up free CFSE) by centrifuging at 500g for 5 minutes. The cells were then resuspended to the desired concentration. For CFSE labelling of purified B cells the above protocol was followed with the exception of no erythrocytes being present.

2.4.5 Generation of M-CSF containing supernatant

L-929 cells are a murine fibrosarcoma cell line which secretes M-CSF (macrophage colony stimulating factor). The conditioned supernatant can be used to induce macrophage differentiation in bone marrow derived cells^{205,206}. L-929 cells were grown to 90% confluence in cRPMI in T75 flasks before being split into T150 flasks and grown to confluence. The cells were left for 3-4 days before the supernatant was collected by centrifugation (500g for 5 minutes). Aliquots were frozen at -20°C and were sterile filtered (0.2µm Minisart filter, Sartorius) before use.

2.4.6 Generation of GM-CSF containing supernatant

X-63 cells are a fibroblast cell line transfected with the murine granulocyte-macrophage colony stimulating factor (GM-CSF) gene. The conditioned supernatant can be used to generate bone marrow derived dendritic cells from bone marrow cells²⁰⁷. X-63 cells were grown in 18ml ISCOVES Modified Medium (IMDM with 2mM L-glutamine, 10% foetal

bovine serum, 100 units/ml Penicillin and 100 units/ml Streptomycin) until confluent. The cells were then washed in IMDM and recultured in 18ml Iscoves Modified Medium with 1mg/ml G418 (Geneticin antibiotic, Promega, USA) for 4 days. The cells were washed in RPMI 1640 and seeded into 25cm² flasks and grown in complete IMDM. When the cells reached log growth they were transferred to 75cm² flasks and grown until confluent. The cells were harvested by centrifugation (500g for 5 minutes) and seeded into 150cm² flasks in complete IMDM. Once confluent and after 4-7 days the supernatant was collected and stored at -20°C.

2.4.7 Harvesting of bone marrow

Mice were sacrificed by CO₂ suffocation and the hind limbs taken and stripped of flesh. The femurs and tibia were flushed with sterile PBS by inserting a 23 gauge needle into the marrow space and washing with PBS loaded into a 20ml syringe. The cells were vortexed thoroughly to break up clumps and broken up by aspirating gently through a 21 gauge needle if necessary. The cells were centrifuged and resuspended in 10ml cRPMI. The cells were passed through a cell strainer to remove clumps and then counted using a haemocytometer and resuspended at 1x10⁷/ml in cRPMI.

2.4.8 Generation of bone marrow derived macrophages

Bone marrow cells were plated out in 90mm Petri dishes (Sterlin, UK) at 5x10⁶ cells in 10ml cRPMI with 20% M-CSF (supernatant from the L-929 cell line) and incubated at 37°C in 5% CO₂. After 4 days the cells were supplemented with 7ml of cRPMI with 20% M-CSF and then used on day 7. Non-adherent cells were removed by aspirating the supernatant and gently washing with 5ml PBS. Adherent cells were harvested by adding 5ml ice cold PBS and scraping off with cell scrapers. Purity was assessed by flow cytometry. Fc receptors were blocked by incubating cells with Fc block (diluted 1:200 per million cells) in 50µl FACS buffer for 10 minutes at 4°C. Cells were then stained

with anti-mouse F4/80 biotin (Biolegend clone BM8, UK) diluted 1:200 per million cells in 50µl FACS buffer or the appropriate isotype control (Rat IgG2ακ biotin, Biolegend, UK) and incubated for 15 minutes at 4°C. The cells were washed in 400µl FACS buffer. The cells were resuspended by flicking the tube and incubated in 50µl FACS buffer with streptavidin APC (Southern Biotech, USA) diluted 1:200 for 15 minutes at 4°C. The cells were then washed twice in 400µl FACS buffer then resuspended in 250µl FACS buffer. Purity was assessed by comparing the percentage of F4/80⁺ cells to the isotype control and was typically >90% F4/80⁺ (example FACS plots in results).

2.4.9 Generation of bone marrow derived dendritic cells

Bone marrow cells were plated out in 90mm petri dishes at 5×10^6 cells in 10ml cRPMI with 10% GM-CSF (supernatant from the X-63 cell line) and cultured at 37°C in 5% CO₂. The cells were supplemented after 4 days with 10ml cRPMI and 10% GM-CSF. The cells were used after 8 days with only the non-adherent cells being taken by gently swirling the plate and taking the supernatant. Purity was assessed using the same protocol as for macrophages (antibodies used were anti-mouse CD11c biotin (BD biosciences, UK), hamster IgG1 isotype control (BD Biosciences, UK) and streptavidin APC, all at a 1:200 dilution per million cells in 50µl FACS buffer). Purity was typically >70% CD11c⁺ as assessed by flow cytometry (example FACS plot in results).

2.5 *In vitro* stimulation of splenocytes, B cells, dendritic cells and macrophages

2.5.1 Stimulation of splenocytes and purified B cells

CFSE labelled cells were prepared as above and resuspended to 1×10^7 cells/ml in cRPMI supplemented with 2-mercaptoethanol and non-essential amino acids. The cells were divided into eppendorfs at 7×10^5 cells in 700µl of supplemented cRPMI and LOS was

added at the desired concentration before mixing. The cells were plated out in a 96 well round bottom plate (Corning, UK) at 2×10^5 cells per well at 1×10^6 cells per ml. The cells were cultured at 37°C with 5% CO_2 for 48 and 72 hours. Following culture, the plates were centrifuged at 400g for 5 minutes and the supernatant collected and stored for further analysis. The cells were resuspended *in-situ* in ice cold FACS buffer containing Fc block diluted 1 in 100 per million cells and incubated on ice for 10 minutes. The cells were then transferred to FACS tubes for further labelling.

2.5.2 Stimulation of bone marrow derived dendritic cells with LOS

Bone marrow derived dendritic cells were generated from C57BL/6 mice. Cells were resuspended to 1×10^7 /ml in cRPMI then transferred to eppendorfs at 1×10^6 /ml in cRPMI. LOS was added to the cells at the appropriate concentration, vortexed then plated out in a 96 well flat bottomed plate (Corning, UK) with 3×10^5 cells in each well. Cells were cultured for 12 hours at 37°C with 5% CO_2 . The supernatant was harvested by centrifuging the plate at 300g for 5 minutes then carefully aspirating 200 μl with a multi-channel pipette. The supernatant was either analysed immediately by ELISA or frozen at -20°C for later analysis. FACS analysis of the cells was carried out by using gentle agitation (pumping the pipette up and down, followed by scraping the well with the tip) to resuspend the cells before transferring them to FACS tubes. Fc receptors were blocked by incubating cells with Fc block (diluted 1:200 per million cells) in 50 μl FACS buffer for 10 minutes at 4°C . Cells were then stained with anti-mouse CD11c biotin and anti-mouse CD40-PE (BD Biosciences, UK) diluted 1:200 per million cells in 50 μl FACS buffer with the appropriate isotype controls (For CD40, Rat IgG2a κ Pe BD Biosciences, UK) and incubated for 15 minutes at 4°C . The cells were washed in 400 μl FACS buffer. The cells were resuspended by flicking the tube and incubated in 50 μl FACS buffer with streptavidin APC (Southern Biotech, USA) diluted 1:200 for 15 minutes at 4°C . The cells were then washed in 400 μl FACS buffer then resuspended in 250 μl FACS buffer.

2.5.3 Quantification of bacteria

C. jejuni were grown and harvested into PBS then heat inactivated. The bacteria were dialysed against dH₂O using 12-14kDa MWCO dialysis tubing. The bacteria were then lyophilised and the dry weight recorded. The lyophilised bacteria were resuspended to 5mg/ml in PBS and a double dilution standard curve was generated comparing the dry weight to the OD600 to generate an equation linking dry weight and optical density at 600nm. For the purposes of estimating the number of bacteria it was assumed the mass of a single bacterium is approximately 1×10^{-12} g (the estimated mass of an *E. coli* cell²⁰⁸) and this value was applied to all the strains being compared.

2.5.4 Stimulation of bone marrow derived dendritic cells with whole *C. jejuni*

Bone marrow derived dendritic cells were generated and prepared as before. 3×10^5 cells were pipetted in 100 μ l of cRPMI into sterile eppendorfs. Heat inactivated *C. jejuni* were defrosted and washed as before. Both strains were diluted to an OD600 of 0.6 in sterile PBS and the quantity of bacteria was estimated using the OD to dry weight formula established above. The bacteria were diluted into cRPMI. The desired ratios of bacteria to dendritic cell was 12:1, 6:1, 3:1 and 1.5:1 and the bacteria were diluted such that the desired number of bacteria for 3×10^5 dendritic cells was present in 200 μ l of cRPMI. The *C. jejuni* were added to the dendritic cells at the diluting titration (200 μ l of bacteria containing cRPMI added to 100 μ l of dendritic cell containing cRPMI making the final concentration of dendritic cells 1×10^6 /ml). The cells were vortexed, then plated out for overnight culture in 96 well flat bottomed tissue culture plates. The supernatant was harvested and stored as before.

2.5.5 Blocking of siglec receptors on bone marrow derived dendritic cells

Bone marrow derived dendritic cells were generated as above. 3×10^5 cells were transferred into eppendorfs at 1×10^7 cells/ml and siglec blocking antibodies (sheep anti-mouse Siglec E, sheep anti-mouse Siglec F and rat anti-mouse Sialoadhesin clones 3D6 and SER-4²⁰⁹) were added at $1 \mu\text{g}$ per million cells. The cells were incubated for 15 minutes on ice then diluted to 1×10^6 cells/ml whereupon LOS was added at $10 \mu\text{g/ml}$. The cells were incubated for 12 hours at 37°C with 5% CO_2 and the supernatant collected for analysis. All blocking antibodies were kind gifts from Prof P Crocker, University of Dundee.

2.5.6 Stimulation of bone marrow derived macrophages with LOS

Bone marrow derived macrophages were generated from C57BL/6 mice as described previously. Cells were resuspended to 1×10^7 /ml in cRPMI then transferred to eppendorfs at 1×10^6 /ml in cRPMI. LOS was added to the cells at the appropriate concentration. The cells were vortexed then plated out in a 96 well flat bottomed plate with 3×10^5 cells in each well. Cells were cultured for 12 hours at 37°C with 5% CO_2 and the supernatant harvested as described for dendritic cells.

2.5.7 Stimulation of bone marrow derived macrophages with whole *C. jejuni*

Bone marrow derived macrophages were generated and prepared as before. The same protocol was used for macrophages as for dendritic cell stimulation by whole bacteria only the bacteria to cell ratios for the diluting titration were 100:1, 50:1, 10:1 and 1:1. The supernatant was harvested and stored as before. For analysis of CD40 upregulation, the macrophages were pulse stimulated with *C. jejuni* at 50:1 bacteria to cell ratio for 15

minutes in eppendorfs while incubated at 37°C with 5% CO₂. The cells were washed with 1.5ml cRPMI by twice centrifuging the tubes at 400g for 5 minutes. The cells were then resuspended to 1x10⁶ per ml and 3x10⁵ were aliquoted into each well in a 96 well round bottom culture plate for overnight culture. The cells were harvested and stained for CD40 upregulation using the same protocol detailed for dendritic cells above only anti-F4/80 antibody was used instead of anti-CD11c.

2.5.8 Stimulation of bone marrow derived dendritic cells and macrophages with exogenous gangliosides and LOS

Bone marrow derived dendritic cells and macrophages were generated from C57BL/6 mice as described previously. Cells were resuspended to 1x10⁷/ml in cRPMI then transferred to eppendorfs at 1x10⁶/ml in cRPMI. The cells were stimulated with PBS, 5µg/ml each of bovine brain derived gangliosides GM1 and GD1a (both from Sigma, UK), 10µg/ml of GB11 wild type LOS, 10µg/ml of GB11 knock out LOS or 10µg/ml of GB11 knock out LOS sonicated with 5µg/ml each of GM1 and GD1a for 5 minutes prior to addition to cells. The gangliosides were prepared by taking 100µl each of GM1 and GD1a (stock was 1mg/ml in 50:50 methanol chloroform) and transferring this to a 15ml falcon tube. The gangliosides were dried by blowing with nitrogen from a compressed gas cylinder (BOC, UK). The gangliosides were then resuspended in 200µl sterile PBS (i.e. still at 1mg/ml) and sonicated and centrifuged repeatedly for 15 minutes. They were then stored in a glass vial until the desired quantity was added to LOS or cells as described above. The cells were vortexed then plated out in a 96 well flat bottomed plate with 3x10⁵ cells in each well. Cells were cultured for 12 hours at 37°C with 5% CO₂ and the supernatant harvested as described for dendritic cells.

2.5.9 Quantification of dead cells by trypan blue exclusion assay

Dendritic cells or macrophages were stimulated overnight with 10µg/ml LOS or PBS as described above. After 200µl of supernatant had been aspirated (leaving 100µl), the plate was placed on ice at 4°C for 15 minutes following which the wells were scraped with a pipette tip to loosen off any adherent cells. 20µl was aspirated from the cells and added to 50µl cRPMI and stored on ice. Shortly before counting, 10µl of trypan blue was added to the cells and a sample transferred to a haemocytometer where the live and dead cells were counted and the percentage of trypan blue positive cells (dead cells) was calculated.

2.6 Analysis of stimulated cells

2.6.1 Preparation and staining of B cells and splenocytes for FACS analysis

Fc receptors were blocked by incubating cells with Fc block (diluted 1:200 per million cells) in 50µl FACS buffer for 10 minutes at 4°C. Cells were then stained with primary fluorophore labelled or biotinylated antibody (diluted 1:200 per million cells) in 50µl FACS buffer and incubated for 15 minutes at 4°C. The cells were washed in 300µl FACS buffer (500g for 5 minutes) and resuspended in 50µl FACS buffer streptavidin conjugated fluorophore (diluted 1:200 per million cells) then incubated for 15 minutes at 4°C. The cells were washed a final time in 500µl FACS buffer then resuspended in 250µl FACS buffer. Immediately before acquisition, counting beads (Caltag laboratories) were added to the tubes according to the manufacturer's instructions. The cells were acquired using a BD FACSCalibur. The data were analysed using FlowJo software (Treestar, USA).

2.6.2 IgG immunoglobulin ELISA

Half area ELISA plates were coated overnight with 50µl of 5µg/ml anti-mouse IgG (Southern Biotech, USA) in sodium carbonate buffer (see appendix 1). The plates were washed three times with 0.3% PBS/Tween then blocked for 1 hour with 100µl of 2% BSA/PBS at room temperature. The plate was washed three times and mouse IgG standard (Bethyl laboratories, USA) was added at 50µl per well starting with 200ng/ml in 0.1% BSA/PBS with doubling dilutions. Supernatant from the splenocyte or B cell cultures was diluted 1:5, 1:10 and 1:20 in 0.1% BSA/PBS and 50µl added to each well. Samples were incubated for 1 hour at room temperature then the plates were washed 3 times. Detection antibody, anti-mouse IgG-HRP, was added (50µl per well, 1:4000 dilution) and incubated for 1 hour. The plate was washed 5 times and 50µl of developing solution was added per well. (1 OPD tablet was added to 14ml Citric acid with 16ml of 0.2M Na₂HPO₄ and 30ml of dH₂O. 20µl of H₂O₂ was added immediately before use). The reaction was stopped using 25µl of 3N H₂SO₄ and the plate was read using a Labsystems Multiscan Ascent plate reader at 490nm within 15 minutes.

2.6.3 IgM Immunoglobulin ELISA

Half area ELISA plates were coated overnight with 50µl of 5µg/ml anti-mouse IgM (Southern Biotech, USA) in sodium carbonate buffer. The plates were washed three times with 0.3% PBS/Tween then blocked for 1 hour with 2% BSA/PBS at room temperature. The plate was washed three times and mouse IgM standard (Bethyl laboratories, USA) was added at 50µl per well starting with 100ng/ml in 0.1% BSA/PBS with 1:3 dilutions. Supernatant from the splenocyte or B cell cultures was diluted 1:250, 1:500 and 1:750 in 0.1% BSA/PBS and 50µl added to each well. Samples were incubated for 1 hour at room temperature then the plates were washed 3 times. Detection antibody, anti-mouse IgM-HRP, was added (50µl per well, 1:4000 dilution) and incubated for 1 hour. The plate was washed 5 times and 50µl of developing solution was

added per well. (1 OPD tablet was added to 14ml Citric acid with 16ml of 0.2M Na₂HPO₄ and 30ml of dH₂O. 20µl of H₂O₂ was added immediately before use.)

2.6.4 Interleukin-10 ELISA

Supernatant from stimulation cultures was assayed using an OptEIA IL-10 ELISA kit (BD Biosciences, UK) as per the manufacturer's instructions except the top standard was extended to 4000pg/ml. The supernatant was either used neat or occasionally had to be diluted 1:2. The plate was developed using Sure Blue TMB solution and read at 450nm in an Ascent Multiscan plate reader.

2.6.5 Interferon Gamma (IFN- γ) ELISA

Supernatant from stimulation cultures was assayed using an OptEIA IFN- γ ELISA kit (BD Biosciences) as per the manufacturer's instructions. Supernatants were used neat and developed as for the IL-10 ELISA.

2.6.6 Interleukin-12 ELISA

Supernatant from stimulation cultures was assayed using an OptEIA IL-12 p70 ELISA kit (BD Biosciences) as per the manufacturer's instructions. Supernatants were used neat and developed as for the IL-10 ELISA.

2.6.7 Tumour Necrosis Factor Alpha (TNF- α) ELISA

Supernatant from stimulation cultures was assayed using an OptEIA TNF- α mono/mono ELISA kit (BD Biosciences) as per the manufacturer's instructions. Supernatants were used neat, 1:10 or 1:20 dilutions, and developed as for the IL-10 ELISA.

2.7 Immunisation of mice with LOS

2.7.1 Injection of mice with LOS

Male C57BL/6 mice aged between 6 and 8 weeks were injected intra-peritoneally with 50µg of GB2 wild type or GB2 CSTII knock out *C. jejuni* LOS in 200µl sterile PBS. Controls included PBS alone, smooth mutant *S. typhimurium* and rough mutant *S. typhimurium* LPS at the same concentration. The mice were sacrificed 18 hours later. The spleens were taken and placed in a 5ml bijoux where they were immersed in Cryo-M-bed (Bright, UK) and transferred to a -80°C freezer.

2.7.2 Immunohistochemical staining of spleen following LOS injection

Spleens from the above mice were cut into 8µm frozen sections using a Bright cryostat (model OTF). The sections were allowed to air dry for two hours and were then permeabilised in ice cold acetone for 10 minutes. After drying, the sections were blocked with 100µl of 5% foetal bovine serum in PBS for 1 hour. The sections were then washed 3 times for 5 minutes in 0.3% PBS/Tween. The sections were stained overnight with antibodies diluted 1:100, 100µl per section. Antibodies used were anti-mouse B220 AlexaFluor 647 (Biolegend, USA) and anti-mouse MOMA-1 FITC. The sections were washed 5 times then mounted using CitiFluor (CitiFluor, UK). Slides were analysed using a Laser Scanning Cytometer (Compucyte) microscope.

2.8 Harvesting and fluorophore labelling of *C. jejuni*

2.8.1 CFSE labelling of bacteria

C. jejuni were grown as before and harvested into sterile PBS. The bacteria were centrifuged at 4500g for 15 minutes, the supernatant discarded and the pellet suspended in PBS. The bacteria were diluted to an OD600 of 1.0 and divided into 10ml aliquots. Stock 5mM CFSE was diluted to 5 μ M in PBS. An equal volume of the 5 μ M CFSE was added to the bacteria and incubated for 30 minutes at 37°C in the dark with regular mixing. The labelled bacteria were transferred to a 65°C water bath and heat inactivated for 1 hour. They were then washed three times with 20ml of sterile PBS by centrifuging at 12,000g for 10 minutes. The concentration of bacteria was standardised between strains using OD600 and then aliquoted to store at -80°C in 10% glycerol. Before use, the aliquots were centrifuged at 13,000g for 5 minutes and the supernatant discarded. The pellet was resuspended and the concentration standardised by OD600.

2.8.2 Quantification of the fluorescence of labelled bacteria

20x10⁶ labelled bacteria were added to 250 μ l FACS buffer and acquired using a BD FACSCalibur flow cytometer. The data were analysed using FlowJo software and the MFI (mean fluorescence intensity) of the fluorophore labelled bacteria was determined. Only those batches where the ganglioside mimicking strain and the control strain exhibited an equal fluorescence were used in phagocytosis experiments. In addition, 20x10⁶ bacteria were centrifuged onto a coated microscope slide using a cytospin (600rpm for 5 minutes) and the bacteria were visualised using a Carl Zeiss Apotome microscope to examine morphology and confirm the fluorescence.

2.8.3 Confirmation CFSE remains bound to bacteria

20x10⁶ CFSE labelled or unlabelled control bacteria were added to 1ml RPMI and incubated for 1 hour at 37°C. The bacteria were removed by twice centrifuging the sample at 12,000g for 10 minutes and aspirating the supernatant. 1x10⁶ mixed mouse splenocytes were then incubated with the supernatant for 30 minutes at 37°C. The cells were centrifuged at 500g for 5 minutes and resuspended in 4% formalin for 10 minutes before being washed and resuspended in FACS buffer. The splenocytes were acquired and the CFSE MFI determined to establish if CFSE had leaked from the labelled bacteria and been taken up by the splenocytes.

2.9 Phagocytosis and cell association of intact bacteria

2.9.1 Association of *C. jejuni* with splenic B cells in the presence or absence of fresh serum

C57BL/6 mice were sacrificed by CO₂ suffocation and a terminal bleed was carried out. The blood was centrifuged at 4000rpm and the serum collected and stored on ice. The spleen was taken and digested using 1ml of cRPMI containing 100µl of DNase and 100µl collagenase (both 10mg/ml) and incubating for 10 minutes at 37°C. A single cell suspension was made and the red cells lysed. The splenocytes were washed and resuspended to 1x10⁷ cells/ml and kept on ice. CFSE labelled GB11 strain *C. jejuni* were defrosted, centrifuged (13,000g for 1 minute) and resuspended in PBS with the OD600 of wild type and CSTII knock out strains matched. The bacteria were then opsonised by adding the bacteria to cRPMI supplemented with 20% fresh homologous mouse serum (taken earlier) at a concentration of 40,000 bacteria per µl. 2x10⁶ splenocytes were transferred into FACS tubes at 1x10⁶/ml in cRPMI supplemented with 5mM NaAzide and 5mM EDTA, and opsonised or non-opsonised wild type or CSTII knock out bacteria were added to the cells at a ratio of 3:1. The cells were vortexed then split into triplicate

tubes before being incubated for 15 minutes at 4°C. The cells were then washed with 3ml of ice cold PBS and, following blocking of Fc receptors, stained for B cells using anti-mouse CD19 APC (Southern Biotech, USA). The cells were analysed using flow cytometry and the percentage of B cells with associated CFSE labelled *C. jejuni* was determined.

Various controls were included to establish the role of complement. The homologous mouse serum was heat inactivated (56°C for 30 minutes) and used for opsonisation and purified exogenous mouse complement (Sigma, UK) was reintroduced (20%) to the heat inactivated serum before opsonisation.

2.9.2 Identification of Sialoadhesin receptor on bone marrow derived macrophages

Bone marrow derived macrophages were grown and harvested as before. The cells were fixed with 4% formalin/PBS then a cytopspin was carried out (450g for 5 minutes). Cells were blocked for 1 hour with 100µl 5% BSA/PBS and 1:100 Fc Block. The slides were then washed once in 0.3% PBS/Tween followed by overnight staining at 1:100 dilution with anti-mouse F4/80 biotin (Biolegend) and anti-mouse MOMA-1 FITC (Serotec, UK). Slides were then washed 3 times before incubating the anti-F4/80 samples with streptavidin Alexa 647 (1:100 dilution) for 1 hour then washed a further 5 times. The slides were mounted using DAPI containing Vectashield and analysed using a laser scanning confocal microscope.

2.9.3 Bone marrow derived macrophage phagocytosis of *C. jejuni*

Bone marrow derived macrophages were grown and harvested as before. Complete RPMI supplemented with Ultra-low IgG foetal bovine serum (Invitrogen, UK) was used at all steps to exclude the possibility of natural Ig affecting phagocytosis. FACS tubes

were labelled for each time point (0, 15, 30 and 60 minutes) and for cells cultured at 37°C and control tubes cultured at 4°C. The cells were resuspended to 1×10^7 per ml and 300,000 cells were transferred into the FACS tubes and kept on ice. CFSE labelled GB11 wild type and CSTII knock out *C. jejuni* were defrosted, centrifuged and resuspended to remove bacterial debris. The OD600 of both strains were matched. *C. jejuni* were diluted in cRPMI then added to the macrophages at a 20:1 ratio so that the final concentration of macrophages was 1×10^6 cells/ml. The cRPMI used in the 4°C control tubes was supplemented with 5mM NaAzide. All tubes were vortexed thoroughly. The 37°C tubes were transferred to an incubator and cultured at 37°C with 5% CO₂, with mixing every ten minutes, for the desired time before being washed with 3ml ice cold PBS with 5mM NaAzide. The cells were stained as for previous FACS analysis using anti-mouse F/480 biotin and streptavidin APC. For analysis, F4/80⁺ cells were gated and the MFI of these cells (representing phagocytosed CFSE labelled bacteria) was determined. The MFI of the 4°C, NaAzide cultured controls was subtracted from the 37°C cultured cells for each time point. The residual sample following FACS analysis was deposited on slides (Superfrost plus, VWR) using a cytospin (450g for 5 minutes) and visualised using an Apotome microscope to confirm the intracellular location of the bacteria.

2.9.4 Inhibition of bone marrow derived macrophage phagocytosis

Bone marrow derived macrophage phagocytosis of *C. jejuni* was carried out as above and cells were analysed at a single 40 minute time point. Prior to addition of the bacteria, the macrophages were incubated with 0.3µg each of Sialoadhesin blocking antibodies SER-4 and 3D6 per million cells for 15 minutes at 4°C. CFSE labelled GB11 wild type and GB11 CSTII knock out *C. jejuni* were added to the cells at a 10:1 ratio and the amount of phagocytosis with and without Sialoadhesin blocking antibody was determined as before. In order to confirm that Sialoadhesin was the only receptor mediating enhanced uptake of the ganglioside mimicking *C. jejuni* strain, a titration of Sialoadhesin blocking antibodies was used ranging from 0 to 0.5µg of SER-4 and 3D6 per million macrophages. In

addition, some cells were incubated with an isotype control antibody for the blocking antibodies at 1µg/million cells before the bacteria were added.

2.9.5 Injection and tracking of labelled *C. jejuni*

Age and sex matched C57BL/6 mice were injected i.v. with 200µl of heat inactivated, CFSE labelled, GB2 wild type and knock out *C. jejuni* diluted to an OD600 of 0.6 in PBS. 200µl of PBS i.v was used as a control. The mice were sacrificed after 1 or 3 hours by CO₂ anaesthesia and harvested for spleen, blood, lymph nodes and liver. For Immunohistology studies, the tissues were transferred to filter paper and deposited on a drop of Cryo-M-bed media then placed in small metal containers and rapidly frozen using liquid nitrogen. They were then stored at -80°C. For FACS studies, the spleens were homogenised to a single cell suspension. Briefly, cell strainers were first wet with 1ml PBS then the spleen tissue was mashed through using a syringe plunger before the strainer was washed with 4ml PBS. The tissue was immediately lightly fixed using 1% paraformaldehyde for 15 minutes before labelling.

2.9.6 Immunohistology of splenic sections

Sections were cut to 8µm thickness using a cryostat and allowed to dry before being stored at -80°C. Following defrosting, the sections were permeabilised with acetone for 10 minutes, air dried and washed with PBS/tween for 10 minutes. Sections were blocked with 10% normal goat serum in PBS/1%BSA for 1 hour. For metallophilic macrophage staining supernatant from a clone producing MOMA1 antibody directed against the Sialoadhesin antigen was used. The MOMA1 clone is Rat IgG2a and the supernatant was kindly gifted by Dr P Leenen, Dept of Immunology, Erasmus MC, the Netherlands. The supernatant was diluted 1:4 in PBS with 1% BSA and 300µl/slide was used for 1 hour at room temperature (control sections were incubated with 1%BSA/PBS alone). Slides were washed for 1 minute then 10 minutes in PBS/tween. The secondary antibody was

goat anti-rat IgG TRITC (Southern Biotech, USA) and was diluted 1:200 as before. Each slide was incubated with 300µl for 1 hour at room temperature. The slides were washed as before. The sections were blocked with 1% normal rat serum before the anti-B220 AlexaFluor 647 antibody was added diluted 1:75 in 1% normal mouse serum (250µl/slide). Slides were washed as before then mounted using CitiFluor mounting medium.

For marginal zone macrophage staining, supernatant from a hybridoma producing an ER TR-9 antibody was used. The ER TR-9 antibody is rat IgM and is directed against the marginal zone macrophage marker SIGN R1. The supernatant was a kind gift from Dr P Leenen, Dept of Immunology, Erasmus MC, the Netherlands. The protocol was the same as above only the supernatant was used at a 1:2 dilution and the secondary antibody was goat anti-rat IgM TRITC (Southern Biotech), used at 1:200 dilution.

Sections were analysed using an Apotome/Zeiss microscope and Axiovision software with the co-localisation module. For co-localisation studies, two sections were cut from each spleen and three follicles in each section were analysed.

2.9.7 FACS analysis of spleen following bacterial injections

Age and sex matched C57BL/6 mice were separated into three groups of three and injected with bacteria as before. After 1 hour the mice were sacrificed by CO₂ suffocation and the spleens were harvested. A single cell suspension was made and the cells were briefly fixed in 1% paraformaldehyde for 15 minutes then kept at 4°C. Collagenase was not used and cells were fixed in paraformaldehyde because pilot studies had shown that the cells have to be analysed very rapidly following harvesting in order to detect the bacteria. The cells were counted and resuspended to 10x10⁶/ml in FACS buffer. 1 million cells were transferred to each FACS tube and the cells were blocked with 50µl of Fc block diluted 1:200. To facilitate better compensation of fluorophores,

each cell population was studied in two colour flow cytometry, that is, *C. jejuni* in FL1 and the cell identifying antibody in FL4. F4/80 biotin, CD11c biotin, GR1 APC and their respective isotype controls were used at 50µl of 1:100 dilution. CD19 APC (Southern Biotech, USA) was used at 1:200 dilution. MOMA1 supernatant was used at 1:4 dilution (secondary antibody alone served as the isotype control for MOMA1). Following a 45 minute incubation the cells were washed and, where appropriate, 50µl of streptavidin APC was added at 1:200 dilution. For the cells labelled with MOMA1, an anti-rat IgG2a biotin was added at 1:200 dilution. After a half hour incubation, the cells were washed and resuspended to 250µl for analysis (a final staining step was carried out on the MOMA1 cells using streptavidin APC as before).

Figure 1: Structure of *E. coli* LPS and *C. jejuni* LOS.

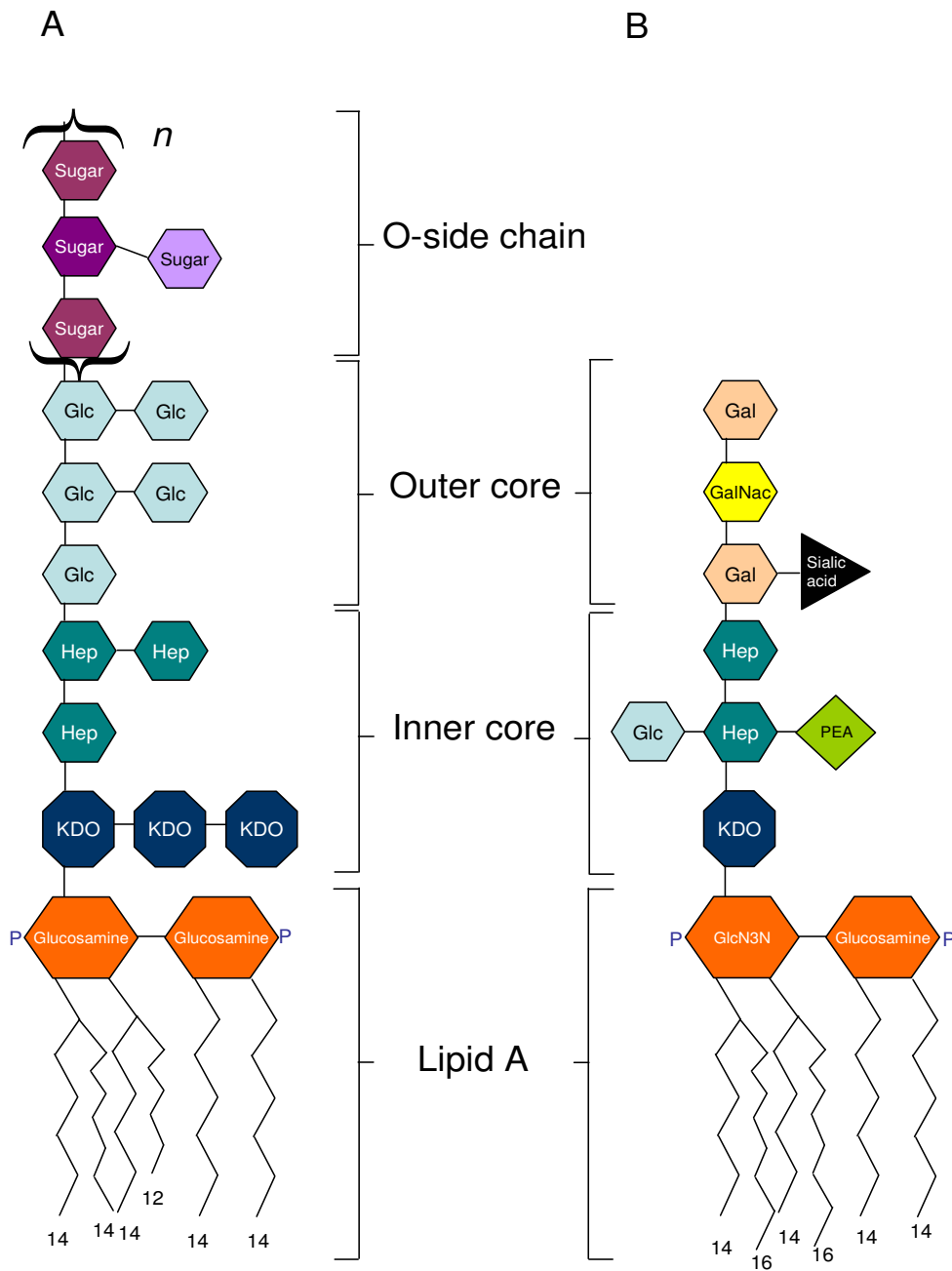


Figure 1. Diagrammatic representation of A) *E. coli* LPS and B) *C. jejuni* LOS (mimicking ganglioside GM1). KDO – 3-deoxy-D-manno-octulosonic acid; HGlcN3N - 2,3-diamino-2,3-dideoxy-D-glucose; Hep - L-glycero-D-manno heptose; Glc – glucose; PEA – phosphorylethanolamine; Gal – galactose; GalNac - N-acetylglucosamine and P – phosphate. Numbers represent length of acyl chain.

3 Isolation and purification of *C. jejuni* LOS

3.1 Introduction

The aims of the experiments presented in this chapter are to purify LOS from *C. jejuni*, eliminate contamination, confirm ganglioside mimicry and accurately quantify the LOS. This will allow us to address one of the central hypotheses of the thesis; that the ganglioside mimicking epitopes found on the LOS molecules of GBS associated strains of *C. jejuni* alter the immunostimulatory properties of the LOS.

Bacterial LPS is found in the outer membrane of gram negative bacteria¹⁰². LPS is a glycolipid molecule that is classically considered as three covalently linked sections^{103,104}: the hydrophobic Lipid A, the core oligosaccharide and the hydrophilic antigenic O-side chain. The Lipid A usually consists of a diglucosamine backbone with attached fatty acyl chains which show inter- and intra-species variability in length and substitution. Lipid A determines endotoxicity^{102,111,210,211}. The inner core oligosaccharide contains bacterial specific sugars such as 3-deoxy-D-manno-octulosonic acid (KDO), while the outer core contains hexoses and hexosamines. The O-side chain consists of repeating saccharide units¹⁰². GBS associated *C. jejuni* synthesise a truncated O-side chain. The resultant molecule, which is essentially Lipid A with attached core sugars, is termed lipo-oligosaccharide (LOS). Figure 1(A) illustrates the structure of a “smooth” mutant *E. coli* LPS with an extended O-side chain and figure 1(B) shows a “rough” mutant *C. jejuni* LOS with a truncated O-side chain.

Figure 2: Structures of HS O:19 and HS O:3 *C. jejuni* LOS.

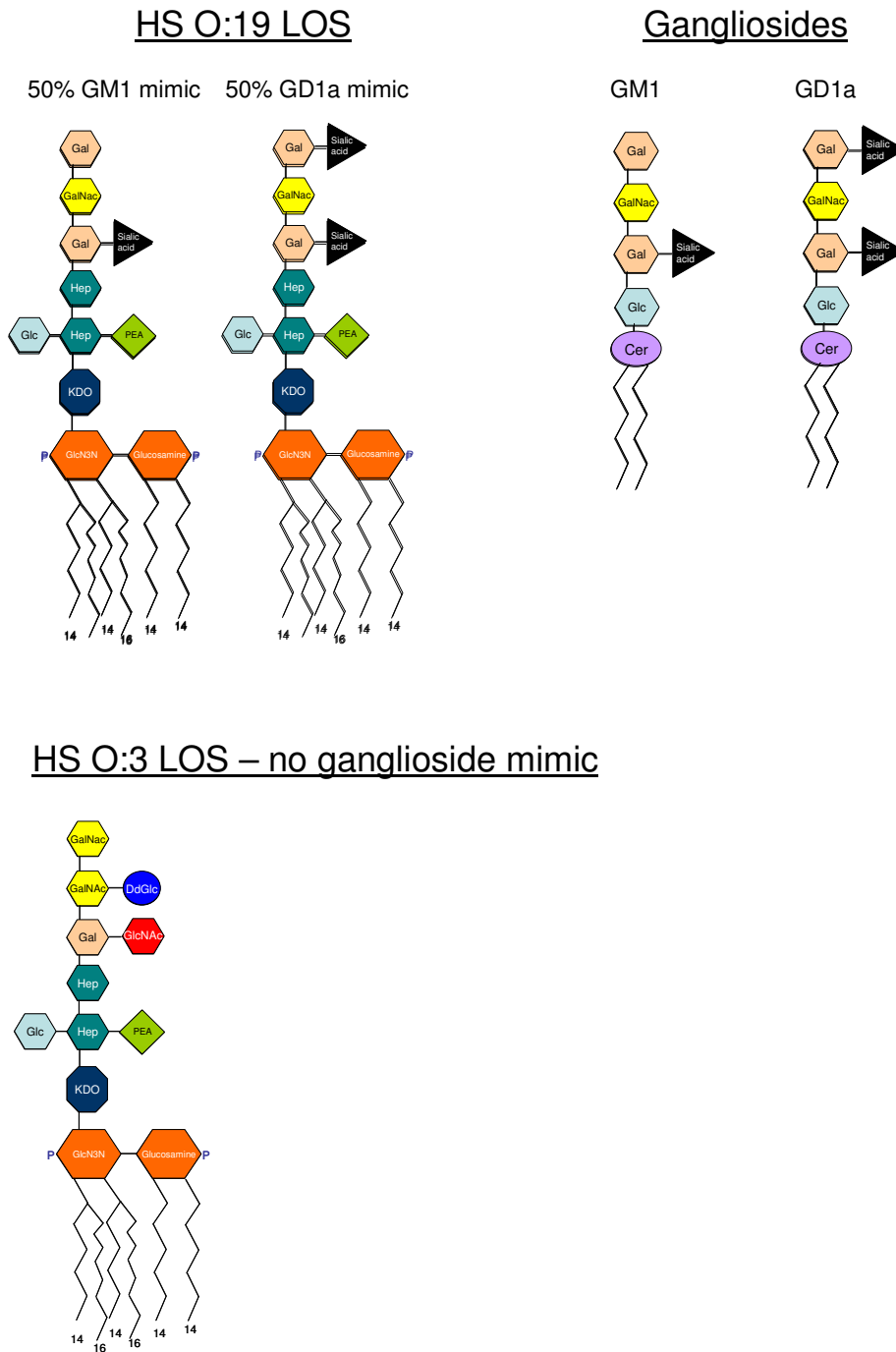
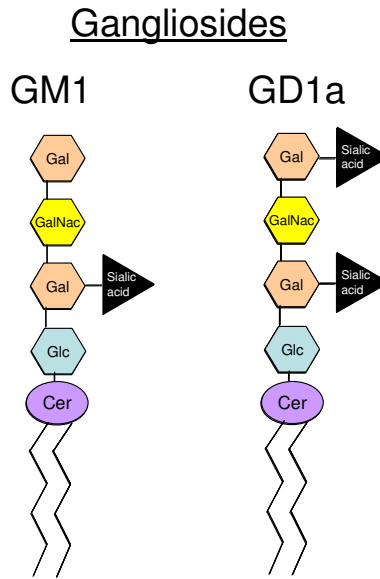


Figure 2. Diagrammatic representation of the LOS structures of the ganglioside mimicking *C. jejuni* strain HS O:19 and non-mimicking strain HS O:3. HS O:19 produces GM1 and GD1a mimicking LOS in equimolar amounts. KDO – 3-deoxy-D-manno-octulosonic acid; HGlcN3N - 2,3-diamino-2,3-dideoxy-D-glucose; Hep - L-glycero-D-manno heptose; Glc – glucose; PEA – phosphorylethanolamine; Gal – galactose; GalNac - N-acetylgalactosamine, P – phosphate, Cer – ceramide, GlcNac – N-acetylglucosamine and DdGlc – dideoxyglucose.

The initial experiments described in this chapter use two strains of *C. jejuni* from the clinical bacteriology departmental collection of *C. jejuni* at the Southern General Hospital, Glasgow. HS O:19 is a GBS associated strain in which the LOS molecules mimic gangliosides GM1 and GD1a at a 50:50 ratio²⁰² while HS O:3 is not associated with GBS and does not mimic gangliosides²⁰³. Both LOS structures are illustrated in figure 2.

For later experiments, through collaboration with Erasmus University, Rotterdam, additional useful strains of *C. jejuni* were used and were supplied as both the parent organism (GB11 and GB2 wild type and CSTII knock out) and as purified LOS (GB11, GB2 and GB19 wild type and CSTII knock out)¹⁰¹. GB11 and GB2 both mimic gangliosides GM1 and GD1a in equimolar amounts. Isogenic knock-out mutants were created lacking the sialyltransferase gene (CSTII) which attaches sialic acid to the core sugars. These strains produce three asialo-sugars as part of their internal core sugar (structures illustrated in figures 3 (A) and 3 (B)) and do not mimic gangliosides. At least two of their core sugars mimic other self glycolipids. Importantly, within the isogenic strains, all other structures in the bacteria and LOS (including Lipid A) are predicted to be identical. GB19 (as distinct from HS O:19) mimics ganglioside GD1c and no information is available about the structure of the CSTII knock out mutant.

Figure 3(A): Structures of GB2 and GB11 wild type *C. jejuni* LOS.



C. jejuni LOS from GB2 and GB11 Wild Type strains

50% GM1 mimic 50% GD1a mimic

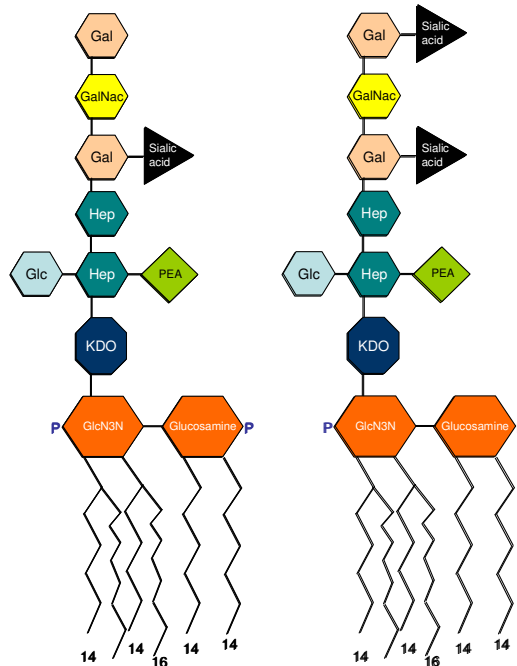


Figure 3 (A). Diagrammatic representation of the structures of the LOS molecules purified from the GB2 and GB11 wild type strains of *C. jejuni* as well as the gangliosides that they mimic. Each LOS molecule is produced by the bacteria in equimolar amounts (i.e. 50:50 ratio). KDO – 3-deoxy-D-manno-octulosonic acid; HGlcN3N - 2,3-diamino-2,3-dideoxy-D-glucose; Hep - L-glycero-D-manno heptose; Glc – glucose; PEA – phosphorylethanolamine; Gal – galactose; GalNac - N-acetylgalactosamine, P – phosphate, Cer – ceramide.

Figure 3(B): Structures of GB2 and GB11 CSTII knock out *C. jejuni* LOS.

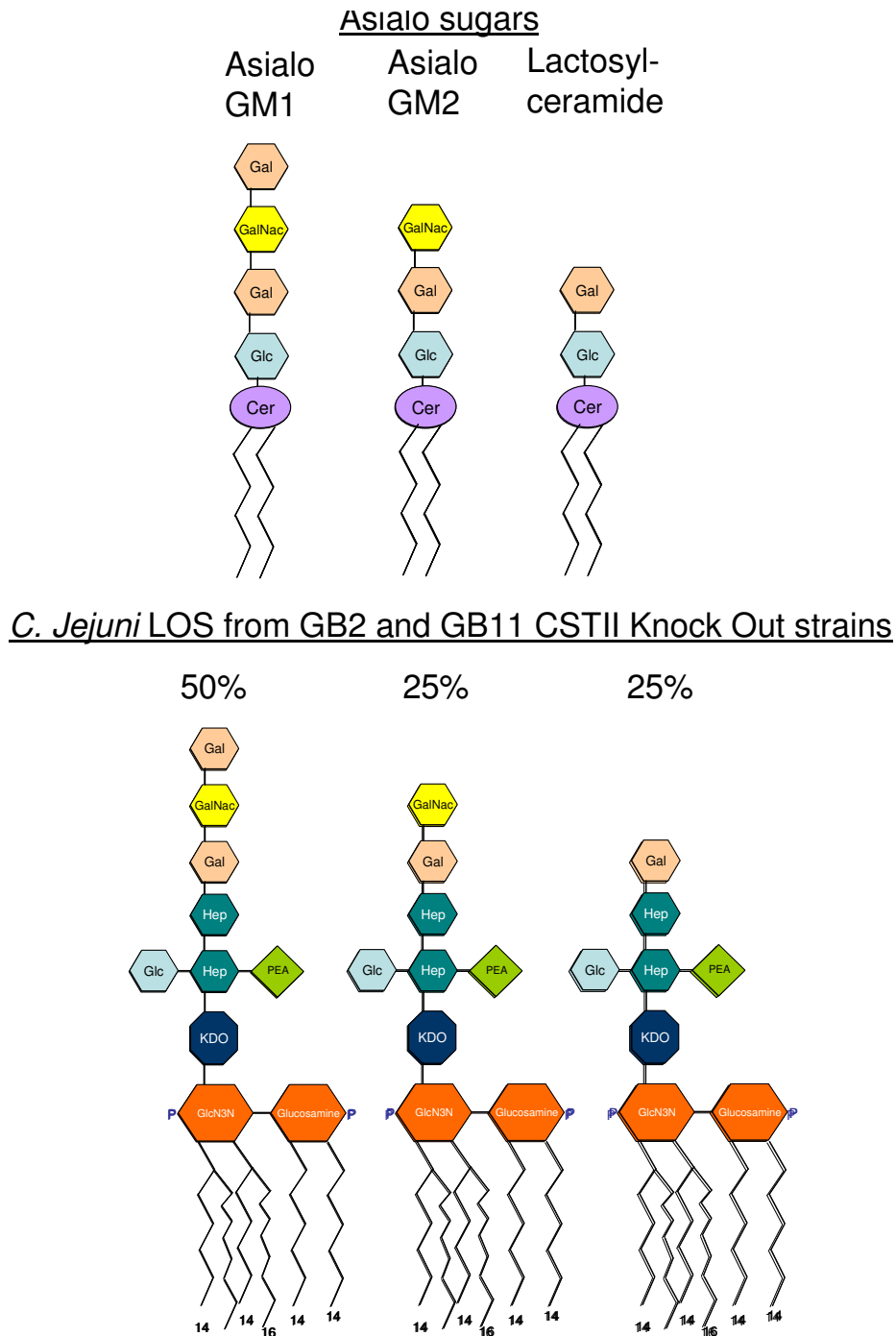


Figure 3 (B). Diagrammatic representation of the structures of the LOS molecules purified from the GB2 and GB11 CSTII knock out strains of *C. jejuni* as well as the asialo-sugars that they mimic. Percentages indicate the proportion of each LOS molecule produced by the bacteria. KDO – 3-deoxy-D-manno-octulosonic acid; HGlcN3N - 2,3-diamino-2,3-dideoxy-D-glucose; Hep - L-glycero-D-manno heptose; Glc – glucose; PEA – phosphorylethanolamine; Gal – galactose; GalNac - N-acetylgalactosamine, P – phosphate, Cer – ceramide.

Figure 4: Silver stain analysis of hot phenol extracted LOS.

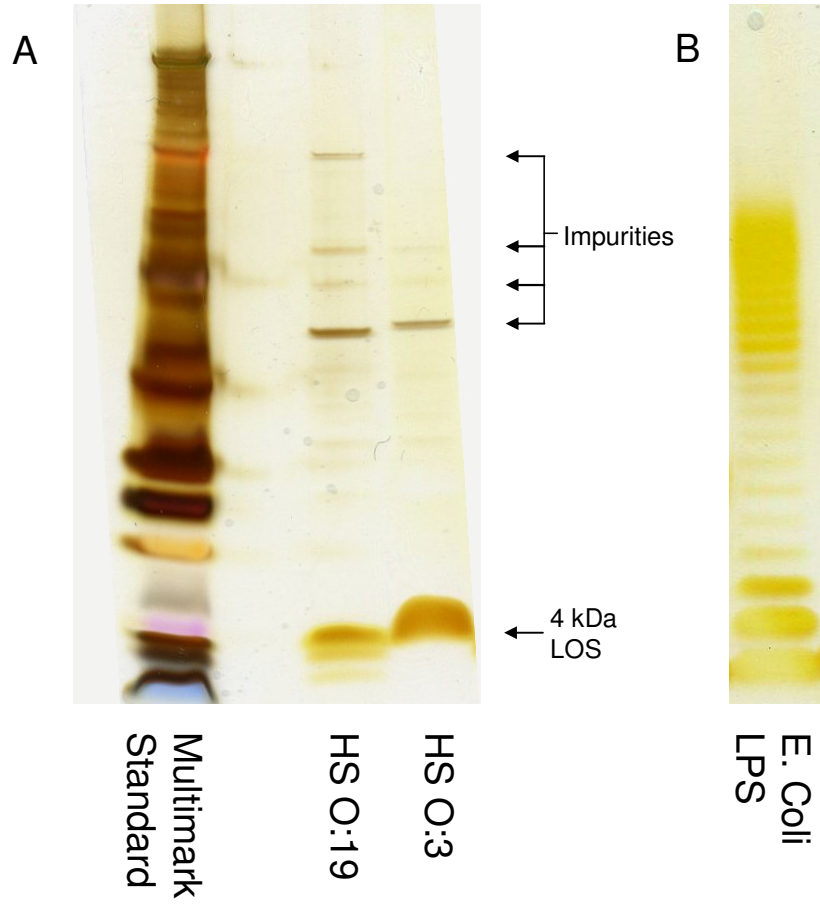


Figure 4. SDS-PAGE and silver stain of hot phenol extracted LOS. (A) *C. jejuni* LOS. (B) Smooth mutant *E. coli* LPS. Each lane contained 5 μ g of LOS (the blank spacer lane contained dH₂O).

3.2 Results

3.2.1 Hot phenol extraction of *C. Jejuni* LOS and assessment of purity

C. jejuni were grown for 48 hours at 37°C in a microaerobic environment on Columbia Agar and Horse Blood plates, harvested into PBS and heat inactivated at 60°C for 1 hour. These bacteria were used as a source for LOS which was extracted using the hot-phenol-water technique. The resultant product was analysed by SDS-PAGE and silver stain to assess purity and mass.

Figure 4 (A) shows that there are distinct high molecular weight bands in the silver stain of the LOS which indicates contamination (the spacer lane with dH₂O shows no such contamination). This contamination is likely to be protein or nucleic acids²¹²⁻²¹⁴. There is a distinct band at 4kDa which is the expected mass of LOS. Figure 4 (B) shows a silver stain of smooth mutant *E. coli* LPS demonstrating the ladder pattern produced by LPS molecules with differing lengths of O-side chain which contrasts with the single mass of rough mutant LOS.

Figure 5: Photograph of LOS solution following enzyme treatment.

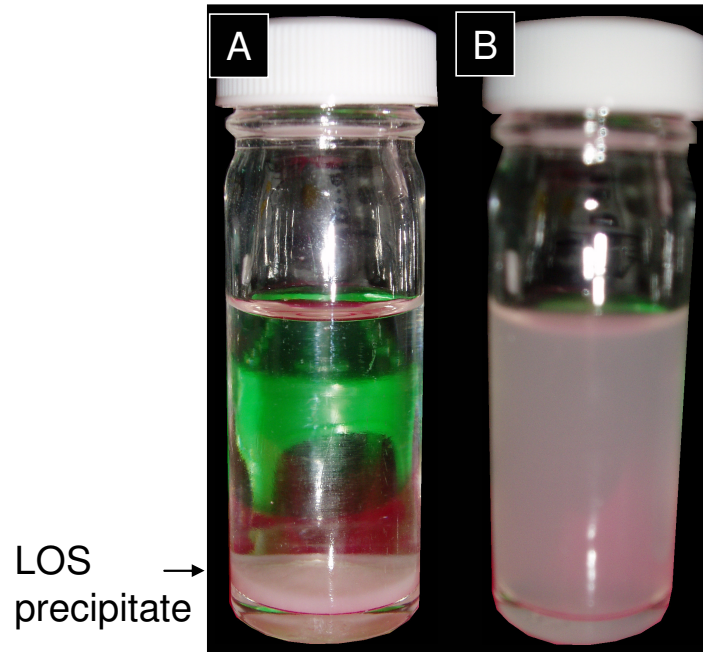


Figure 5. Photographs of LOS purified in enzyme buffer using DNase, RNase, lysozyme and Proteinase K. (A) Photograph of the settled precipitate. (B) Photograph the opaque colloid solution after agitation.

3.2.2 Purification of hot phenol extracted LOS

To obtain a purified sample of LOS it was necessary to remove the contaminating DNA/RNA, glycolipids and protein. To do this hot phenol extracted LOS was treated with DNase, RNase, lysozyme and Proteinase K.

LOS was resuspended in enzyme buffer (0.1M TrisHCL, 5mM CaCl₂ and 5mM MgCl₂, pH 7.5) and the enzymes added sequentially. The enzyme buffer was derived from LPS purification protocols²¹⁵ using suggested cation concentrations from the enzyme product data sheets. Although the LOS solution was initially clear, the addition of lysozyme caused a precipitate to form which came out of suspension and settled in the universal. Figure 5 (A) and 5 (B) show photographs of the LOS solution containing the settled precipitate and the precipitate in a colloid suspension following vortexing.

Figure 6: Silver stain analysis of LOS precipitate.

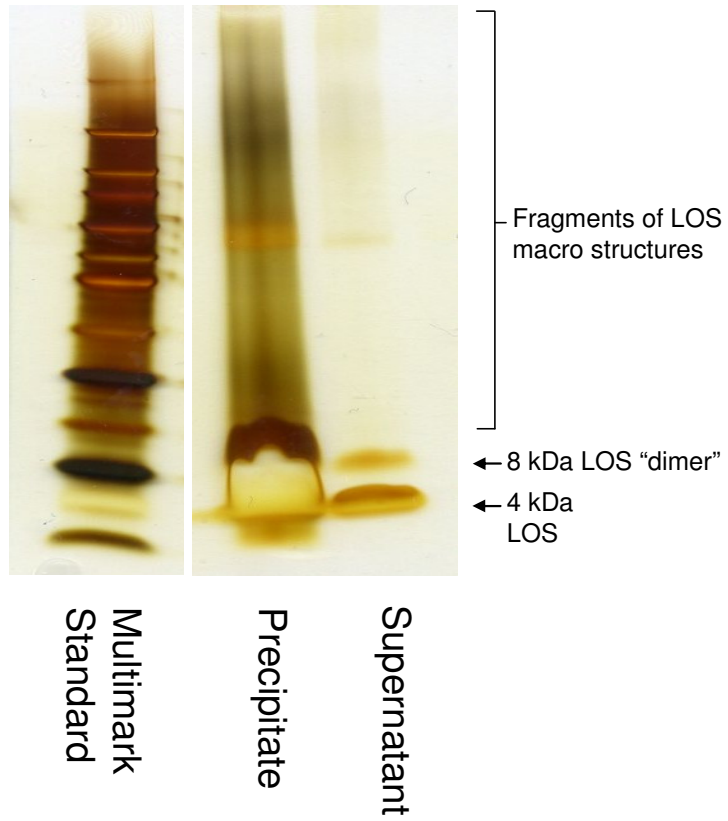


Figure 6. SDS-PAGE and silver stain of HS O:3 LOS precipitate and supernatant. The precipitate shows a continuous smear with no distinct bands. The clear supernatant resolves into two distinct bands, one of which is double the mass of the other.

3.2.3 Assessment of purity and determination of the nature of the precipitate

SDS-PAGE and silver staining was used to analyse the precipitate and the supernatant (5µg of each). Figure 6 shows that the precipitate consists of a continuous smear of material with the staining characteristics of LOS and that there are no distinct bands of contamination like those seen in figure 4 (A). The supernatant also contains LOS although it resolves into two bands, one at 8kDa and one at 4kDa.

The two bands produced by the supernatant in lane 3 were interpreted to represent single LOS molecules (4kDa) and LOS “dimers” (8kDa). These dimers probably consist of two LOS molecules held together, tail to tail, by hydrophobic interactions (illustrated in figure 16 (B)).

In order to test this hypothesis, HS O:19 LOS was subjected to SDS-PAGE and Western blotting. HS O:19 produces two LOS molecules in equimolar amounts, one mimicking ganglioside GM1 and the other mimicking ganglioside GD1a. The Western blot was labelled using cholera toxin (to identify GM1) and MOG35 monoclonal antibody (to identify GD1a).

Figure 7: Western blot analysis of ganglioside mimicking LOS epitopes.

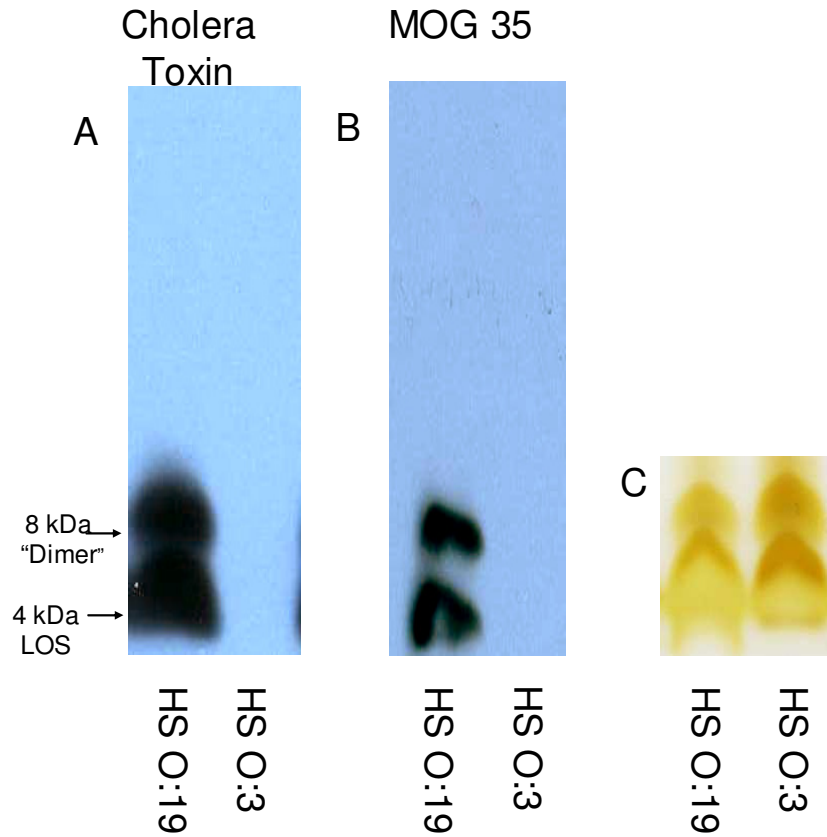


Figure 7. SDS-PAGE, Western blot and silver stain of HS O:19 and HS O:3 LOS demonstrating ganglioside epitopes. (A) Labelled with cholera toxin (binding GM1 epitope) and (B) Labelled with MOG35 mAb (binding GD1a epitope). (C) Loading control showing a silver stain of a gel run in parallel to (A) and (B).

The Western blot in Figure 7 shows that both epitopes (GM1 and GD1a) are present in both the 4kDa and 8kDa bands. This is consistent with LOS dimers being responsible for the 8kDa band. In addition, the HS O:3 strain only produces a single LOS species and yet silver staining resolves into two bands (figure 6) consistent with an LOS homodimer.

The continuous smear produced by the precipitate was interpreted to represent incompletely fragmented lamellar LOS macro-structures. Such structures form in solution as a consequence of the amphipathic nature of LOS. They are held together by lateral electrostatic interactions and bilayer hydrophobic interactions (illustrated in figure 16 (A)). The smear indicates that they were incompletely separated by the electrophoresis process.

Figure 8: Silver stain analysis of LOS following micelle dispersal.

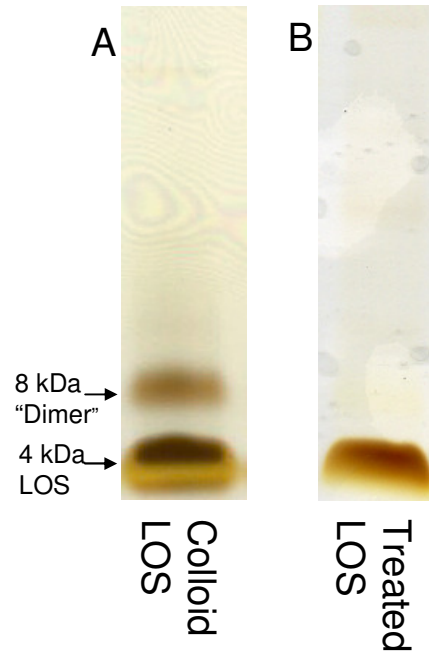


Figure 8. SDS-PAGE and silver stain of HS O:3 LOS or HS O:3 LOS treated with EDTA and Triton X detergent. (A) LOS prior to treatment. (B) The same LOS sample after treatment.

3.2.4 Control of macro-molecular structures

Macro-molecular structures, such as micelles and lamellar sheets, can potentially influence LPS activity and so it was decided to regulate their formation.

Eliminating lysozyme from the protocol prevented the formation of the settled precipitate. However, the LOS continued to form a stable opaque colloidal solution which resolved into double bands following SDS-PAGE and silver stain (figure 8 (A)). The opaque appearance of the solution and the dual band on silver stain were interpreted to represent continued aggregation into macro-molecular structures.

LOS was subjected to treatment to disperse the macromolecular structures. This was done by altering the pH (titration of NaOH), removing cations (addition of EDTA) or adding detergents. A combination of treatments (EDTA with Triton X detergent) caused a visual dispersal of the colloid solution. SDS-PAGE and silver stain of the treated LOS (figure 8, (B)) shows that it resolves into a single band of approximately 4kDa. The LOS solution in figure 8 (A) was an opaque colloid solution while the solution in figure 8 (B) was clear. This confirms that double bands seen by silver stain correspond with macro-molecular structures in the LOS and that these are visible as an opaque colloid solution. The clarification of the solution allowed spectrophotometry to be carried out on the LOS and no DNA, RNA or protein was detected.

Figure 9: Western blot analysis of LOS epitopes following neuraminidase treatment.

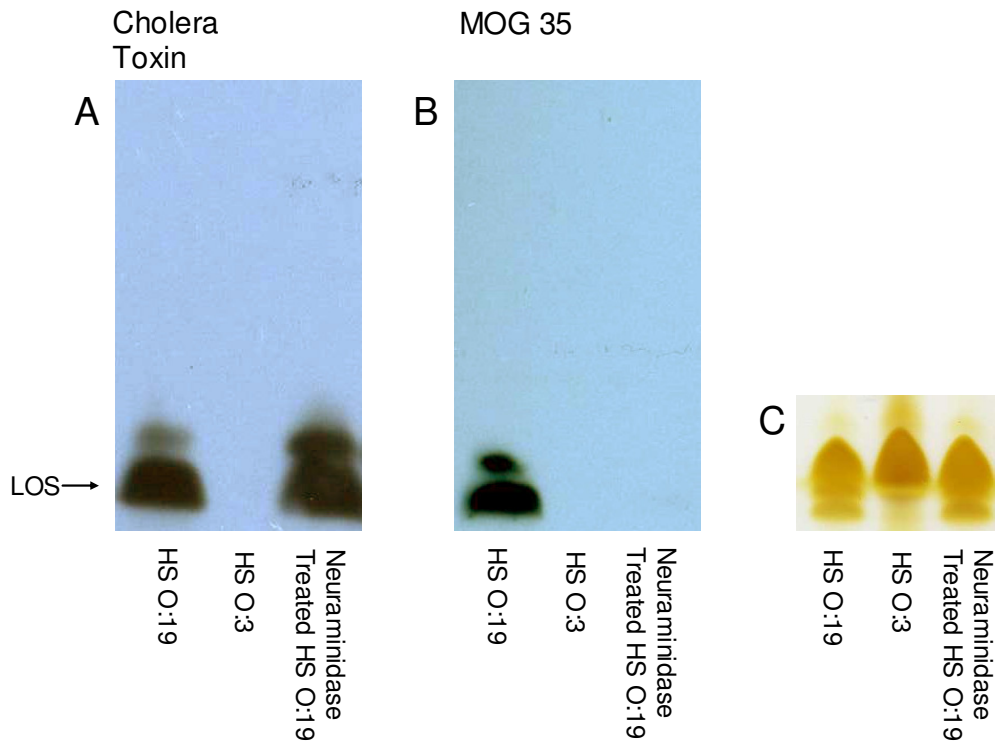


Figure 9. SDS-PAGE, Western blot and silver stain of HS O:19, HS O:3 and neuraminidase treated HS O:19 LOS demonstrating ganglioside mimicking epitopes. (A) Shows all three strains incubated with cholera toxin (binds GM1 epitope). (B) Shows all three strains incubated with MOG35 mAb (binds GD1a epitope). Cholera toxin labels HS O:19 and neuraminidase treated HS O:19 while MOG35 only labels HS O:19. (C) Loading control showing a silver stain of a gel run in parallel to the gels used in (A) and (B). (These samples had not been pre-treated with detergent/EDTA).

3.2.5 Generation of a control strain of LOS and confirmation of ganglioside mimicking epitopes

Intra-species differences in the structure of LOS Lipid A may alter LOS potency. HS O:19 LOS was treated with cholera neuraminidase to remove sialic acid and provide a control strain with an identical Lipid A but without ganglioside mimicry.

A Western blot was carried out, using cholera toxin and MOG35, in order to confirm the ganglioside mimicry of HS O:19, the non-mimicry of the neuraminidase treated HS O:19 and the non-mimicry of HS O:3. Figure 9 (A) and (B) confirms that HS O:19 LOS mimics ganglioside GM1 and GD1a respectively. HS O:3 LOS does not mimic either of these gangliosides. However, neuraminidase treated HS O:19 LOS continues to mimic GM1 (figure 9(A)) but no longer mimics GD1a (figure 9(B)).

Figure 10: Silver stain analysis of enzyme purified LOS.

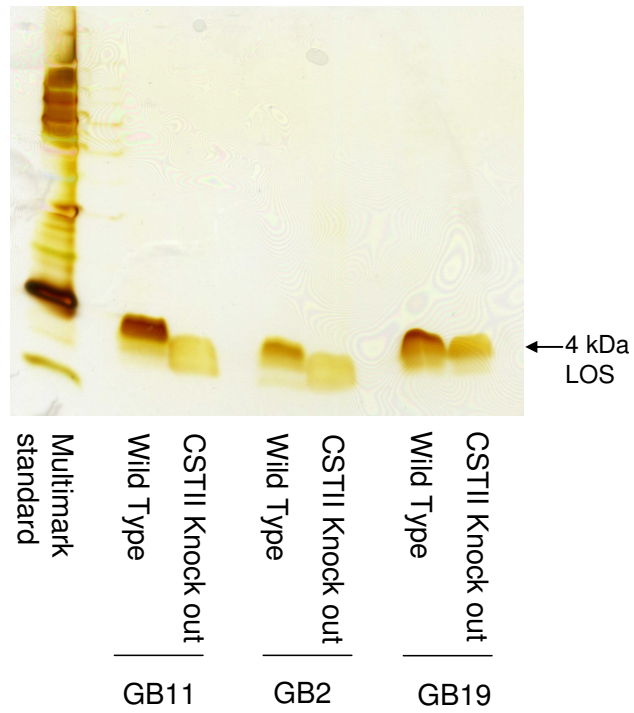


Figure 10. SDS-PAGE and silver stain of new strains of LOS, purified in Milli-Q. 5 μ g of LOS loaded per well.

3.2.6 Isolation and purification of GB11 wild type, GB11 CSTII knock out, GB2 wild type and GB2 CSTII knock out LOS

New strains of *C. jejuni* were provided by collaborators as both the parent organism and as pre-purified LOS. Isolation and purification was done using an identical protocol with the exception that Milli-Q distilled and deionised H₂O was used at all steps of the procedure in place of enzyme buffer. Silver stain was carried out on the LOS to establish if the new protocol successfully removed impurities. Figure 10 shows that there is no evidence of impurities using silver stain, indicating that the purification enzymes remained active in the absence of calcium and magnesium. In addition, the LOS formed a clear solution and resolved primarily into a single band. All subsequent purifications used this protocol.

Figure 11: Alcian blue and silver stain analysis of purified LOS and whole cell lysate.

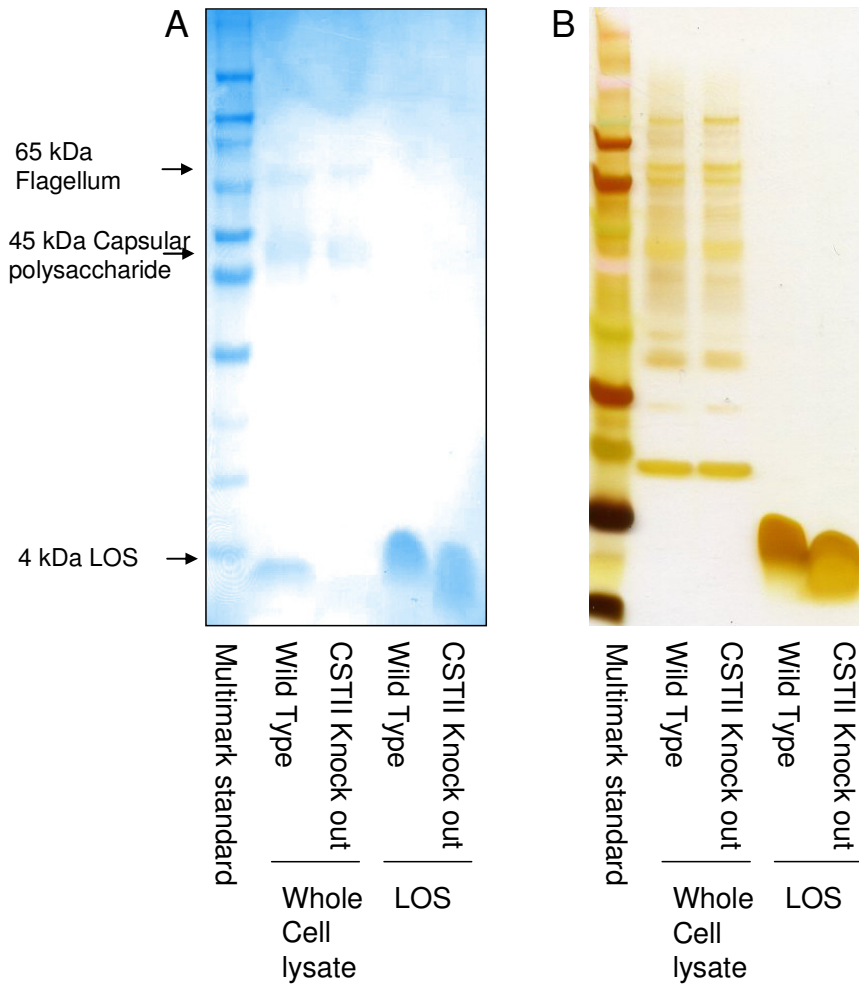


Figure 11. SDS-PAGE with alcian blue and silver stain of a whole cell lysate of GB2 *C. jejuni* and purified GB2 LOS (5 μ g of each). (A) Shows alcian blue stain and (B) shows silver stain.

3.2.7 Detection of capsular polysaccharide contamination

Capsular polysaccharide (CPS) is a glycolipid molecule with similar chemical properties to LOS and LPS. Although steps were taken to eliminate nucleic acid and protein contamination, no precautions had been taken to eliminate CPS. CPS can potentially signal through TLR2²¹⁶ which would result in inaccurate measurements of LOS potency. LOS was tested for CPS contamination using an alcian blue stain. A positive control was generated using whole cell *C. jejuni* lysate. Figure 11(A) shows the alcian blue stain of the LOS and whole cell lysate and figure 11(B) shows the silver stain. In the lanes containing cell lysate, there is a faint band of alcian blue staining at 45kDa which is the reported mass of *C. jejuni* CPS²¹⁷. There are additional bands at 65kDa (consistent with flagellum) and 4kDa (consistent with LOS). In the lanes containing purified LOS there is a single LOS band at 4kDa. No contaminating CPS is detected in the purified LOS.

Figure 12: Western blot analysis of gangliosides mimicry by GB11 and GB2 LOS.

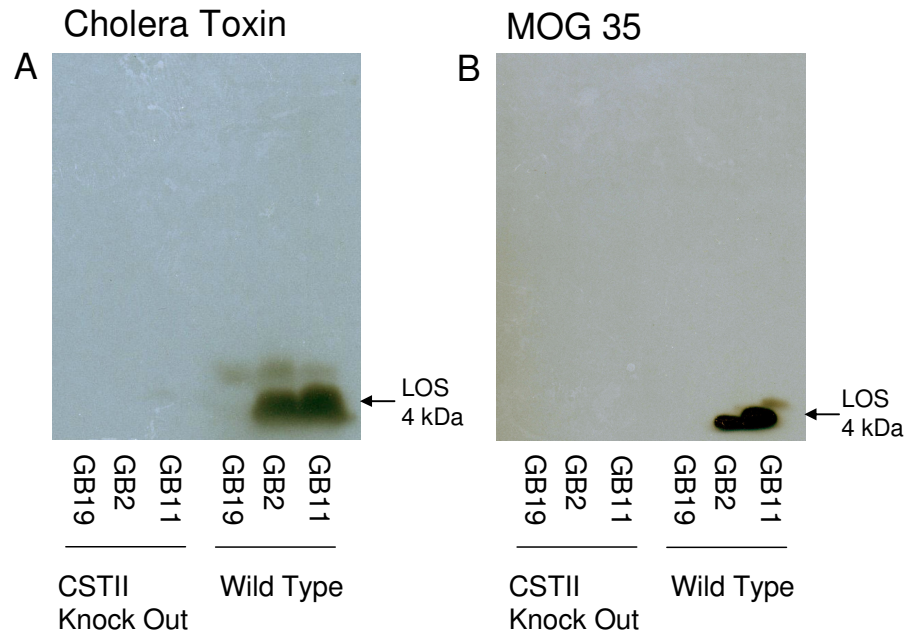


Figure 12. SDS-PAGE and Western blot of GB11 and GB2 strains of LOS demonstrating ganglioside mimicry. 5 μ g of LOS was used in each well. (A) shows membrane incubated with cholera toxin (specific for GM1 epitope) and (B) membrane incubated with MOG35 mAb (specific for GD1a epitope).

3.2.8 Confirmation of GM1 and GD1a epitopes on GB11 and GB2 wild type LOS.

GB11 and GB2 wild type LOS are reported to mimic gangliosides GM1 and GD1a at a 50:50 ratio. SDS-PAGE and Western blot was carried out to confirm the ganglioside mimicry. Figure 12 shows that GB11 and GB2 wild type LOS mimic gangliosides GM1 and GD1a and that the CSTII knock out LOS strains do not mimic these gangliosides. GB19 LOS is reported to mimic GD1c and as expected does not label with cholera toxin or MOG35. The Western blot also confirms that the LOS resolves primarily into a single 4kDa band although very weak labelling was present at 8kDa.

Figure 13: LOS concentration determined by thiobarbituric acid assay.

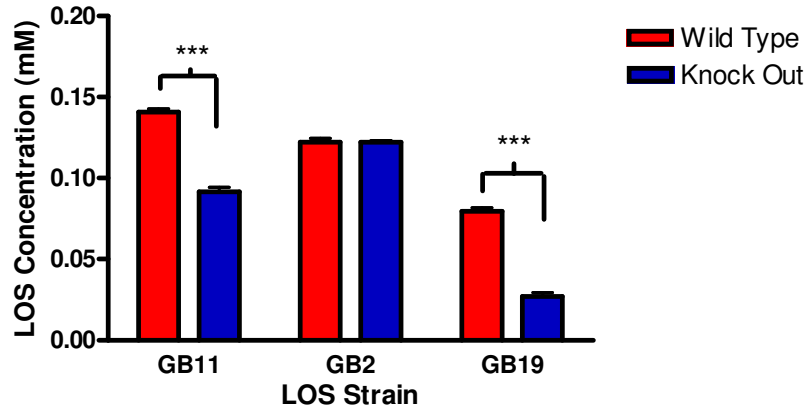


Figure 13. Concentration of LOS determined using the thiobarbituric acid assay. There is a significant difference in LOS concentration ($p < 0.001$) between GB11 wild type and knock out, and GB19 wild type and knock out. Mean and SEM calculated from triplicate tubes with Students two tailed t test. Experiment repeated twice.

3.2.9 Determination of LOS concentration by thiobarbituric acid assay

In all experiments described above, LOS was quantified by dry weight following lyophilisation. The thiobarbituric acid assay was used to confirm the concentration and ensure that wild type and CSTII knock out strains were equimolar. The thiobarbituric acid assay measures the concentration of KDO, a core sugar unique to bacteria. Figure 13 shows the concentration of GB11, GB2 and GB19 wild type and CSTII knock out LOS. There is a statistically significant difference ($p < 0.001$) in the concentration of GB11 wild type and GB11 CSTII knock out strains as well as the GB19 wild type and GB19 CSTII knock out strains. In both cases the sialylated strains are more concentrated. The GB2 wild type and CSTII knock out strains are equimolar.

Figure 14: Thiobarbituric acid assay of GM1 and sialic acid.

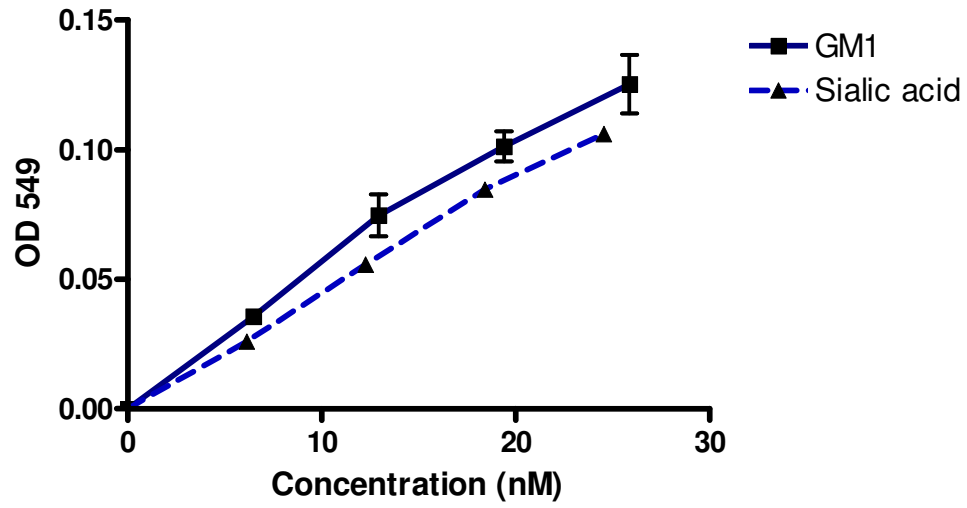


Figure 14. Thiobarbituric acid assay of native GM1 and native sialic acid. There is an increase in OD549 for both molecules. Mean and SEM calculated from triplicate tubes. Single experiment.

3.2.10 Assessment of the validity of the thiobarbituric acid assay

A potential cause for the difference in molarity is interference in the assay. Sialic acids are 2-keto-3-deoxy sugars which are similar in structure to KDO. To test whether sialic acid in the ganglioside mimicking LOS is interfering with the thiobarbituric acid assay, native GM1 ganglioside and native sialic acid molecules were used as substrates in the assay. Figure 14 shows that both GM1 and sialic acid cause an increase in absorbance at OD549 in the thiobarbituric acid assay.

A second experiment was carried out to determine if sialic acid makes a significant contribution to the colour change when compared to KDO. Native KDO molecules and native sialic acid molecules were used in the thiobarbituric acid assay. Figure 15 (note that the graph x and y axes have been reversed) indicates that an approximately four times greater concentration, by molarity, of sialic acid is required to produce the same absorbance at OD549 as KDO. Sialic acid and KDO exist in LOS at a 1.5:1 ratio in GB11 and GB2 LOS strains.

Figure 15: Thiobarbituric acid assay of KDO and sialic acid.

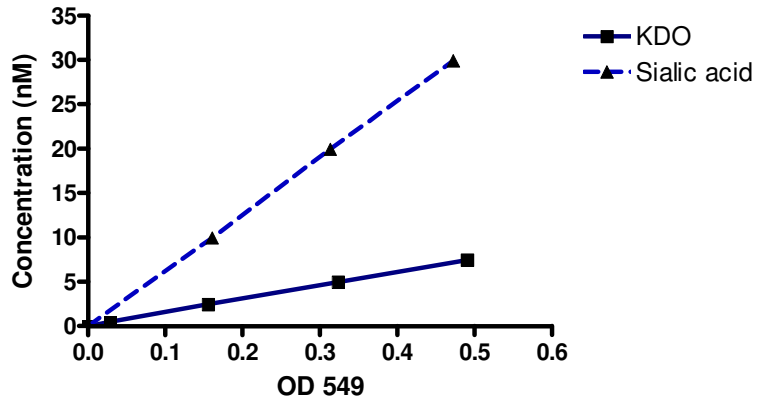


Figure 15. Thiobarbituric acid assay of native KDO and native sialic acid comparing potency in inducing colour change at OD 549. (Note that the graph x and y axes have been reversed). Single experiment.

3.3 Discussion

The principal concerns when isolating LOS were purity, ganglioside mimicry and accurate quantification. The additional issue of secondary structures (how the LOS molecules associate with each other in solution) became apparent during the purification process.

The technique of isolating LPS or LOS using hot phenol and water has been described previously²¹⁸. This involves disrupting bacterial cells in a hot water phenol mix and allowing the LOS to partition into the aqueous phase while cooling the mixture. This method is not entirely specific as it relies solely on the relative solubility of the LOS for separation from other constituents. Bacteria contain a number of immunostimulatory molecules such as proteins, glycolipids and DNA/RNA, all of which can be sources of contamination. There are a number of variations of this technique optimised for different types of LPS. My particular technique was chosen because the major studies on the structure on *C. jejuni* LOS have used the basic hot phenol technique to extract LOS^{202,203}.

My initial studies show that hot phenol extraction of LOS does not yield a pure product. The use of DNase, RNase and Proteinase K in an appropriate enzyme buffer to remove contamination is an established technique²¹⁹ and this was employed to improve purity. SilverXpress[™] staining is exquisitely sensitive for proteins (detecting sub-nanogram quantities) and DNA (detecting nanogram quantities). SilverXpress[™] staining detected no evidence of contamination in LOS purified using the final protocol. In support of this, after LOS solutions had been clarified using detergent and EDTA, biophotometry detected no evidence of DNA, RNA or protein.

Lysozyme was initially used to remove CPS. However, lysozyme caused a precipitate to form which was interpreted as the formation of LOS lamellar macro-structures. Studies have shown that lysozyme interacts electrostatically with phosphate groups on the Lipid

A in Re (rough mutant) LOS causing increased rigidity of the acyl chains which affects the LOS aggregate structures²²⁰. This is a likely explanation for my observations of precipitate formation, although changes in the pH or ionic concentration of the solution might also account for this. For this reason it was decided to eliminate lysozyme from the protocol. Capsular polysaccharide produced by *C. jejuni* is detectable using alcian blue staining²¹⁷. LOS purified without lysozyme was tested by this method. No evidence of CPS is seen in the LOS while a band at the expected molecular mass was visible in the whole cell lysate positive control. Based on these findings it was concluded that CPS is either absent or present at levels below the limits of the alcian blue assay sensitivity.

The structures of LOS molecules produced by HS O:19, HS O:3, GB11 wild type, GB2 wild type, GB11 CSTII knock out and GB2 CSTII knock out have been established^{101,202,203}. Western blot analysis using reagents directed against gangliosides GM1 and GD1a confirms the expected ganglioside mimicry and shows no evidence of such mimicry in the control strains. An attempt was made to produce an additional control strain for HS O:19 by treating the LOS with cholera neuraminidase. However, this resulted in the GD1a epitopes being converted to GM1 which can be explained by the fact that cholera neuraminidase is only active against external sialic acids^{221,222}. Additional neuraminidase enzymes capable of cleaving internal sialic acids, such as *Arthrobacter ureafaciens* sialidase²²³, could have been used alongside cholera neuraminidase to completely remove all sialic acid residues.

Figure 16: Diagram of LOS macromolecular structures.

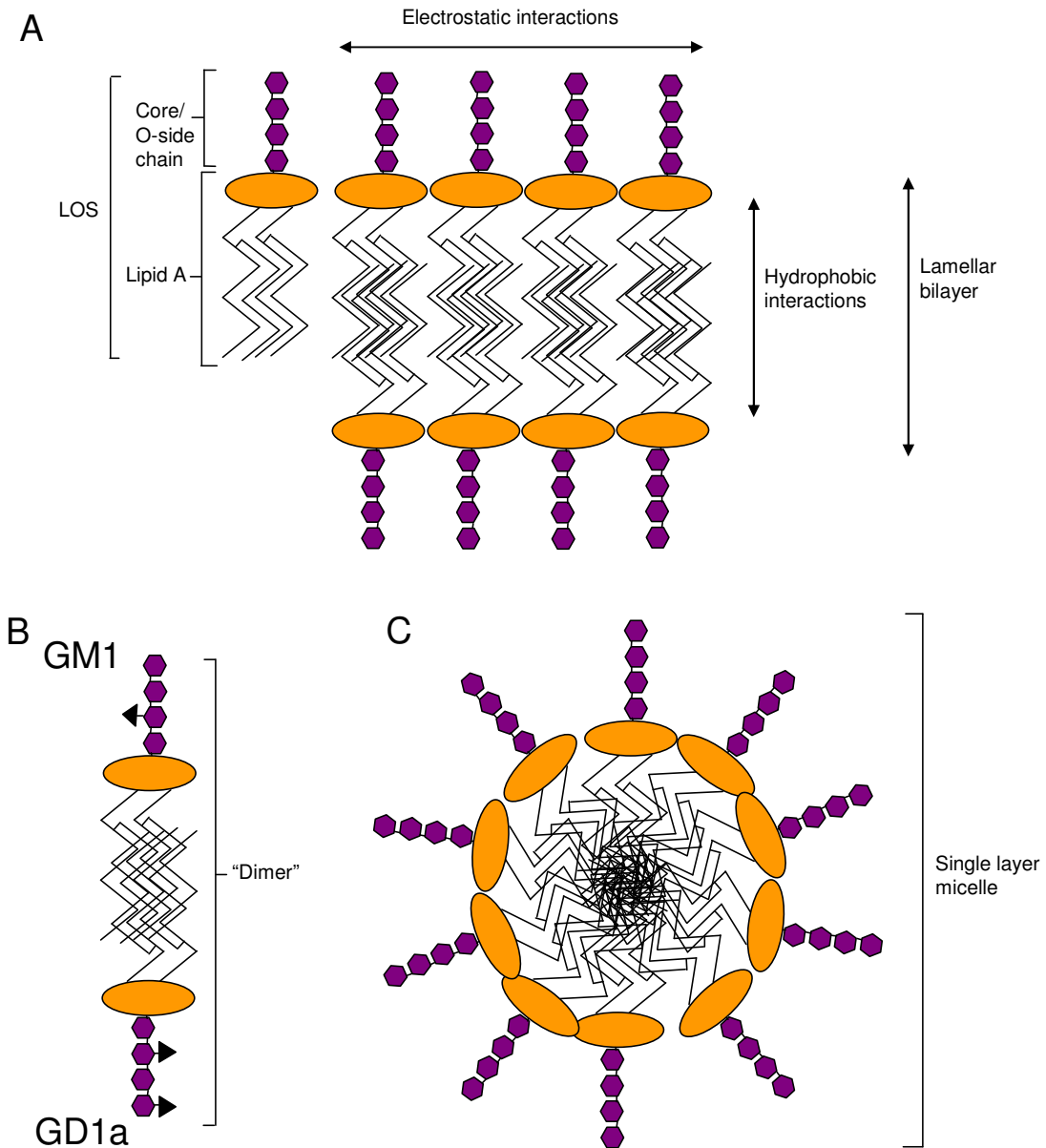


Figure 16. Diagrammatic representation illustrating potential macro-molecular LOS structures. (A) represents a lamellar bilayer. (B) shows a "dimer" structure comprising GM1 and GD1a mimicking LOS molecules linked by hydrophobic bonds. (C) shows a monolayer micelle.

LPS is an amphipathic molecule consisting of a hydrophobic tail and hydrophilic head. In aqueous solutions LPS spontaneously forms a variety of macro-molecular structures²²⁴⁻²²⁶. These include lamellar bilayers, micelle bilayers, single layer micelles and dimer structures¹⁰² (illustrated in figure 16). The precise nature of these macro-molecular structures depends on a variety of factors including LPS concentration, ionic concentration, pH and temperature. LOS is more hydrophobic than LPS and has a greater tendency to form these structures. Divalent cations, required for activity of the DNase²²⁷, RNase²²⁸ and Proteinase K²²⁹, increase the tendency for such structures to form. A number of different purification protocols were tested to try and prevent colloid formation and these included varying the pH and cation concentrations.

Macromolecular structures are a concern because several studies report aggregated LPS to be more potent than monodisperse LPS²³⁰⁻²³² and aggregate dependent differences in mAb binding to LPS have been demonstrated²³². This means that important epitopes might be hidden by secondary structures, for example ganglioside availability for antibody binding can be influenced by neighbouring gangliosides²³³. To allow a comparison of potency of the ganglioside mimicking versus non-mimicking strains without the confounding influence of aggregate effects, it was decided to regulate the micelle structures. Micelles could be dispersed by treating the colloidal LOS with EDTA and detergent and dispersal was confirmed by changes in the silver staining properties. However, EDTA and detergent proved difficult to remove by dialysis.

New strains of *C. jejuni* and LOS were provided by a collaborating group. In addition to eliminating potential differences in the Lipid A, the GB2, GB11 and GB19 strains of LOS were purified using a procedure that omitted divalent cations and minimised micelle formation. Tests of LOS purity under these alternative conditions confirmed that the DNase, RNase and proteinase remained effective in removing contamination. Presumably residual cations chelated by the LOS were available to activate the enzymes. The visual appearance of the LOS and the resolution of the LOS into a mainly single

band by SDS-PAGE and silver stain indicate that the omission of divalent cations at all stages of purification provides a simple solution to colloidal aggregate formation.

It was noted that the bands formed by silver staining of these LOS strains showed variations in size and intensity. It is thought that silver staining binds to the carbohydrate rather than the lipid portion of LPS/LOS^{234,235}. Therefore differences in staining intensity are probably due to differences in the carbohydrate structure of wild type and knock out LOS rather than differences in concentration.

The LOS was quantified using a combination of dry weight and the thiobarbituric acid assay. This chemical assay relies on the cleavage of a diol grouping in 3 deoxy-D-manno-oct-2-ulosonic acid (KDO) which is a unique sugar found in the LOS/LPS core region. This releases a derivative which reacts with thiobarbituric acid to produce a chromophore²³⁶. LOS concentration is determined by comparing to a known concentration of KDO. The initial assay shows that wild type and knock out strains of LOS are not equimolar. There are a number of potential explanations including inaccuracy in the dry weight, differences in molecular mass and inaccuracy of the KDO assay.

Variants of the thiobarbituric acid assay are used to measure sialic acid. Due to differences in the chemical structure of these molecules, sialic acid requires harsher acid treatment in order to contribute to colour change in this assay²³⁶. Several variations of this assay were tested and the least harsh protocol was employed to measure the LOS. However, both free sialic acid and GM1 causes a colour change using my protocol, confirming inaccuracy in the KDO assay.

A further attempt at quantification was done using the Limulus Ameobocyte Assay although due to its exquisite sensitivity it was found to be impractical. Quantification was therefore done using dry weight alone as this was considered the most convenient and reliable method of quantification. It is recognised that this does not take into account differences in molecular mass.

In conclusion, I have purified LOS to such a degree that no contamination can be demonstrated using standard detection techniques. I have verified that my LOS strains either mimic or do not mimic gangliosides as predicted. In addition, I have shown that the thiobarbituric acid assay is unreliable for quantifying sialylated LOS and concluded that dry weight is the most suitable alternative. There is no evidence of differences in macromolecular structures between the wild type and knock out strains although I have not shown this definitively. Overall, I judge the LOS to be suitable for testing my hypotheses.

4 Interaction of ganglioside mimicking LOS and whole *C. jejuni* with ganglioside specific cellular receptors and complement components

4.1 Introduction

The aim of the experiments presented in this chapter is to establish if the ganglioside mimicking side chain of LOS can act as a ligand for cellular receptors and complement proteins which are believed to bind to endogenous gangliosides.

The pathophysiology of GBS is thought to involve the generation of LOS specific antibodies that cross react with gangliosides on self-cells resulting in autoimmune damage^{40,237}. This model of pathogenesis relies on gangliosides substituting for ganglioside mimicking LOS as a target for antibodies and this cross-reactivity has been confirmed^{238,239}. I wish to establish if ganglioside mimicking LOS can substitute for gangliosides as a ligand for immune system receptors.

A number of ganglioside binding cellular receptors are known. The best characterised family of receptors are siglecs (sialic acid binding immunoglobulin like lectins)^{144,146,240}. The precise specificities and physiological roles of these receptors are still being investigated. It has been shown that Siglec 7 binds to GT1a/GM1 mimicking *C. jejuni* and its purified LOS¹⁴⁸. The myeloid expressed mouse siglecs, Sialoadhesin, Siglec E and Siglec F, are predicted to bind to GD1a/GM1 mimicking *C. jejuni* and its LOS although this has not yet been confirmed experimentally. (See Appendix 3 and 4 for siglec structure, cellular expression and binding profiles).

The complement regulatory protein Factor H has a sialic acid binding site^{241,242}. Factor H inhibits the alternative complement pathway and this protects self-cells from aberrant complement activation²⁴¹. Non-campylobacter pathogens are thought to use sialylation and fH binding to enhance complement resistance²⁴³⁻²⁴⁵. It has not been established if ganglioside mimicry by *C. jejuni* facilitates fH binding or if this affects complement activation on GBS associated strains.

Figure 17: Sialoadhesin binding to whole *C. jejuni*.

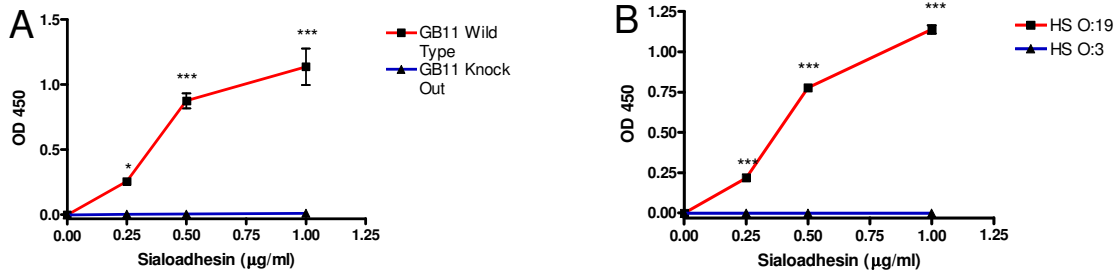


Figure 17. Sialoadhesin-Fc fusion protein binding to whole *C. jejuni*. (A) whole GB11 wild type and GB11 knock out *C. jejuni* and (B) whole HS O:19 and HS O:3 *C. jejuni*. There is statistically significant binding of Sialoadhesin to ganglioside mimicking strains of *C. jejuni* (GB11 wild type and HS O:19) compared to their control strains (GB11 knock out and HS O:3) at each concentration of Sialoadhesin tested (A and B). Mean and SEM calculated from triplicate wells. Significance compares binding to ganglioside mimicking and control strain at each Sialoadhesin concentration using 2way ANOVA with Bonferroni's post tests (*= $p < 0.05$, ***= $p < 0.001$). Graphs representative of 3 experiments.

4.2 Results

4.2.1 Sialoadhesin binding to *C. jejuni*.

Murine Sialoadhesin-human-Fc fusion protein binding to whole, formalin fixed, *C. jejuni*, pre-adsorbed onto ELISA plates, was measured. Figures 17 (A) and (B) show that Sialoadhesin binds to both of the ganglioside mimicking strains (GB11 wild type (A) and HS O:19 (B)). Sialoadhesin does not bind to the non-mimicking control strains (GB11 knock out (A) and HS O:3 (B)). The difference in binding between ganglioside mimicking strains and control strains is statistically significant (GB11 wild type v knock out: $p < 0.001$ at $1\mu\text{g/ml}$ and $0.5\mu\text{g/ml}$, $p < 0.05$ at $0.25\mu\text{g/ml}$. HS O:19 v HS O:3: $p < 0.001$ at 1, 0.5 and $0.25\mu\text{g/ml}$).

Sialoadhesin is predicted to bind GD1a and GT1b. Sialoadhesin binding to gangliosides and ganglioside mimicking LOS was assessed using ELISA. The target gangliosides tested were GM1, GD1a and GT1b, and the asialo-glycolipids were asialo-GM1, asialo-GM2 and lactosyl ceramide (the core components of GB11 knock out *C. jejuni* LOS). Sialoadhesin binding to GB11 wild type and knock out LOS, and HS O:19 and HS O:3 LOS was also assessed. No Sialoadhesin binding was detected to any of these targets (data not shown).

Figure 18: Immunocytochemistry of Sialoadhesin binding to *C. jejuni*.

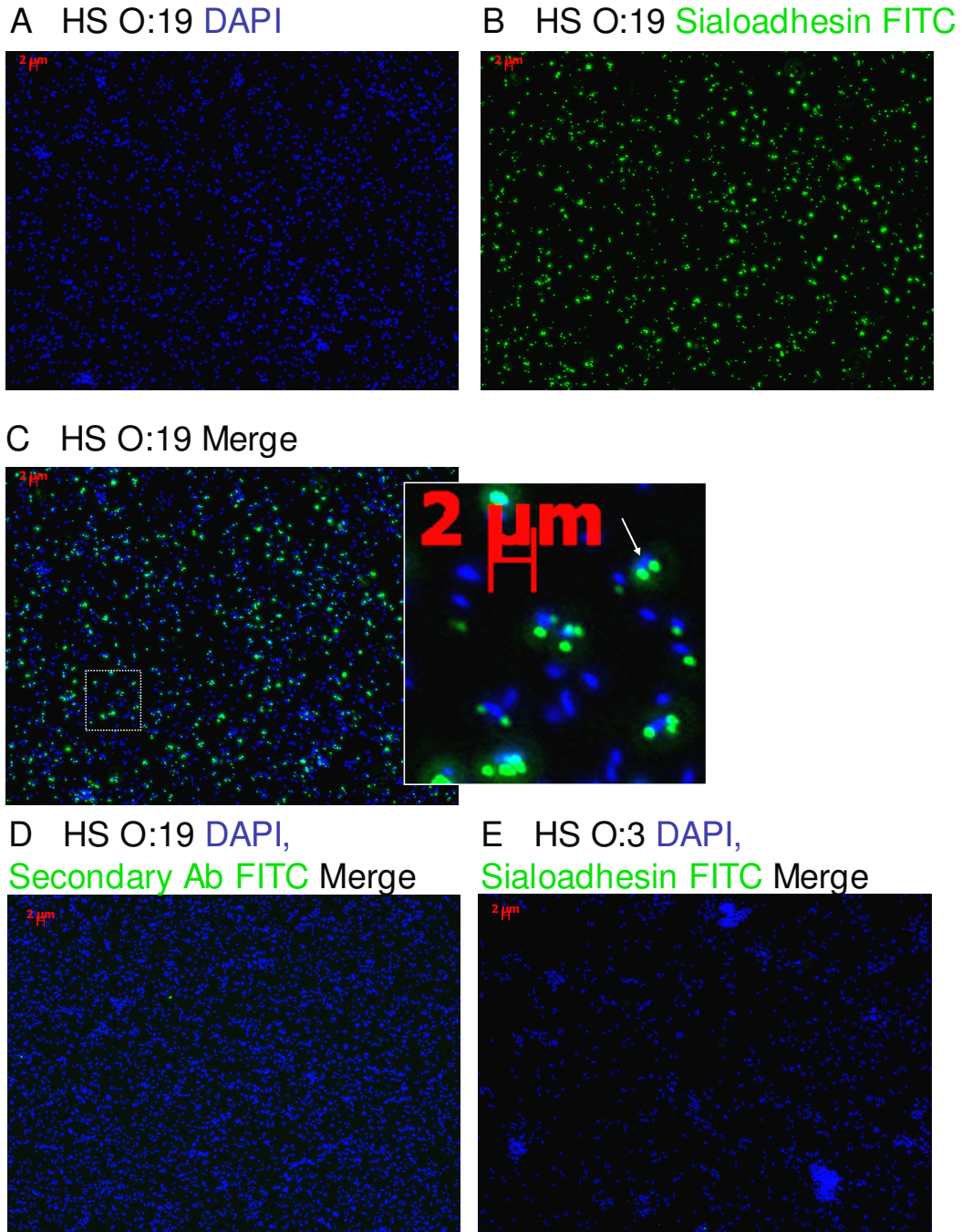


Figure 18. Immunocytochemistry of Sialoadhesin binding to *C. jejuni*. (A) DAPI labelled HS O:19. (B) HS O:19 labelled with Sialoadhesin-Fc fusion protein and anti-human IgG FITC. (C) Merge of (A) and (B). Inset is digital magnification of (C); arrow shows punctate staining of the bacteria. (D) Control 1 – merged image of DAPI labelled HS O:19 and anti-human IgG FITC (secondary Ab only). (E) Control 2 – merged image of DAPI labelled HS O:3 with Sialoadhesin-Fc fusion protein and anti-human IgG FITC. Single experiment.

4.2.2 Visualisation of Sialoadhesin binding to *C. jejuni*

Sialoadhesin was found to bind whole bacteria but not the LOS or native ganglioside. It was decided to confirm the binding specificity by using Sialoadhesin to fluorescently label the bacteria. Formalin fixed *C. jejuni* were adsorbed onto slides and labelled with Sialoadhesin-Fc fusion protein pre-complexed with anti-human IgG FITC labelled antibodies. The DNA binding fluorophore DAPI was used to localise the bacteria. Two test strains were chosen, HS O:19 and HS O:3, both of which are wild type strains of *C. jejuni* which mimic and do not mimic gangliosides respectively. Figure 18 (A) shows DAPI labelled HS O:19 *C. jejuni*. Figure 18 (B) shows Sialoadhesin labelled HS O:19 *C. jejuni*. Figure 18 (C) shows the merged and digitally magnified image which confirms that the Sialoadhesin binding is associated specifically with the bacteria. Interestingly, the Sialoadhesin appears to show a punctuate pattern of staining (white arrow) which is often localised to one or both poles of the bacterium. In addition, not all of the bacteria were labelled with Sialoadhesin. Figures 18 (D) and (E) show the secondary antibody alone and Sialoadhesin labelling of the HS O:3 strain respectively. These show no detectable binding. These controls confirm the specificity of Sialoadhesin binding.

Figure 19: Sialoadhesin binding to *C. jejuni* following neuraminidase treatment.

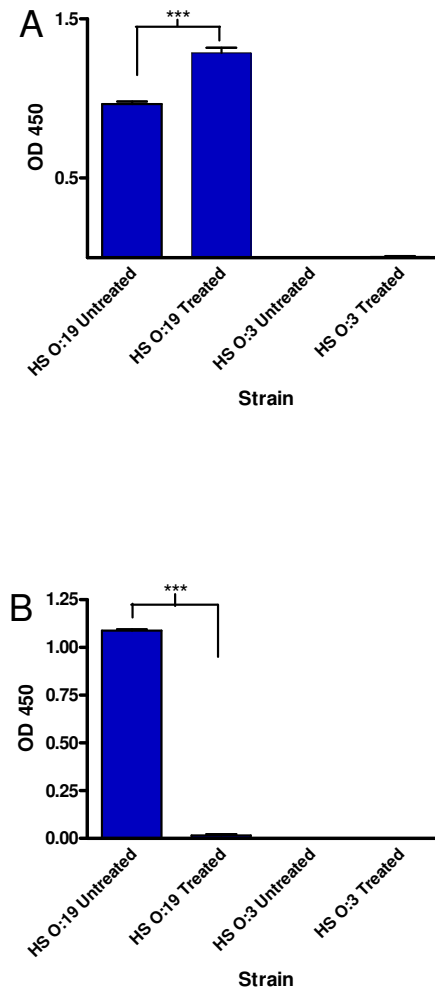


Figure 19. Effect of removal of GD1a on Sialoadhesin binding. (A) ELISA showing GM1 specific mAb DG2 binding to *C. jejuni*. There is a statistically significant increase in binding to HS O:19 *C. jejuni* following neuraminidase treatment. (B) ELISA showing Sialoadhesin binding to neuraminidase treated *C. jejuni*. Sialoadhesin binding to HS O:19 is completely obliterated by neuraminidase treatment. Mean and SEM calculated from triplicate wells and analysed using students 2 tailed t test (***)= $p < 0.001$). Single experiment.

4.2.3 Confirmation of Sialoadhesin binding to the GD1a epitope

In order to confirm that Sialoadhesin was binding to the GD1a epitope, HS O:19 and HS O:3 whole *C. jejuni* were treated with cholera neuraminidase. The experiment in chapter 3.2.5 (figure 9) demonstrates that cholera neuraminidase cleaves the external sialic acid on LOS and converts GD1a to GM1. The prediction is that neuraminidase treatment will result in an increase in GM1 epitopes on the surface of HS O:19 bacteria and a decrease in GD1a with a subsequent decrease in Sialoadhesin binding. Figure 19 (A) shows binding of the GM1 specific mAb DG2 to HS O:19 and HS O:3 before and after neuraminidase treatment. As expected, there is a significant ($p < 0.001$) increase in DG2 binding following neuraminidase treatment of HS O:19, which is consistent with an increase in GM1 epitopes. There is no DG2 binding to HS O:3. Figure 19 (B) shows Sialoadhesin binding to HS O:19 and HS O:3 before and after neuraminidase treatment. Neuraminidase treatment completely abrogates Sialoadhesin binding to HS O:19 ($p < 0.001$) consistent with a loss of the GD1a epitope. There is no binding to the HS O:3 control strain. This experiment confirms that GD1a mimicry is necessary for Sialoadhesin binding.

Figure 20: Siglec F binding to gangliosides, LOS and *C. jejuni*.

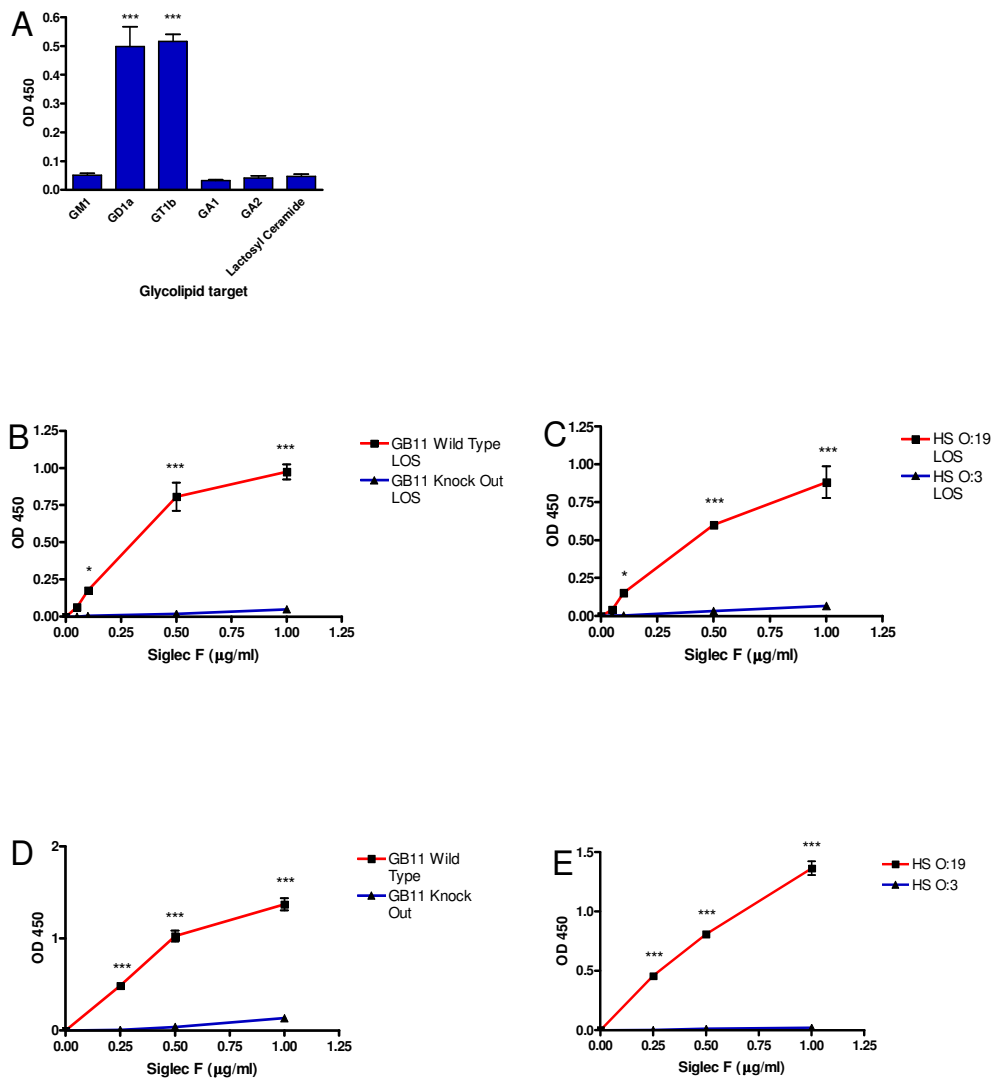


Figure 20. ELISAs measuring Siglec F-Fc fusion protein binding to (A) glycolipids (Siglec F used at 1µg/ml); (B) LOS from GB11 wild type and knock out strains of *C. jejuni*; (C) LOS from HS O:19 and HS O:3 strains of *C. jejuni*; (D) whole GB11 wild type and GB11 knock out *C. jejuni* and (E) whole HS O:19 and HS O:3 *C. jejuni*. Siglec F shows statistically greater binding to gangliosides GD1a and GT1b when compared to ganglioside GM1 and the asialo-sugars (A). Siglec F shows significantly greater binding to ganglioside mimicking LOS (GB11 wild type and HS O:19) when compared to the non-mimicking counterparts (GB11 knock out and HS O:3) (B and C). In addition, there is significantly greater binding of Siglec F to ganglioside mimicking strains of whole *C. jejuni* compared to their control strains at each concentration of Siglec F tested (D and E). Mean and SEM calculated from triplicate wells. Significance compares Siglec F binding to GD1a and GT1b compared to each other glycolipid using 1way ANOVA and Bonferroni's multiple comparison post test (A). Significance compares binding to ganglioside mimicking and control strain at each Siglec F concentration using 2way ANOVA with Bonferroni's post tests (B to E) (*= $p < 0.05$, ***= $p < 0.001$). Graphs representative of 3 experiments.

4.2.4 Siglec F binding to gangliosides, LOS and *C. jejuni*

Siglec F binding to glycolipids was assessed by ELISA. In contrast to Sialoadhesin, figure 20 (A) demonstrates that Siglec F (used at 1 μ g/ml) can bind to native gangliosides. Comparing GD1a and GT1b to the other glycolipids, the difference in binding is statistically significant ($p < 0.001$) with no difference between GD1a and GT1b themselves. Siglec F binding to GD1a mimicking LOS was tested by comparing ganglioside mimicking LOS to control strains. Figures 20 (B) and (C) show significantly greater binding of Siglec F to the ganglioside mimicking strains GB11 wild type and HS O:19 respectively compared to the control strains GB11 knock out and HS O:3 ($p < 0.001$ at 1 μ g/ml and 0.5 μ g/ml, $p < 0.05$ at 0.1 μ g/ml). This dose dependent effect indicates specific binding. Finally, Siglec F binding to whole, formalin fixed, *C. jejuni* was assessed. Figures 20 (D) and (E) show statistically greater binding of Siglec F to ganglioside mimicking strains (GB11 wild type and HS O:19 respectively) than to their relevant control strains ($p < 0.001$ over the complete range of concentrations).

Figure 21: Immunocytometry of Siglec F binding to *C. jejuni*.

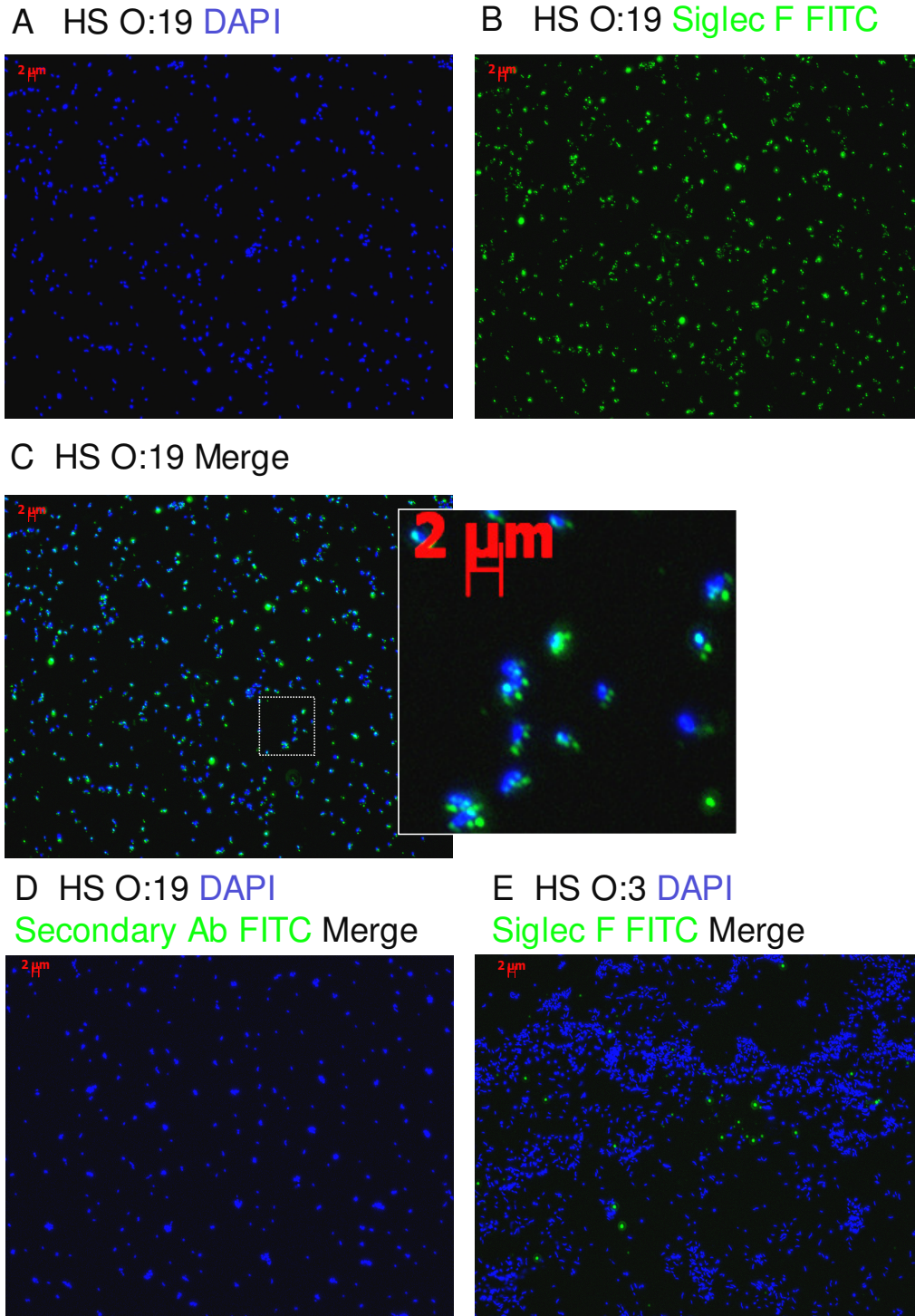


Figure 21. Immunocytometry of Siglec F binding to *C. jejuni*. (A) DAPI labelled HS O:19. (B) HS O:19 labelled with Siglec F-Fc fusion protein and anti-human IgG FITC. (C) Merge of (A) and (B). Inset digital magnification of (C). (D) Control 1 – merged image of DAPI labelled HS O:19 and anti-human IgG FITC (secondary Ab only). (E) Control 2 – merged image of DAPI labelled HS O:3 with Siglec F-Fc fusion protein and anti-human IgG FITC. Single experiment.

4.2.5 Visualisation of Siglec F binding to *C. jejuni*

Siglec F binding to formalin fixed HS O:19 and HS O:3 *C. jejuni* was visualised using the same method as for Sialoadhesin.

Figures 21 (A) and (B) show DAPI labelled HS O:19 and Siglec F-Fc anti human IgG FITC labelled HS O:19. Figure 21 (C) shows the merged and digitally magnified image. These show specific Siglec F labelling of HS O:19 and they also reveal a punctate staining pattern similar to that of Sialoadhesin. Figures 21 (D) and (E) show secondary antibody alone and Siglec F labelling of the HS O:3 strain respectively and confirm that Siglec F binds specifically to the ganglioside mimicking HS O:19 strain.

Figure 22: Siglec E binding to gangliosides, LOS and *C. jejuni*.

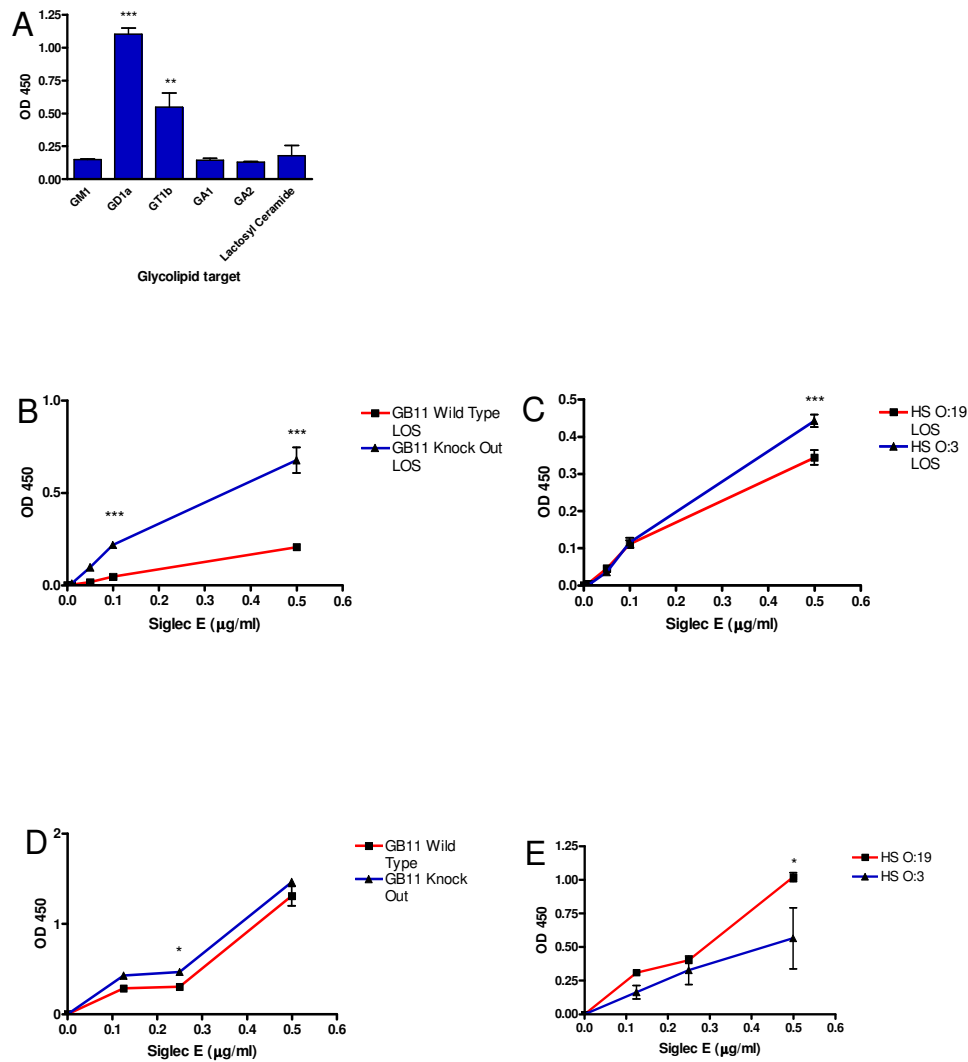


Figure 22. ELISAs measuring Siglec E-Fc fusion protein binding to (A) glycolipids (Siglec E used at 0.5µg/ml); (B) LOS from GB11 wild type and knock out strains of *C. jejuni*; (C) LOS from HS O:19 and HS O:3 strains of *C. jejuni*; (D) whole GB11 wild type and GB11 knock out *C. jejuni* and (E) whole HS O:19 and HS O:3 *C. jejuni*. Siglec E shows significantly greater binding to gangliosides GD1a and GT1b when compared to ganglioside GM1 and the asialo-sugars (A) (analysis by 1way ANOVA and Bonferroni's multiple comparison posttest.). Siglec E shows statistically greater binding to non-ganglioside mimicking LOS (GB11 knock out and HS O:3) when compared to the mimicking counterparts (GB11 wild type and HS O:19) at higher concentrations of Siglec E (B and C). Siglec E binding to whole *C. jejuni* showed significantly increased binding to GB11 knock out compared to GB11 wild type at a single concentration and significantly increased binding to HS O:19 over HS O:3 at a single concentration. Mean and SEM calculated from triplicate wells. Significance was calculated using 2way ANOVA with Bonferroni's posttest analysis. (*=p<0.05, **=p<0.01, ***=p<0.001). Graphs representative of 3 experiments.

4.2.6 Siglec E binding to gangliosides, LOS and *C. jejuni*

Siglec E binding to selected gangliosides and asialo-glycolipids was assessed as before (Siglec E used at 0.5µg/ml). Figure 22 (A) shows significantly greater binding of Siglec E to GD1a ($p<0.001$) than any other glycolipid and to GT1b compared to GM1 and the asialo-glycolipids ($p<0.01$). Figures 22 (B) and (C), which show Siglec E binding to LOS, reveal unexpected findings. Siglec E shows statistically greater binding at higher concentrations to the non-ganglioside mimicking strains, GB11 knock out (B) and HS O:3 (C), than the ganglioside mimicking strains (GB11 wild type v knock out: $p<0.001$ at 0.5 and 0.1µg/ml. HS O:19 v HS O:3: $p<0.001$ at 0.5µg/ml). Figures 22 (D) and (E) show Siglec E binding to both ganglioside mimicking and non-mimicking strains of *C. jejuni*. Siglec E does not show any clear trend as there is greater binding to GB11 knock out than wild type ($p<0.05$ at 0.25µg/ml) and greater binding to HS O:19 than HS O:3 ($p<0.05$ at 0.5µg/ml) at a single concentration point in each titration.

Figure 23: Immunocytochemistry of Siglec E binding to *C. jejuni*.

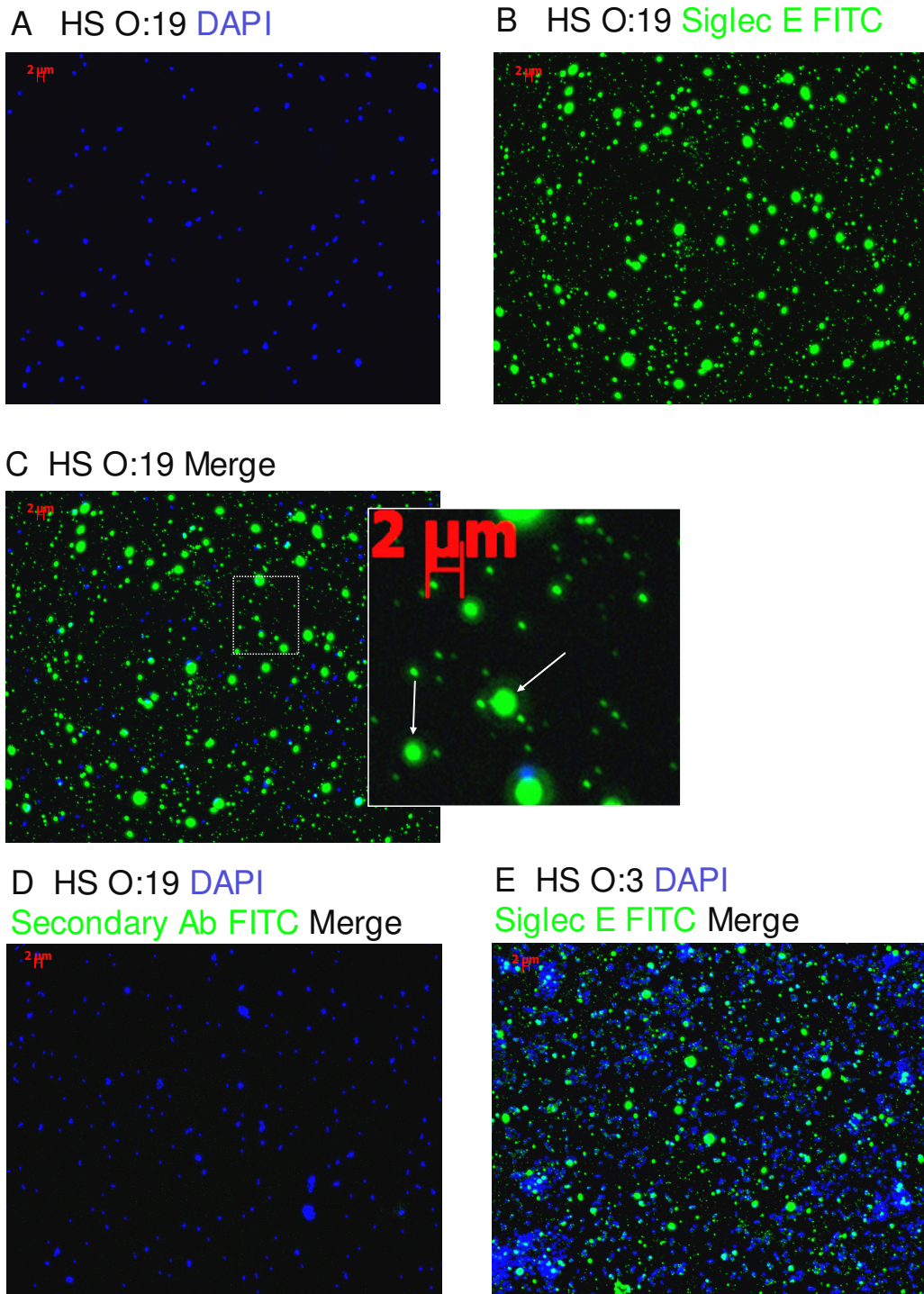


Figure 23. Immunocytochemistry of Siglec E binding to *C. jejuni*. (A) DAPI labeled HS O:19. (B) HS O:19 labeled with Siglec E-Fc fusion protein and anti-human IgG FITC. (C) Merge of (A) and (B). Inset digital magnification of (C). (D) Control 1 – merged image of DAPI labelled HS O:19 and anti-human IgG FITC (secondary Ab only). (E) Control 2 – merged image of DAPI labelled HS O:3 with Siglec E-Fc fusion protein and anti-human IgG FITC. Arrows in (C) show non-specific background binding of Siglec E-Fc fusion protein in the HS O:19 strains which is also present in HS O:3.

4.2.7 Visualisation of Siglec E binding to *C. jejuni*

In order to further understand this unexpected finding, Siglec E binding to formalin fixed *C. jejuni* was visualised as before. Figures 23 (A) and (B) show DAPI labelled HS O:19 and Siglec E-Fc anti-human IgG FITC labelled HS O:19 respectively. Figure 23 (C) shows the merged and digitally magnified images. Figure 23 (D) shows secondary antibody alone. Figure 23 (E) shows merged DAPI and Siglec E-Fc anti-human IgG FITC labelled HS O:3 *C. jejuni*. Figures 23 (C) and (E) show that some Siglec E is associated with both strains of bacteria. However, intense non-specific staining (white arrows in (D)) and speckled background staining is also present. These results show that Siglec E is binding non-specifically to the background material and not specifically to either strain of bacteria.

Figure 24: Siglec E binding to LOS, gangliosides and complexed gangliosides.

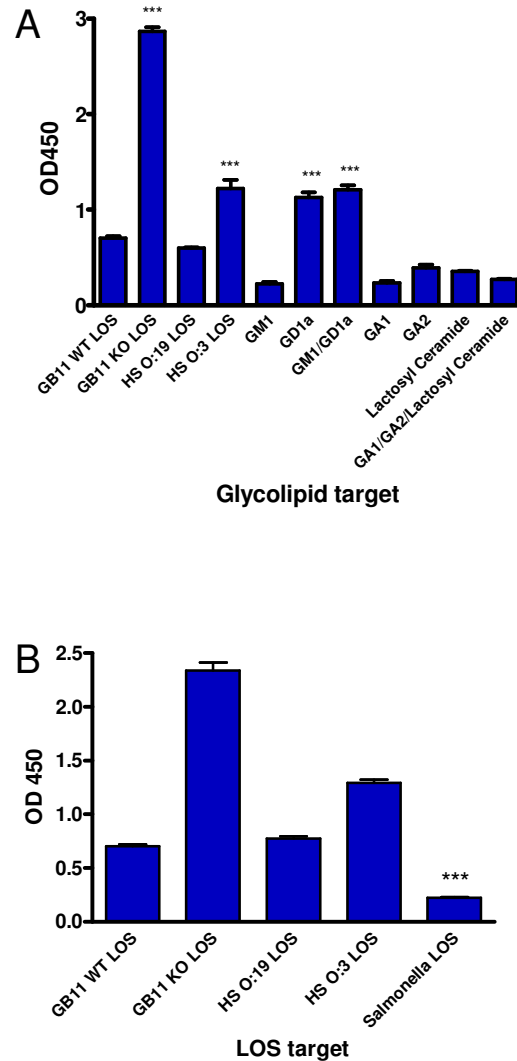


Figure 24. Siglec E binding to LOS, gangliosides and complexed gangliosides using ELISA. (A) Siglec E binding to LOS compared to gangliosides and complexed gangliosides. The strongest binding observed was to GB11 knock out LOS which reached saturation ($p < 0.001$ compared to all other targets). There was strong and equal binding to HS O:3 LOS, GD1a and GD1a/GM1 complexes ($p < 0.001$ compared to other targets but not to each other). There was no statistical difference between GB11 wild type LOS and HS O:19 LOS but both of these showed greater binding than GM1 and all the asialo-sugars ($p < 0.001$). There was no difference between GM1 and all of the asialo-sugars. (B) Siglec E binding to *C. jejuni* LOS was compared to binding to *S. typhimurium* LOS. Similar to (A), GB11 knock out LOS shows greater binding than all the other targets ($p < 0.001$) and HS O:3 shows greater binding than the two ganglioside mimicking strains ($p < 0.001$). There is no difference between GB11 wild type and HS O:19. There is significantly less binding to *S. typhimurium* LOS ($p < 0.001$) than any of the *C. jejuni* LOS strains. Only the key statistical differences have been marked for clarity. Mean and SEM calculated from triplicate tubes. Statistical analysis was by 1 way ANOVA and Bonferroni's posttests. (**= $p < 0.001$). Single experiment.

4.2.8 Siglec E binding to LOS, gangliosides and ganglioside complexes

In order to investigate the specificity of the binding of the Siglec E reagent it was decided to directly compare LOS to ganglioside binding, and to include complexes of mixed gangliosides and asialo-sugars. Ganglioside complexes were included as LOS consists of mixed GM1 and GD1a mimics and such complexes might be important in altering epitopes. Figure 24 (A) shows Siglec E binding to gangliosides and to LOS. Siglec E binding to GB11 knock out LOS is significantly greater than any other LOS or, surprisingly, the asialo-sugars (asialo-GM1, asialo-GM2 and lactosyl ceramide) which constitute the core sugars of the GB11 knock out LOS itself ($p < 0.001$). There is no statistical difference in binding to HS O:3 LOS, native GD1a alone and GD1a/GM1 complexes. Binding to these three glycolipids is greater than to the other glycolipids tested ($p < 0.001$) other than GB11 knock out LOS. Interestingly, binding to GM1 and GD1a targets is significantly greater ($p < 0.001$) than binding to the LOS strains that mimic these gangliosides.

There is an inconsistency between Siglec E binding to LOS and the native sugars found in the LOS core. This is seen in both the ganglioside mimicking strains and the non-mimicking GB11 knock out strain. This raises the question of whether the Siglec E target is the external core sugars or another part of the molecule such as Lipid A. To address this, a rough mutant LOS from *S. typhimurium* was used as a target to provide an independent Lipid A i.e. not from *C. jejuni*. Figure 24 (B) shows binding of Siglec E to *C. jejuni* LOS and *S. typhimurium* LOS. There was significantly less binding to *S. typhimurium* LOS than to any of the *C. jejuni* strains ($p < 0.001$).

Figure 25: Factor H binding to *C. jejuni*.

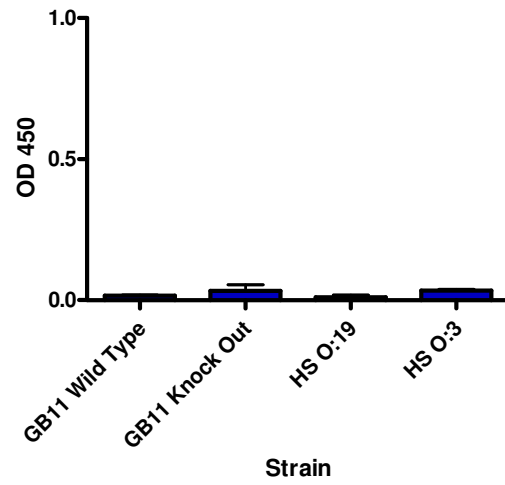


Figure 25. Purified human fH binding to whole *C. jejuni* using ELISA. Mean and SEM calculated from triplicate wells. Graph representative of 3 experiments.

4.2.9 Purified human complement Factor H binding to *C. jejuni*

Purified human fH binding to formalin fixed *C. jejuni* was assessed using an ELISA technique. Bacteria were adsorbed onto an ELISA plate and incubated with purified fH for 1 hour at 37°C. Binding was assessed using a monoclonal anti-human fH antibody. Figure 25 shows that no fH binding, above the limits of sensitivity, to either ganglioside mimicking or non-mimicking strains could be detected. In order to confirm this finding, fH binding to heat killed bacteria was measured using FACS analysis (figure 26). *C. jejuni* were incubated with 10µg purified fH for 30 minutes at 37°C and a mouse anti-fH mAb with anti mouse Ig-FITC were used for detection. There is no evidence of fH binding to ganglioside mimicking or non-mimicking strains of *C. jejuni*. Binding to formalin fixed bacteria was assessed using immunocytometry (figure 27). None of the methods employed showed evidence of purified fH binding to either sialylated or non-sialylated strains whether heat inactivated or formalin fixed. Although no suitable positive control was available to test the purified fH reagent, subsequent experiments, detailed below, indicate that the anti-fH mAb works. In addition, the FACS analysis protocol works as I have used this technique to demonstrate cholera toxin-FITC binding to ganglioside mimicking strains of *C. jejuni* in other projects²³³ (data shown in figure 26 (B)).

Figure 26: FACS of Factor H binding to *C. jejuni*.

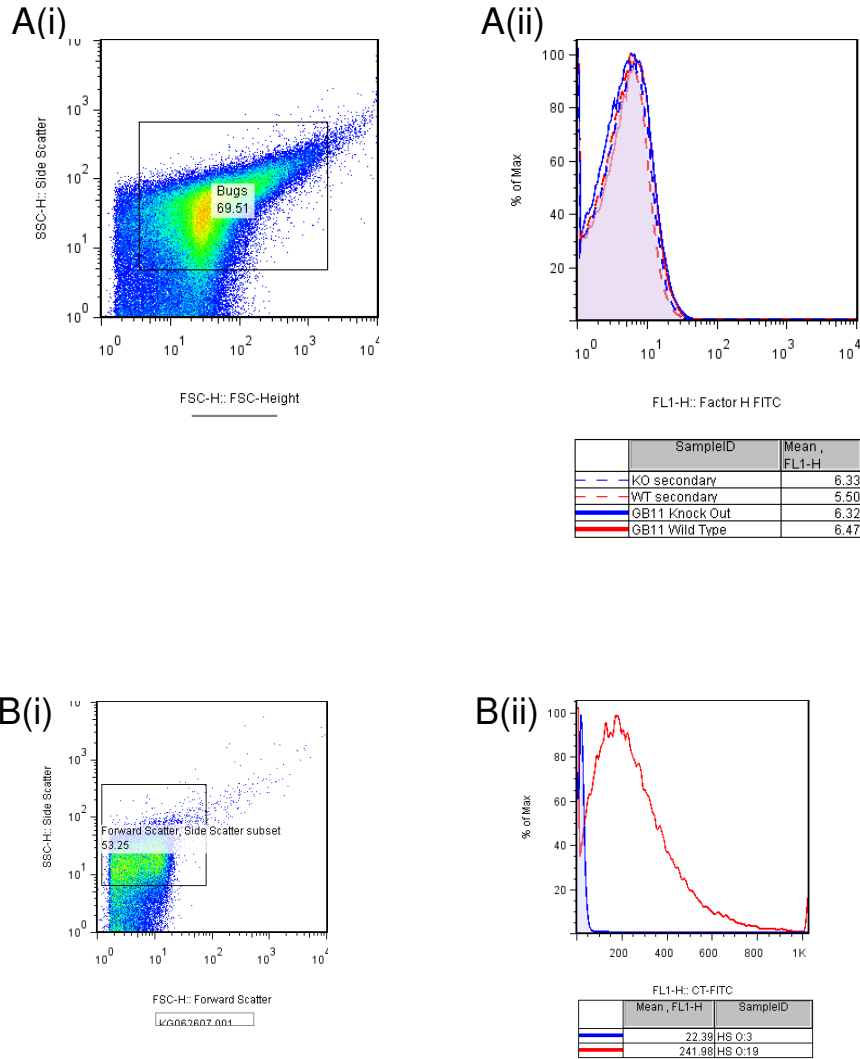


Figure 26 . Purified human fH binding to heat inactivated GB11 wild type or GB11 knock out *C. jejuni* using FACS analysis. Dot plot (A)(i) shows bacteria gate. (A)(ii) Shows histograms of bacteria showing the FITC MFI as a measure of fH binding. Anti-mouse Ig-FITC only (secondary) was used as a control. (B) Shows a separate experiment in which HS O:19 and HS O:3 bacteria were labelled with cholera toxin FITC which binds to GM1. (B)(ii) shows binding of cholera toxin to O:19 but not O:3 confirming that labelled bacteria can be detected by FACS analysis with this protocol. Representative of triplicate tubes.

Figure 27: Immunocytometry of Factor H binding to *C. jejuni*.

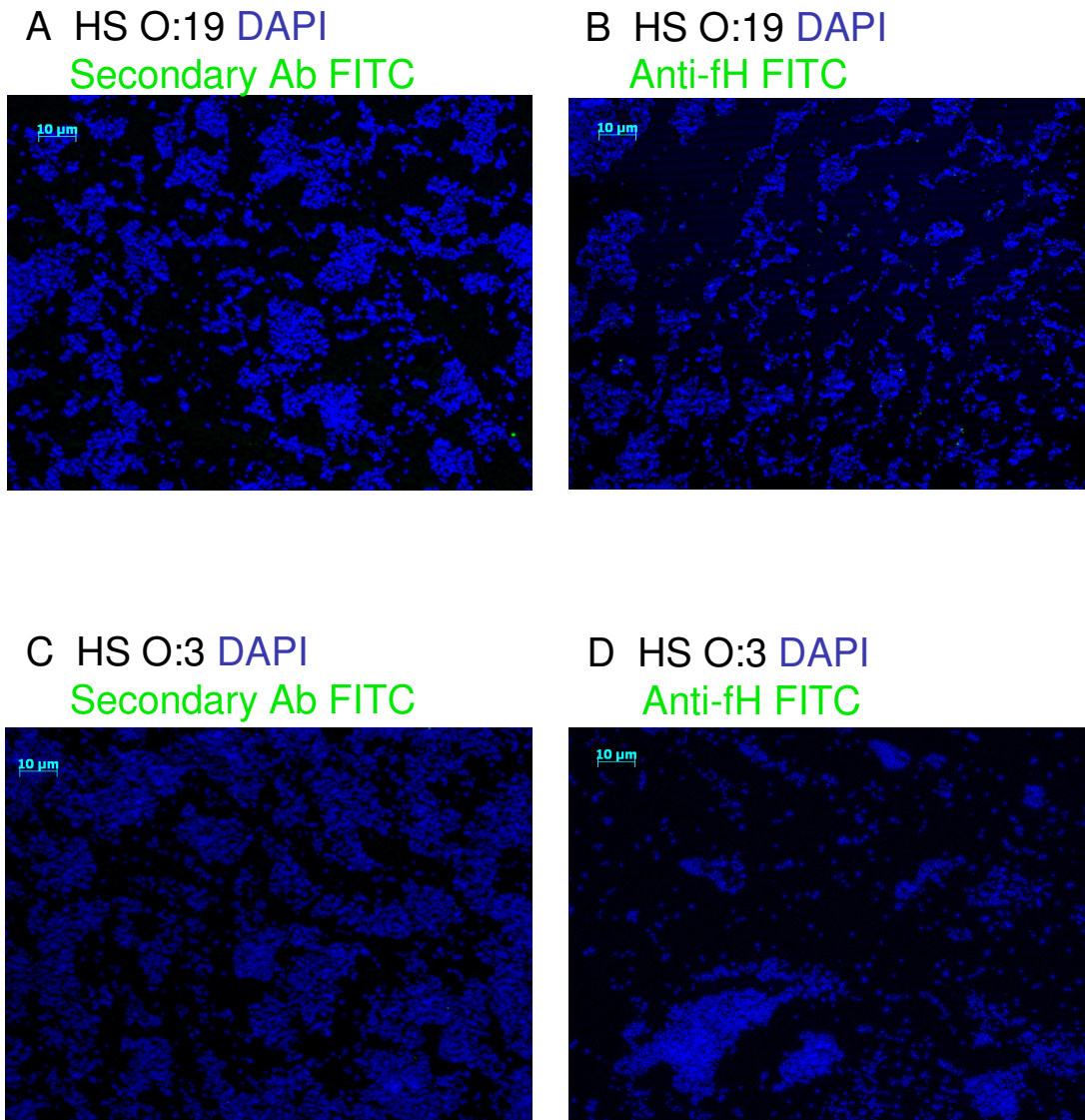


Figure 27. Immunocytometry of purified human fH binding to HS O:19 and HS O:3 *C. jejuni*. (A) and (C) show mAb anti-fH and anti-mouse IgG FITC only (negative control). (B) and (D) shows *C. jejuni* incubated with 5 μ g purified human fH followed by anti-fH mAb and anti-mouse IgG FITC. Experiment repeated twice.

Figure 28: Factor H binding following incubation with serum.

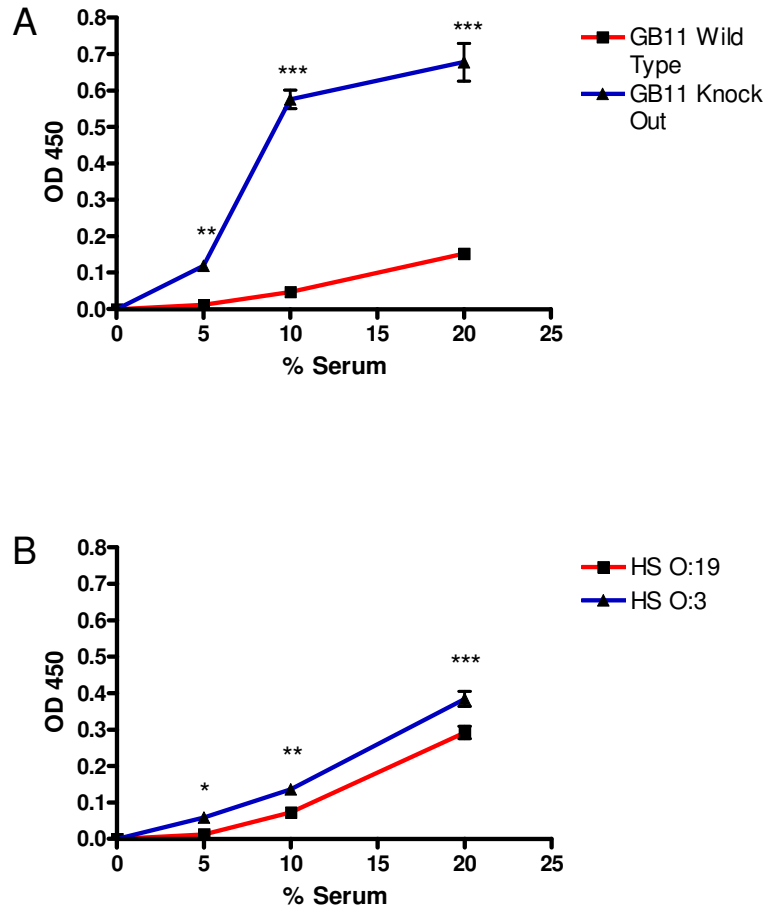


Figure 28. Serum fH binding to whole *C. jejuni* following incubation with active naïve human serum using ELISA. (A) Shows fH binding to GB11 wild type and knock out *C. jejuni*. (B) Shows binding to HS O:19 and HS O:3 *C. jejuni*. There are statistically significant differences in binding with increased fH binding to the non-sialylated strains. Mean and SEM calculated from triplicate wells. Statistical analysis was done using a 2way ANOVA with Bonferroni's posttests. (*= $p < 0.05$, **= $p < 0.01$, ***= $p < 0.001$). Graphs representative of three donors.

Factor H has a binding site for C3b and activated complement provides binding sites for fH by depositing C3b on target structures. In order to test if activated serum provides binding sites for fH, and to confirm that the anti-fH mAb works, formalin fixed *C. jejuni* were adsorbed onto an ELISA plate and incubated with naïve human serum for 20 minutes at 37°C. Serum fH binding was assayed as before using the monoclonal anti-fH antibody. Figures 28 (A) and (B) show significantly greater binding of serum fH to non-sialylated strains of *C. jejuni* compared to sialylated strains (GB11 wild type v knock out: $p < 0.001$ at 20% and 10% serum, $p < 0.005$ at 5% serum. HS O:19 v HS O:3: $p < 0.001$ at 20%, $p < 0.005$ at 10% and $p < 0.05$ at 5% serum).

Figure 29: Complement C3c and C9 deposition on *C. jejuni*.

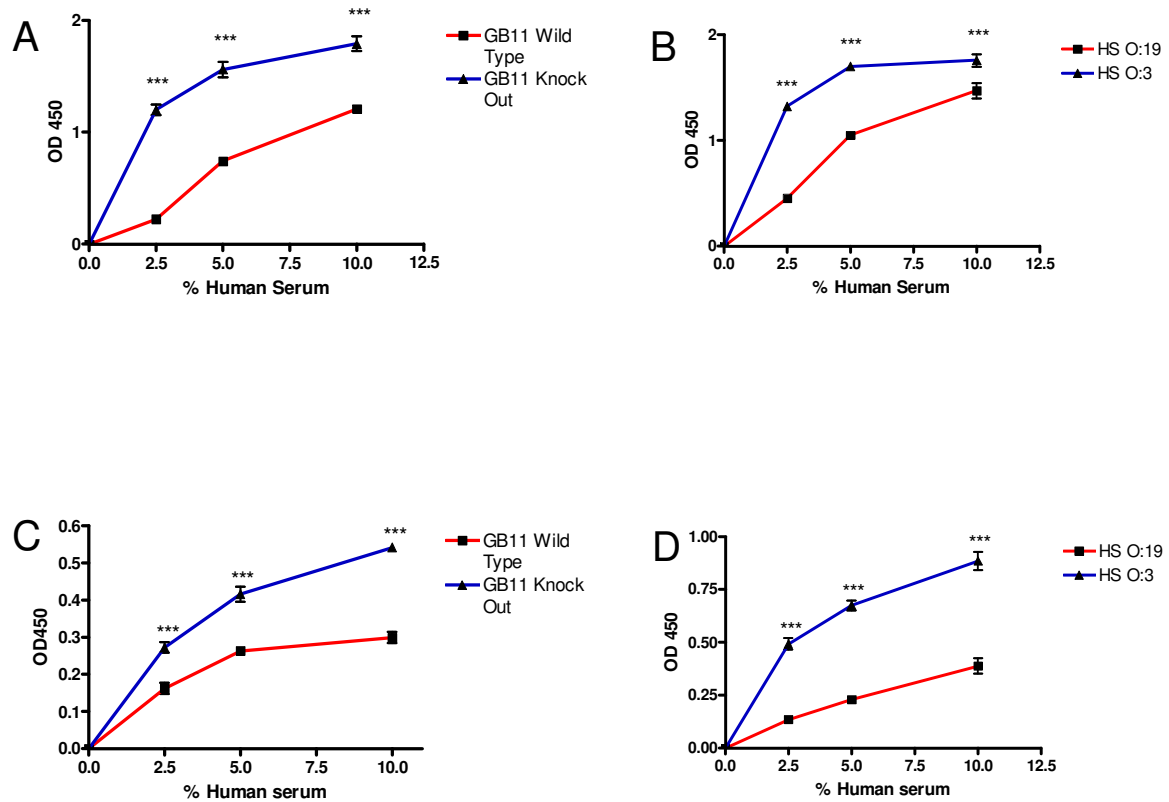


Figure 29. C3c and C9 deposition on whole *C. jejuni* after incubation with naïve human serum for 20 minutes using ELISA. (A) and (B) show human C3c deposition on GB11 wild type v knock out and HS O:19 v HS O:3 respectively. (C) and (D) show human C9 deposition on GB11 wild type v knock out and HS O:19 v HS O:3 respectively. Deposition was measured using rabbit anti-C3 or anti-C9 with an anti-rabbit Ig-HRP detection antibody. All graphs show greater C3 and C9 deposition on the non-ganglioside mimicking *C. jejuni* strains. Mean and SEM calculated from triplicate wells. Significance measured using two way ANOVA with Bonferroni's posttests (***= $p < 0.001$). Graphs representative of 3 naïve donors.

4.2.10 Human C3c and C9 complement deposition on *C. jejuni*

Purified fH alone shows no binding to sialylated *C. jejuni*. The previous results show enhanced serum fH binding to non-sialylated *C. jejuni* that had been incubated with active serum. As complement activation provides fH binding sites, this suggests there is greater complement activation on the surface of non-ganglioside mimicking strains. To test this hypothesis, deposition of C3c and C9 (the main component of membrane attack complex) on *C. jejuni* was measured following incubation with naïve human serum. Figures 29 (A) and (B) show binding of complement C3c to whole formalin fixed *C. jejuni* following incubation with human serum for 20 minutes at 37°C. Although C3c is deposited on all the *C. jejuni* strains, there is significantly greater C3c deposited on the non-sialylated strains, GB11 knock out (B) and HS O:3 (C), than the corresponding sialylated strains ($p < 0.001$ over the range of serum concentrations). Figures 29 (C) and (D) show significantly increased Complement C9 deposition on the non-ganglioside mimicking *C. jejuni* strains when compared to the ganglioside mimicking strains under the same conditions ($p < 0.001$ over the range of serum concentrations). Serum from three naïve individuals showed the same pattern of C3c and C9 deposition.

Figure 30: Anti-LOS natural IgM and IgG antibody.

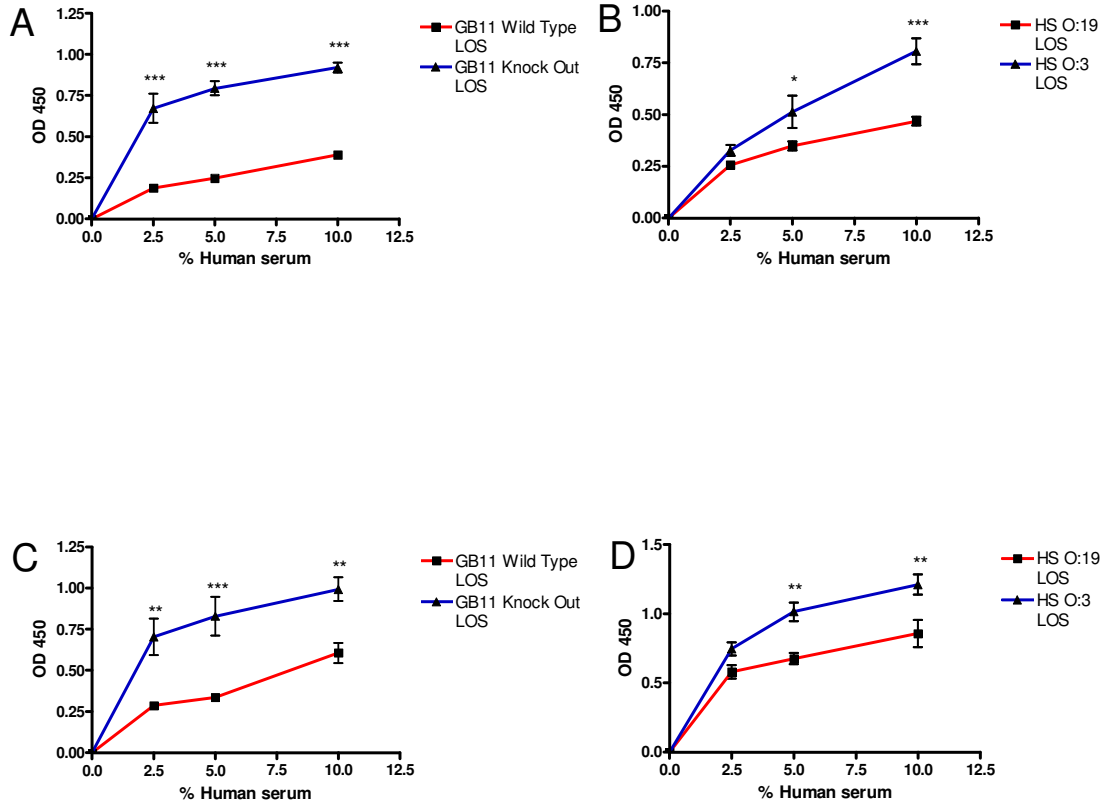


Figure 30. IgM and IgG binding to LOS following incubation with naïve human serum for 1 hour using ELISA. (A) IgM binding to GB11 wild type and knock out LOS; (B) IgM binding to HS O:19 and HS O:3 LOS; (C) IgG binding to GB11 wild type and knock out LOS and (D) IgG binding to HS O:19 and HS O:3 LOS. There is significantly greater IgM and IgG specific for non-ganglioside mimicking strains of LOS. Mean and SEM calculated from triplicate wells. Significance was calculated using 2way ANOVA with Bonferroni's posttest analysis (*= $p < 0.05$, **= $p < 0.01$, ***= $p < 0.001$). Graphs representative of 3 naïve donors.

4.2.11 Natural IgM and IgG binding to *C. jejuni* LOS

A potential explanation for increased complement deposition on non-sialylated strains is the presence of pre-existing “natural” antibodies which can activate the classical pathway. Self-tolerance predicts that there will be less natural antibody specific for ganglioside mimicking strains of LOS. To test this hypothesis, relative levels of IgM or IgG to ganglioside mimicking and non-mimicking LOS were compared using sera from three naïve human donors (each donor serum was tested individually). Figures 30 (A) and (B) show significantly greater levels of IgM to the non-ganglioside mimicking LOS compared to the relevant ganglioside mimicking LOS (GB11 wild type v knock out: $p < 0.001$ at 10%, 5% and 2.5% serum. HS O:19 v HS O:3: $p < 0.001$ at 10% serum and $p < 0.05$ at 5 % serum). Figures 30 (C) and (D) show significantly greater levels of IgG to the non-ganglioside mimicking LOS compared to the relevant ganglioside mimicking LOS (GB11 wild type v knock out: $p < 0.01$ at 10% and 2.5% serum, $p < 0.001$ at 5% serum. HS O:19 v HS O:3: $p < 0.01$ at 10 and 5% serum).

Figure 31: Anti-*C. jejuni* natural IgM and IgG.

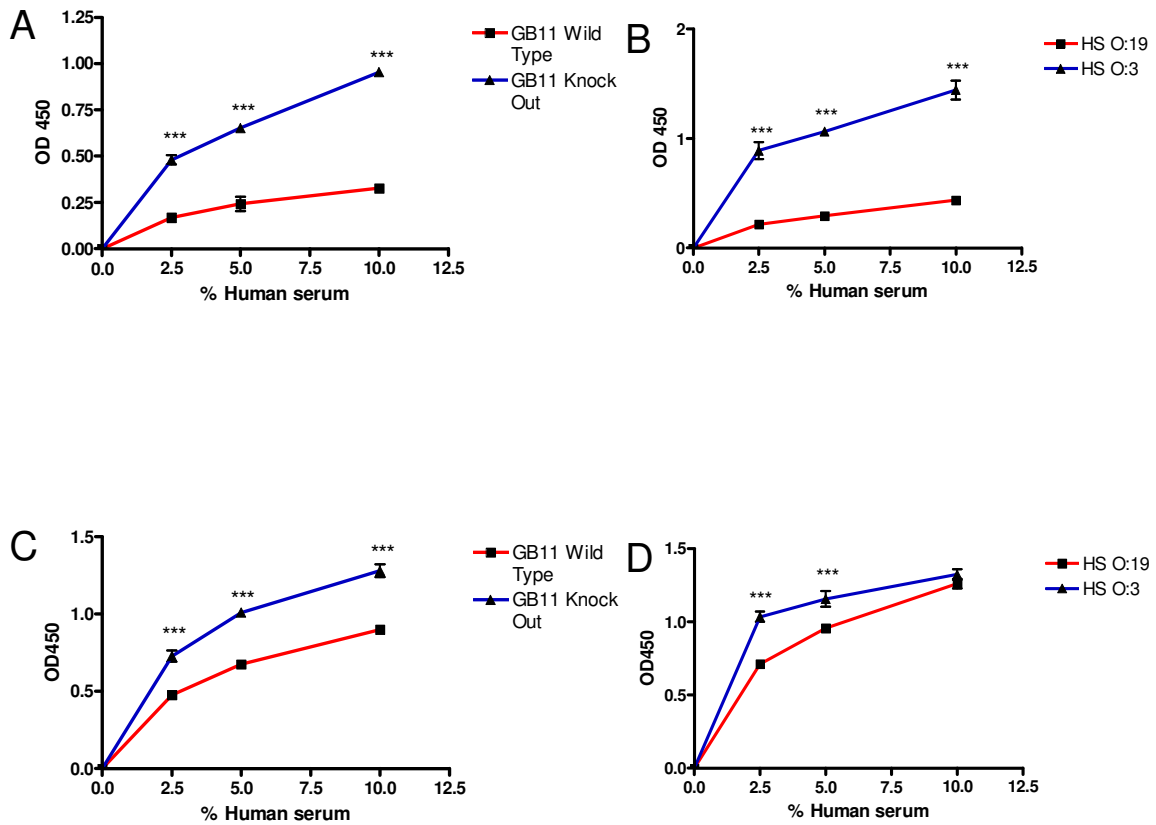


Figure 31. IgM and IgG to whole *C. jejuni* in naïve human serum using ELISA. (A) IgM binding to GB11 wild type and knock out *C. jejuni*; (B) IgM binding to HS O:19 and HS O:3 *C. jejuni*; (C) IgG binding to GB11 wild type and knock out *C. jejuni* (D) IgG binding to HS O:19 and HS O:3 *C. jejuni*. There are significantly more natural antibodies (IgM and IgG) to non-sialylated strains of *C. jejuni*. Mean and SEM calculated from triplicate wells. Significance was calculated using 2way ANOVA with Bonferroni's post test analysis (***)= $p < 0.001$). Graphs representative of 3 naïve donors.

4.2.12 Natural IgM and IgG binding to whole *C. jejuni*

Having demonstrated that there are fewer natural antibodies specific for purified ganglioside mimicking LOS than non-mimicking LOS it was hypothesised that there will be less natural antibodies specific for whole *C. jejuni* in ganglioside mimicking strains. Whole formalin fixed bacteria were adsorbed onto an ELISA plate and incubated with naïve human serum following which the *C. jejuni* specific antibodies were measured. Figures 31 (A) and (B) show IgM binding to ganglioside mimicking and non-mimicking strains. Figures 31 (C) and (D) show IgG binding. There is statistically more IgM (GB11 wild type v knock out: $p < 0.001$ over the whole titration. HS O:19 v HS O:3: $p < 0.001$ over the whole titration) and IgG (GB11 wild type v knock out: $p < 0.001$ over the whole titration. HS O:19 v HS O:3: $p < 0.001$ at 5 and 2.5% serum) to the non-ganglioside mimicking strains of *C. jejuni* when compared to the relevant ganglioside mimicking strains. Serum from three separate naïve individuals was tested and showed the same trend.

4.3 Discussion

Sialoadhesin (Siglec-1 or CD169) is a type 1 membrane protein with 17 extracellular immunoglobulin like domains²⁴⁶. Purified sialoadhesin is approximately 40nm²⁴⁷ in length and it is the largest member of the siglec family. In contrast to most siglecs, Sialoadhesin lacks tyrosine based signalling motifs. Sialoadhesin is constitutively expressed at high levels on specific subpopulations of macrophage including the metallophilic macrophages of the spleen and subcapsular sinus macrophages in the lymph node. It is also expressed at lower levels by tissue resident macrophage populations of the bone marrow and liver^{209,248}. Sialoadhesin expression can be modulated by a number of factors, for example IL4 inhibits Sialoadhesin expression²⁴⁹ while type 1 interferons and specific TLR agonists can increase expression²⁵⁰. Sialoadhesin has affinity for the terminal oligosaccharide sequence Neu5Ac α 2 \rightarrow 3Gal β 1 \rightarrow 3GalNac and has been shown to bind the ganglioside GD1a. It does not bind to GM1²⁴⁷. The function of Sialoadhesin is still being explored. It has been postulated as a lymphocyte adhesion molecule²⁵¹ and is believed to inhibit the function of regulatory T cells²⁵². Sialoadhesin knock out mice have reduced inflammation in experimental autoimmune uveoretinitis suggesting a possible pro-inflammatory role for Sialoadhesin²⁵³. In addition, knock out mice have subtle changes in B and T cell populations and reduced levels of IgM suggesting Sialoadhesin may have a role in antibody or B cell population regulation²⁵⁴. Sialoadhesin has also been shown to bind sialylated *N. meningitidis* resulting in enhanced phagocytosis²⁵⁵.

Due to its affinity for Neu5Ac α 2 \rightarrow 3Gal β 1 \rightarrow 3GalNac it was predicted that the Sialoadhesin-Fc fusion proteins would bind to GD1a and GD1a mimicking LOS. However, in my assays I found no evidence of binding. Contrary to this, I found that Sialoadhesin binds to GD1a mimicking whole *C. jejuni*. GD1a mimicking LOS, *in-situ*, was confirmed as the target on the native bacterium. The isogenic control strain, which differs only in its lack of ganglioside mimicry by the LOS, was unable to interact with Sialoadhesin. Direct visualisation of the binding and the loss of binding after specific

removal of the GD1a epitope further confirmed that Sialoadhesin is binding to GD1a on the bacteria.

A number of possible explanations for the lack of binding to LOS and native gangliosides were addressed by varying the protocol. Epitope density of the GD1a and LOS was increased by increasing the target concentration. The effects of secondary micelle structures were addressed by altering the buffer. Low Sialoadhesin avidity was addressed by pre-complexing it with biotin labelled anti-Fc and streptavidin-HRP. None of the changes to the protocol resulted in Sialoadhesin binding to gangliosides or ganglioside mimicking LOS. The Sialoadhesin-Fc reagent is composed of a truncated Sialoadhesin molecule (comprising the four N-terminal Ig domains – see Appendix 4 for structure) and it may therefore have a reduced capacity to bind its ligand. My results reflect the complexity of carbohydrate ligand binding in which repetitive epitopes and three dimensional structures can be essential for increasing avidity and this might explain why the Sialoadhesin reagent binds whole bacteria but not the LOS.

An additional unexpected finding is that Sialoadhesin does not bind to all of the GD1a mimicking *C. jejuni* and the binding tends to be localised to one or both poles of the bacterium. Manual counting of three fields found that 34% (ranging from 26% to 39%) of the ganglioside mimicking bacteria are labelled with Sialoadhesin and that 16% (ranging from 11% to 21%) are labelled at both poles. There are a number of possible explanations for this. Phase variation within the population might alter LOS expression and the two types of ganglioside mimicking LOS (GM1 and GD1a) might not be evenly dispersed across the surface of the bacterium. The *C. jejuni* polysaccharide capsule^{217,256} might be limiting access of the Siglec-Fc complexes to the poles of the organism where the flagellum penetrates the capsule. In addition, it is known in standard immunohistochemistry that formalin fixation can alter epitope expression by allowing soluble epitopes to diffuse off the target.

Siglec F has four extracellular immunoglobulin-like domains with an immunoreceptor tyrosine-based inhibitory motif on its cytoplasmic tail²⁵⁷. It has specificity for α 2-3 linked sialic acids and its constitutive expression is restricted to precursor cells of myeloid lineages²⁵⁷ and mature eosinophils²⁵⁸. Siglec F is also expressed by a subset of CD4⁺ T cells following induction of allergic lung inflammation²⁵⁹. As well as signalling, Siglec F has endocytic properties, delivering ligands to lysosomes²⁶⁰. The human homologue, Siglec 8, is restricted to eosinophils and basophils. Cross-linking Siglec F induces apoptosis in eosinophils and it has been postulated that upregulation of Siglec F ligands during allergic inflammation may contribute to a negative feedback loop, limiting disease²⁵⁹.

My assay shows Siglec F binding to GD1a and GT1b. Consistent with this affinity for GD1a, for the first time, Siglec F binding to ganglioside mimicking LOS and whole *C. jejuni* is shown. When visualised, the binding pattern was similar to Sialoadhesin although it appeared that more of the ganglioside mimicking bacteria were labelled. Manual counting of three fields found that 87% (ranging from 86% to 89%) of ganglioside mimicking bacteria labelled for Siglec F. In addition, 22% of these (ranging from 17% to 30%) had distinct labelling at both poles. However, subjectively, the Siglec F binding was more diffuse around the edge of the bacteria instead of the distinct punctate staining seen with Sialoadhesin. Siglec F binds native ganglioside, LOS and whole bacteria, therefore the different binding pattern might reflect it being a better reagent than Sialoadhesin. Alternatively, it might bind to a more conserved part of GD1a or, being a smaller siglec than Sialoadhesin, it might gain easier access to its target epitopes. Further studies could be carried out using FACS analysis to gain an objective measure of siglec binding and ideally heat inactivated or live bacteria should be used to exclude fixation artefact.

Siglec E has three extracellular immunoglobulin-like domains while its intracellular domain contains two immunoreceptor tyrosine based inhibitory motifs²⁶¹. It appears to be a functional orthologue of human siglecs 7 and 9. Siglec E shows differing affinity for

a number of sialic acid arrangements in the order α 2,8 disialic acid> α 2,3 sialylactose> α 2,6 sialylactose²⁵⁸. Siglec E is expressed on neutrophils, peritoneal macrophages, splenic myeloid dendritic cells and subsets of NK cells²⁵⁸. Weak Siglec E expression is also found on peritoneal B1a B cells as well as splenic T2 and MZ B cells²⁵⁸.

Siglec E shows strongest binding to ganglioside GD1a with less binding to GT1b. There was weak binding to the asialo-glycolipids, which are mimicked by the GB11 knock out strain. However, in contrast to these findings, Siglec E shows very high affinity for the GB11 knock out LOS (significantly greater than the wild type strain) with greater binding to HS O:3 LOS compared to HS O:19 at high concentrations. Binding to the whole *C. jejuni* shows a mixed profile.

Binding to GB11 knock out LOS and its respective asialo-glycolipids was compared directly at matching concentrations. Binding to LOS was significantly greater than to the respective asialo-sugars suggesting that the epitope is not the core sugars of the LOS. Using complexed asialo-glycolipid molecules (i.e. asialo-GM1, asialo-GM2 and lactosyl ceramide together) did not replicate the LOS binding. Further, an additional species of LOS (salmonella) was compared to establish if the lipid A or internal core sugars might provide a conserved epitope unique to LOS but not found in asialo-glycolipids. There was no evidence that this is the case.

Direct visualisation of Siglec E binding to whole *C. jejuni* reveals high levels of non-specific background staining. One possibility is that epitopes are shed from whole killed *C. jejuni* perhaps during the freeze/thaw process. However, the bacteria were formalin fixed specifically to preserve their structural integrity and there is no evidence of this problem with either Sialoadhesin or Siglec F. The binding buffer (methanol) and blocking buffer (3% BSA) were also tested for Siglec E binding and, while the

background was higher than for other siglecs, this did not account for the strong GB11 knock out LOS binding.

Siglec E is known to have a wider specificity than the other siglecs tested and the α 2,3 sialylactose epitope found on LOS is not its preferred epitope. However, this does not provide an explanation for the observed binding. No satisfactory conclusion could be drawn as to the epitope in GB11 knock out LOS that Siglec E binds to. The visualisation studies suggest the reagent is sticky and non-specific. This further confirms the complexity and difficulty of studying carbohydrate epitopes.

The siglec binding results confirm one of the central hypotheses; that ganglioside mimicking LOS and whole ganglioside mimicking *C. jejuni* can bind to cellular receptors via their ganglioside mimics. Only three receptors, out of many potential ganglioside receptors, were tested and their binding specificities were very idiosyncratic. Although the function of siglecs is poorly understood, in principle this could result in additional LOS signalling events (in combination with TLR4) or altered trafficking of bacteria. Experiments designed to test these hypotheses are reported later in the thesis.

Complement is a conserved component of the innate immune system which consists of ~40 serum and cell associated proteins. Complement functions to opsonise and lyse bacteria; link the innate and adaptive immune systems and remove immune complexes and apoptotic cells before they trigger unwanted inflammation. There are three pathways of complement activation: the classical pathway, the alternative pathway and the mannose-binding lectin pathway. The alternative pathway is continuously activated at a low level by the hydrolysis of C3. Self-damage and amplification is kept in check by a number of complement regulatory proteins. The classical pathway is activated by C1q binding to antibody bound to the surface of a target. The classical and alternative complement cascades converge at the level of C3 convertase. The final common

pathway involves the formation of a Membrane Attack Complex pore on the surface of the target by polymerisation of C9²⁶².

Factor H is 150kDa glycoprotein consisting of 20 short consensus repeats²⁶³. It is synthesised predominantly in the liver and is part of a structurally related family of proteins. Factor H functions as a complement regulatory protein that inhibits the classical and alternate complement cascades by interfering with C3 convertase^{199,200}. Factor H competes with Factor B and inhibits convertase formation²⁶⁴, it facilitates the dissociation of the convertase²⁶⁵ and fH is a cofactor for Factor I mediated cleavage of C3b²⁶⁵. Factor H binds to a number of ligands including C3b, C3d, heparin, self-glycosaminoglycans and bacterial virulence factors^{266,267}. Sialic acid is an important target for fH binding on self-cells and this protects against complement activation^{268,269}. However, sialylation is also used by pathogens where it is believed to increase their resistance to complement mediated lysis²⁴²

Using a variety of techniques, my assays showed no evidence of purified fH binding to either sialylated or non-sialylated strains of *C. jejuni*. This was unexpected given the known binding site for sialic acid present on fH. Previous publications have shown that fH binds to GM1 ganglioside and inhibits Complement activation on liposomes²⁷⁰. Factor H binding to sialylated *N. gonorrhoeae*²⁴² has also been demonstrated. However, it has become clear that the gonococcal porin Por1B is responsible for fH binding to *N. gonorrhoeae*²⁴⁵ while *N. meningitidis* produces a Factor H Binding Protein capable of mimicking charged carbohydrates and binding fH²⁷¹. In support of my negative results, some sialylated strains of *N. gonorrhoeae* do not bind fH²⁴². The contribution of sialylation to complement resistance in these species is not clear and it appears that sialic acid is neither necessary nor sufficient for fH binding. I could not show fH binding to sialylated *C. jejuni* and this may be due to complexities in the role of sialic acid in fH binding, due to a problem with the purified fH reagent or due to alterations of the sialic acid fH binding sites on the heat killed or fixed bacteria.

Following incubation with active human serum, fH was detected at higher levels on the non-sialylated strains. I believe this is due to deposition of C3b on the *C. jejuni* providing a binding site for fH. Alternatively, this may be due to the anti-fH mAb binding to the Factor H Related Proteins which are present in serum and share a similar structure to fH. In support of the former hypothesis, I showed greater C3 and C9 complement deposition on the non-sialylated strains. C3c is a breakdown product of C3b under the influence of Factor I and Factor H. Anti-C3c antibodies are not able to distinguish between C3c and the C3c portion of native C3 or C3b. However measuring C3c has the advantage of not being sensitive to complement consumption as it gives a total measure of recent complement activation (i.e. native C3b and metabolised C3b).

It was hypothesised that the difference in complement activation is due to enhanced classical pathway activation through the action of natural antibody and it was expected that there are less natural antibodies specific for the sialylated strains of LOS because of self-tolerance. This was investigated by measuring IgM and IgG specific for the ganglioside mimicking or non-mimicking LOS. In addition, I show that there are less natural antibodies to the ganglioside mimicking whole bacteria when compared to the non-mimicking control strains. The complement and antibody experiments used sera of three naïve humans (that is, subjects who self-reported no known previous exposure to *C. jejuni*). However, this is too small a number to draw definitive conclusions and further studies using pooled human serum from many donors are necessary.

Further experiments are required to support these hypotheses. For example, measuring complement deposition in the absence of immunoglobulin (purified human complement) would confirm or refute the role of natural antibody. My findings that all of the serum components tested (fH, C3, C9 and Ab) bound more to non-sialylated bacteria could be due to an experimental flaw. For example, my method of quantifying the bacteria might be inaccurate (if one strain is stickier than the other it might clump and affect the OD600 reading). The strong negative charge of sialic acid might reduce binding of these strains to the ELISA plate or it might repel complement and antibodies in a non-specific manner.

My studies could be made more relevant by measuring serum resistance, that is, the ability of live bacteria to survive incubation with human serum. The differences I measured in complement and antibody binding are relatively small therefore such studies would give a better idea of the physiological importance of these findings. This could not be done in my laboratory due to restrictions on the use of live pathogens.

In conclusion, by demonstrating Sialoadhesin binding to GD1a mimicking *C. jejuni* and Siglec F binding to ganglioside mimicking LOS and *C. jejuni* I have confirmed my hypothesis that the ganglioside mimics on GBS associated strains of *C. jejuni* can interact with endogenous immune system receptors. Siglec E did not show specific binding. In addition, and in contrast to my initial expectations, I found no evidence of fH binding to sialylated *C. jejuni*. However, *C. jejuni* ganglioside mimicry results in less complement activation which may be related to my finding of lower natural antibody levels against these strains. These findings require further clarification.

5 Immunostimulatory effects and potency of purified *C. jejuni* LOS

5.1 Introduction

The aim of the experiments presented in this chapter is to investigate the immunostimulatory properties of *C. jejuni* LOS and to establish if ganglioside mimicry has an effect on potency.

Ganglioside mimicking *C. jejuni* LOS can be conceptually divided into two portions; the Lipid A tail and the ganglioside mimicking external core. Lipid A is the “endotoxic principal” of lipopolysaccharides^{111,210-212,272} and mediates a plethora of immunostimulatory effects via signalling through the LPS receptor complex, TLR4-MD2, in conjunction with co-receptor CD14^{116,119}. The primary responder cells to LPS are those of the myeloid lineage; monocytes, macrophages, dendritic cells and neutrophils, which constitutively express CD14 and TLR4¹⁰⁵⁻¹⁰⁸. B cells are also sensitive to LPS although the receptors employed are less well characterised. While TLR4 is not expressed on human B cells^{108,197} a structurally related complex, RP105-MD1, appears to confer sensitivity to LPS²⁷³. In mouse models, the absence of either RP105 or MD1 results in B cell hyporesponsiveness, although absence of TLR4 or MD2 results in a complete loss of sensitivity^{127,274-276}. This illustrates potential murine-human disparities and the complexity of the LPS sensing system.

Myeloid cells respond to LPS stimulation at picomolar concentrations. LPS has a panoply of effects, principal amongst them being secretion of acute phase cytokines; TNF- α , IL-1 and IL-6, as well as immunomodulatory cytokines such as IL-12 and IL-10²⁷⁷⁻²⁸². LPS has important adjuvant effects which include maturation of antigen presenting cells coinciding with increased co-receptor expression and enhanced antigen presentation²⁸³⁻²⁸⁶.

The B cell compartment is broadly divided into two subsets. The B1 subset comprises B1a and B1b B cells and the B2 subset comprises MZ and FO B cells. B1 B cells are located primarily in the peritoneal and pleural cavities¹⁵⁸ while MZ B cells are located in close proximity to the marginal zone and Sialoadhesin expressing metallophilic macrophage populations near the marginal sinuses of the spleen¹³¹. Both B1 B cells and MZ B cells are important in T-independent antibody responses, have a tendency towards polyreactivity and autoreactivity, and produce natural antibodies against carbohydrate antigens^{131,158}. In addition, and in contrast to FO B cells, they are highly responsive to LPS stimulation which results in proliferation, maturation and antibody secretion¹⁰⁹. Marginal zone B cells are mobilised by LPS and play a role in transporting antigen into the follicle²⁸⁷⁻²⁹⁰ where they can function as potent antigen presenting cells¹⁶⁸. In addition, following LPS stimulation, they are an important source of the cytokine IL-10²⁹¹. LPS is a Type I TI antigen which is capable of directly triggering polyclonal B cell activation and proliferation²⁹².

Bacteria exhibit substantial inter-species differences in LPS structure¹⁰². LPS and LPS analogues, derived from diverse bacterial species, in addition to causing TLR4-MD2 homodimerisation, appear capable of interacting with different receptor clusters, recruiting unique combinations of signalling proteins and stimulating different cellular responses²⁹³⁻²⁹⁶. While differences in LPS potency clearly exist, such studies are inevitably complicated by impurities present in the LPS preparation and must be interpreted with caution.

C. jejuni LOS, while structurally similar to related species, has a number of unique differences. A glucosamine residue of the Lipid A backbone is replaced with a related sugar, 2,3-diamino-2,3-dideoxy-D-glucose, and the inner core contains a unique tetrasaccharide (Glc-Hep-Hep-Kdo)^{102,112}. In addition, the acyl chains are particularly long which, combined with the absence of an O-side chain, makes the molecule highly hydrophobic.

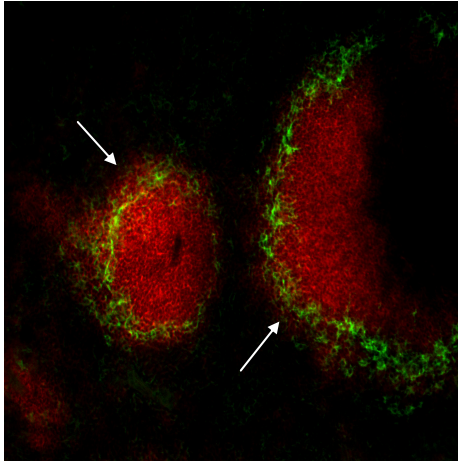
GBS associated *C. jejuni* LOS are exclusively rough mutant. Substantial differences are thought to exist between sensing and signalling of smooth mutant LPS (S-form) and rough mutant LPS (R-form). While S-form LPS requires LBP and CD14 in order to signal, R-form LPS can bind to TLR4/MD-2 directly^{99,123} and cells lacking CD14 (such as mast cells and B cells) can recognise R-form LPS without the CD14 and LBP accessory molecules⁹⁹. In addition, signalling by R-form LPS, in the absence of LBP and CD14, results in signal transduction via the MyD88 dependent pathway with only weak signalling via the TRIF dependent pathway^{99,123,297}.

Gangliosides have long been recognised as immune system modulators¹³⁴. Incubation of human dendritic cells with purified GD1a ganglioside causes inhibition of IL-12 production and enhanced IL-10 production, although subsequent co-culture with naïve T cells results in a blunting of both Th1 and Th2 differentiation²⁹⁸. Pre-incubation of dendritic cells with GD1a also inhibits subsequent co-stimulator upregulation and cytokine production following LPS stimulation²⁹⁹. T cells incubated with GD1b, GT1c or GQ1b show enhanced Th1 cytokine production when stimulated with PHA (phytohaemagglutinin)³⁰⁰ while human B cells incubated with GM2 or GM3 show inhibited immunoglobulin production and reduced thymidine uptake (GM1 and GD1a have no effect)³⁰¹. Although gangliosides are generally considered immunosuppressive, there is no clear consensus on their specific effects or the mechanisms by which they produce these effects. The complexity of the ganglioside repertoire complicates such studies. Gangliosides, and ganglioside mimicking LOS, are capable of engaging immune system receptors such as siglecs (demonstrated previously in 4.2.4 and 4.2.5). In addition, gangliosides are important self ligands for presentation in the CD1 family of glycolipid antigen presentation molecules and this allows them to interact with specific subsets of T cells³⁰²⁻³⁰⁴. Due to the ubiquitous nature of gangliosides, and their co-localisation on plasma membrane lipid rafts with a wide array of signalling molecules in lymphocytes^{305,306}, there is potential for exogenous gangliosides, or ganglioside mimics, to insert into membranes and disrupt signalling.

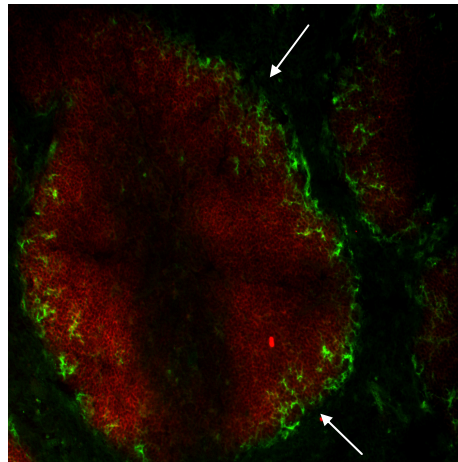
One of my central hypotheses is that ganglioside mimicry alters the potency of LOS. In the experiments in this chapter I compare ganglioside mimicking LOS to LOS derived from isogenic, non-mimicking, control strains in their ability to stimulate those cell types most likely responsible for the effector stage (B cells) and induction stage (myeloid cells) of GBS. This hypothesis is not without precedent. I have demonstrated ganglioside mimicking LOS engaging siglec receptors through the O-side chain and this may alter adjuvant activity in a similar manner to *E. coli* and Klebsiella LPS strains which contain mannose in the carbohydrate O-side chain and which show enhanced adjuvant activity through binding to the mannose receptor on myeloid cells^{150-152,307-309}.

Figure 32: *In vivo* mobilisation of marginal zone B cells by LPS.

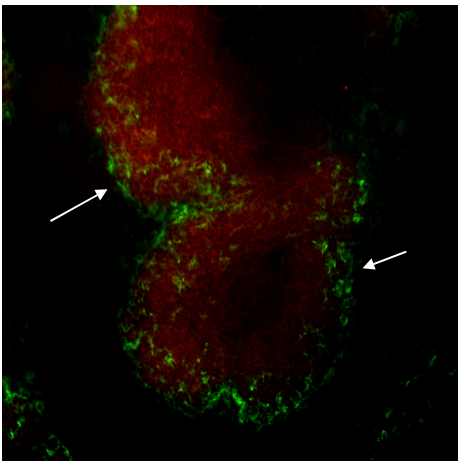
A) PBS injected
MOMA1 FITC
B220 Alexa 647



B) *S. typhimurium* LPS injected
MOMA1 FITC
B220 Alexa 647



C) GB2 Wild type LOS injected
MOMA1 FITC
B220 Alexa 647



D) GB2 Knock out LOS injected
MOMA1 FITC
B220 Alexa 647

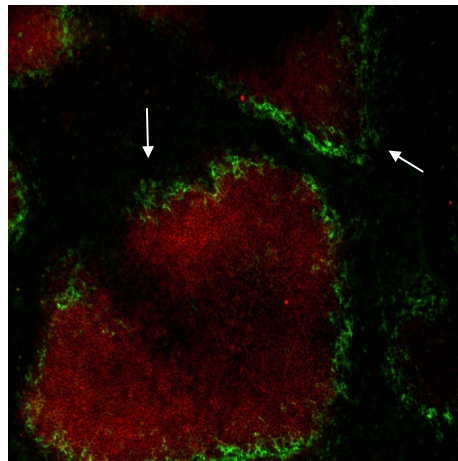


Figure 32. Immunohistology of murine spleens following LOS injection. Metallophilic macrophages (MOMA1 positive, green) mark the edge of the follicles. B cells, including MZ B cells, are labelled with B220 (red). (A) PBS injected. White arrows show B cells outwith the metallophilic macrophages. (B) Smooth mutant *S. typhimurium* LPS injected mouse spleen. (C) GB2 wild type *C. jejuni* LOS injected spleen. (D) GB2 knock out *C. jejuni* LOS injected spleen. (B, C, D) White arrows show absence of B cells in the marginal zone following LPS or LOS injection. Images representative of three experiments.

5.2 Results

5.2.1 *In vivo* mobilisation of Marginal Zone B cells

Marginal zone B cells are potentially important in GBS because they are a source of antibodies directed against carbohydrate antigens^{131,158}, they are responsive to LPS¹⁰⁹ and they are believed to contain auto-reactive specificities within their repertoire. Marginal zone B cells are also potent antigen presenting cells¹⁶⁸ and have been shown to migrate and carry antigen from the marginal zone of splenic follicles into the follicle^{287,289,290}. This mobilisation occurs rapidly in response to LPS stimulation and the aim of my initial experiments was to test whether or not *C. jejuni* LOS could do the same.

Mice were injected intra-peritoneally with 50µg of GB2 wild type LOS, GB2 knock out LOS, *S. typhimurium* LPS (smooth mutant) and PBS (the latter two being positive and negative controls respectively). After 18 hours, spleens were harvested and frozen. Frozen sections were stained with the mAb MOMA1, which is specific for the metallophilic macrophage marker Sialoadhesin and distinguishes the edge of the follicle, and a mAb specific for the B cell marker B220. Figure 32 shows immunohistology of splenic sections. Figure 32 (A) shows a section from a mouse injected with PBS. The white arrows indicate the position of B220 positive marginal zone B cells (red) outwith the MOMA1 positive metallophilic macrophage population (green). Follicular B cells also stain positive for B220 and are present within the follicle which is surrounded by the MOMA1 positive macrophage population. Figures 32 (B), (C) and (D) show sections following injection with *S. typhimurium* LPS, GB2 wild type LOS and GB2 knock out LOS respectively. B cells are no longer present in the marginal zone (white arrows) indicating that LOS is capable of mobilising MZ B cells. Ganglioside mimicry does not affect this property.

Figure 33: Example FACS plots of labelled B cells.

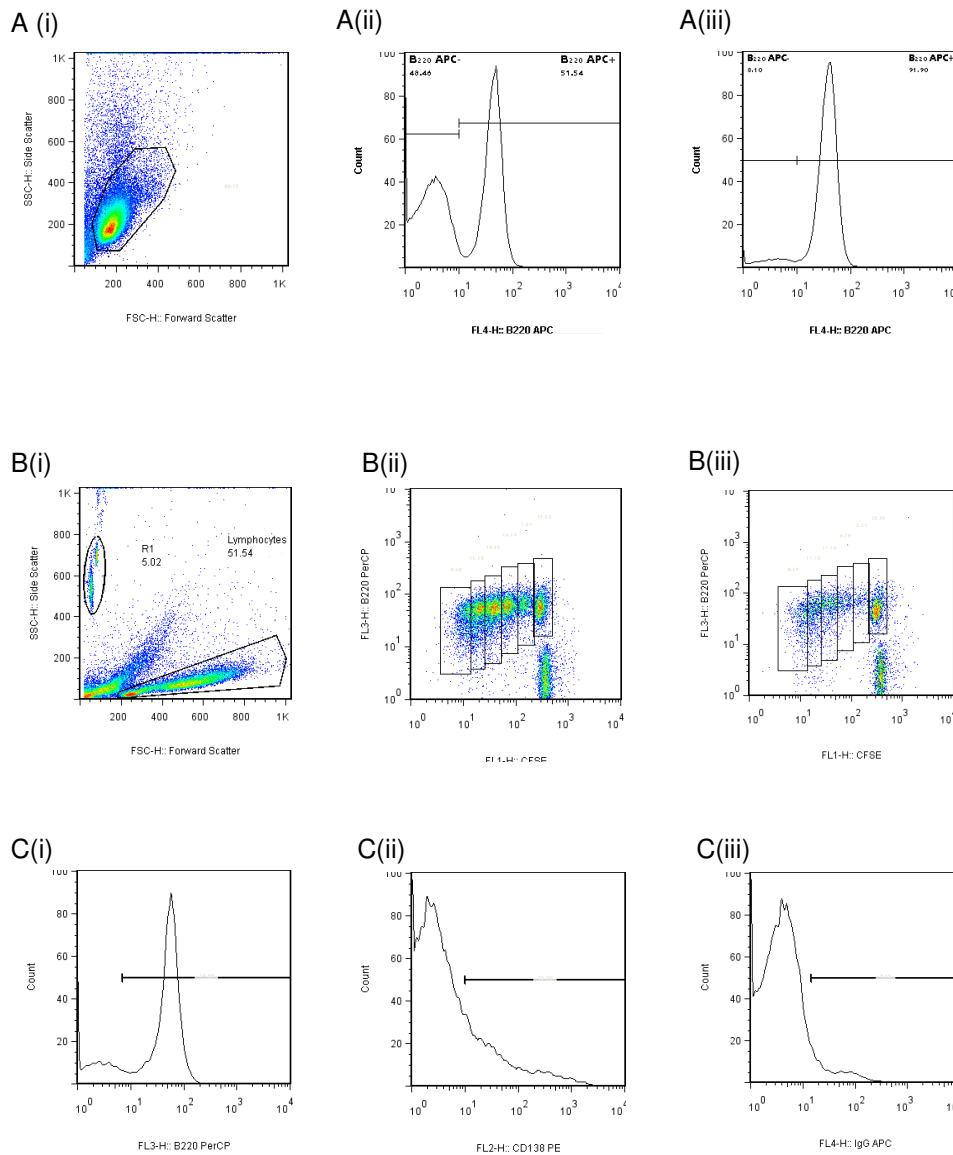


Figure 33. Example FACS plots of (A) B cell selection, (B) tracking B cell division using CFSE and (C) B cell subpopulations. B cells were purified from mixed splenocytes using the EasySep B cell negative selection kit. (A) FACS analysis showing B cell purity before and after magnetic bead negative selection. (A) (i) Parent lymphocyte gate on forward and side scatter, (A) (ii) Pre-selection purity (51.24% B220+). (A) (iii) Post selection purity (>91% B220+). (B) FACS analysis of cell division. (B) (i) Forward v side scatter of mixed splenocytes including the parent lymphocyte gate and the Caltag counting beads (R1). (B) (ii) Dot plot showing CFSE v B220. Each gate is a B cell population in a particular round of division 72 hours after *E. coli* LPS stimulation. (B) (iii) as before except *C. jejuni* LOS stimulation. (C) Examples of gates used to determine the size of each population (C) (i) B220+ B cell population (parent population to C (ii) and (iii)). C (ii) CD138 positive B cell population. C (iii) IgG positive B cell population.

5.2.2 B cell activation by ganglioside mimicking and non-mimicking *C. jejuni* LOS in a purified B cell culture

To test the B cell stimulatory potency of *C. jejuni* LOS in a pure B cell culture, B cells were purified using negative selection from a mixed splenocyte population. The EasySep B cell negative selection kit uses a panel of antibodies, directed against non-B cells, magnetic nanoparticles and a magnetic sleeve to remove unwanted cells without antibodies binding to the B cells. Figure 33 (A) shows B cell purity before and after negative selection by labelling with the B cell marker B220 (all experiments resulted in purity of >90%). To assess mitogenic potency, cells were labelled with the cell tracking fluorophore CFSE^{310,311}. CFSE forms covalent bonds with intracellular molecules and the fluorescence of the cell halves with each round of mitosis. Cell division can be tracked using flow cytometry and Figure 33 (B) shows example FACS plots of *E. coli* LPS and *C. jejuni* LOS stimulated B cells co-labelled with the B cell marker B220. Each gate is a B cell population in the same round of division. The concentration of cells was derived from the FACS data using Caltag counting beads, a known concentration of which was added to the samples prior to analysis and from which the cell concentration can be mathematically derived (according to the manufacturers lot specific instructions). B cells were stimulated with 20µg/ml ganglioside mimicking (GB2 wild type) or non-mimicking (GB2 CSTII knock out) *C. jejuni* LOS or *E. coli* LPS as a control. Plasma cell differentiation was measured by co-labelling with the plasma cell differentiation marker CD138³¹² (Syndecan1) and IgG isotype switching measured by co-labelling with anti-IgG (example FACS plots shown in figure 33 (C)).

Figure 34: B cell responses to *C. jejuni* LOS in a purified B cell population.

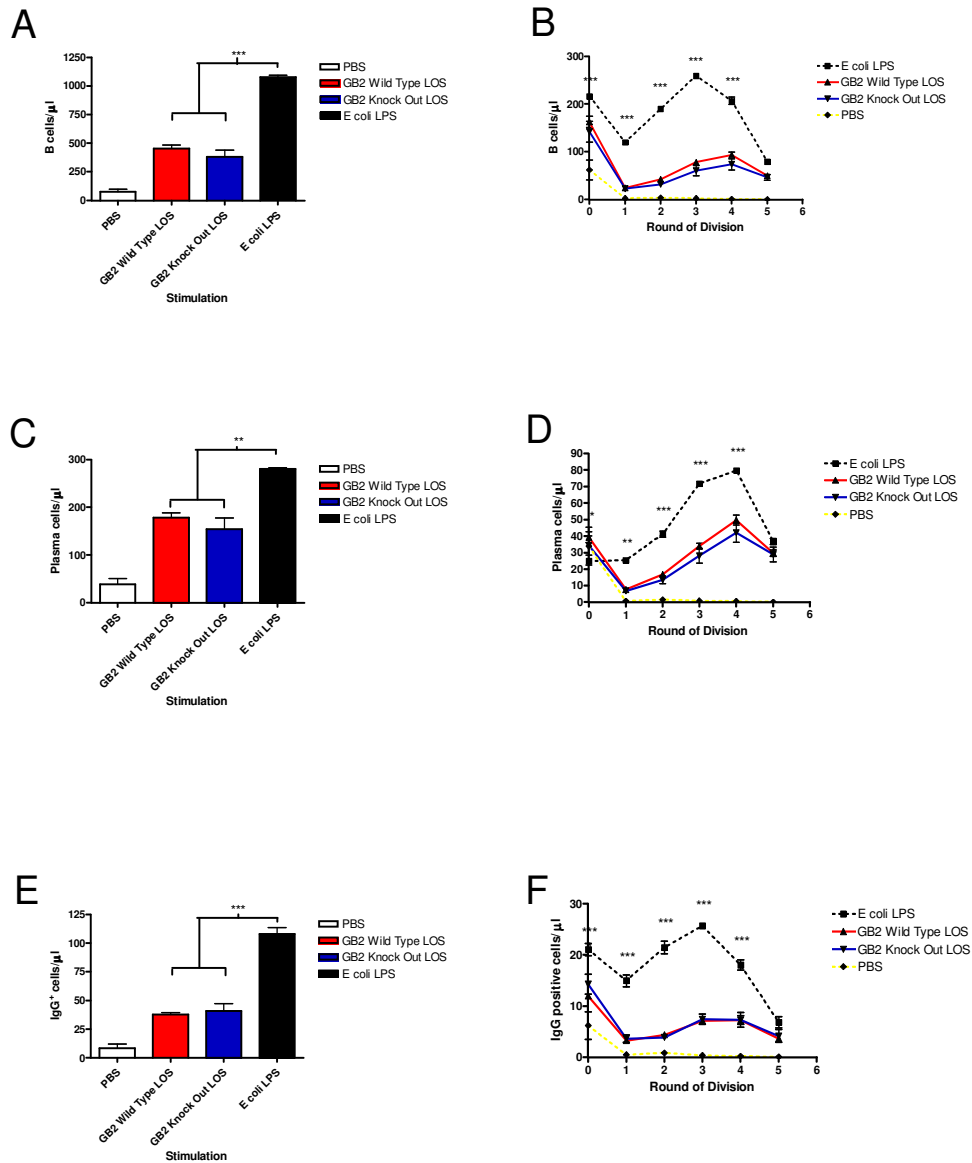


Figure 34. Purified B cells responses to LOS/LPS stimulation measured by FACS analysis. The cells were harvested and labelled for the B cell marker B220, the plasma cell marker CD138 and surface IgG expression. Cells were enumerated using Caltag counting beads. (A) concentration of B cells (B220 positive). (B) concentration of B cells in each round of division. (C) concentration of CD138 positive cells. (D) Concentration of CD138 positive cells in each round of division. (E) Concentration of IgG positive B cells. (F) Concentration of IgG positive B cells in each round of division. Mean and SEM calculated from triplicate tubes. Representative of two experiments. Bar graphs analysed using 1way ANOVA with Bonferroni's multiple comparison test, Line graphs analysed using 2way ANOVA with Bonferroni's posttests (*= $p < 0.05$, **= $p < 0.005$, ***= $p < 0.001$).

Figure 34 (A) shows the total B cell concentration at 72 hours after stimulation with 20µg/ml wild type LOS, knock out LOS or *E. coli* LPS. There is no statistical difference between either of the *C. jejuni* LOS strains. However, twice as many B cells are present following *E. coli* LPS stimulation ($p<0.001$). Figure 34 (B) shows the concentration of B cells in each round of division. *C. jejuni* LOS and *E. coli* LPS both induced B cell division. However, there are significantly more B cells in rounds 0, 1, 2, 3 and 4 of division following *E. coli* LPS stimulation ($p<0.001$) compared to *C. jejuni* LOS stimulation. There is no statistical difference between the *C. jejuni* LOS strains. These results suggest *E. coli* LPS is more potent at stimulating B cell mitosis in a pure B cell culture than *C. jejuni* LOS and that ganglioside mimicry has no effect on LOS potency.

The ability of *C. jejuni* LOS to stimulate plasma cell differentiation in a purified B cell culture was assessed by co-staining the B cells with the plasma cell differentiation marker CD138. Figure 34 (C) shows the concentration of CD138 positive cells present after 72 hours. There is no statistical difference between the *C. jejuni* LOS strains. However, the *E. coli* LPS has stimulated greater CD138 positive cell differentiation ($p<0.01$). Figure 34 (D) shows the concentration of CD138 positive cells in each round of division. A greater number of CD138 positive cells did not divide (remaining in round 0) following *C. jejuni* LOS stimulation compared to *E. coli* LPS stimulation ($p<0.05$). A greater number of CD138 positive cells were in each subsequent round of division (except round 5) following *E. coli* LPS stimulation (Round 1 $p<0.01$, rounds 2 to 4 $p<0.001$). There was no difference in potency at generating CD138 positive cells between the *C. jejuni* LOS strains.

To assess the capacity of *C. jejuni* LOS to stimulate isotype switching to IgG, B cells were co-stained with an IgG specific antibody. Figure 34 (E) shows the concentration of IgG positive B cells after 72 hours of stimulation. There is no statistical difference between the ganglioside mimicking and non-mimicking *C. jejuni* LOS strains. However, *E. coli* LPS stimulation resulted in more than twice as many IgG positive B cells ($p<0.001$). Figure 34 (F) shows the concentration of IgG positive B cells in each round

of division. There are no differences between either LOS strains. *E. coli* LPS stimulation resulted in more IgG positive B cells in all rounds of division except round 6 ($p < 0.001$).

Figure 35: B cell responses to *C. jejuni* LOS in a mixed splenocyte population.

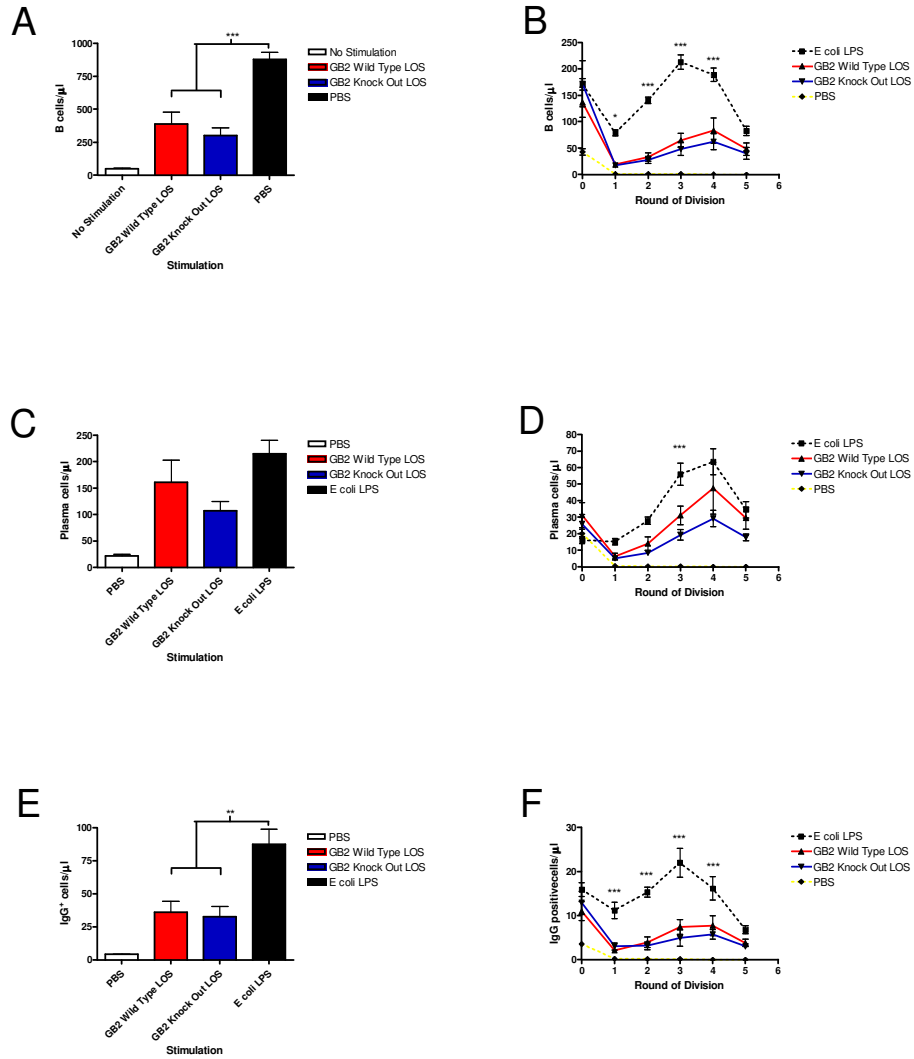


Figure 35. Mixed splenocyte response to LOS/LPS stimulation measured by FACS analysis. The cells were harvested and labelled for the B cell marker B220, the plasma cell marker CD138 and IgG expression. The number of cells was enumerated using Caltag counting beads. (A) Concentration of B cells (B220 positive) (B) Concentration of B cells in each round of division. (C) Concentration of CD138 positive cells. (D) Concentration of CD138 positive cells in each round of division. (E) Concentration of IgG positive B cells. (F) Concentration of IgG positive B cells in each round of division. Mean and SEM calculated from triplicate tubes. Representative of two experiments. Bar graphs analysed using 1way ANOVA with Bonferroni's multiple comparison Test, Line graphs analysed using 2way ANOVA with Bonferroni's posttests (*= $p < 0.05$, **= $p < 0.01$, ***= $p < 0.001$).

5.2.3 B cell activation by ganglioside mimicking and non-mimicking LOS in a mixed splenocyte culture

Myeloid lineage cells can act as accessory cells for B cell activation and survival³¹³ and are sensitive to LPS. It was decided to compare the B cell activating potency of ganglioside mimicking and non-mimicking LOS in a mixed splenocyte culture (i.e. including accessory cells). The methods used were the same as before.

Figure 35 (A) shows the total B cell concentration in a mixed splenocyte culture. There are more remaining B cells after 72 hours following *E. coli* LPS stimulation than *C. jejuni* wild type or knock out LOS ($p < 0.001$). There is no statistical difference between either of the *C. jejuni* LOS strains. Figure 35 (B) shows the concentration of B cells in each round of division. LOS and LPS have both stimulated B cell mitosis although there are significantly more B cells in rounds 1 ($p < 0.05$), 2 ($p < 0.001$), 3 ($p < 0.001$), and 4 ($p < 0.001$) of division following *E. coli* LPS stimulation. There is no statistical difference between the *C. jejuni* LOS strains. These results confirm *E. coli* LPS is more potent at stimulating B cell mitosis than *C. jejuni* LOS. Ganglioside mimicry has no effect on LOS induced B cell mitogenicity.

Figure 35 (C) shows the concentration of CD138 positive cells present after 72 hours. There is no statistical difference between either of the *C. jejuni* LOS strains or the *E. coli* LPS. Figure 35 (D) shows the concentration of CD138 positive cells in each round of division. There are more CD138 positive cells in round 3 of division following *E. coli* LPS stimulation ($p < 0.001$). There are no statistical differences between the wild type of knock out LOS strains.

Figure 35 (E) shows the concentration of IgG positive B cells. *E. coli* LPS stimulation results in more IgG positive B cells after 72 hours ($p < 0.01$), while there is no difference between the *C. jejuni* LOS strains. Figure 35 (F) shows the concentration of IgG positive

B cells in each round of division. There are more IgG positive B cells in rounds 1, 2, 3 and 4 ($p < 0.001$) following *E. coli* LPS stimulation compared to *C. jejuni* LOS stimulation. There is no difference between either of the *C. jejuni* strains.

Combined, these results show *E. coli* LPS to be more potent than *C. jejuni* LOS. Ganglioside mimicry does not appear to enhance *C. jejuni* LOS potency.

Figure 36: Immunoglobulin production by LOS stimulated B cells and splenocytes.

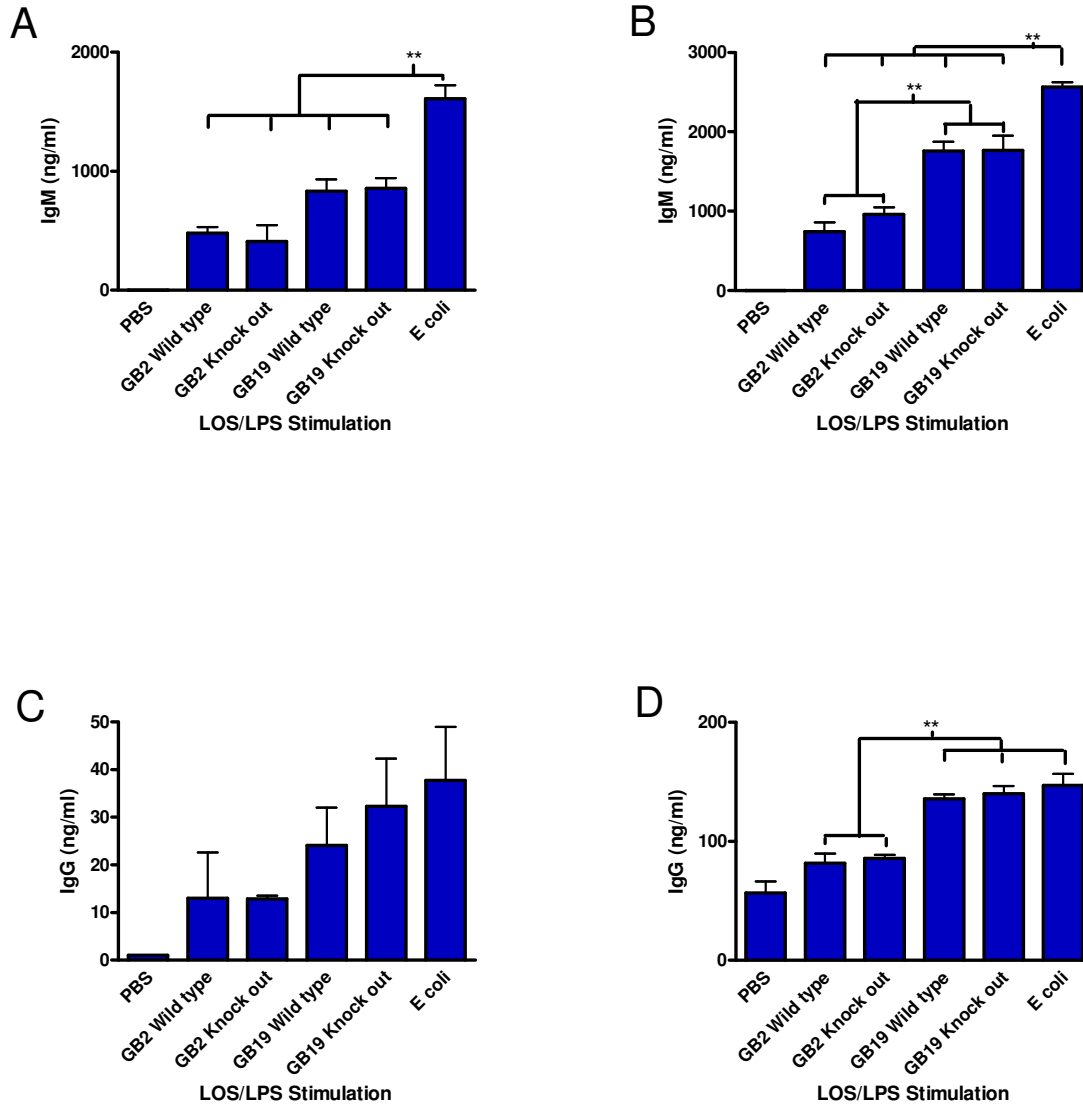


Figure 36. Purified B cells or mixed splenocytes were stimulated with 10 μ g/ml of GB2 or GB19 strains of *C. jejuni* LOS or *E. coli* LPS for 72 hours and immunoglobulin secretion was measured in the supernatant using ELISA. (A) Shows IgM production by purified B cells. (B) Shows IgM production by mixed splenocytes. (C) Shows IgG production by purified B cells. (D) Shows IgG production by mixed splenocytes. Mean and SEM calculated from triplicate wells. Analysed using 1way ANOVA with Bonferroni's multiple comparisons test (**= $p < 0.01$, ***= $p < 0.001$). Representative of three experiments.

5.2.4 Comparison of LOS potency at stimulating antibody secretion

Having compared the potency of ganglioside mimicking and non-mimicking LOS at stimulating B cell mitosis and CD138 positive cell differentiation it was decided to compare immunoglobulin secretion as another measure of potency.

Purified B cells or mixed splenocytes were cultured for 72 hours with 10 μ g/ml LOS and antibody secretion into the supernatant was measured using an ELISA. An additional ganglioside mimicking LOS, GB19 wild type mimicking GD1c, and the CSTII knock out control was included in the assay. Figure 36 (A) shows IgM production by a purified B cell population. There is no difference in IgM production between wild type and knock out LOS in both the GB2 and GB19 strains. There is also no statistical difference between both GB2 and both GB19 strains. *E. coli* LPS is more potent than both GB2 ($p < 0.001$) and both GB19 ($p < 0.01$) strains.

Figure 36 (B) shows IgM production by a mixed splenocyte population. There is no difference in IgM production between wild type and knock out LOS in both the GB2 and GB19 strains. However, both GB19 LOS strains are more potent than both GB2 LOS strains ($p < 0.01$) and *E. coli* LPS is more potent than both GB2 strains ($p < 0.001$) and both GB19 strains ($p < 0.01$).

Figure 36 (C) shows IgG production by a purified B cell population. Very low quantities of IgG were produced in the absence of accessory cells (compare to figure 36 (D)). There was no statistical difference in IgG production between any of the strains of LOS or LPS. Figure 36 (D) shows IgG production by a mixed splenocyte population. There is no difference in IgG production between wild type and knock out LOS in both the GB2 and GB19 strains. Both GB19 strains are more potent than both GB2 strains ($p < 0.01$).

and *E. coli* LPS is more potent than both GB2 strains (WT $p < 0.001$, KO $p < 0.01$) but is not statistically different from either GB19 strain.

These results show that ganglioside mimicry does not affect the potency of *C. jejuni* LOS at stimulating IgM or IgG secretion from purified B cells or mixed splenocytes. They highlight intra-species differences, as both GB19 LOS strains appear more potent than both GB2 LOS strains. Inter-species differences are also apparent as *E. coli* LPS is generally more potent than either *C. jejuni* strain.

Figure 37: Cytokine production by LOS stimulated B cells and splenocytes.

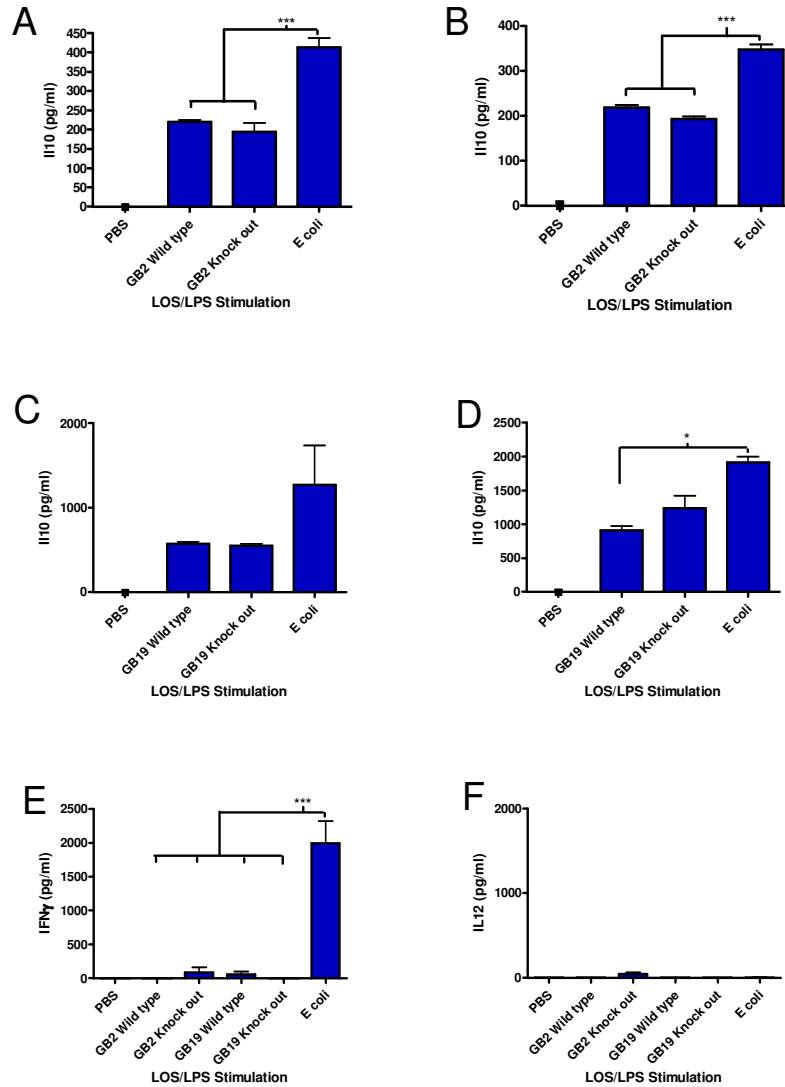


Figure 37. Purified B cells or mixed splenocytes were stimulated with 10 μ g/ml *C jejuni* LOS or *E. coli* LPS and cytokine secretion was measured using ELISA after 72 hours. (A) IL-10 production by purified B cells following GB2 wild type and knock out LOS or *E. coli* LPS stimulation. (B) IL-10 production by mixed splenocytes following GB2 wild type and knock out LOS or *E. coli* LPS stimulation. (C) IL-10 production by purified B cells following GB19 wild type and knock out LOS or *E. coli* LPS stimulation. (D) IL-10 production by mixed splenocytes following GB19 wild type and knock out LOS or *E. coli* LPS stimulation. (E) IFN- γ production by mixed splenocytes following 10 μ g/ml LOS or *E. coli* LPS stimulation. (F) IL-12 production by mixed splenocytes following 10 μ g/ml LOS or *E. coli* LPS stimulation. Mean and SEM calculated from triplicate wells. Analysed using 1way ANOVA with Bonferroni's multiple comparison test (*=p<0.05, ***=p<0.001). Representative of four experiments.

5.2.5 Comparison of LOS potency at stimulating cytokine secretion

A further functional measure of LOS potency is cytokine secretion. Purified B cells or mixed splenocytes were stimulated with ganglioside mimicking or non-mimicking LOS, and *E. coli* LPS. Cytokine secretion was measured after 72 hours. Figure 37 (A) shows IL-10 production in a purified B cell culture and figure 37 (B) shows IL-10 production in a mixed splenocyte culture, following GB2 wild type and knock out LOS stimulation. In both cases, there is no difference between ganglioside mimicking and non-mimicking strains. However, *E. coli* LPS is more potent than either of the *C. jejuni* LOS strains in both cases ($p < 0.001$). Figures 37 (C) and (D) show similar experiments as before only using GB19 strains of LOS. Again, there is no difference between the ganglioside mimicking and non-mimicking variants of LOS. *E. coli* is more potent ($p < 0.05$) than GB19 wild type *C. jejuni* LOS (with no statistical advantage over knock out LOS) in the mixed splenocyte culture, but not the pure B cell culture.

IFN- γ production was measured in a mixed splenocyte culture (figure 37(E)). None of the *C. jejuni* LOS strains induced detectable IFN- γ secretion although the *E. coli* LPS stimulated large quantities of IFN- γ . In addition, no IL-12 could be detected from mixed splenocytes following LPS or LOS stimulation (figure 37 (F)).

Figure 38: Cytokine production by rough v smooth LPS stimulated mixed splenocytes.

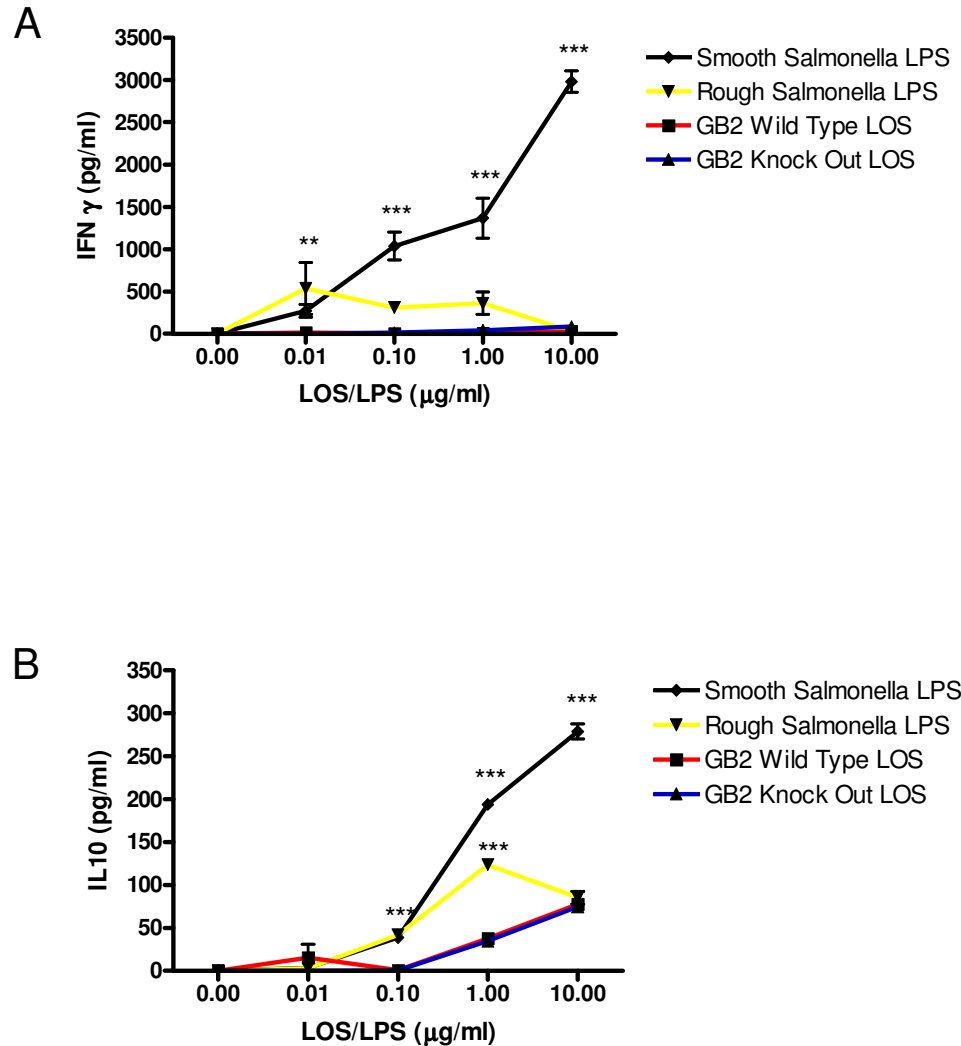


Figure 38. Mixed splenocytes were stimulated with a titrating dose of smooth (Ra) and rough (Re) mutant *S. typhimurium* LPS and GB2 *C. jejuni* LOS following which IFN- γ and IL-10 secretion into the supernatant was measured by ELISA. (A) IFN- γ production following stimulation. (B) IL-10 production following stimulation. Mean and SEM calculated from triplicate wells. Analysed using 2way ANOVA with Bonferroni's post tests (**= $p < 0.01$, ***= $p < 0.001$).

To test if an inability to stimulate IFN- γ production is a property unique to *C. jejuni* LOS or a general property of rough mutant LPS, a number of additional strains of LPS were tested. Re (deep rough mutant) and Ra (smooth mutant) *S. typhimurium* LPS strains were used in an IFN- γ , mixed splenocyte assay (figure 38 (A)). The smooth mutant *S. typhimurium* LPS induces more IFN- γ over a range of concentrations (10 μ g/ml, 1 μ g/ml and 0.1 μ g/ml ($p < 0.001$)) than any of the rough mutant strains, including the rough *S. typhimurium* LPS. *C. jejuni* LOS does not induce IFN- γ . Figure 38 (B) shows IL-10 production in the same experiment. Smooth *S. typhimurium* LPS is statistically more potent than the rough mutant strains (greater than *C. jejuni* LOS at 10 μ g/ml, 1 μ g/ml and 0.1 μ g/ml ($p < .001$) and greater than rough *S. typhimurium* LPS at 10 μ g/ml and 1 μ g/ml ($p < 0.001$)). Rough *S. typhimurium* LPS is more potent than *C. jejuni* LOS at 1 μ g/ml and 0.1 μ g/ml ($p < 0.001$). There is no difference between the ganglioside mimicking and non-mimicking *C. jejuni* GB2 LOS strains

These cytokine experiments showed a small degree inter-experiment variability. In two IL-10 repeats the GB2 knock out *C. jejuni* LOS induced slightly more IL-10 from mixed splenocytes ($p < 0.05$) than the wild type strains while in two experiments there was no difference. Where a difference was present it could be attributed to a single outlier. Although the rough *S. typhimurium* resulted in detectable IFN- γ (including statistically more than *C. jejuni* LOS at 0.01 μ g/ml ($p < 0.01$)), a number of subsequent repeats (data not shown) using single concentration points (2 μ g/ml, 5 μ g/ml and 20 μ g/ml) resulted in no detectable IFN- γ following rough *S. typhimurium* stimulation. The balance of results suggests that rough mutant LPS/LOS from either *S. typhimurium* or *C. jejuni* do not induce significant amounts of IFN- γ from mixed splenocytes. These results also demonstrate no difference in potency between ganglioside mimicking and non-mimicking LOS in stimulating IL-10 secretion from purified B cells or mixed splenocytes.

Figure 39: Bone marrow derived dendritic cell and macrophage purity assessed by FACS.

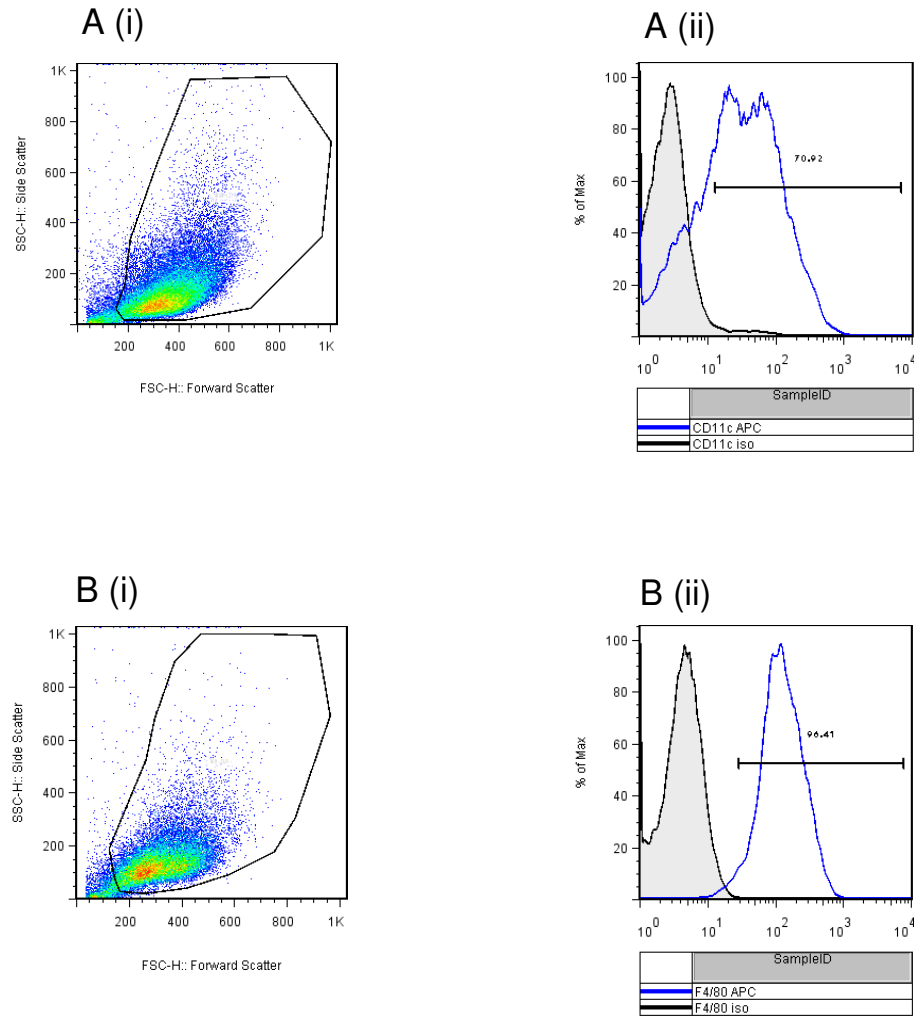


Figure 39. Bone marrow derived dendritic cell and bone marrow derived macrophage purity assessed using FACS analysis (monoclonal antibody to CD11c (dendritic cells) or F4/80 (macrophages)). (A)(i) Forward v side scatter of BMDC parent cells. (A)(ii) histogram showing CD11c positive cells (blue, 70%) against isotype control (black). (B)(i) forward v side scatter of BM macrophage parent cells. (B)(ii) histogram showing F4/80 positive cells (blue, 96%) against isotype control (black).

5.2.6 Potency of ganglioside mimicking and non-ganglioside mimicking LOS at stimulating myeloid antigen presenting cells

Bone marrow derived dendritic cells (BMDC) and bone marrow derived macrophages are innate immune cells of myeloid lineage. Myeloid cells express numerous pathogen recognition receptors such as TLRs (including TLR4) and also express members of the siglec family of ganglioside receptors. Bone marrow derived dendritic cells and macrophages were stimulated with LOS in order to test if ganglioside mimicry alters the potency of LOS.

Bone marrow derived dendritic cells were differentiated from bone marrow cells using GM-CSF containing supernatant from the X-63 cell line. Before use, cells were harvested and labelled with the dendritic cell marker CD11c in order to establish purity. Figure 39 (A) shows harvested cells labelled with anti-CD11c and the isotype control. Dendritic cell purity was greater than 70%. Bone marrow derived macrophages were differentiated from bone marrow using M-CSF containing supernatant from the L-929 cell line and purity was confirmed by labelling with the macrophage marker F4/80. Figure 39(B) shows F4/80 positive cells against isotype control. Macrophage purity was greater than 90%.

Figure 40: Cytokine production by LOS stimulated dendritic cells and macrophages.

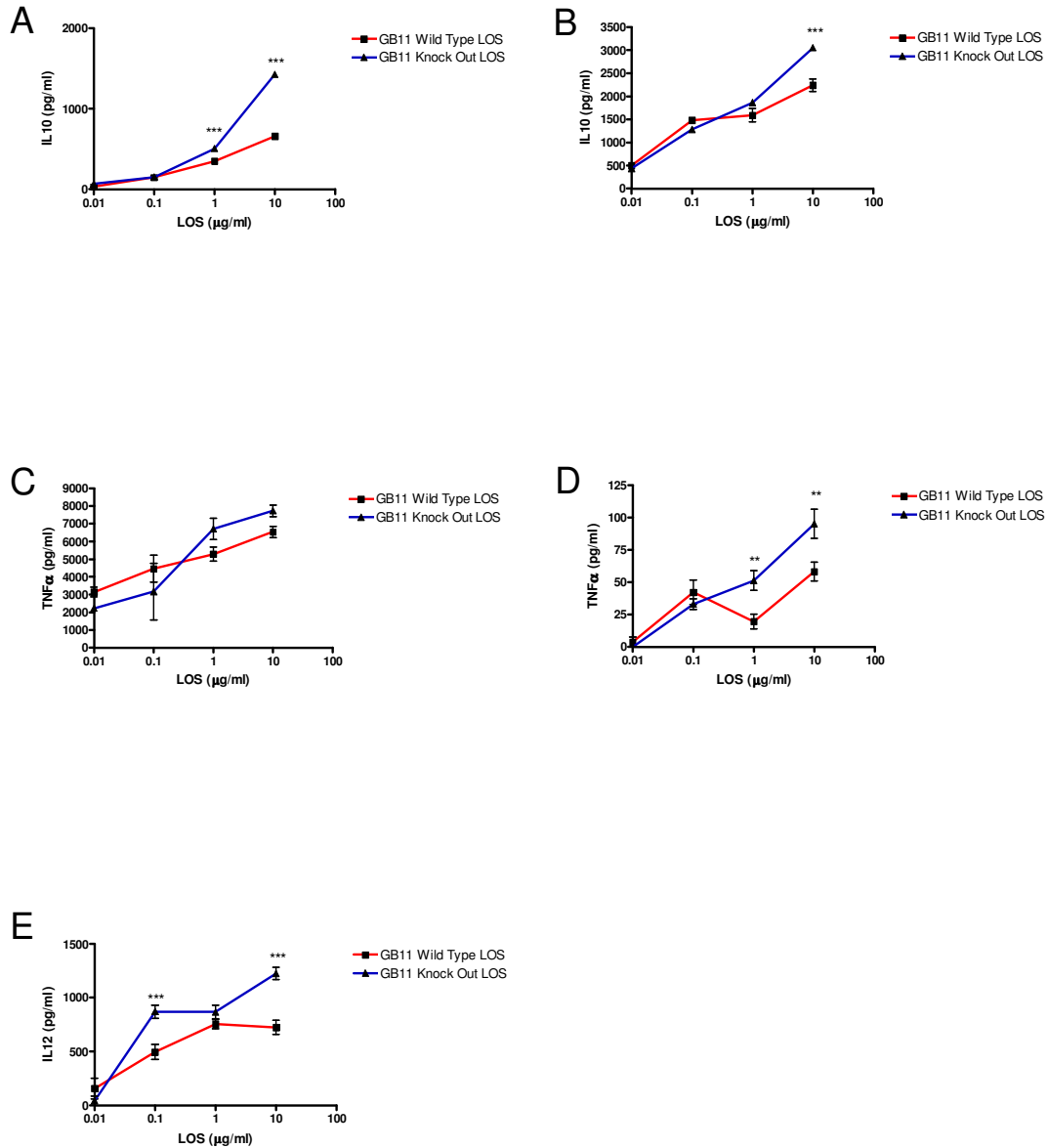


Figure 40. Dendritic cell or macrophage responses to wild type or knock out *C. jejuni* GB11 LOS. The supernatants were harvested and analysed for cytokine production using OptEIA ELISA kits. (A) BMDC IL-10 production following overnight stimulation with GB11 wild type or knock out LOS. (B) BM macrophage IL-10 production following overnight stimulation with GB11 wild type or knock out LOS. (C) BMDC TNF- α production following overnight stimulation with GB11 wild type or knock out LOS. (D) BM macrophage TNF- α production following overnight stimulation with GB11 wild type or knock out LOS. (E) BMDC IL-12 production following overnight stimulation with GB11 wild type or knock out LOS. Mean and SEM calculated from triplicate wells. Analysed using 2way ANOVA with Bonferroni's posttests (**= $p < 0.01$, ***= $p < 0.001$). Representative of three titration experiments.

Bone marrow derived dendritic cells or macrophages were stimulated with a titrating dose of wild type or knock out GB11 *C. jejuni* LOS and the supernatants were harvested after overnight incubation. Cytokine production was assayed using cytokine ELISAs. Figures 40(A) and (B) shows IL-10 production by dendritic cells and macrophages respectively. Dendritic cells produce double the amount of IL-10 (1433 pg/ml v 665 pg/ml) following stimulation with 10µg/ml knock out LOS than compared to wild type LOS (p<0.001) and almost 50% more (509 pg/ml v 354 pg/ml) when stimulated with 1µg/ml (p<0.001). 1µg/ml of knock out LOS has potency comparable to 10µg/ml of wild type LOS. Macrophages produce one third more IL-10 when stimulated with 10µg/ml knock out LOS as compared to wild type LOS (p<0.01) although no difference in potency is apparent at lower concentrations.

Figures 40(C) and (D) show dendritic cell and macrophage TNF-α production under the same conditions. There is no statistical difference in dendritic cell TNF-α secretion following GB11 knock out LOS or GB11 wild type LOS stimulation. There is greater TNF-α production by macrophages at 10µg/ml and 1µg/ml (p<0.01) with knock out LOS having approximately double the potency of wild type LOS at each concentration.

Figure 40 (E) shows bone marrow derived dendritic cell IL-12 production. GB11 knock out LOS is more potent at 0.1µg/ml and 10µg/ml (p<0.001) than wild type LOS producing just under twice as much IL-12 at each concentration.

The differences in dendritic cell IL-10 production were reliably reproduced each time it was tested (over eight separate repeats) with similar levels of cytokines, high levels of statistical significance and consistent dose response curves. However, the other cytokines showed marked inter-experiment variability with inconsistent dose response curves. Small differences in macrophage IL-10 production at high concentrations (10µg/ml) of LOS were generally consistent while macrophage TNF-α production showed fluctuations in the dose response curves with knock out LOS being more potent

at higher concentrations. Dendritic cell IL-12 responses were extremely variable over a number of repeats making it difficult to draw definite conclusions.

Figure 41: Dendritic cell IL10 production in response to alternative *C. jejuni* LOS strains.

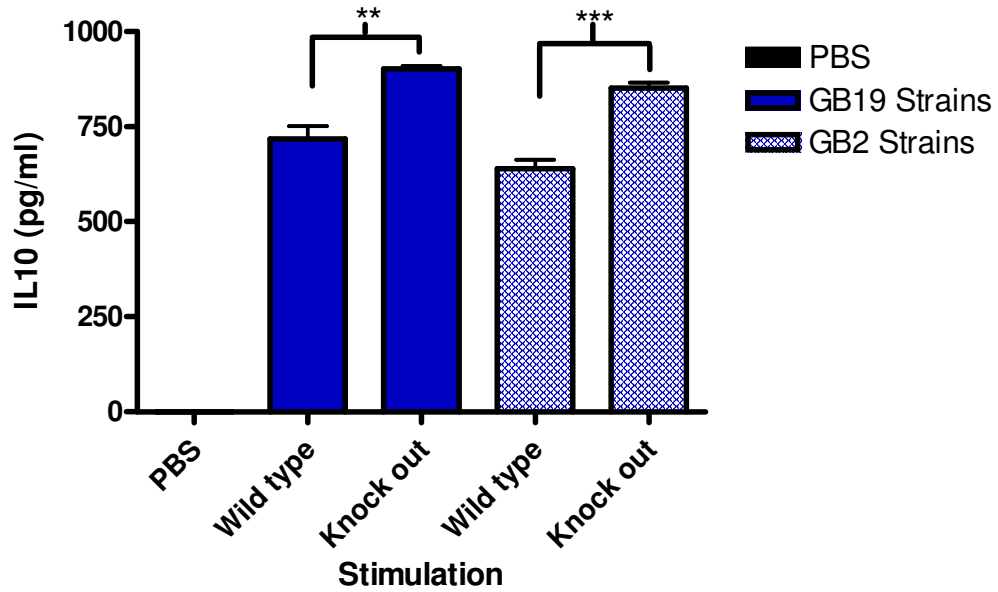


Figure 41. IL-10 production by bone marrow derived dendritic cells following overnight stimulation with 10 μ g/ml of wild type or knock out GB2 or GB19 *C. jejuni* LOS assayed using an OptEIA ELISA kit. Mean and SEM calculated from triplicate wells. Analysed using 1way ANOVA with Bonferroni's multiple comparison test. (**= $p < 0.01$, ***= $p < 0.001$). Single experiment.

In order to confirm that the difference in dendritic cell IL-10 production could be reliably related to the presence of ganglioside mimicry, dendritic cells were stimulated with an additional two strains of ganglioside mimicking LOS and their non-mimicking control strains (GB2 and GB19 wild type and knock out). Figure 41 shows IL-10 production and confirms a similar trend to the previous results with knock out strains being more potent (GB19 $p < 0.01$, GB2 $p < 0.001$) than the wild type strains although the magnitude of the difference is less marked than with GB11 strains.

Figure 42: Whole *C. jejuni* stimulation of dendritic cells and macrophages.

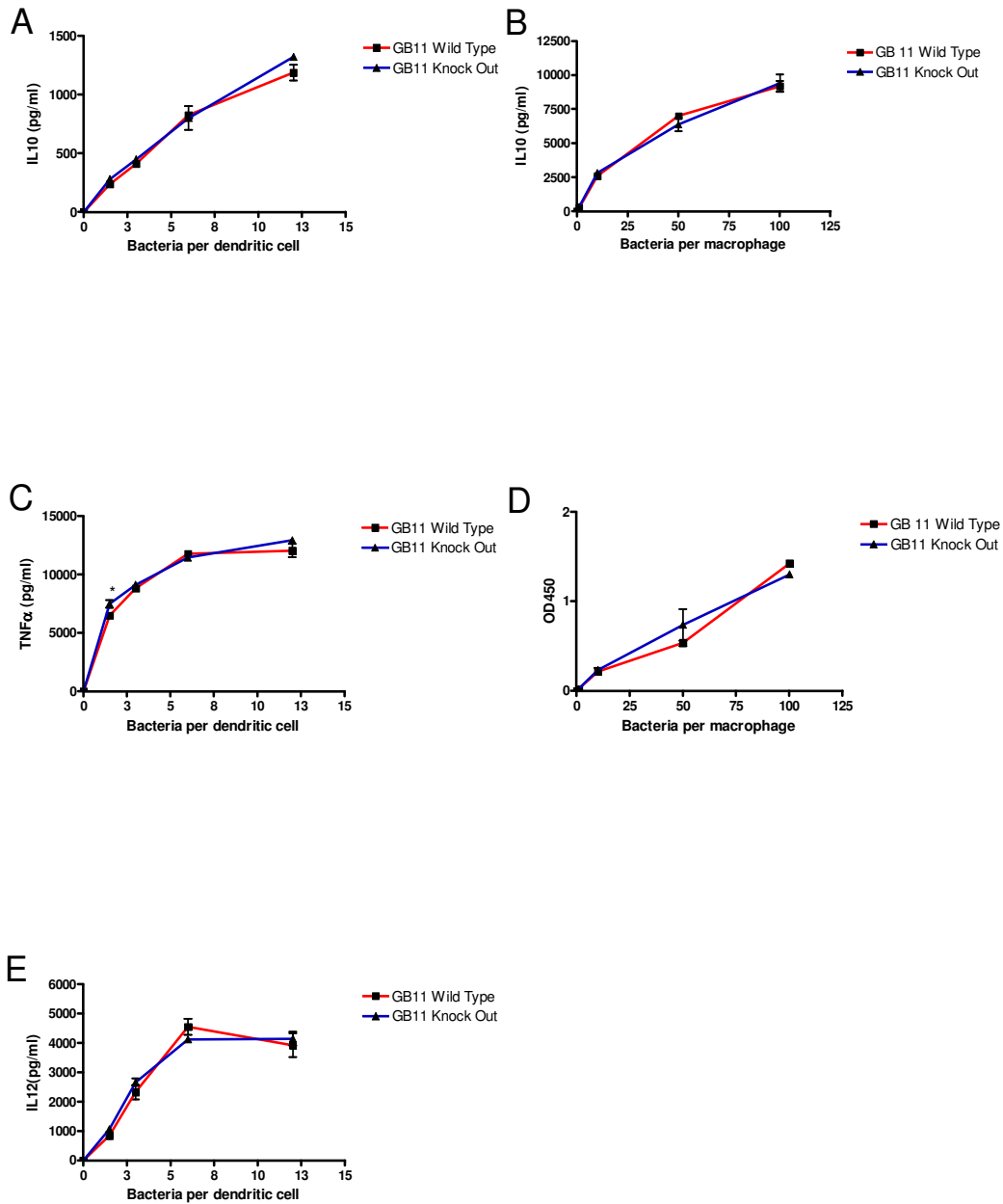


Figure 42. Bone marrow derived dendritic cells or macrophages were stimulated overnight with a titrating dose of whole heat inactivated GB11 wild type or knock out *C. jejuni*. Cytokine production was measured using ELISA. (A) BMDC IL-10 production following stimulation with whole *C. jejuni*. (B) BM macrophage IL-10 production following stimulation with whole *C. jejuni*. (C) BMDC TNF- α production following stimulation with whole *C. jejuni*. (D) BM macrophage TNF- α production following stimulation with whole *C. jejuni*. (E) BMDC IL-12 production following stimulation with whole *C. jejuni*. Mean and SEM calculated from triplicate wells. Analysed using 2way ANOVA with Bonferroni's posttests (*= $p < 0.05$). Representative of three experiments.

5.2.7 Potency of whole *C. jejuni* at stimulating myeloid antigen presenting cells

To investigate the role of ganglioside mimicry in differences in potency, dendritic cells and macrophages were stimulated with whole ganglioside mimicking or non-mimicking bacteria. The cells were stimulated overnight with whole heat killed *C. jejuni*. Figures 42(A) and (B) show dendritic cell and macrophage IL-10 production following stimulation. There is no difference in potency between the wild type and knock out strains in stimulating either cell type. Figures 42(C) and (D) show TNF- α production. Although there is a small statistical difference in dendritic cell responses at a bacteria to cell ratio of 1.5:1 ($p < 0.05$) there is no substantial difference in potency between the GB11 wild type and knock out strains. Figure 42 (E) shows dendritic cell IL-12 production following whole bacteria stimulation and there is no difference in potency between ganglioside mimicking and non-mimicking strains.

Figure 43: LOS and ganglioside stimulation of dendritic cells and macrophages.

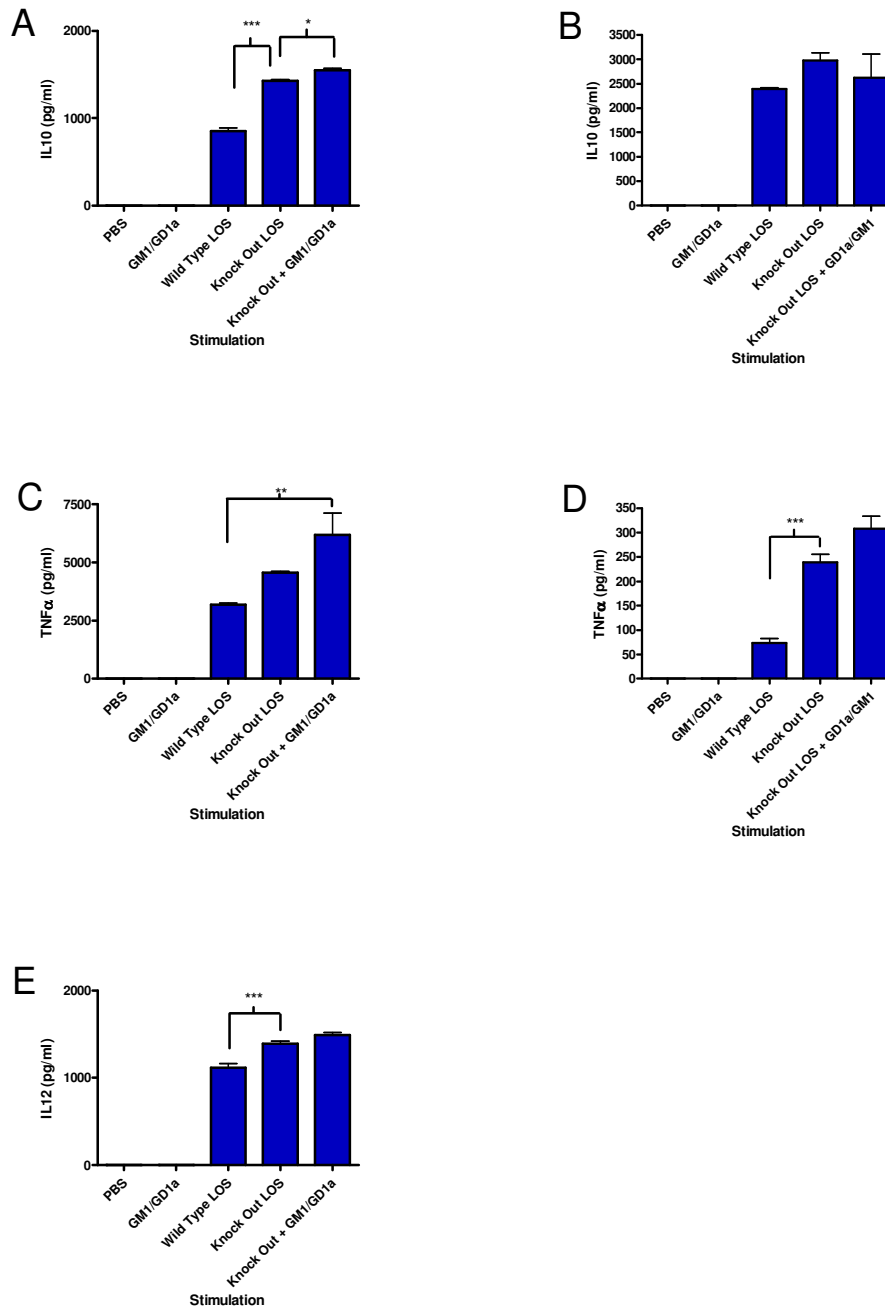


Figure 43. Bone marrow derived dendritic cells or macrophages were incubated with 10 μ g/ml gangliosides GD1a and GM1 alone, GB11 wild type LOS, knock out LOS, and knock out LOS which had been sonicated with 10 μ g/ml GD1a and GM1. The cells were incubated overnight and cytokine production was measured in the supernatant using ELISA. (A) BMDC IL-10 production (B) BM macrophage IL-10 production. (C) BMDC TNF- α production (D) BM macrophage TNF- α production. (E) BMDC IL-12 production. Mean and SEM calculated from triplicate wells. Analysed using 1way ANOVA with Bonferroni's multiple comparison test (*= $p < 0.05$, **= $p < 0.01$, ***= $p < 0.001$). Representative of three experiments.

5.2.8 Effect of exogenous gangliosides on knock out LOS potency

Exogenous gangliosides have been shown to alter activation of immune cells. To establish if the measured differences in potency between ganglioside mimicking and non-mimicking LOS are due to the ganglioside mimic, and to gain an insight into the mechanism, myeloid cells were stimulated with knock out LOS in the presence of exogenous gangliosides. The cells were stimulated with 10 μ g/ml non-ganglioside mimicking LOS which was first sonicated in solution with 5 μ g/ml each of gangliosides GM1 and GD1a. The cells were also stimulated with PBS, ganglioside alone or wild type LOS. Contrary to expectations, rather than reduce the potency of knock out LOS to that of wild type LOS, the general trend was for GM1 and GD1a to slightly increase the potency of knock out LOS (although this was subject to inter-experiment variability and was usually not statistically significant). Figures 43(A) and (B) show dendritic cell and macrophage IL-10 secretion. Addition of exogenous gangliosides slightly increased the potency of knock out LOS ($p < 0.05$) at stimulating IL-10 from dendritic cells although it had no effect on macrophages. Figures 43 (C) and (D) show dendritic cell and macrophage TNF- α secretion. There was no statistical difference in TNF- α production for either population when gangliosides were added to knock out LOS. Figure 43 (E) shows dendritic cell IL-12 secretion. Addition of gangliosides to knock out LOS had no effect on the LOS potency. Gangliosides alone had no effect on the dendritic cells or macrophages.

Figure 44: IL10 production by dendritic cells following blocking of siglec receptors.

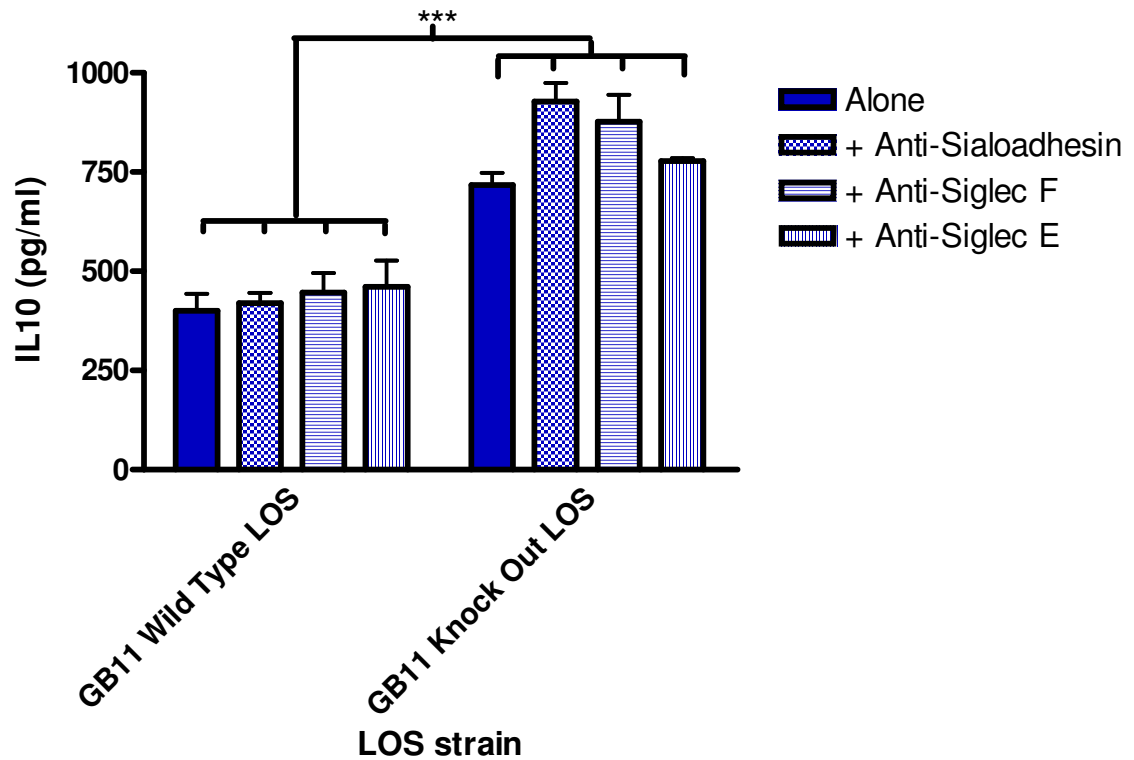


Figure 44. Bone marrow derived dendritic cell IL10 production following Sialoadhesin, Siglec E or Siglec F blockade and LOS stimulation. The supernatants were harvested and assayed for IL10 production using an ELISA. Mean calculated from triplicate wells. Analysed using 2way ANOVA with Bonferroni's posttests (**= $p < 0.001$). Representative of three experiments.

5.2.9 Effect of siglec blockade on LOS potency

The greatest and most reproducible difference in LOS potency was observed with dendritic cell IL-10 secretion following 10µg/ml of GB11 LOS stimulation. It was hypothesised that wild type LOS is less potent than knock out LOS because of inhibitory signalling through a siglec receptor. A restricted set of blocking antibodies against candidate myeloid expressed siglec receptors was used to block potential signals mediated by the ganglioside mimicking LOS. Figure 44 shows IL-10 secretion by dendritic cells following LOS stimulation in combination with blocking anti-Sialoadhesin (3D6 and SER-4²⁰⁹), anti-Siglec F²⁵⁸ or anti-Siglec E²⁵⁸ antibodies (1µg/million cells). The cells were incubated with blocking antibody at 4°C for 15 minutes before 10µg/ml LOS was added, and then cultured overnight. The addition of siglec blocking antibodies has no effect on wild type LOS potency which remained less potent than knock out LOS under all the conditions (p<0.001). Surprisingly, addition of siglec blocking antibody to knock out LOS had a trend of increasing potency although not with statistical significance.

Figure 45: Upregulation of co-stimulator CD40 by LOS and whole *C. jejuni* stimulated dendritic cells and macrophages.

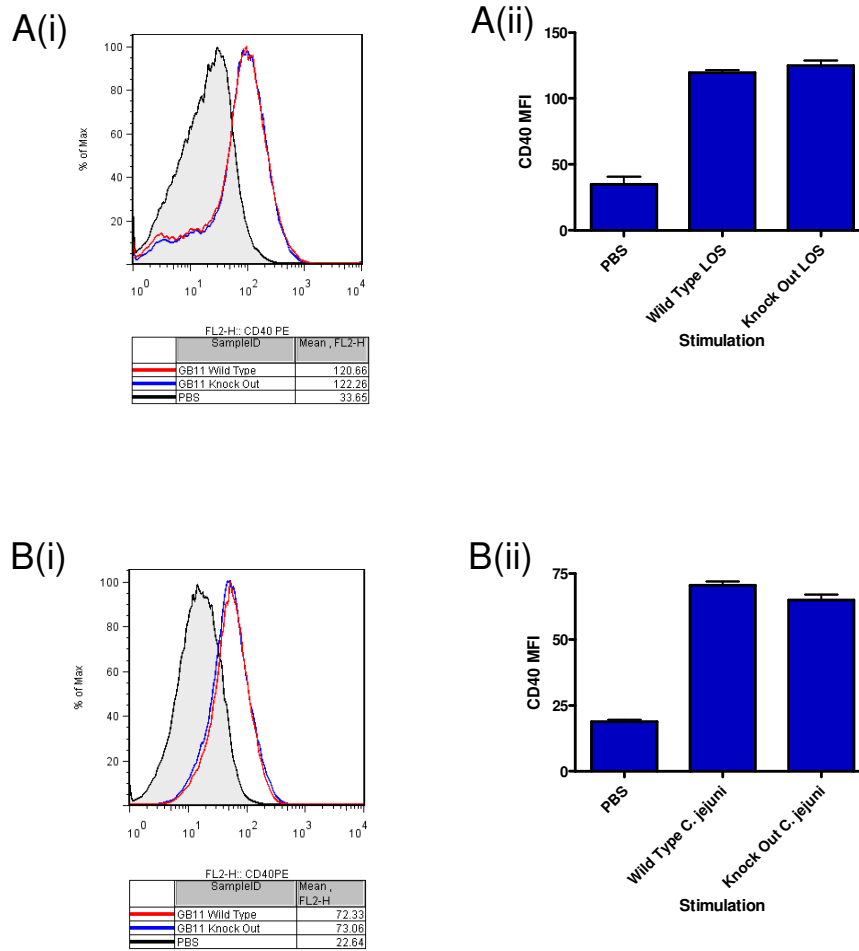


Figure 45. (A) (i) Bone marrow derived dendritic cells were stimulated with 10 μ g/ml GB11 wild type or knock out LOS and incubated overnight. CD40 upregulation was measured by FACS analysis (increase in CD40-PE MFI shown in histogram). (A)(ii) Graphical representation. (B)(i) Bone marrow derived macrophages were pulsed with heat inactivated whole GB11 *C. jejuni* for 15 minutes, washed, and then incubated overnight. Upregulation of CD40 was measured by increased MFI. (B)(ii) Graphical representation. Mean and SEM calculated from triplicate tubes. Analysed using 1way ANOVA with bonferroni's multiple comparisons test. Representative of three experiments.

5.2.10 Upregulation of co-stimulatory molecule CD40 following LOS stimulation

CD40 is a co-stimulatory molecule expressed on a number of cells of the immune system including dendritic cells and macrophages. CD40 is up-regulated on dendritic cells following stimulation via TLRs and is a useful marker of dendritic cell maturation as ligation of CD40 leads to increased expression of other co-stimulators such as CD80 and CD86 as well as pro-inflammatory cytokine production³¹⁴. CD40 plays a similar role in macrophages³¹⁵.

Having established differences in the potency of ganglioside mimicking and non-mimicking LOS at inducing cytokines, it was decided to test if there were differences in the up-regulation of the co-stimulatory molecule CD40. Dendritic cells were stimulated with ganglioside mimicking or non-mimicking LOS while macrophages were pulse stimulated with ganglioside mimicking or non-mimicking whole *C. jejuni*. The cells were stained with anti-CD11c mAb and F4/80 respectively and co-stained for CD40. Example FACS histograms are shown in Figure 45(A)(i) and (B)(i) (an isotype control antibody for CD40 showed no increase beyond PBS stimulated cells). Upregulation was measured using the change in the MFI. Figures 45 (A)(ii) shows the change in dendritic cell CD40 expression and indicates no difference between wild type and knock out LOS. (B)(ii) shows macrophage CD40 upregulation and no difference is noted between wild type and knock out whole *C. jejuni*.

Figure 46: Dendritic cell and macrophage death following LOS stimulation.

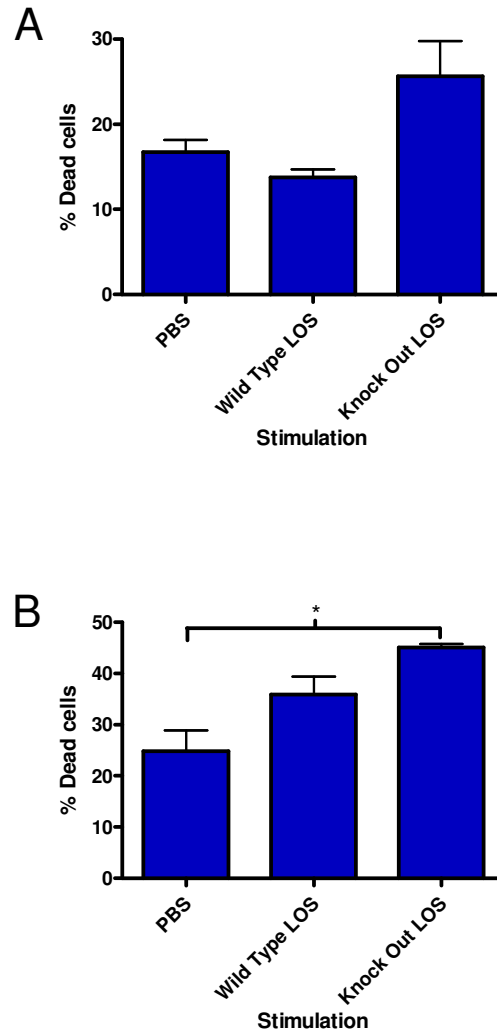


Figure 46. Percentage of dead cells determined by trypan blue exclusion assay. (A) Bone marrow derived dendritic cells, (B) bone marrow derived macrophages. Each population was stimulated with 10 μ g/ml wild type or knock out GB11 *C. jejuni* LOS and incubated overnight. Mean and SEM calculated from triplicate wells. Analysed using 1way ANOVA with bonferroni's multiple comparisons test (*=p<0.05). Representative of three experiments.

5.2.11 Effect of LOS on cell death

The inter-experimental variation in cytokine production could be due to cell death because of the high concentrations of LOS being used. Dendritic cells and macrophages were stimulated overnight with 10µg/ml wild type or knock out LOS and cell death was assayed using a trypan blue exclusion assay. Figure 46 (A) shows the percentage of dead dendritic cells. There is no statistical difference in dead cells when stimulated with wild type LOS, knock out LOS or PBS. Figure 46(B) shows the percentage of dead macrophages. There is no statistical difference between wild type and knock out LOS although knock out LOS caused more cell death than PBS alone ($p < 0.05$). The trend for increased cell death associated with knock out strains of LOS (GB11, GB2 and GB19) was seen in a number of dendritic cell and macrophage experiments, although the trend was not statistically significant. To confirm these findings a single experiment was done using the 7AAD viability probe in conjunction with FACS analysis. This confirmed the trend but was not statistically significant.

Figure 47: C3H/HeJ and TLR2^{-/-} dendritic cell IL10 production following LOS stimulation.

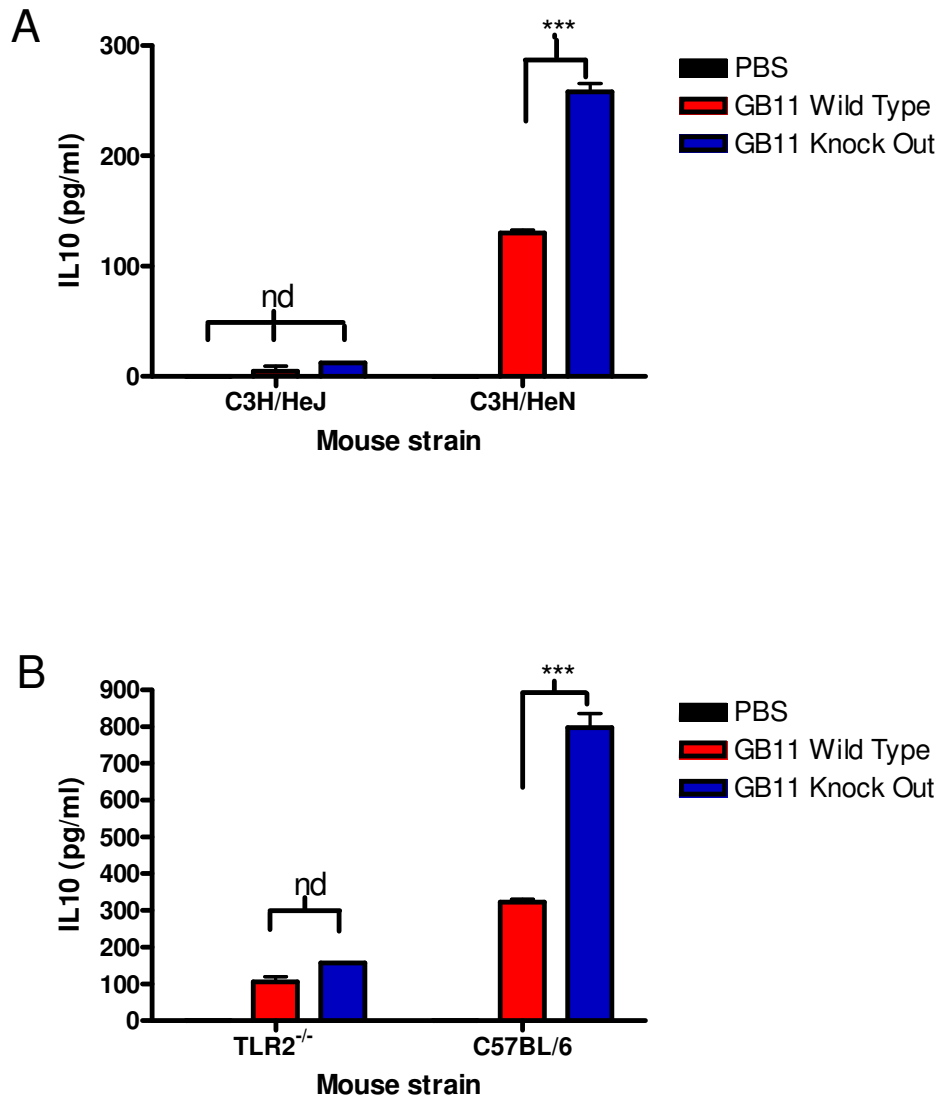


Figure 47. Bone marrow derived dendritic cells from (A) C3H/HeJ and C3H/HeN and (B) TLR2 Knock Out and C57BL/6 mice were stimulated with 10 μ g/ml wild type or knock out LOS and IL-10 was measured by ELISA in the supernatant after overnight culture. There is no statistical difference between PBS and LOS stimulation of C3H/HeJ cells. There is no statistical difference between wild type and knock out LOS in TLR2^{-/-} cells. Mean and SEM calculated from triplicate wells. Analysed using 2way ANOVA with Bonferroni's posttest (nd=no statistical difference, ***=p<0.001). Single experiment.

5.2.12 LOS stimulation of dendritic cells from C3H/HeJ LPS hyporesponsive mice and TLR2^{-/-} mice

Capsular polysaccharide is a frequent and tenacious contaminant of LPS preparations. It is sensed by immune cells using TLR2²¹⁶. In order to test for contamination, bone marrow derived dendritic cells from the LPS hyporesponsive mouse strain, C3H/HeJ, and the normo-responsive control strain, C3H/HeN, as well as a TLR2^{-/-} strain and the C57BL/6 background strain, were stimulated overnight with *C. jejuni* LOS and the supernatant assayed for IL-10 production. Figure 47(A) shows that C3H/HeN dendritic cells, consistent with previous results for C57BL/6 derived cells, produce IL-10 and that knock out is more potent than wild type LOS (p<0.001 for knock out v wild type LOS and for both types of LOS v PBS alone). The C3H/HeJ dendritic cells do not respond to LOS, consistent with their LPS hyporesponsive phenotype (no statistical difference between either LOS and PBS).

Figure 47(B) shows that C57BL/6 dendritic cells respond as before with knock out LOS generating more IL-10 than wild type LOS (and both being greater than PBS) (p<0.001). The dendritic cells from TLR2^{-/-} mice produce IL-10 at low levels but both were significantly greater than PBS (wild type p<0.01, knock out p<0.001). However, in contrast to the C57BL/6 derived control cells, there is no statistical difference between the wild type and knock out LOS at inducing IL-10.

5.3 Discussion

The aim of these experiments was to investigate the immunostimulatory properties of *C. jejuni* LOS and any potential effect of ganglioside mimicry. There are a number of ways ganglioside mimicry can potentially modulate the subsequent immune activation following TLR4/Lipid A interactions. Firstly, as shown in chapter 4, the ganglioside mimic can act as ligand for siglec receptors. Secondly, sialic acid plays a direct role in TLR4 signalling which has been demonstrated in Neu1 (neuraminidase 1) deficient mice and with the use of pharmacological neuraminidase inhibitors such as Tamiflu. Neu1 is expressed by macrophages and it associates with TLR4 where it specifically cleaves α 2-3 linked sialic acid residues, such as those found on gangliosides GM1 and GD1a, linked to β -galactoside of TLR4. When Neu1 activity is blocked or absent there is a reduction in the ability of TLR4 to signal with significant reductions in inflammatory cytokine production such as IL-6 and TNF- α ^{153,154}. If the α 2-3 linked sialic acids on ganglioside mimicking LOS can substitute for the α 2-3 linked sialic acid residues on β -galactoside of TLR4 then this may alter signalling.

LPS mobilises MZ B cells causing them to migrate into the follicle where they deliver antigen to FO B cells²⁸⁷⁻²⁹⁰. Marginal Zone B cells are important effector cells in the response to carbohydrate antigens and are believed to harbour auto-reactive specificities^{131,158}, making them potentially important in GBS. Results presented in this chapter provide evidence for the first time that *C. jejuni* LOS is capable of mobilising MZ B cells *in vivo* and the results also show that ganglioside mimicry has no effect on this. However, an alternative explanation for my observations is that LOS kills all of the MZ B cells. My methodology, which does not differentiate between B cell subsets, does not exclude this. My original intention was to label FO and MZ B cells separately using anti-IgD and anti-IgM, but for technical reasons related to reagents, this did not work.

A number of immune cell populations were stimulated with wild type and knock out LOS in order to test for the effects of ganglioside mimicry. B cells were chosen as they are the effector cells responsible for producing auto-reactive antibodies in GBS. Both purified B cells and B cells as part of a mixed splenocyte population were used in order to examine direct ganglioside effects on B cells as well as more complex multiple cell lineage interactions. My results show that *C. jejuni* LOS triggers B cell division and CD138 positive cell differentiation and that a number of the cells which divided were, or became, IgG positive. However, this probably does not represent *de-novo* class switching as 72 hours is too early for this to occur. There is no difference in potency between ganglioside mimicking and non-mimicking LOS strains in this assay. Interestingly, *E. coli* LPS stimulation results in statistically greater division, CD138 positive cell differentiation and class switching than either *C. jejuni* LOS strain.

In addition to cell division and maturation, IgM and IgG antibody production was measured. Consistent with the previous results, no difference is observed between ganglioside mimicking and non-mimicking *C. jejuni* LOS, although *E. coli* LPS is more potent at stimulating purified B cell and mixed splenocyte IgM production. In addition, there is an inter-strain difference in mixed splenocyte IgM production with the GB19 strains (both wild type and knock out) inducing more IgM than the GB2 strains (wild type and knock out). There is a similar trend in IgM production from purified B cells. This suggests that the specific strain of *C. jejuni* from which the LOS is derived is more important at determining potency than ganglioside mimicry. This in turn suggests that the Lipid A portion is the only important part of the molecule in determining B cell stimulating potency. A similar trend is seen for IgG production by purified B cells, although it is not statistically significant. The GB19 strains of *C. jejuni* LOS and *E. coli* LPS are equally potent and both are more potent than GB2 strains of *C. jejuni* LOS at stimulating IgG production by mixed splenocytes.

An additional measure of potency is cytokine secretion and IL-10 was chosen as it is an important immune modulating cytokine secreted by both B cells and myeloid cells²⁹¹.

My results show no difference in IL-10 production by B cells or mixed splenocytes when stimulated with LOS from ganglioside mimicking or non-mimicking strains of *C. jejuni*, and this was seen with both GB2 and GB19 strains. Consistent with previous findings, *E. coli* LPS is more potent than GB2 strains of *C. jejuni* LOS and have a trend for greater potency than GB19 *C. jejuni* LOS.

Previous studies of *C. jejuni* LOS show that it is 50% less toxic to galactosamine sensitised mice, 30 to 50 fold less pyrogenic in rabbits and induces 100 fold less TNF- α from peritoneal macrophages than LPS from salmonella species³¹⁶. The studies presented here demonstrate for the first time the potency of *C. jejuni* LOS in stimulating purified murine B cells and B cells as part of a mixed splenocyte population. They show that *C. jejuni* LOS shares similar immunostimulatory properties as other types of LPS. However, consistent with previous publications, they show *C. jejuni* LOS to be generally less potent than other species of LPS (in this case *E. coli* LPS). Some authors have suggested that the low potency is linked to a higher phase transition (lower fluidity) of *C. jejuni* LOS and the unique diaminoglucose structure in the Lipid A³¹⁶. This evidence of low potency is reinforced when the molarity of my LOS is considered. S-form LPS can have up to 100 times the mass of R-form LPS (LOS) which means that the *C. jejuni* LOS was used at significantly higher molar concentrations than the *E. coli* LPS. S-form LPS is heterogeneous in size, so there is no definitive mass with which to calculate molarity and make a direct comparison to the *C. jejuni* LOS.

No difference in B cell stimulation is obvious between the wild type and knock out strains. Given that LPS is one of the most potent immune stimulators known, it is possible that any additional signal from a ganglioside receptor is overwhelmed by the TLR4 signal or that ganglioside specific receptors are unable to engage soluble LOS. To address this possibility some assays were done with LOS pre-adsorbed onto the tissue culture plate, but this had no effect. Siglec receptors are known to be held in *cis* interactions and require “liberating” from these bonds before they can engage in *trans* binding with external gangliosides. Further experiments could address this issue by pre-

treating the cells with a neuraminidase to release any siglec receptors from *cis* bonds prior to exposing them to LOS.

IFN- γ secretion by mixed splenocytes was tested to establish if ganglioside mimicry affects production of polarising cytokines. Intriguingly, no IFN- γ is secreted when splenocytes are stimulated with *C. jejuni* LOS, while *E. coli* LPS stimulates ample IFN- γ production. No IL-12 production is detected from splenocytes following stimulation with any of the LPS/LOS types and this might be due to consumption of the cytokine by the cells themselves.

To test if a lack of IFN- γ was unique to *C. jejuni* LOS, or a general property of R-form LPS, splenocytes were stimulated with a titration of *C. jejuni* LOS, R-form *S. typhimurium* LPS and S-form *S. typhimurium* LPS. The data presented shows large quantities of IFN- γ production by splenocytes stimulated with S-form *S. typhimurium* LPS with significantly lower quantities from R-form *S. typhimurium* LPS and none from *C. jejuni* LOS. In a number of subsequent repeats at varying concentrations, no IFN- γ could be detected following R-form *S. typhimurium* LPS stimulation. These results indicate that R-form LPS, and especially *C. jejuni* LOS, does not stimulate IFN- γ secretion by mixed splenocytes. This has not been reported before. Analysis of the same supernatant shows that IL-10 secretion remains intact and confirms that S-form *S. typhimurium* LPS is more potent than R-forms of LPS. 10 μ g/ml is considered a very high concentration for LPS stimulation so it is unlikely the lack of IFN- γ is due to the LPS concentration being too low.

The mechanisms underlying these differences have not been investigated. It is possible that IL-10 is inhibiting the IL-12/IL-18 – IFN- γ axis. However, S-form LPS induces more IL-10 than R-form LPS and yet continues to induce IFN- γ . R-form LPS signals principally through the MyD88 dependent pathway in the absence of CD14 and this might skew the resultant cytokine response towards Th2 and away from Th1 For

example, Mast cells are TLR4 positive/CD14 negative and are a potent source of cytokines such as IL-5, IL-13 and IL-10. The antibody isotypes commonly (but not exclusively) associated with GBS are IgG1 and IgG3 and this is classically thought to be a manifestation of a Th1 dominated response. Therefore, confirming that *C. jejuni* LOS polarises towards Th2 under normal circumstances would be an important discovery.

These results must be interpreted with caution. Although all of the LPS types were treated with enzymes to improve purity, the two *S. typhimurium* strains were purified using different methods (the S-form by hot phenol extraction and the R-form by the phenol-chloroform-petroleum ether method) and both *S. typhimurium* strains were bought commercially. It is possible that they contain different quantities of contaminating bacterial immune stimulators, such as capsular polysaccharide, from each other, or the *C. jejuni* LOS. The observed phenomena can only be adequately investigated using sources of ultra-pure LPS and TLR^{-/-} mouse strains to exclude confounding effects.

Myeloid cells, such as dendritic cells and macrophages, play an important early role in shaping the immune response. LPS stimulates maturation of dendritic cells and macrophages into potent antigen presenting cells whereupon they can secrete cytokines such as IL-10, IL-12 and TNF- α ²⁷⁷⁻²⁸⁶. In order to compare the potency of ganglioside mimicking and non-mimicking *C. jejuni* LOS, and to establish if there is any difference in the production of polarising cytokines, bone marrow derived dendritic cells and bone marrow derived macrophages were stimulated with LOS and the resultant production of TNF- α (an acute phase inflammatory cytokine), IL-10 (a cytokine generally considered to be anti-inflammatory/Th2) and IL-12 (a Th1 cytokine) was measured.

Dendritic cells stimulated with GB11 knock out LOS produce approximately twice as much IL-10 as wild type LOS at 10 μ g/ml stimulation. This difference is consistent, entirely reproducible (being present in at least eight separate repeats), always highly statistically significant and is considered a good candidate for biological significance due

to the magnitude of the difference. Importantly, this effect follows a dose response curve although the difference in potency only becomes significant above 1µg/ml. In addition, the increased IL-10 production seen with knock out LOS (or reduced IL-10 production seen with wild type LOS) is also present when GB2 and GB19 strains (mimicking GM1/GD1a and GD1c respectively) of LOS are used. This too is consistent and reproducible. However, the magnitudes of the differences for these strains of LOS are not as great as for GB11.

The experiments measuring IL-12 and TNF- α suffered from a degree of inter-experimental variation and the results presented offer a fair reflection of the general trends of the experiments. While the GB11 knock out LOS appears to be generally more potent at inducing cytokines from both dendritic cells and macrophages, the differences between knock out and wild type strains for TNF- α and IL-12 production is variable, not always statistically significant and therefore of questionable biological significance. Further experiments studying an alternative marker of dendritic cell activation, upregulation of the co-stimulator molecule CD40, show no difference between wild type and knock out strains of LOS confirming differences in potency is largely specific to the cytokine IL-10.

In order to further investigate the role of ganglioside mimicry and its affect on potency, dendritic cells and macrophages were stimulated with heat killed whole bacteria. In contrast to the purified LOS, this does not reveal any difference in potency between ganglioside mimicking and non-mimicking strains in inducing IL-10, IL-12 or TNF- α . This casts some doubt on the effect or biological relevance of ganglioside mimicry. In the context of multiple separate immunostimulators (LOS, bacterial DNA, RNA, flagellum etc) it is possible that subtle effects are lost. Macrophages pulse stimulated with whole *C. jejuni* show no difference in upregulation of the co-stimulator molecule CD40.

Exogenous gangliosides directly affect activation of both dendritic cells and macrophages through what are believed to be non-receptor specific interactions^{139,299} (i.e. gangliosides may insert into membranes or lipid rafts). Interestingly, such studies tend to use gangliosides at concentrations in the region of tens of micrograms per ml, which is within the range at which differences become apparent between ganglioside mimicking and non-mimicking LOS. It is possible that both halves of the ganglioside mimicking LOS molecule are biologically active at different concentration ranges, with the lipid A portion being highly potent and active at sub-microgram concentrations, and the ganglioside mimic being less potent and active at tens of micrograms. Studies of ganglioside effects tend to show an inhibitory function which is consistent with the reduced cytokine production, and in particular reduced IL-10, seen with ganglioside mimicking LOS. To explore non-receptor specific effects of ganglioside mimicry, dendritic cells and macrophages were stimulated with ganglioside alone, ganglioside mimicking LOS or non-ganglioside mimicking LOS with exogenous gangliosides added at 10µg/ml. The knock out LOS was first sonicated with the exogenous ganglioside in order to incorporate the LOS and gangliosides together in micelles to recapitulate the epitope structure of ganglioside mimicking wild type LOS.

In contrast to the reduced potency of ganglioside mimicking LOS, knock out LOS combined with exogenous gangliosides has no effect on cytokine production or weakly increases cytokine production. This effectively rules out the hypothesis that differences in potency are due to non-receptor specific effects of ganglioside mimicry.

An alternative mechanism for differences in potency is receptor specific signals delivered by the ganglioside mimic. Siglec receptors are generally inhibitory which is consistent with the reduced IL-10 production seen with wild type LOS. In order to test this hypothesis, dendritic cells were stimulated with wild type or knock out LOS in the presence of blocking antibodies to a restricted set of myeloid expressed siglecs; Sialoadhesin, Siglec F and Siglec E. The presence of blocking antibodies has no effect on the amount of IL-10 produced following wild type LOS stimulation. Although this

casts doubt on this hypothesis, it is possible that signalling is taking place via an alternative receptor not included in my panel of antibodies. In addition, these antibodies were affinity purified from sheep serum and presumably contain mixed specificities. Apart from the anti-Sialoadhesin antibodies, which showed blocking activity in later experiments (chapter 6.2.8), it cannot be certain that anti-Siglec E and anti-Siglec F have a blocking function as there was no suitable positive control. It is also possible that the antibodies were used at an insufficient concentration.

A possible explanation for the inter-experimental variability seen with TNF- α and IL-12 production is the extremely high doses of LOS being used to stimulate the cells. For *in vitro* stimulation of myeloid cells, 10 μ g/ml of LPS is an exceptionally high concentration and possibly toxic, although it is difficult to draw comparisons between the more commonly used types of LPS (such as salmonella or *E. coli*) and *C. jejuni*. Experiments were done to quantify cell death using both trypan blue exclusion and 7AAD uptake. There is no statistical difference in dendritic cell death between either LOS strains or PBS although there was a trend seen over a number of experiments for more cell death associated with knock out LOS.

Having excluded non-receptor specific ganglioside effects and receptor specific effects (as far as is possible with limited reagents) a remaining possibility is that the difference in IL-10 production, and indeed the inter-experimental variability, is due to contamination present at higher levels in the knock out LOS strains. An experiment was carried out to determine if bacterial capsular polysaccharide was present in the LOS and if this could account for differences in potency between wild type and knock out strains. The C3H/HeJ mouse strain is hyporesponsive to LPS due to a mutation in the Tlr4 gene¹¹⁶. Before proceeding with this experiment it was recognised that there are a number of potential flaws in using this strain. Firstly, C3H/HeJ mice are hyporesponsive but not necessarily non-responsive to LPS³¹⁷ and secondly there has been one report that C3H/HeJ derived cells remain sensitive to R-type LPS³¹⁸. In addition, if the ganglioside mimic is delivering an additional signal it may be impossible to distinguish this signal

from signals due to contamination. A better model may have been the TLR4^{-/-} mouse, but it was not available.

My results show that neither the wild type nor the knock out LOS stimulates IL-10 secretion from dendritic cells derived from the C3H/HeJ strain. This indicates that contamination is not present in the LOS and does not account for the difference in IL-10 secretion that is demonstrated in the C3H/HeN control strain. To confirm this interpretation, dendritic cells derived from a TLR2^{-/-} mouse strain were stimulated with LOS. The TLR2 receptor senses capsular polysaccharide although it is more promiscuous than TLR4 in its specificity²¹⁶. If capsular polysaccharide contamination is responsible for the differences in IL-10 secretion then there should be no difference in IL10 production by TLR2^{-/-} dendritic cells stimulated with wild type or knock out LOS. This is what was found.

It was noted that TLR2^{-/-} dendritic cells produce IL-10 at a lower level than the C57BL/6 controls. However, this phenomenon, and the resultant IL-10 levels, are entirely consistent with a previous publication using *E. coli* LPS and TLR2^{-/-} derived dendritic cells³¹⁹. These results suggest that a TLR2 ligand, such as capsular polysaccharide, could be responsible for the difference in IL-10 production and therefore this finding is at odds with my interpretation of the C3H/HeJ results.

A recent study shows that bone marrow derived dendritic cells produce large quantities of TNF- α and IL-12 in response to highly purified LPS signalling through TLR4, but that IL-10 is only produced in very low quantities unless there is additional signalling through TLR2. The same study demonstrates that TLR2 signalling alone (achieved using the TLR2 agonist Pam3CSK4) does not lead to IL-10 secretion. TLR2 was shown to act synergistically with TLR4 to increase IL-10 but not TNF- α or IL-12 secretion from dendritic cells³¹⁹. Applying this paradigm to the data presented here suggests that the C3H/HeJ experiment does not exclude the presence of a TLR2 agonist as the cytokine

tested was IL-10, which a TLR2 agonist alone does not induce in dendritic cells. However, this contrasts with previous published work, again using Pam3CSK4 to stimulate dendritic cells, which shows ample IL-10 production in response to TLR2 signalling³²⁰. These conflicting studies used substantially different techniques to purify dendritic cells with the former paper bearing a closer protocol to my own, while the latter paper used spleen derived dendritic cells.

In order to definitively exclude TLR2 signalling in the C3H/HeJ experiment, the supernatant should also have been tested for an additional cytokine such as TNF- α or IL-12. Although a TNF- α assay was done on the supernatant, none could be detected in either the C3H/HeJ or the control C3H/HeN cells. Unfortunately, the supernatants had undergone multiple freeze/thaw cycles and the need for additional assays only became apparent at a late stage. This would be a suitable experiment to exclude contamination, however due to pressing limitations in time and reagents, these experiments have not been carried out.

The presence of a TLR2 agonist contaminating the knock out LOS is in keeping with a number of observations. Firstly, the difference in potency was only consistent for IL-10. This can be explained in the context of TLR2 signalling acting synergistically to boost IL-10, but not TNF- α or IL-12³¹⁹. Secondly, the difference in potency only emerges at high concentrations. This can be explained if trace concentrations of contamination reach an active dose only when the LOS is used at high concentrations. Thirdly, the difference in potency was only consistent in dendritic cells, in which this synergistic action of TLR2 and TLR4 signalling for IL-10 has been described. Although ligands for TLR2 and TLR4 have been extensively studied it is clear that this is a very complicated area full of potential pitfalls.

Although it has been assumed that ganglioside mimics will signal through siglec receptors, an additional possibility is that the ganglioside mimics signals through TLR2. TLR2 is known to be a promiscuous receptor and although GD1a is not a known ligand for TLR2 it has been shown to be a co-receptor for TLR2 with certain ligands³²¹. This scenario might explain the results seen in the TLR2^{-/-} cells. It is also important to establish if the ganglioside mimicking LOS actively inhibits IL-10 secretion or simply causes less stimulation.

Reduced IL-10 secretion by dendritic cells when stimulated by ganglioside mimicking LOS potentially has wide ranging consequences in autoimmune disease. IL-10 has multiple immunosuppressive effects³²². In dendritic cells and macrophages it is a potent inhibitor of antigen presentation, reducing MHCII expression and expression of co-stimulators CD80 and CD86. Through its inhibitory effects on antigen presenting cells it inhibits both Th1 associated cytokines (such as IL-2 and IFN- γ) as well as Th2 associated cytokines (such as IL-4 and IL-5). IL-10 also suppresses myeloid derived pro-inflammatory cytokines such as IL-1, IL-6, IL-12 and TNF- α . Modulation of these latter two cytokines by IL-10 dependent feedback loops might explain the variability seen in my assays looking at these cytokines. It is conceivable that a localised deficiency of IL-10 production by dendritic cells could perturb the cytokine milieu sufficiently to facilitate greater inflammation and lead to a break in tolerance, leading to autoimmunity. This scenario would be more plausible if it can be shown that ganglioside mimicry actually suppresses IL-10 rather than being less potent at inducing it, although the data suggests that ganglioside mimicking LOS is less potent in general. It should of course be noted that this a simplification of the properties of IL-10 which is also immunostimulatory under certain circumstances with positive effects on B cell survival and class switching as well as natural killer cell proliferation and cytokine secretion.

In summary, in relation to B cells, I show *C. jejuni* LOS to be less potent than *E. coli* LPS by a number of measures. I find no differences in *C. jejuni* LOS potency related to ganglioside mimicry. In relation to myeloid cells, and in particular dendritic cells, I show an intriguing phenomenon of less IL10 production associated with ganglioside mimicking LOS. I am unable to establish a mechanism for this effect but have taken several steps to rule out contamination, although so far my experiments fall short of definitively excluding this.

6 *In vitro* and *in vivo* tracking of ganglioside mimicking and non-mimicking *C. jejuni*

6.1 Introduction

The aims of the experiments in this chapter are to establish if differences in receptor binding and/or opsonisation between ganglioside mimicking and non-mimicking strains of *C. jejuni* translate into altered cellular association and uptake, both *in vitro* and *in vivo*.

My third core hypothesis, that ganglioside mimicry alters *C. jejuni* trafficking, is not without precedent. The results presented in chapter four demonstrate that ganglioside mimicry by *C. jejuni* enables the bacteria to bind to specific myeloid expressed siglec receptors *in vitro*, namely Sialoadhesin and Siglec F. It has been shown by other groups that Sialoadhesin enhances phagocytosis of sialylated meningococci²⁵⁵ and I aim to investigate if this also occurs with *C. jejuni*. In addition to receptor mediated effects, the reduced natural antibody levels and complement activation directed against the ganglioside mimicking *C. jejuni* could also affect cellular association and trafficking and I aim to investigate this further.

Figure 48: Analysis of CFSE labelled *C. jejuni*.

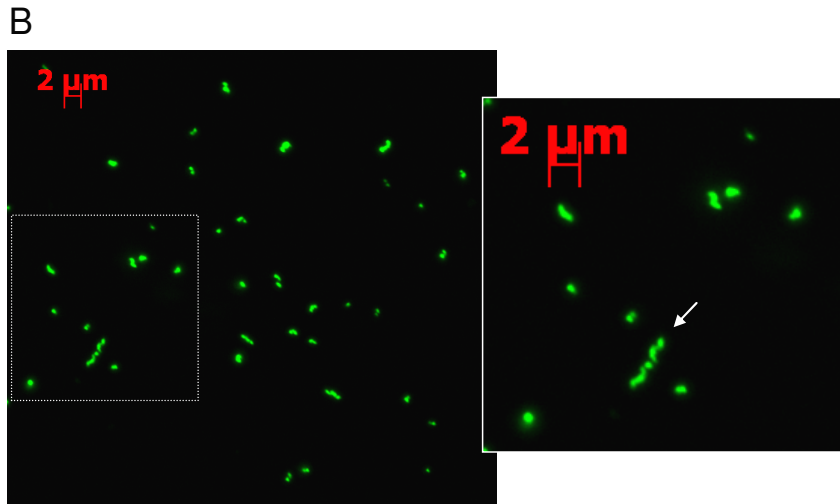
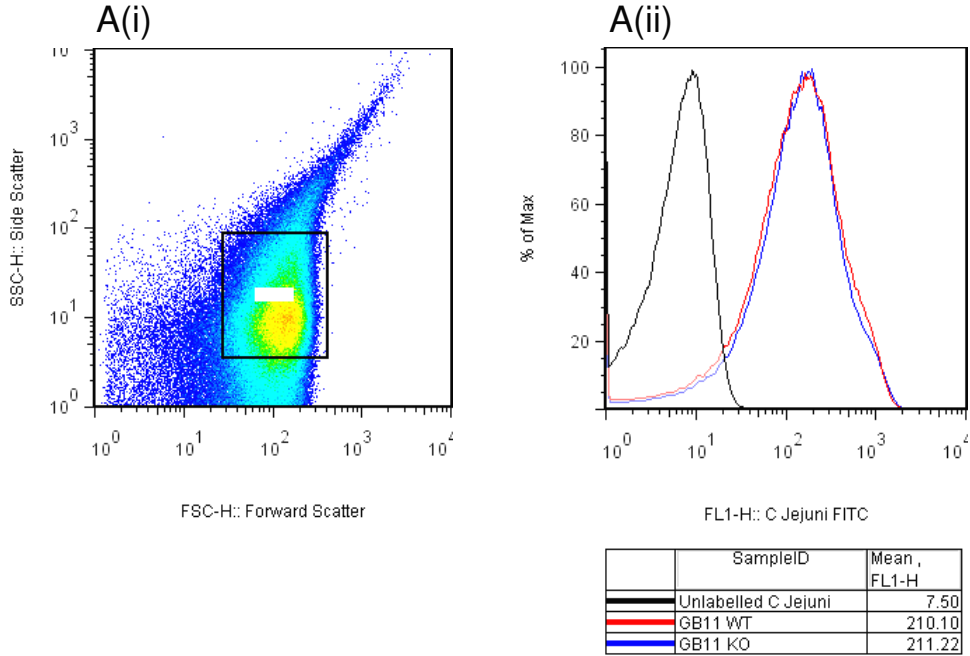


Figure 48. Wild type and knock out *C. jejuni* were incubated with 2.5 μ M CFSE for 30 minutes before heat inactivation. The fluorescence was assessed using FACS analysis. (A) (i) is a representative forward side scatter FACS plot of *C. jejuni* (ii) is a histogram plot showing CFSE MFI of both strains including unlabelled control bacteria. (B) labelled bacteria visualised using a fluorescent microscope. Inset - mixtures of corkscrew (white arrow), C-shaped bacilli and coccoid morphology were often present.

6.2 Results

6.2.1 Fluorophore labelling of *C. jejuni*

In order to track *C. jejuni* both *in vitro* and *in vivo*, without altering the surface epitopes, it was decided to develop a protocol to label the bacteria with the stable intracellular fluorophore CFSE. Ganglioside mimicking and non-mimicking strains were grown as before and incubated with CFSE, washed, then heat inactivated. As the bacteria were intended for use in quantification experiments using MFI they were first analysed by Flow Cytometry to ensure the GBS associated strains and control strains had acquired an equal fluorescence. Figure 48 (A) shows the dot plot (i) and MFI (ii) of the bacteria. This figure shows that both the wild type and knock out bacteria are labelled with an equal fluorescence. All batches were tested for fluorescence to ensure they were suitable for comparison.

In addition to ensuring the consistency of fluorescence it is important ensure the bacteria have not been damaged by the labelling process. Figure 48 (B) shows immunocytometry of CFSE labelled bacteria. The bacteria in this particular batch have retained their corkscrew morphology (white arrow). It was noted in subsequent batches that there is a phase variation in morphology with coccoid forms being more common in aged agar cultures (48 to 72 hours old) and it is known that prolonged culture or oxygen exposure can induce this morphological change. For the purposes of consistency, wild type and knock out strains were always grown and labelled simultaneously and bacteria from the same batch were used in each experiment.

Figure 49: Confirmation of durable CFSE binding.

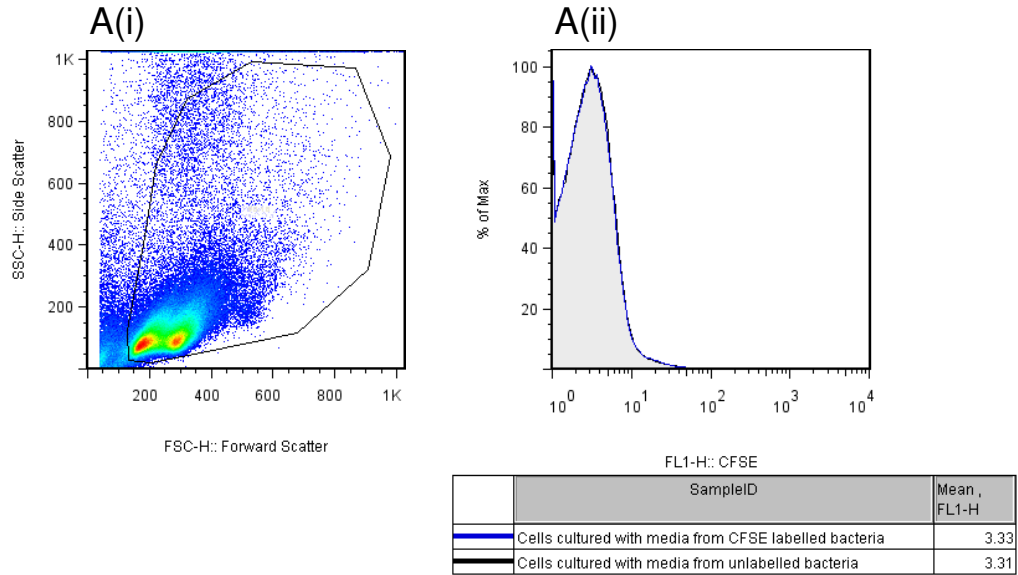


Figure 49. Confirmation that CFSE remains permanently bound to bacteria. Labelled or unlabelled bacteria were incubated in RPMI for 1 hour, removed by centrifugation and then splenocytes were incubated with the RPMI. (A)(i) FACS forward, side scatter dot plot of splenocytes. (ii) Histogram showing CFSE MFI of splenocytes following culture in RPMI which had, or had not, been incubated with CFSE labelled bacteria. Single experiment.

6.2.2 Confirmation that CFSE is retained by the *C. jejuni*

CFSE is used as a fluorophore label for mammalian cells and is exceptionally bright. For this reason it is necessary to confirm that it remains durably bound to *C. jejuni* and will not leak into co-cultured cells. Labelled or unlabelled *C. jejuni* were incubated in RPMI for 1 hour at 37°C then removed by centrifugation. Mixed splenocytes were then cultured in the RPMI for 30 minutes. The MFI of splenocytes cultured with RPMI from non-labelled *C. jejuni* was compared to the MFI of splenocytes cultured in RPMI from labelled *C. jejuni*. Figure 49 shows a FACS plot of the mixed splenocytes (i) and the MFI of the cells (ii). The histograms show no increase in MFI of the splenocytes cultured with RPMI which had previously been exposed to labelled *C. jejuni* indicating that leakage of fluorophore and subsequent uptake by cells is not a confounding factor.

Figure 50: Quantification of *C. jejuni* by optical density.

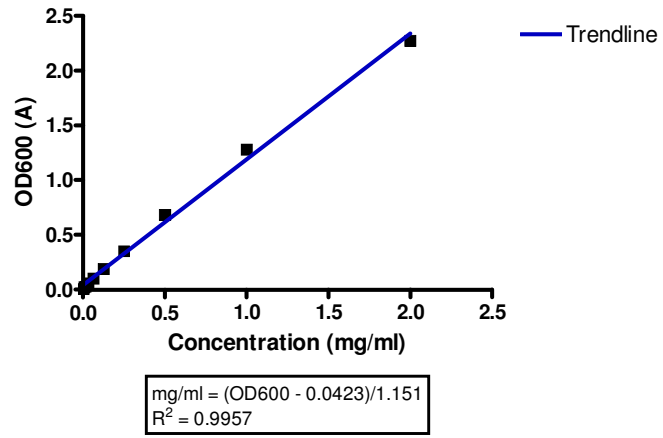


Figure 50. Quantification of *C. jejuni*. Graph showing dry weight v OD600. Mean calculated from two tubes. Single experiment.

6.2.3 Development of a convenient and reliable method for quantification of *C. jejuni*

C. jejuni had to be grown off-site (in a fully regulated diagnostic microbiology facility) because of restrictions on the use of genetically modified class 2 pathogens in my laboratory complex. In addition, GBS associated *C. jejuni* are rough mutant which rapidly form an amorphous growth pattern making quantification by traditional colony forming units impractical. Due to these difficulties a convenient method of quantifying killed *C. jejuni* was established. A mixed population of *C. jejuni* were heat killed, lyophilised and the dry weight established. After being resuspended in PBS, a doubling dilution was carried out and OD600 measured. Figure 50 shows a linear relationship between dry weight and OD600. For experiments where an estimate of bacteria to cell ratio was required, the mass of one organism was taken to be 1×10^{-12} g (the estimated mass of an *E. coli* cell²⁰⁸).

Figure 51: Association of opsonised *C. jejuni* with B cells.

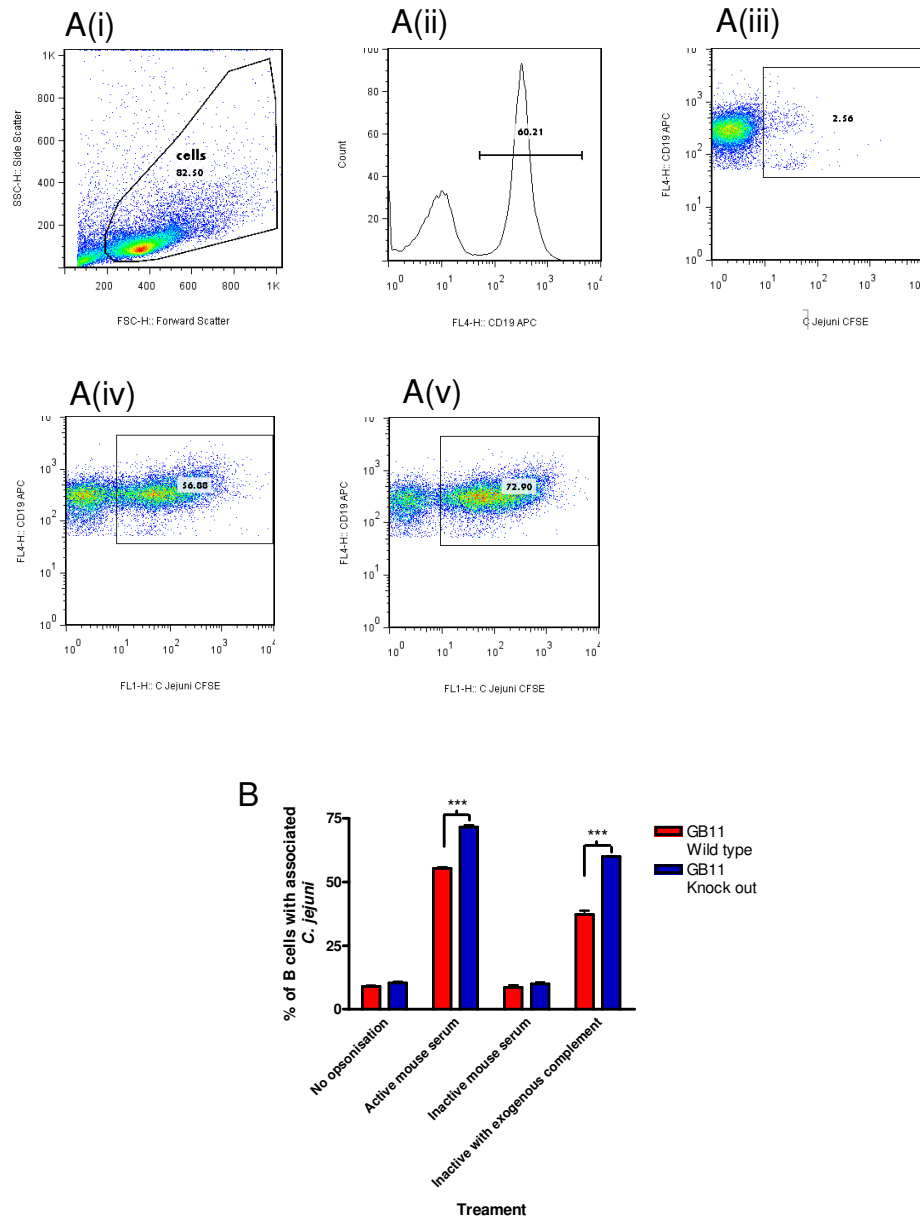


Figure 51. Heat inactivated, CFSE labelled, *C. jejuni* were opsonised for 1 minute in fresh autologous mouse serum, heat inactivated serum or heat inactivated serum with added exogenous purified mouse serum complement. They were then incubated with mixed splenocytes derived from collagenase treated spleens. Association of *C. jejuni* with B cells was assayed using FACS. (A) Representative FACS plots showing (i) Splenocyte gate, (ii) CD19 positive B cells, (iii) B cells incubated without bacteria, (iv) B cells incubated with opsonised wild type bacteria and (v) B cells incubated with opsonised knock out bacteria. (B) Graph showing the percentage of B cells associated with *C. jejuni* following different opsonisation conditions (corrected for background A(iii)). Following opsonisation, more B cells were associated with knock out bacteria than wild type bacteria ($p < 0.001$). There is no difference following heat inactivation of serum. The difference reappears following addition of exogenous complement ($p < 0.001$). Mean and SEM calculated from triplicate wells. Analysed using two way ANOVA with Bonferroni's posttests. (***)= $p < 0.001$). Representative of three experiments.

6.2.4 Effect of complement opsonisation of *C. jejuni* on B cell association *in vitro*

My previous results demonstrate that non-ganglioside mimicking strains of *C. jejuni* are more readily opsonised by complement and that this corresponds with increased natural antibody present in naïve sera against these strains. In order to establish if this is likely to affect *C. jejuni* cell association *in vivo* it was decided to opsonise CFSE labelled bacteria and track cell association *in vitro* in a mixed splenocyte population derived from collagenase treated spleens. B cells were chosen as the target cell as they are considered the main effector cell in GBS and express complement receptors.

Wild type and knock out *C. jejuni* were opsonised for 1 minute in fresh homologous mouse serum before being incubated with splenocytes at a 3:1 ratio. The cells were kept at 4°C in the presence of 5mM Na Azide and 5mM EDTA to prevent phagocytosis by other populations and to prevent further complement activation. Figure 51(A) shows representative FACS plots. (A)(i) is the splenocyte gate. (A)(ii) shows the CD19 positive gate (B cells) and A(iii), (iv) and (v) show the percentage of *C. jejuni* positive B cells following incubation with no bacteria (used for background correction), wild type bacteria and knock out bacteria respectively. Figure 51(B) is the graphed data and shows the percentage of B cells with associated *C. jejuni* under different opsonisation conditions.

The results show that opsonisation of knock out *C. jejuni* leads to greater association with B cells than wild type *C. jejuni* ($p < 0.001$). To confirm the role of complement in this association, heat inactivated homologous serum was used to opsonise the bacteria. Inactivation results in no difference between wild type and knock out *C. jejuni* B cell association. When exogenous purified-mouse-serum-complement was reintroduced into the heat inactivated serum prior to opsonisation, the increased B cell association of non-ganglioside mimicking strains is restored ($p < 0.001$). This experiment also shows the same trend when the data is analysed using the MFI of B cells rather than percentage positive.

These results support the earlier finding that ganglioside mimicking strains show less opsonisation and indicate that this will potentially affect cell association and trafficking *in vivo*.

Figure 52: Immunocytochemistry of Sialoadhesin on bone marrow derived macrophages.

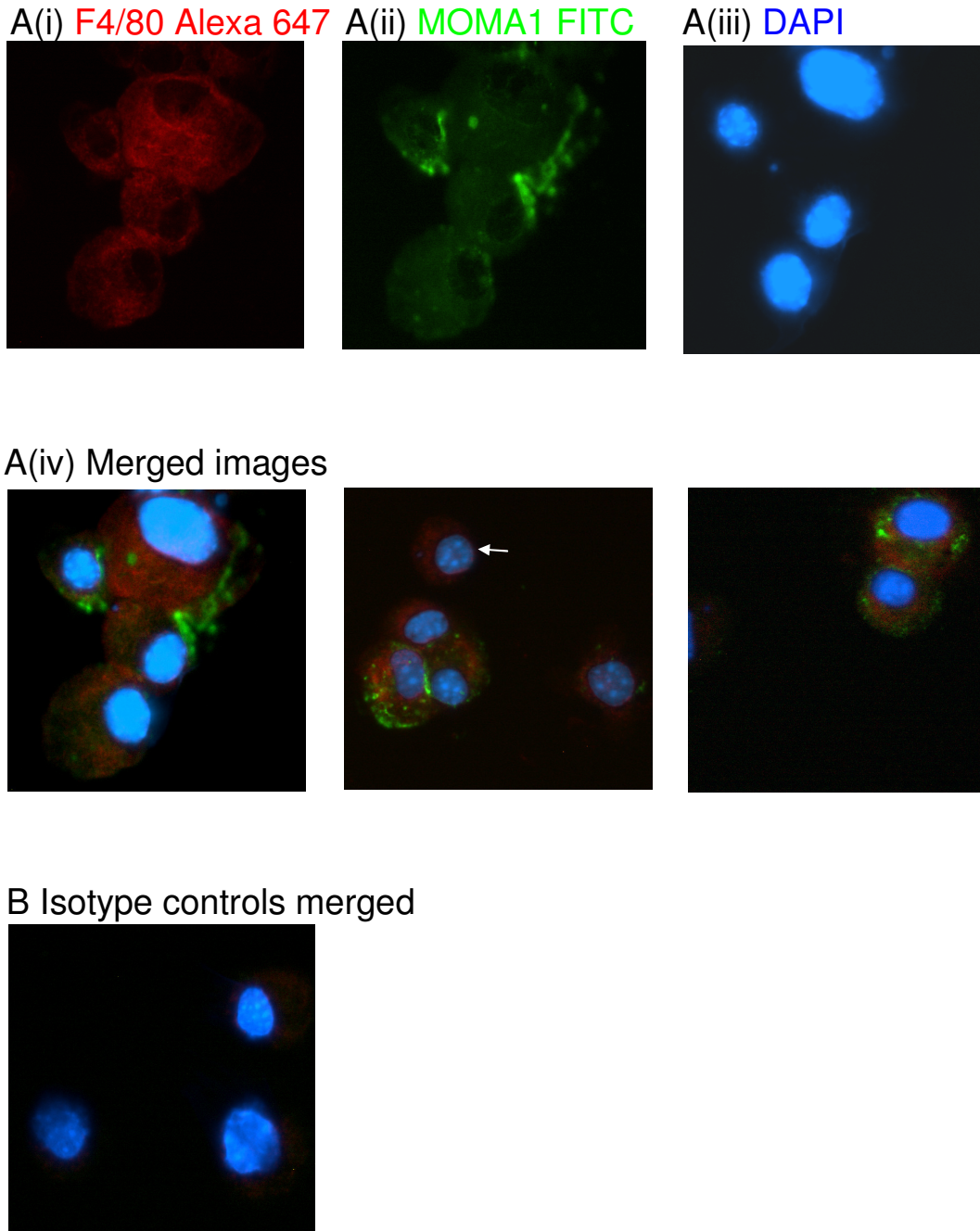


Figure 52. Detection of Sialoadhesin expression by bone marrow derived macrophages. A cytospin of formalin fixed bone marrow derived macrophages was prepared then labelled overnight with F4/80 and MOMA1. Sialoadhesin could be detected on some, but not all F4/80 positive macrophages (white arrow shows Sialoadhesin negative cell). (A)(i) to (iii) Single labels. (iv) Merged images. (B) Merged isotype controls. Single experiment.

6.2.5 Identification of the Sialoadhesin receptor on bone marrow derived macrophages

High levels of Sialoadhesin expression are found on specific subpopulations of macrophage, notably the lymph node subcapsular sinus macrophages and splenic metallophilic macrophages. Sialoadhesin is also expressed at low levels by conventional populations of macrophages^{209,248}. In order to establish if bone marrow derived macrophages would be a suitable population to study Sialoadhesin-*C. jejuni* interactions, a population of these macrophages was labelled with the Sialoadhesin specific antibody MOMA1 and the macrophage marker F4/80, and analysed using immunofluorescence microscopy.

Figure 52 shows immunocytology of these macrophages. Image (A) (i) to (iii) are single stains. (A)(iv) shows that, following overnight incubation with the MOMA1 antibody, Sialoadhesin expression by F4/80 positive macrophages could be detected. Interestingly Sialoadhesin could not be detected on all of the F4/80 positive cells (white arrow). Although labelling with MOMA1 appeared weak and patchy, the MOMA1 isotype control was negative. The fluorophore used in conjunction with F4/80 was AlexaFluor-647 which is adversely affected by DAPI (present in the mounting medium) and this is probably the reason for the weak F4/80 signal.

Figure 53: Macrophage phagocytosis of *C. jejuni* analysed by FACS.

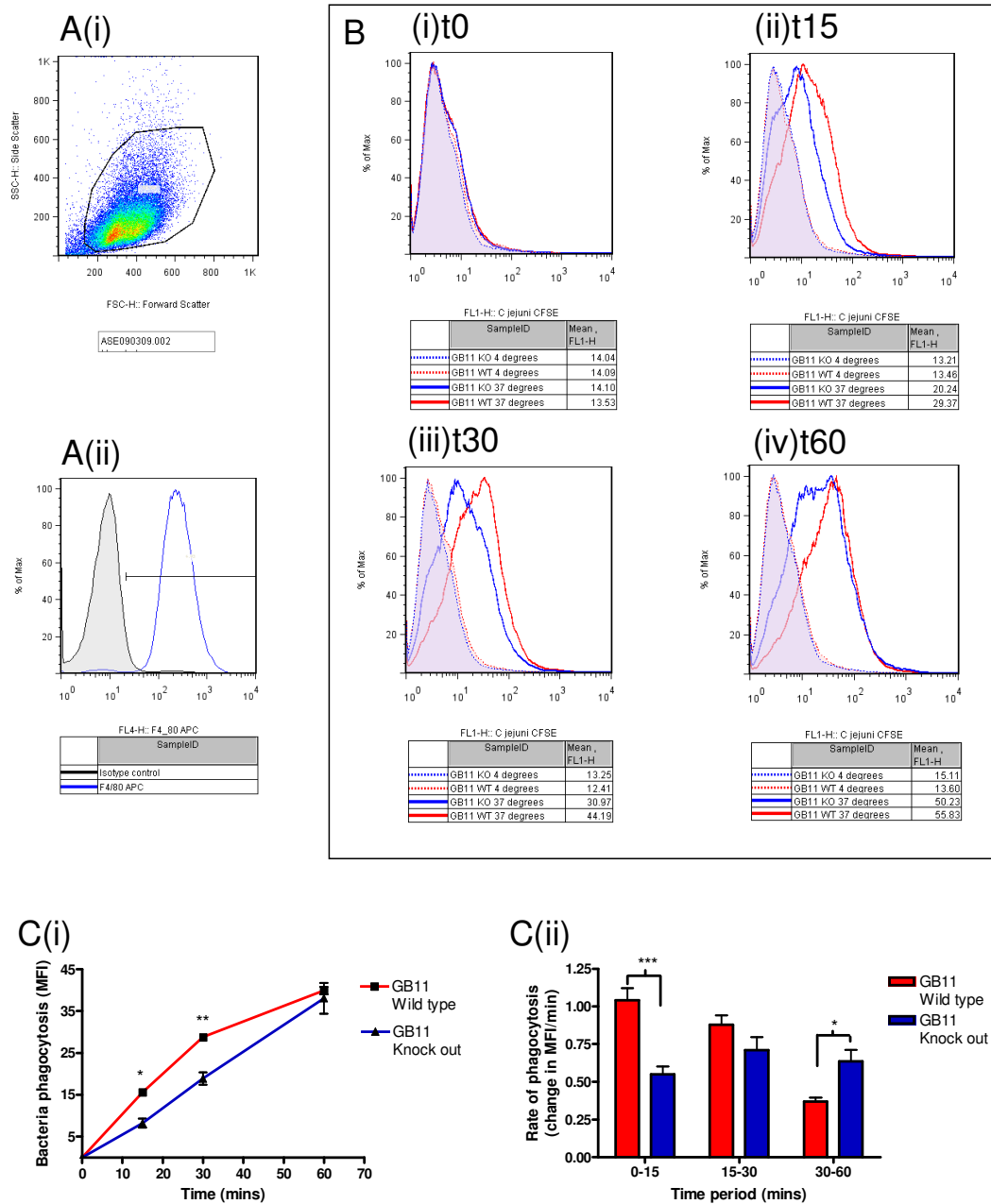


Figure 53. Bone marrow derived macrophages were incubated with wild type or knock out *C. jejuni* (20:1 bacteria:cell ratio) and phagocytosis was measured using the increase in CFSE MFI of the macrophages. The fluorescence of cells kept at 4°C in cRPMI with 5mM NaAzide was subtracted as the control. (A)(i) and (ii) Cell gate and F4/80 positive gate with isotype control. (B) Histogram FACS plots showing the CFSE MFI of macrophages at (i) 0 minutes, (ii) 15 minutes, (iii) 30 minutes and (iv) 60 minutes. 4°C/NaAzide controls are included and were subtracted from the final MFI. (C)(i) Graph of the MFI against time. There is increased phagocytosis of the wild type strain after 15 and 30 minutes compared to knock out. C(ii) Graph showing the rate of phagocytosis over each time period and demonstrates an initial rapid uptake of wild type *C. jejuni* greater than knock out. Mean and SEM calculated from triplicate tubes. Analysed using 2way ANOVA with Bonferroni's posttests (*= $p < 0.05$, ***= $p < 0.001$). Representative of three experiments.

6.2.6 Bone marrow derived macrophage phagocytosis of *C. jejuni*

Sialoadhesin has been shown to facilitate phagocytosis²⁵⁵. Results presented earlier in this thesis (chapter 4.2.1) demonstrate Sialoadhesin binding to ganglioside mimicking *C. jejuni*. In order to test the hypothesis that Sialoadhesin binding will increase the rate of phagocytosis of ganglioside mimicking *C. jejuni*, bone marrow derived macrophages were cultured with CFSE labelled wild type or knock out *C. jejuni* at a 20:1 bacteria to cell ratio and phagocytosis was assessed by measuring the increase in CFSE MFI in the macrophages. To exclude confounding effects of natural antibody opsonisation, ultra-low immunoglobulin foetal bovine serum was used to supplement the media. In addition, to eliminate the effect of surface binding without phagocytosis, a control population of macrophages was incubated with *C. jejuni* at 4°C in the presence of 5mM Na Azide.

Figure 53 (A) shows the F4/80 positive macrophage population. Figure 53(B) (i) to (iv) shows representative histograms of the MFI of the macrophages following incubation with CFSE labelled bacteria at 0, 15, 30 and 60 minutes. As the MFI increases, it can be seen that phagocytosis of the ganglioside mimicking strain is more rapid than the non-ganglioside mimicking strain. Figure 53(C)(i) illustrates the increase in MFI graphically and is corrected for background fluorescence (the shaded histograms in figure 53(B)). The difference between wild type and knock out is statistically significant after 15 minutes ($p < 0.05$) and 30 minutes ($p < 0.01$). Of three experiments, the wild type and knock out reached equivalent phagocytosis by sixty minutes in one, and were close to equivalent in two, with the wild type still being ahead. Figure 53(C) (ii) shows the same data illustrated as a rate of phagocytosis over each time period and shows that the enhanced rate of uptake of the ganglioside mimicking strain is an early phenomenon ($p < 0.001$) with the rate equalising, and then reversing.

Figure 54: Immunocytometry of phagocytosed *C. jejuni*.

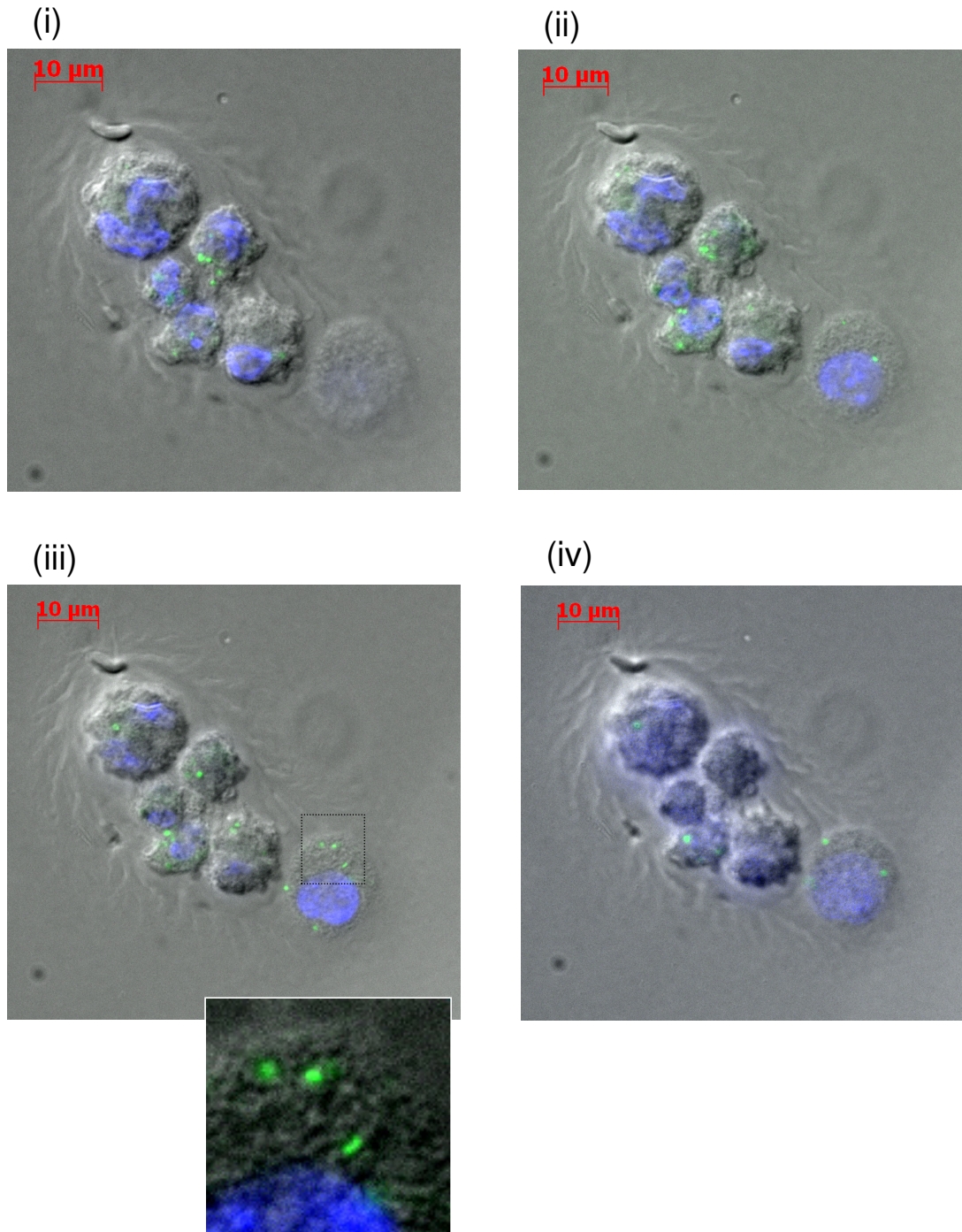


Figure 54. Visualised of macrophage phagocytosis of *C. jejuni* using light and fluorescent microscopy with Z-stacking to demonstrate the intracellular location of the bacteria. (i) to (iv) is a Z-stack in which multiple bacteria can be seen in levels (ii) and (iii) which are absent in (i) and (iv) indicating their presence inside the cytoplasm (see inset). This was confirmed for wild type and knock out strains in single experiments.

6.2.7 Microscopy of phagocytosed *C. jejuni*

To confirm that phagocytosis of *C. jejuni* was occurring, a cytopsin was made of macrophages that had been incubated with *C. jejuni* for 1 hour. The cytopsin was examined using light microscopy with overlaid fluorescence microscopy to identify the bacteria. A Z-stack was made to confirm the intracellular location of the bacteria.

Figure 54 (i) to (iv) shows selected images from the Z-stack of a representative slide. A number of bacteria can be seen present in the middle two layers (highlighted by the insert) which are absent in the external layers, confirming that at least a proportion of the bacteria are intracellular. Phagocytosis of both wild type and knock out strains was confirmed by this method.

Figure 55: Inhibition of phagocytosis by Sialoadhesin blockade.

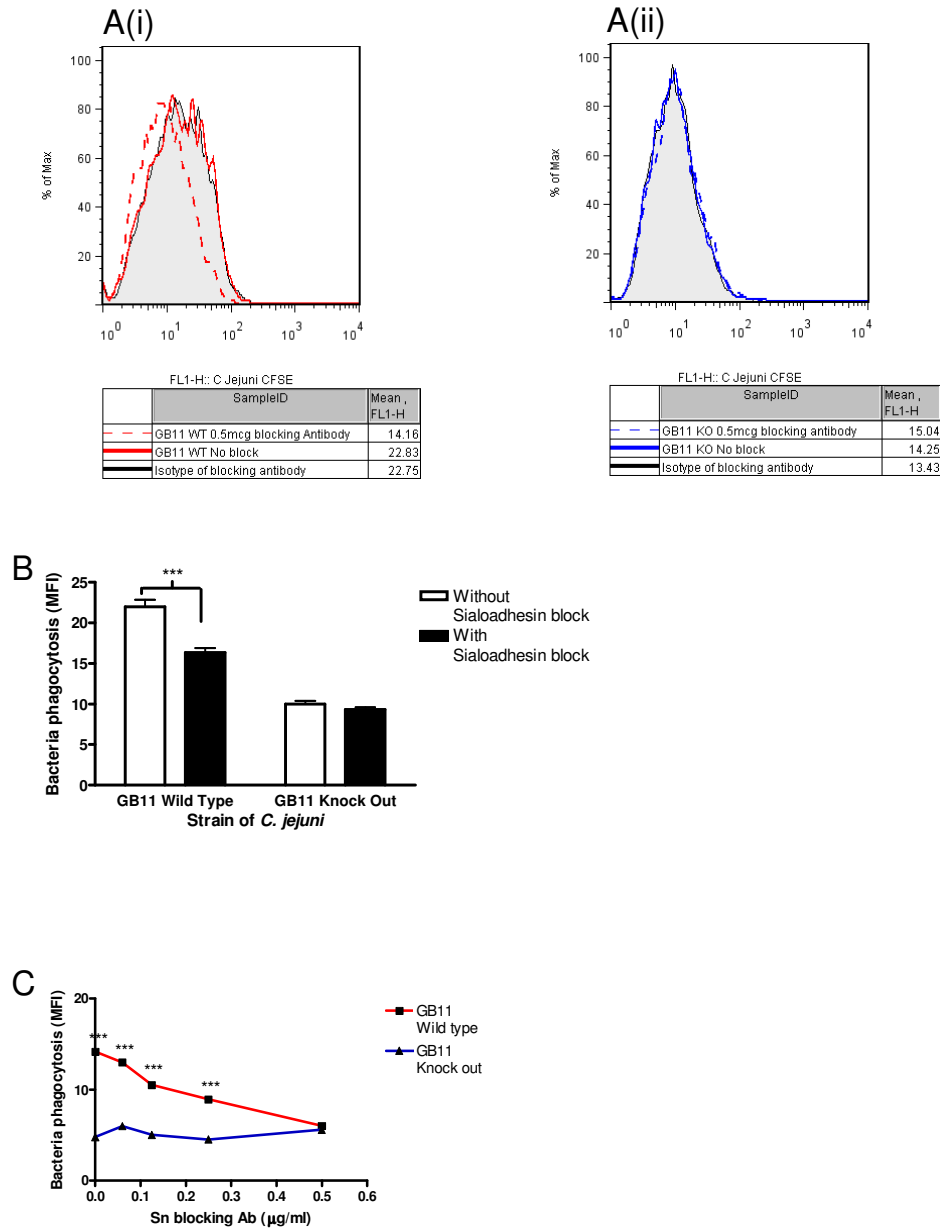


Figure 55. Bone marrow derived macrophages were incubated with labelled *C. jejuni* (10:1 bacteria to cell ratio) for 40 minutes in the presence of a single concentration or a titrated dose of Sialoadhesin blocking antibodies SER4 and 3D6 and phagocytosis was measured as before. (A)(i) and (ii) shows the MFI of macrophages incubated with labelled wild type and knock out bacteria respectively. The unbroken line is with no blocking antibody, the broken is with Sialoadhesin blocking antibody and the shaded histogram is the isotype control. $4^{\circ}\text{C}/\text{NaAzide}$ controls are not included in the histogram for clarity, but were subtracted for the final MFI calculation. (B) Graph showing inhibition of phagocytosis of wild type *C. jejuni* in the presence of a single concentration of Sialoadhesin blocking antibody with no effect on knock out phagocytosis. (C) Titration of blocking antibody until equivalence is reached. Mean and SEM calculated from triplicate tubes. Analysed using 2way ANOVA with Bonferroni's posttests (***)= $p < 0.001$. (B) representative of three experiments, (C) single experiment.

6.2.8 Phagocytosis following incubation with Sialoadhesin blocking antibodies

To confirm that Sialoadhesin is the receptor mediating the enhanced phagocytosis of ganglioside mimicking *C. jejuni*, a phagocytosis assay was carried out at a single time point, at a bacteria to cell ratio of 10:1, in the presence of the Sialoadhesin blocking antibodies 3D6 and SER-4.

Figures 55(A) (i) and (ii) respectively show representative histograms of the MFI of macrophages incubated for 40 minutes with labelled wild type (red lines) and knock out (blue lines) *C. jejuni*. The histograms show bacterial uptake. The unbroken line is phagocytosis with no blocking antibody. The broken line is phagocytosis following prior incubation with 3D6 and SER-4. The shaded histogram is a 3D6 and SER-4 isotype control. The 4°C, Na Azide controls are not shown in the histogram to aid clarity, but were subtracted from the final fluorescence. This figure shows a reduction in the right-shift of the wild type histogram in the presence of blocking antibodies with no such reduction in the knock out histogram.

Figure 55(B) shows a phagocytosis blocking experiment at a single concentration of blocking antibody (0.3µg/million cells) (4°C controls subtracted) and shows a statistically significant reduction in phagocytosis of wild type *C. jejuni* (p<0.001) with no reduction in knock out phagocytosis when Sialoadhesin blocking antibodies are present.

After it was established that Sialoadhesin blocking antibody inhibited wild type but not knock out *C. jejuni* phagocytosis, it was decided to do a titration of blocking antibody to establish if the rate of wild type phagocytosis could be reduced to match that of knock out. Figure 55(C) shows the effect of increasing the dose of blocking antibody on the amount of wild type and knock out phagocytosis. At 0.5 μ g/ml each of blocking antibodies 3D6 and SER-4, there is no statistical difference between phagocytosis of wild type and knock out *C. jejuni*.

6.2.9 *In vivo* tracking of i.v. injected *C. jejuni* to metallophilic macrophages

Having established *in vitro* differences in complement opsonisation and cell association as well as differences in receptor mediated phagocytosis of ganglioside mimicking and non-mimicking strains of *C. jejuni* it was decided to inject the bacteria into mice i.v. and establish which cell populations the ganglioside mimicking or non-mimicking bacteria associate with. As Sialoadhesin is expressed at high levels by metallophilic macrophages I hypothesised that the wild type strains would associate with this cell population. As the knock out strain is targeted by complement, I hypothesised that these bacteria would either be rapidly lysed in the serum or associate with complement receptor expressing cells such as marginal zone macrophages or MZ B cells.

Age and sex matched C57BL/6 mice were injected i.v. with 200µl of heat inactivated bacteria at an OD600 of 0.6 in PBS. Control mice were injected with PBS alone. After 1 hour or 3 hours the mice were sacrificed and the spleen, lymphoid tissue and serum harvested and stored at -80°C. Following sectioning, the spleen was stained with a B220 specific antibody to identify the follicles and a MOMA1 antibody to identify the metallophilic macrophages.

Figure 56(A) (i) to (iii) shows single stains. (A)(iv) shows a representative image of a splenic follicle from a wild type strain injected mouse. The inset shows labelled *C. jejuni* lying in association with MOMA1 positive macrophages (white arrows (a)). In addition, bacteria can also be seen lying external to the MOMA1 positive population (white arrow (b)). Figure 56(B) shows a representative section from a PBS injected mouse and the inset illustrates the background auto-fluorescence that can be distinguished from bacteria.

Figure 57(A) (iv) shows a representative image of a splenic follicle from a knock out strain injected mouse. The inset shows that knock out bacteria are also found in association with the MOMA1 positive metallophilic macrophages.

Figure 56: *In vivo* association of wild type *C. jejuni* with metallophilic macrophages.

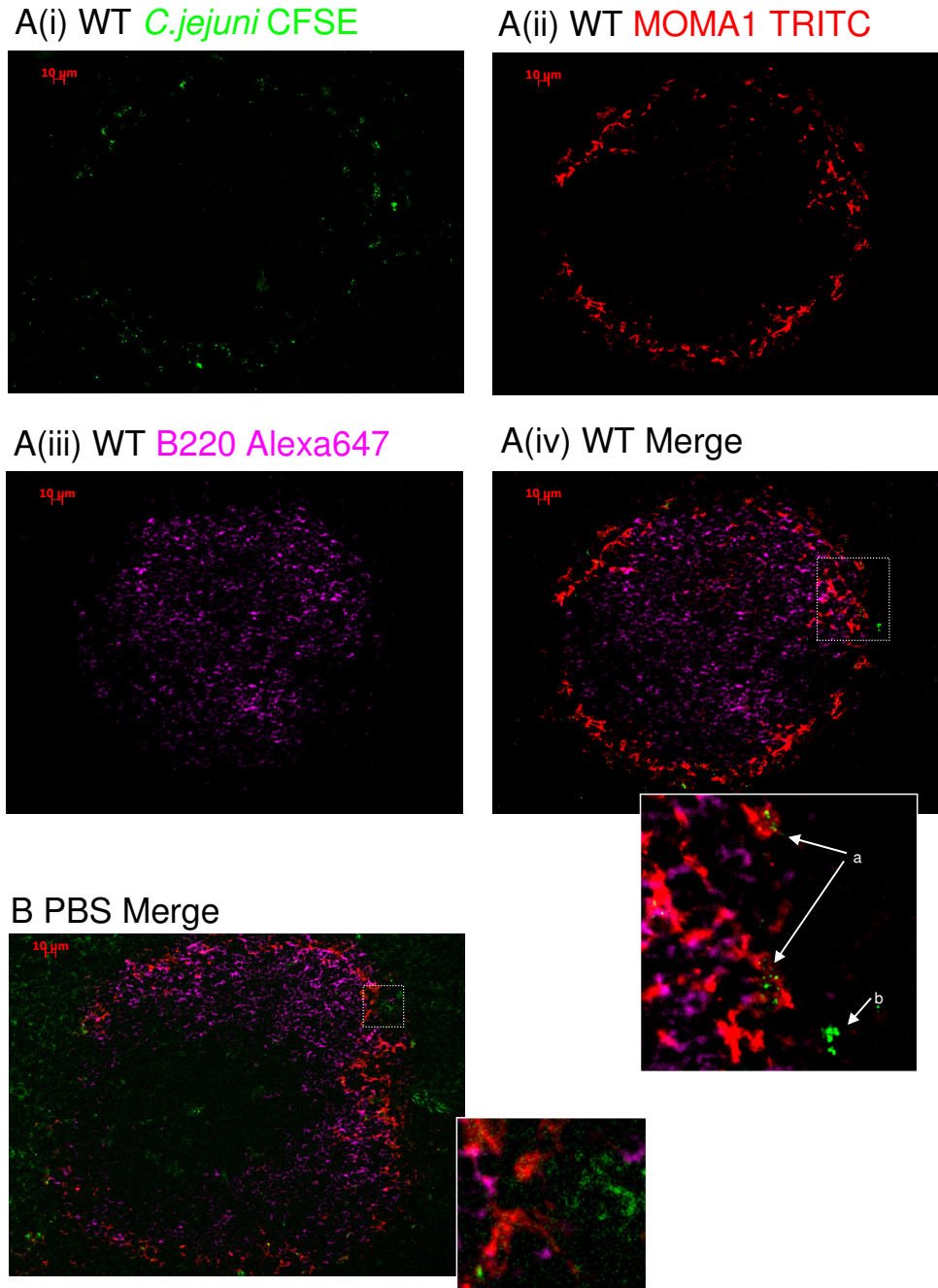


Figure 56. Fluorescent microscopy images of spleens from wild type *C. jejuni* injected mice after 1 hour. Spleen was stained for metallophilic macrophages (MOMA1) and B cells (B220). (A) (i) to (iii) are single stains. (iv) Shows the merged images of a splenic B cell follicle and the inset shows wild type *C. jejuni* in association with metallophilic macrophages (a) and external to the metallophilic macrophages (b). (B) Is a splenic section following i.v. PBS injection and the inset shows FITC auto-fluorescence clearly distinguishable from the labelled bacteria in (A)(iv). (n=4 for 1 hour time point and n=2 for 3 hour time point).

Figure 57: *In vivo* association of knock out *C. jejuni* with metallophilic macrophages.

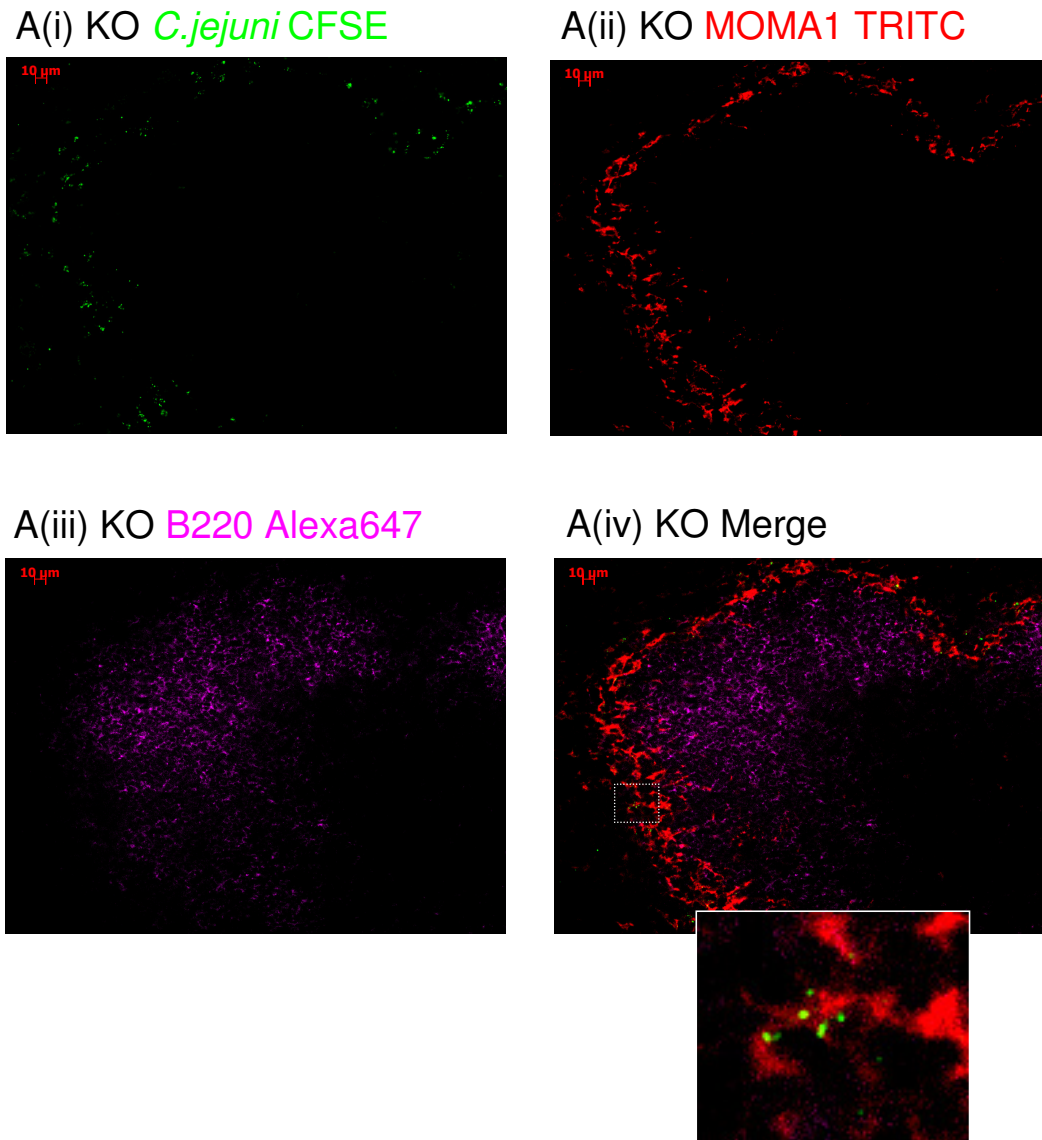


Figure 57. Fluorescent microscopy images of spleens from knock out *C. jejuni* injected mice after 1 hour. Spleen was stained for metallophilic macrophages (MOMA1) and B cells (B220). (A) (i) to (iii) is single stains. (iv) Shows the merged images of a splenic B cell follicle and the inset shows knock out *C. jejuni* in association with metallophilic macrophages. (n=4 for 1 hour time point, n=2 for 3 hour time point).

6.2.10 *In vivo* tracking of i.v. injected *C. jejuni* to marginal zone macrophages

Both wild type and knock out bacteria were identified outside the rim of metallophilic macrophages, lying in a region which is populated by marginal zone macrophages. To test if these bacteria were associating with marginal zone macrophages the sections were stained with the marginal zone macrophage marker ER-TR9. Figure 58(A) (iv) shows a representative image of a follicle from a wild type injected mouse. Bacteria can be seen lying in association with the ER-TR9 positive marginal zone macrophages (inset white arrow (a)) and also internal to this population (white arrow (b)) in association with ER-TR9 negative cells (presumably metallophilic macrophages). Figure 58(B) shows a follicle from a PBS injected control mouse and again illustrates background autofluorescence.

Figure 59 (A) (iv) shows a representative image of a splenic follicle from a mouse injected with knock out bacteria. The inset shows bacteria lying in association with ER-TR9 positive marginal zone macrophages (white arrow (a)) and also lying internal to this (white arrow (b)) in association with ER-TR9 negative cells (again, presumably metallophilic macrophages).

Figure 58: *In vivo* association of wild type *C. jejuni* with marginal zone macrophages.

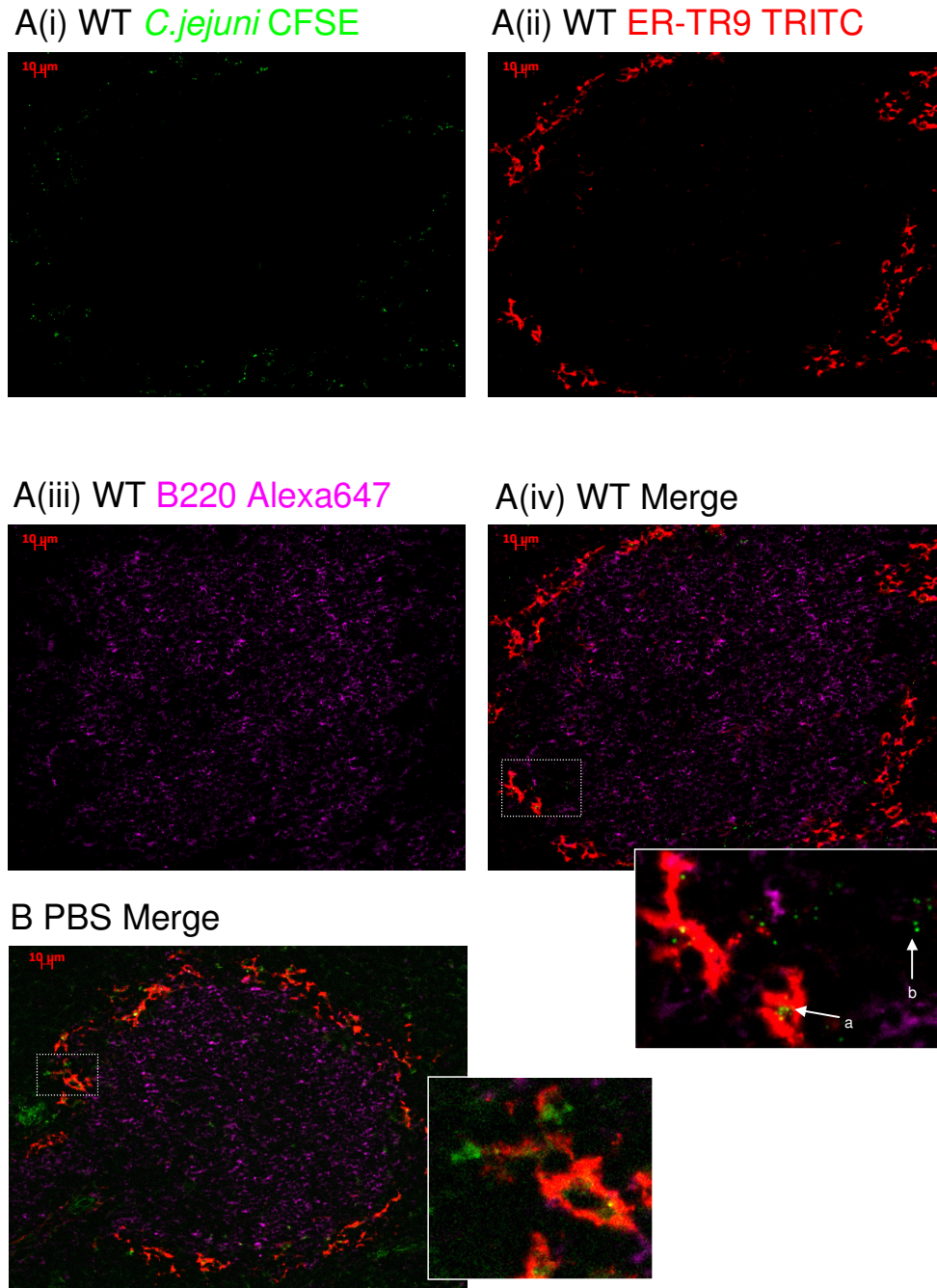


Figure 58. Fluorescent microscopy images of splenic sections 1 hour following i.v. administration of labelled wild type *C. jejuni*. Spleen was stained for marginal zone macrophages (ER-TR9) and B cells (B220). (A) (i) to (iii) are single stains. (iv) Shows the merged images of a splenic B cell follicle and the inset shows wild type *C. jejuni* in association with marginal zone macrophages (a) and internal to the marginal zone macrophages (b). (B) Is a splenic section following i.v. PBS injection and the inset shows FITC auto-fluorescence clearly distinguishable from the labelled bacteria in (A)(iv). (n=4 for 1 hour time point, n=2 for 3 hour time point).

Figure 59: *In vivo* association of knock out *C. jejuni* with marginal zone macrophages.

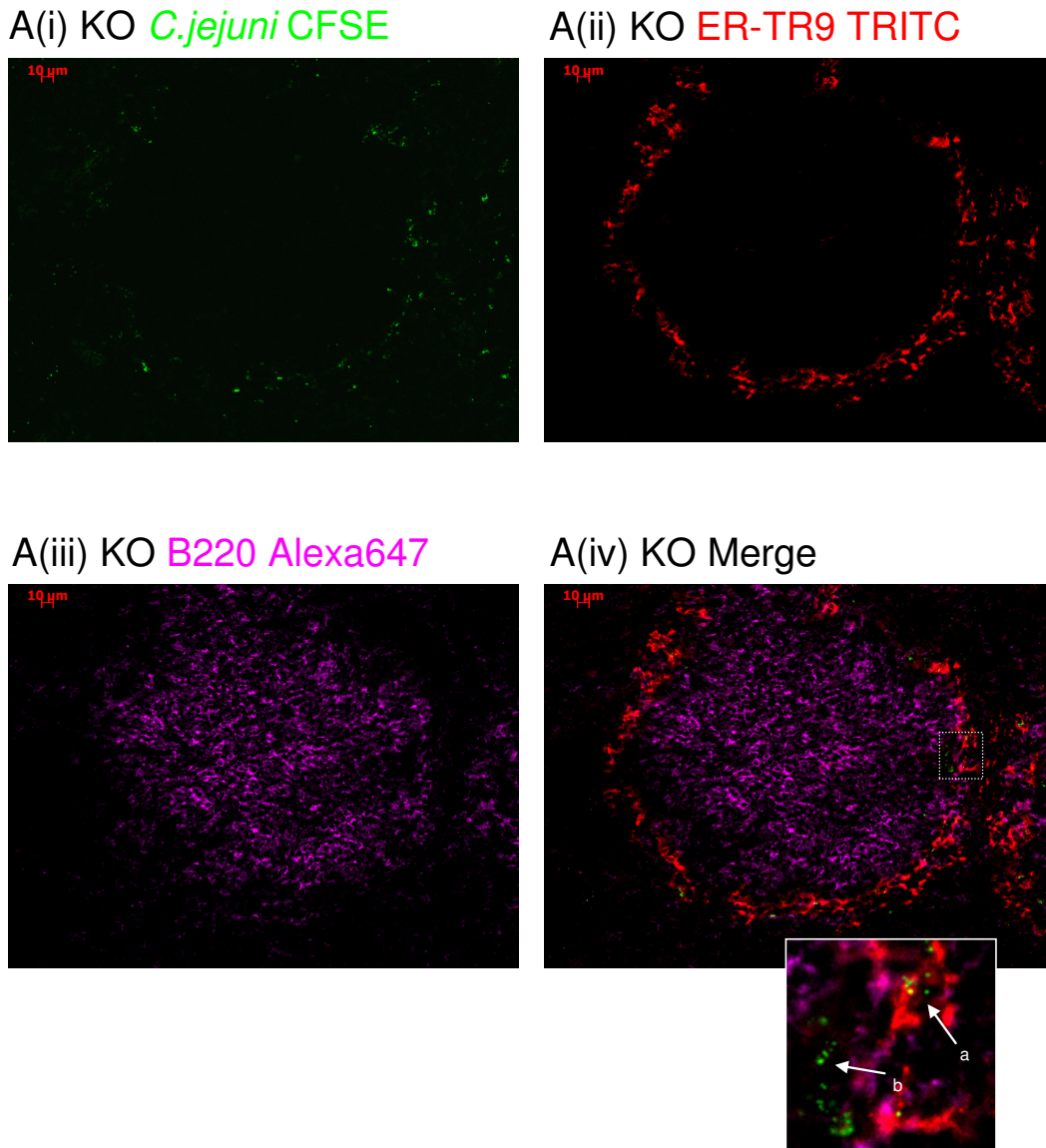


Figure 59. Fluorescent microscopy images of splenic sections 1 hour following i.v. administration of labelled knock out *C. jejuni*. Spleen was stained for marginal zone macrophages (ER-TR9) and B cells (B220). (A) (i) to (iii) show single stains. (iv) Shows the merged images of a splenic B cell follicle and the inset shows knock out *C. jejuni* in association with marginal zone macrophages (a) and internal to the marginal zone macrophages (b). (n=4 at 1 hour time point, n=2 at 3 hour time point).

Figure 60: Analysis of *C. jejuni* and macrophage *in vivo* co-localisation.

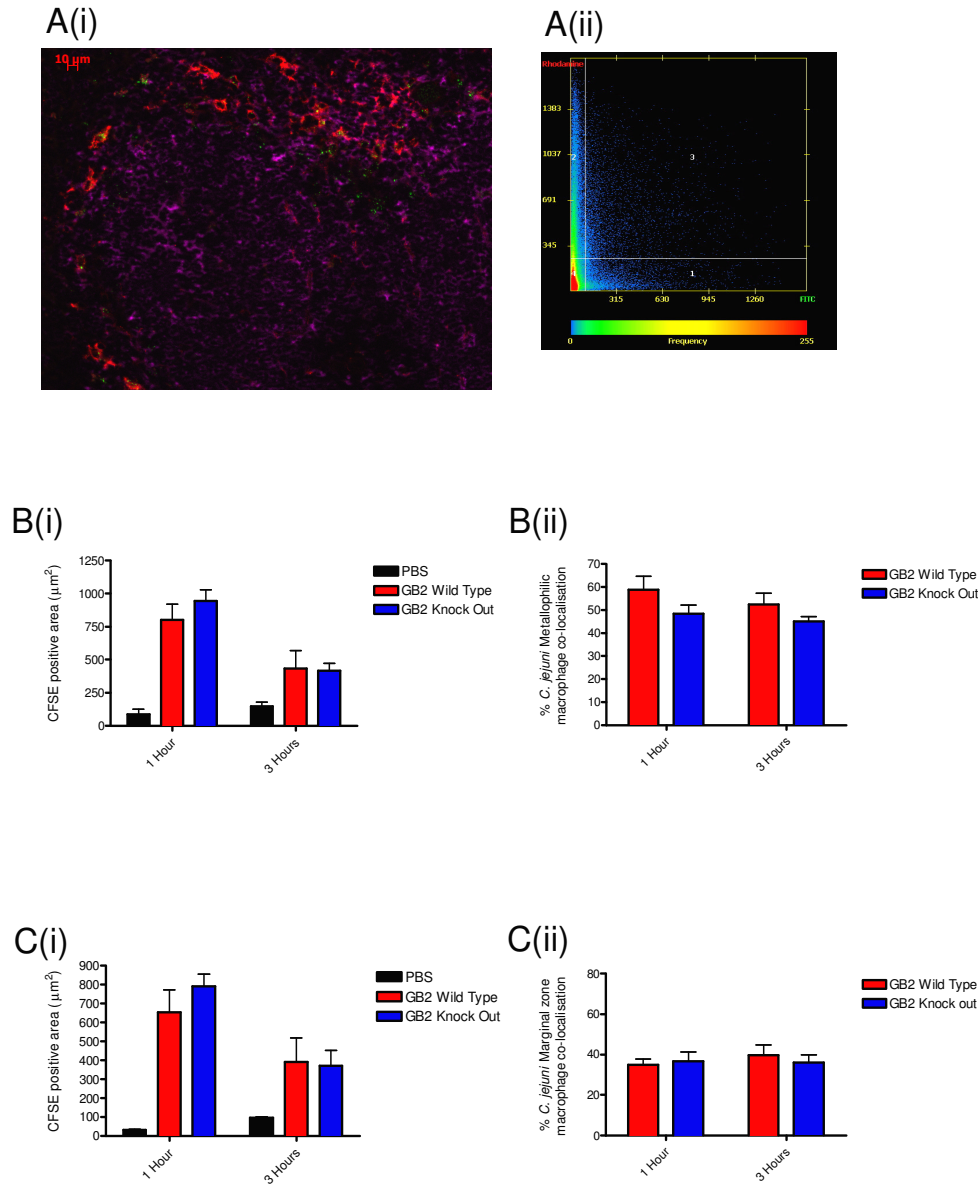


Figure 60. The co-localisation of wild type and knock out *C. jejuni* with metallophilic and marginal zone macrophage populations was quantified. A(i) representative follicle. A(ii) representative scatter plot analysis. Co-localisation software identified the number of pixels in which CFSE (bacteria) and TRITC (macrophage population) were co-localised. (B) Metallophilic macrophages (i) Shows the total CFSE positive area after 1 hour and 3 hours. (B)(ii) Shows the percentage of *C. jejuni* and metallophilic macrophage co-localisation ((co-localised area/total CFSE area) *100)). There is no statistical difference between wild type and knock out *C. jejuni* at either time point. (C) Marginal zone macrophages. (i) Shows the total CFSE positive area after 1 hour and 3 hours in the ER-TR9 stained sections. (C) (ii) Shows the percentage of *C. jejuni* and marginal zone macrophage co-localisation ((co-localised area/total CFSE area) *100)). There is no statistical difference between wild type and knock out *C. jejuni* at either time point. Analysed using two way ANOVA with Bonferroni's posttest. (n=4 at 1 hour, n=2 at 3 hours. 3 follicles in each of 2 sections analysed per mouse).

6.2.11 Quantification of *C. jejuni* association with macrophage populations

In order to determine if there are quantitative differences in the association of the different strains of *C. jejuni* with metallophilic and marginal zone macrophages, co-localisation software was used to quantify amount of CFSE (*C. jejuni*) positive area and establish how much it co-localises with the different macrophage populations.

Figure 60 (A) (i) shows a representative follicle and figure 60 (A) (ii) shows the scatter plot generated when a follicle is analysed. The number of pixels positive for both CFSE and TRITC are identified in the top right quadrant. Two sections were taken per spleen and three follicles were analysed per section. Four wild type and four knock out *C. jejuni* injected mice spleens were analysed at 1 hour and two each at 3 hours.

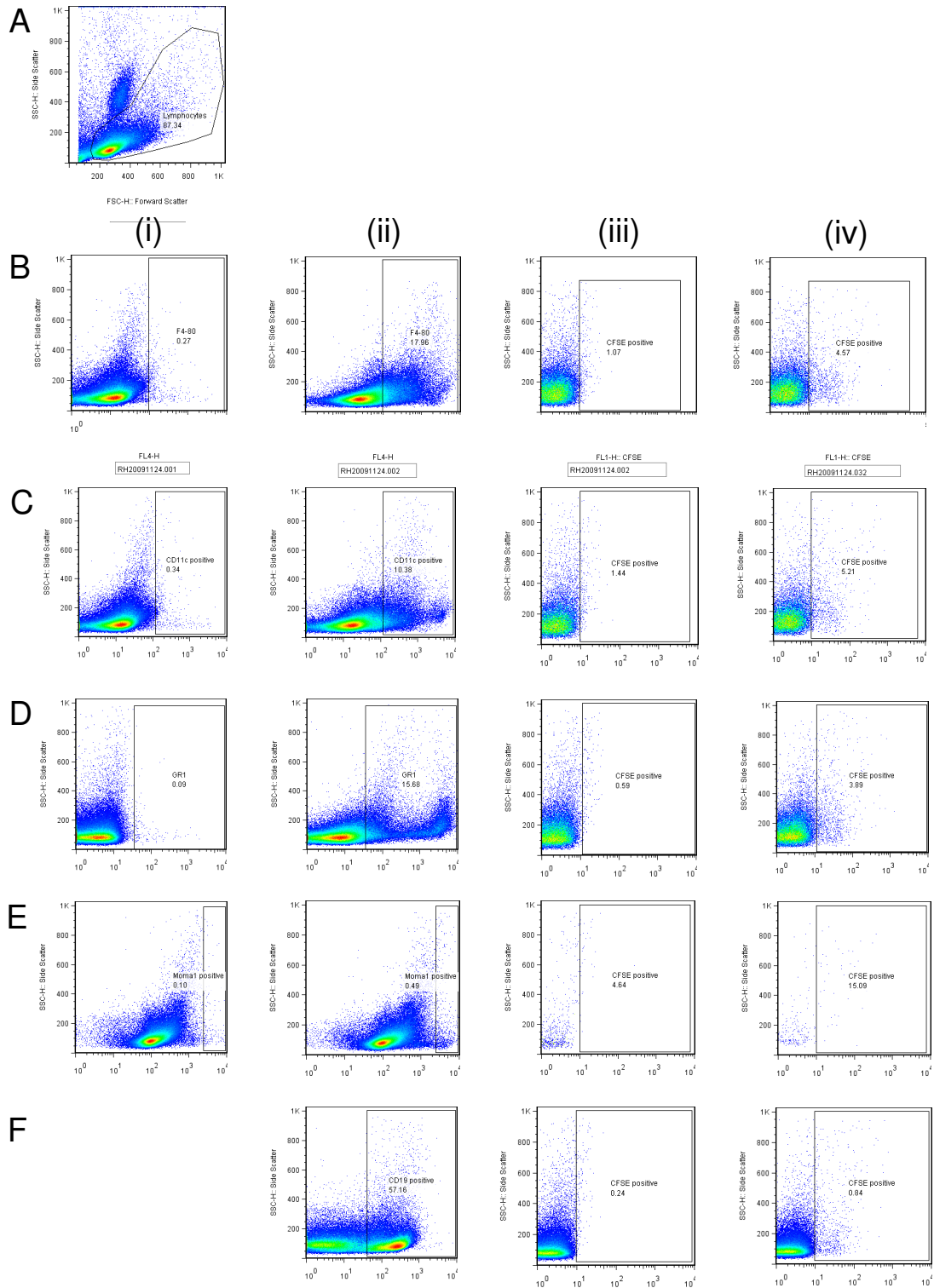
Figure 60 (B) (i) shows the average total CFSE positive area per follicle in the MOMA1 stained sections at 1 hour and 3 hours post injection, and demonstrates the steep drop off in fluorescence over this time period. This rapid loss of fluorescence demonstrates one of the technical challenges in tracking the labelled bacteria. There is no statistical difference between the total CFSE positive area for wild type and knock out injected mice at either time point showing that the same quantity of bacteria reached, and were retained in, the spleen for both wild type and knock out strains.

Figure 60 (B) (ii) shows the percentage of *C. jejuni* co-localising with metallophilic macrophages. This demonstrates that both strains of bacteria localise to this macrophage population and that these macrophages are associated with approximately half of all the bacteria that are present in the spleen. There is no statistical difference between the two strains of *C. jejuni* at either time point.

Figure 60 (C) (i) shows the average total CFSE positive area per follicle in the ER-TR9 stained sections at 1 hour and 3 hours post injection. As expected, the results are similar to the MOMA1 stained sections with no statistical difference between the total CFSE positive area for wild type and knock out injected mice at either time point.

Figure 60 (C) (ii) shows the percentage of *C. jejuni* co-localising with marginal zone macrophages. Both *C. jejuni* strains localise with this macrophage population. There is no statistical difference between the two strains at either time point. A smaller percentage of the bacteria localise with marginal zone macrophages than with the metallophilic macrophages. However, between the metallophils and marginal zone macrophages it appears that that virtually all of the *C. jejuni* depositing in the spleen will be associated with these populations.

Figure 61: FACS analysis of *C. jejuni* co-localisation with splenocytes *in vivo*.



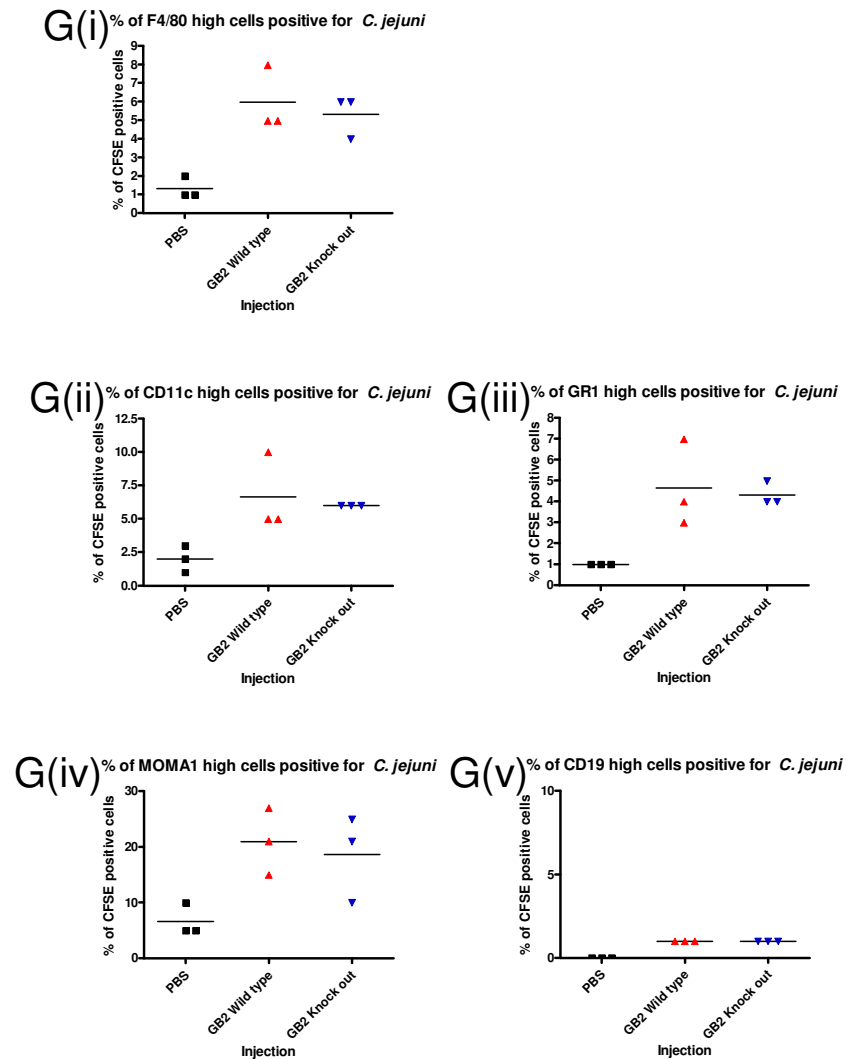


Figure 61. Mice were injected i.v. with 200 μ l of labelled wild type or knock out bacteria at an OD600 of 0.6. The mice were sacrificed after 1 hour and a single cell suspension was made of the spleens without collagenase. The cells were briefly fixed with paraformaldehyde then labelled for various cell populations. (A) to (F) Representative FACS plots. (A) Lymphocyte gate, (B) F4/80 positive cells (macrophages), (C) CD11c positive cells (dendritic cells), (D) GR1 positive cells (granulocytes), (E) MOMA 1 positive cells (metalophilic macrophages), (F) CD19 positive cells (B cells). Column (i) isotype control (not available for CD19), (ii) antibody marker for lymphocyte population (x axis, all APC), (iii) CFSE (*C. jejuni*) high in PBS injected mouse (negative control) and (iv) CFSE high from *C. jejuni* injected mouse.

(G) (i) to (v) graphical representation of FACS data comparing association of wild type *C. jejuni* and knock out *C. jejuni* with different spleen populations (i) F4/80 positive, *C. jejuni* positive, (ii) CD11c positive, *C. jejuni* positive, (iii) GR1 positive, *C. jejuni* positive, (iv) MOMA1 positive, *C. jejuni* positive and (v) CD19 positive, *C. jejuni* positive. There are no statistically significant differences between wild type and knock out populations. Analysed using 1 way ANOVA with Bonferroni's multiple comparison test. (n=3 mice for each injection, FACS tubes in triplicate).

6.2.12 Analysis of *C. jejuni* association with different splenic cell populations using FACS

In order to confirm the immunohistology results and to test a broader range of cell types, spleens from injected mice were analysed using Flow Cytometry.

Nine age and sex matched C57BL/6 mice were divided into three groups and injected with *C. jejuni* or PBS as before. After one hour the spleens were harvested and a single cell suspension was made. The immunohistology results and pilot FACS studies had shown that bacteria, or the CFSE fluorescence, disappear rapidly *in vivo*. The spleens were therefore fixed for 15 minutes in 1% paraformaldehyde and the usual red cell lysis step was omitted so that surface associated bacteria would remain intact.

The cell populations studied were F4/80 high macrophages, CD11c high dendritic cells, GR1 positive granulocytes (using the anti-Ly-6G neutrophil specific clone 1A8), MOMA1 high metallophilic macrophages and CD19 positive B cells. Figures 61 (A) to (F) show representative FACS plots (detailed in the figure legend) and includes isotype controls where available and PBS injected controls.

Figure 61 (G) (i) to (v) shows the percentage of CFSE (*C. jejuni*) positive cells in each of the populations studied. There is no statistical difference in the association of wild type or knock out *C. jejuni* with any of the cell types studied.

6.3 Discussion

These results and the technical challenges that were met in achieving them led to a number of novel observations. An ideal method of tracking *C. jejuni* involves an intrinsic fluorophore label which is stable and resistant to bleaching. Plasmid transformation with green fluorescent protein (GFP) is one possible solution with the added advantage that the label is stable through multiple rounds of division. Although such transformations have been done, they are technically challenging as commercially available *gfp* plasmids are not suitable for use in *C. jejuni* because the antibiotic resistance genes and origins of replication are not active in this species³²³. In addition, making the *C. jejuni* chemically competent would require prolonged periods of handling which was impossible due to safety restrictions which prevented the use of live, genetically modified, pathogens in the lab. The off-site clinical bacteriology lab where the bacteria were cultured does not have the facilities to carry out such work.

To overcome these difficulties, the cell tracking fluorophore CFSE was used to label the live bacteria which were then heat inactivated to prevent dilution of the dye. CFSE enters bacteria where it is metabolised by esterases resulting in covalent intracellular binding³²⁴. This makes it a suitable alternative to GFP as it is stable and is unlikely to alter surface epitopes. CFSE has been used to label and track *C. trachomatis*, *borreliae Sp.*, *H. pylori* and *S. pneumoniae*³²⁵⁻³²⁸. However, it shows species specific differences in uptake with poor labelling of *S. aureus* and no labelling of *E. coli*³²⁸. This is the first time that CFSE labelling of *C. jejuni* is demonstrated and I also show that identical levels of labelling can be achieved within related strains of *C. jejuni* which allows tracking the bacteria while comparing individual genetic traits, in this case the expression of ganglioside mimics on LOS. Durable binding of CFSE is important (i.e. the CFSE won't leak out). This has already been demonstrated using *S. pneumoniae*³²⁸ and I confirm this quality in *C. jejuni* as there is no evidence of CFSE leakage into culture media.

Previous studies in this thesis have demonstrated reduced complement deposition on ganglioside mimicking strains of *C. jejuni* compared to control strains (chapter 4.2.10). These studies looked at formalin fixed bacteria which had been adsorbed onto an ELISA plate. In this chapter I demonstrate that this difference in complement opsonisation affects association of heat inactivated *C. jejuni* with splenic B cells *in vitro*. This study suggests that ganglioside mimicry might affect which immune cells the bacteria associate with *in vivo* and that ganglioside mimicry begins to shape the interaction with the immune system at a very early stage, i.e. when bacteria are first exposed to serum.

B cells express complement receptors³²⁹⁻³³¹ and complement plays a vital role in B cell responses both directly through signalling and indirectly by controlling delivery of antigens. Deficiency of complement components results in defective antibody responses³³²⁻³³⁵. There are a number of mechanisms by which complement facilitates humoral immunity. The complement receptors CD21/CD35 link antigen to the B cell, they act synergistically with B cell receptor signalling and they co-aggregate with CD19 to modulate signalling³³⁶⁻³⁴¹. In addition, MZ B cells deliver IgM opsonised antigen to follicular dendritic cells in a complement and complement receptor dependent manner²⁸⁹. Although the complexities of an *in vivo* system make it impossible to predict how small differences in opsonisation will affect immunity, in theory, my observations regarding opsonisation and cell association suggest the ganglioside mimicking strains should be less immunogenic due to less opsonisation.

The results presented here show relatively more B cell association of non-ganglioside mimicking bacteria and that this is complement dependent. Results presented earlier suggest that natural antibody is the important factor determining levels of complement opsonisation (chapter 4.2.12). How efficiently *C. jejuni* are opsonised and delivered to follicular dendritic cells could be down to variations in an individual's anti-ganglioside natural antibody levels and repertoires. This is an important area for further work as it was not proven definitively that natural antibody was the sole cause of differences in complement activation.

Sialoadhesin has affinity for ganglioside mimicking *C. jejuni* (chapter 4.2.1). Sialoadhesin mediates phagocytosis of sialylated *meningococci*²⁵⁵. The studies presented in this chapter show, for the first time, that ganglioside mimicking *C. jejuni* are phagocytosed more rapidly than control strains and that this difference can be completely inhibited by blocking Sialoadhesin. The margin of difference was very small, but had consistent statistical significance across several repeats. The small margin might be due to the population of macrophages being used in the assay. The presence of Sialoadhesin on bone marrow derived macrophages was demonstrated by immunocytology. However, the cells required an overnight incubation with the MOMA1 antibody and the receptor was not detectable on all of the F4/80 positive cells. This is not surprising as Sialoadhesin is highly expressed by only particular subpopulations of macrophages. These populations cannot be isolated and studied without altering their physiology as the only reliable marker is Sialoadhesin itself. It is therefore possible that any biological significance is not with the conventional macrophage populations but may lie with the specialised subpopulations. If an assay could be designed to study *C. jejuni* phagocytosis by these cells it might show marked differences when ganglioside mimicry is present.

Up until this point a number of *in vitro* phenomena have been demonstrated which have potential to alter trafficking and delivery of ganglioside mimicking *C. jejuni* to the follicle. Importantly, differences in behaviour between these strains and control strains have been by degree rather than absolute. In order to establish the biological significance

of these observations, ganglioside mimicking and control strains were injected i.v. into wild type mice. It was hypothesised that ganglioside mimicking strains can evade the complement cascade and localise to Sialoadhesin positive metallophilic macrophages.

No such study tracking antigen trapping of labelled *C. jejuni* has been done previously and in particular no studies have addressed trapping of a pathogen which expresses surface ligands for the metallophilic macrophage receptor, Sialoadhesin. The studies presented here show a trend for increased association of ganglioside mimicking *C. jejuni* with the metallophil population but this is not statistically significant. There is no statistical difference between strains when association with marginal zone macrophages is measured either. In addition, a number of *C. jejuni* can be seen in the splenic medulla not associated with either of these macrophage populations. Although I did not investigate this further, this may be association with medullary macrophages. The methods used in this study cannot reliably distinguish between phagocytosis and surface association.

Although not the expected outcome, association of both wild type and knock out strains with both the metallophilic and marginal zone populations of macrophages is an important finding, demonstrated for the first time. With hindsight, these findings are unsurprising as marginal zone and metallophilic macrophages both contribute to trapping of diverse types of particulate antigen³⁴²⁻³⁴⁵. Marginal zone macrophages are reported to express high levels of CR3³⁴² and my own experiments show efficient complement opsonisation of both strains of *C. jejuni*, albeit with inter-strain differences. The design of these experiments was insufficient to demonstrate the contribution of Sialoadhesin binding because both strains could be associating with both marginal zone and metallophilic macrophage populations via complement receptors. Another confounding factor is that the MOMA1 positive macrophage population overlies and interdigitates with the outermost B220 positive MZ B cell population and this might affect the ability of co-localisation software to discriminate between metallophil association and B cell association.

An interesting observation is that the B220 positive MZ B cells are not visible beyond the edge of the follicle indicating that the MZ B cells have been mobilised in a manner similar to that shown following purified LOS injection (chapter 5.2.1). Presumably LOS is shed from the bacteria during heat inactivation and is present in the injected whole bacteria sample. The rapid kinetics demonstrated here (1 hour versus 18 hours in 5.2.1) might be due to the intravenous versus intraperitoneal routes of administration.

Metallophilic macrophages are believed to be less phagocytic than conventional macrophages^{346,347} while their lymph node counterparts, subcapsular sinus macrophages, have been shown to transfer intact antigen on their surface into follicles. Future work might establish if ganglioside mimicking *C. jejuni* are endocytosed (through Sialoadhesin mediated phagocytic activity) while control strains might remain surface associated (and available to B cell receptors). There were a number of occasions where both wild type and knock out metallophilic macrophage associated *C. jejuni* appeared convincingly intracellular but confocal microscopy is required to formally establish this. In addition, cell sorting was employed to separate out the CFSE positive cells from a splenocyte suspension 1 hour after injection. Cytospins of the sorted cells, which will reveal the location of the bacteria, await analysis.

Functional outcomes might also prove important. The metallophilic macrophage population has been shown to be an important source of IFN- α/β following i.v. herpes simplex virus injection³⁴⁸. In my experiments, serum was taken at early and late time points, and combined with immunofluorescence labelling of the splenic sections, might yet reveal differences between *C. jejuni* strains at stimulating cytokines *in vivo*.

The association of *C. jejuni* with a number of different cell types *in vivo* was studied using FACS analysis. *C. jejuni* association with F4/80 positive macrophages, CD11c positive dendritic cells, GR1 positive granulocytes, MOMA1 positive macrophages and

CD19 positive B cells was measured and no difference between the *C. jejuni* strains is detected. These studies were difficult for practical reasons. The CFSE fluorophore is very bright and has a tendency to bleed in to other channels. Each cell type had to therefore be analysed as a double stain with *C. jejuni* in FL1 and the cell identifying antibody in FL4 (i.e. as far apart as possible in the spectrum). In addition, pilot studies showed that *C. jejuni* fluorescence rapidly disappears (presumably due to being destroyed by complement lysis or lysosomal enzymes in phagocytes) and we therefore had to omit potentially important but time consuming steps in the protocol, such as collagenase treatment of the spleens. As this is used to enhance the release of populations of antigen presenting cells it may have affected our results. Brief paraformaldehyde fixation was also used to preserve the bacteria. Despite these difficulties, the FACS analysis appears to confirm the immunohistology results, that is, there is no apparent difference in cell association between *C. jejuni* strains.

In conclusion, I show *in vitro* differences between ganglioside mimicking and non-mimicking strains in B cell association and macrophage phagocytosis. These differences are due to differential complement activation and receptor binding. However, *in vivo* I am unable to demonstrate differences in cell association. This might be due to practical considerations, such as the use of heat inactivated dead bacteria, which can only be tracked for a short period of time. In addition, alternative measures of outcome, such as IFN production, might yield positive results.

7 Conclusion

The experiments presented in this thesis were intended to address the following hypotheses:

1. LOS derived from a GBS associated strain of *C. jejuni* is able to bind to cellular or humoral ganglioside specific receptors through the ganglioside mimicking core sugars.
2. Binding of LOS to these ganglioside specific receptors alters the potency or polarising properties of ganglioside mimicking LOS compared to non-mimicking LOS.
3. Binding of ganglioside mimics to these ganglioside receptors alters trafficking of the *C. jejuni* within the immune system.

The maintenance of self-tolerance is an active process which is tightly regulated by the immune system. The over-arching hypothesis is that the breaking of tolerance which occurs in GBS following exposure to *C. jejuni* LOS is not an idiopathic event, but is driven by both Lipid A-TLR4 stimulation and ganglioside mimic-ganglioside receptor interactions. It is these additional signals that subvert the normal immune system homeostasis, and allow, or promote, the survival and expansion of auto-reactive B cell clones.

Studies of GBS are numerous, but until now have focussed largely on the clinical aspects of the disease or the function and fine specificity of the anti-ganglioside/anti-LOS antibodies and their role in neuroinflammation^{233,349,350}. In addition, the physiology of *C. jejuni* has been well studied with particular reference to the biochemical synthesis of ganglioside mimicking LOS^{101,202,203}. The general immunology of *C. jejuni* infection has also been the subject of much interest due to its role as an important food borne

pathogen^{76,351,352}. However, very few studies have looked closely at the induction phase of GBS, how ganglioside mimicking *C. jejuni*, specifically, interact with the immune system and if the ganglioside mimic is simply a passive target for autoreactive B cell receptors (antibodies) or if it influences the evolution of the response via ganglioside receptor interactions.

Studying potential interactions between ganglioside mimicking LOS and the immune system has become possible in recent years due to the identification and characterisation of ganglioside specific receptors such as members of the siglec family^{144,240} or galectin 1³⁵³. In addition, an understanding of the biochemical pathways involved in LOS synthesis allowed the generation of *C. jejuni* control strains, isogenic with the GBS associated ganglioside mimicking strains, which lack the CSTII enzyme required to add sialic acid to the LOS and generate a ganglioside mimic¹⁰¹. These provide an excellent source of non-ganglioside mimicking control LOS with which to compare the ganglioside mimicking LOS in function and potency.

To the best of my knowledge there is currently only one study which has reported binding of a ganglioside mimicking *C. jejuni* strain and its LOS to a lymphocyte expressed ganglioside receptor (a GM1/GT1a mimicking strain binding to the NK cell receptor, Siglec 7)¹⁴⁸ and no functional outcomes were measured. I sought to investigate LOS and *C. jejuni* interactions with ganglioside specific receptors and identify functional outcomes dependent on these interactions and idiosyncratic to ganglioside mimicking strains. It was hoped that this study would improve our understanding of the immune response to ganglioside mimicking *C. jejuni* and shed light on the evolution of autoimmunity in GBS.

7.1.1 LOS purification

In order to test my hypothesis I needed highly pure forms of wild type and CSTII knock out LOS which were standardised both by primary structure (the actual concentration of LOS molecules) and by secondary structure (the size and nature of the spontaneous LOS aggregates that form during hot phenol extraction). The secondary aggregate structures are important because they affect the rate at which LPS is taken up by cells¹⁰⁶ and LPS stimulated cytokine secretion²³².

Protocols for purifying LOS are well established³¹⁶, however this turned out to be a frustratingly difficult task. The nature of my experiments, comparing two strains of LOS, meant that quantification, purity and secondary structures were of paramount importance which contrasts with previous studies in which the chemical structure of the LOS was the prime concern. The thiobarbituric acid assay, for example, is commonly used to quantify LOS. However, I demonstrated that ganglioside derived sialic acid interferes with this assay making it inappropriate for comparing concentrations of ganglioside mimicking and non-mimicking strains. It is debatable whether the ganglioside effect is sufficient to render this assay useless. However, when dry weight and the thiobarbituric acid assay gave contrasting results (as they did) it was decided to work with dry weight as this is the standard method of quantifying LOS/LPS in immunological methods.

It was recognised that silver stains and Western blots can only act as surrogate markers when trying to determine the nature of the aggregate structures adopted by the LOS in aqueous solution. This level of organic chemistry is beyond the scope of the study and beyond the levels of expertise available in the department. However, the interpretation that “dimers” present in the silver stain represented two LOS molecules in a hydrophobic embrace, via their extensive acyl chains, is in fact consistent with previous, more specialised, work showing that dispersed LPS forms dimers, dependent on hydrophobic interactions, when in solution^{226,354}. The nature of such secondary structures is an

important consideration in the light of recent work showing that juxtaposed gangliosides form complexes which can dramatically alter the binding properties of antibodies and receptors^{233,355,356} and this might also be the case for ganglioside mimicking LOS. More importantly, when LOS forming dense precipitates was used in pilot studies it proved virtually inactive, or highly toxic, as the cells barely responded.

It is impossible to predict how the micelle structure of LOS will be affected by culture conditions. Clearly tissue culture media will contain cations. However, the LOS is diluted massively when added to culture media which presumably makes secondary structures less likely to form de novo. However, if they are already present they may not be affected. In addition, the serum added to RPMI media to make complete RPMI will contain numerous proteins and lipoproteins (such as high density lipoprotein, chylomicrons and LPS binding protein) which are known to have a physiological capacity to bind LPS and affect its transport, activity and detoxification³⁵⁷⁻³⁶¹. Provided the wild type and knock out strains have comparable micelle structures before addition to cultures then any of these immeasurable considerations should be controlled for.

The initial attempts to regulate aggregate structure by dispersal with Triton X detergent were stymied by an inability to remove the large detergent molecule using dialysis. Pilot studies using the small planar detergent, sodium cholate (used frequently for this very purpose²³²) looked more promising. However, an alternative strategy, which avoided adding divalent cations, which facilitate aggregate formation^{362,363}, was used by a collaborating group who provided us with the aforementioned wild type and CSTII knock out *C. jejuni* and LOS. The fact that the enzymes remained active can be explained by the high concentrations of Ca^{2+} and Mg^{2+} which associate with LPS during purification from bacteria³⁵⁴. I showed in my silver stain and Western blot analysis that using this technique resulted in only faint dimers and, combined with the visual appearance of the solution, interpreted this as meaning the LOS was no longer forming large secondary structures. This purification could have been improved by combining the strategies of avoiding cations in the enzyme buffer with using cholate dispersal to produce mono-

disperse LOS which could then be reconstituted into its spontaneous micelle forms under controlled buffer conditions to ensure parity between the wild type and knock out strains.

Bacterial LPS is frequently contaminated by other bacterial immunostimulators³⁶⁴⁻³⁶⁶. Glycolipids, such as capsular polysaccharide, represent the most tenacious contaminants because of their similar chemical properties to LPS, meaning that they do not necessarily partition differently during chemical extraction techniques such as hot phenol. In addition, it cannot be digested out using enzymes, and although some protocols use lysozyme for this purpose, I showed it to be inappropriate with my R-form LOS where it caused dramatic changes to the secondary LOS structures. Prolonged ultra-centrifugation is included in many protocols possibly to take advantage of differing solubilities between LOS and capsular polysaccharide. However, in my hands this resulted in a significant loss of reagent. It was not included in my collaborators protocol as it was thought to be of dubious benefit.

I established that contamination of my LOS is minimal using silver stain for protein/nucleic acids (sensitive to picogram quantities), alcian blue staining for capsular polysaccharide and spectrophotometry (again for protein and nucleic acids). A biological assay was also employed by stimulating dendritic cells from the LPS hyporesponsive C3H/HeJ mouse strain and measuring IL-10 secretion which had been established as a cytokine reliably excreted by *C. jejuni* LOS stimulated C57BL/6 derived dendritic cells.

Establishing purity could have been improved by using a more robust biological assay. However, the TLR4^{-/-} strain of mouse was not available and doing more extensive tests using the natural Tlr4 mutated C3H/HeJ strain might only have served to muddy the waters as this strain is idiosyncratic in its response to LPS. For example, priming C3H/HeJ derived mononuclear cells with IFN- γ restores LPS responsiveness³¹⁷. There has also been a report of these strains being responsive to rough, but not smooth, forms of LPS³¹⁸. An alternative and highly sensitive biological method of detecting contamination

is using TLR transfected reporter cell lines which are commercially available (for example Invivogen's HEK-Blue™ C3H/WT murine embryonic fibroblasts). These cells are transfected with a TLR of interest and a reporter gene is placed under an NFκB inducible promoter which results in visible colour change in the media when the transfected TLR receptor is activated. This represents a more definitive method of excluding contamination or demonstrating that the contamination is present in equal amounts in wild type and knock out purified LOS.

I believe that I achieved a high standard of purity and that the GBS associated and control strains of LOS were comparable in purity, concentration and secondary structures. Any subtle differences in concentration, due to the differing molecular weights of the two strains, could be best addressed by using titrations of LOS. I therefore felt it was possible to compare these strains of LOS to each other to establish if the ganglioside mimicking strain exhibited any unique receptor binding or immune stimulating properties.

7.1.2 Binding of LOS to ganglioside specific receptors

Using ganglioside specific antibodies, I demonstrated that the expected ganglioside epitopes were present on LOS. My first task in confirming my central hypothesis was to show that ganglioside specific receptors can also bind to the ganglioside mimicking epitopes. As is common in carbohydrate immunology, receptor specificity for gangliosides is not clear-cut and often defined by relative levels of affinity for closely related glycan structures, or indeed complexes of different glycan structures^{144,146,356}. A number of receptors showing affinity for GD1a and GM1 exist and are expressed on several lineages of immune cells. It was decided to focus on siglecs expressed by myeloid cells as these cells play an important role in B cell responses^{367,368} and the necessary reagents were kindly provided by a collaborating group.

Surprisingly, I could not demonstrate binding of the macrophage expressed siglec, Sialoadhesin, to either native ganglioside or purified LOS under a number of conditions. In contrast to the native ganglioside and LOS findings, Sialoadhesin showed clear affinity for ganglioside mimicking whole bacteria, demonstrating dose dependent binding. The ganglioside mimic was confirmed as the epitope. Firstly, the Sialoadhesin did not bind to the control CSTII knock out strain which differs only in its lack of ganglioside mimicry and secondly because Sialoadhesin binding was lost when the GD1a epitope was converted to GM1 by neuraminidase treatment. This experiment demonstrated perfectly the difficulties in studying carbohydrate interactions where the context of the antigen (i.e. on a whole bacterium) appears to be crucial for binding to occur in this particular system.

It is possible that the lack of binding to LOS is due to the Sialoadhesin-Fc fusion protein reagent, which is a truncated form of the mouse molecule comprising the distal three Ig domains rather than the entire seventeen Ig domain molecule. This may reduce spacing of the Sialoadhesin molecule leading to a requirement for the target GD1a to be closely packed, which might be the case on the bacteria surface but not with native GD1a in an ELISA. The binding of Sialoadhesin to *C. jejuni* could have been further characterised and the specificity proven definitively by the use of the SnR97A mutant Sialoadhesin reagent which has an amino acid substitution in the sialic acid binding pocket which obliterates sialic acid binding³⁶⁹. This reagent was not available for my experiments.

Binding of Sialoadhesin to ganglioside mimicking *C. jejuni* is an interesting finding for a number of reasons. GBS is an antibody mediated autoimmune disease³⁷⁰ in which the target is a carbohydrate³⁷¹⁻³⁷³ TI antigen. The antibody isotypes commonly, but not exclusively, associated with GBS are the Th1 associated isotypes, IgG1 and IgG3^{53,54,374}, which is atypical for a carbohydrate antigen as these tend to induce antibodies of the IgG2 subclass in humans^{58,59}. The macrophage populations which constitutively express high levels of Sialoadhesin are intimately involved in a number of facets of antibody responses and antigen retention by these macrophages greatly enhances B cell activation³⁶⁸.

Lymph node, Sialoadhesin positive, subcapsular sinus macrophages acquire particulate antigen in the sinus and transport it to B cells in the medullary region³⁷⁵ where it is taken up by B cells and transported throughout the follicle^{376,377}. In addition, the macrophages appear to discriminate between antigens. Although subcapsular sinus macrophages display a lower phagocytic capacity compared to medullary macrophages³⁷⁸ and appear to transport antigen, intact, on their surface to the B cells, degraded viral particles have been demonstrated within the macrophages³⁷⁵. It is not known what discriminates the different antigens to their differing fates but it has been suggested that it may be a function of different receptor interactions³⁶⁸. For example, lectin, complement or antibody Fc receptor binding might determine whether it is endocytosed or delivered intact on the surface. As Sialoadhesin is a receptor expressed at high levels by these cells, and I have demonstrated Sialoadhesin binding to ganglioside mimicking *C. jejuni*, the fact that Sialoadhesin has been shown to enhance phagocytosis on conventional macrophages²⁵⁵ might have important implications for how GD1a mimicking, GBS associated strains, are presented to B cells.

Sialoadhesin is also constitutively expressed by splenic metallophilic macrophages which in mice delineate the marginal zone of the follicles³⁴⁷ and in humans are present in the perifollicular zone³⁷⁹. This places them in an ideal location to interact with MZ B cells which are a candidate population for the source of anti-ganglioside antibodies due to their participation in responses to T independent antigens and their tendency to harbour auto-reactive specificities. Depletion of the metallophilic macrophage population results in a marked decrease in antibody responses to T dependent antigens, although responses to T independent antigens remain intact but with a notable increased bias towards Th2 isotypes³⁸⁰. This can be explained by the findings that metallophilic macrophages are an important source of Type 1 interferons³⁴⁸ and IFN- γ ³⁸⁰ which are believed to drive antibody class switching towards Th1 isotypes³⁸¹⁻³⁸⁴, such as IgG2a in mice (the equivalent of the pathogenic human isotypes in GBS).

My finding of Sialoadhesin binding to ganglioside mimicking *C. jejuni* confirms my initial hypothesis that the ganglioside mimic can engage endogenous receptors. It also fits well with the over-arching hypothesis that such binding could significantly alter the antibody response and subvert tolerance. My findings specifically link a GBS associated strain of *C. jejuni* with a receptor expressed by a specialised population of macrophages which provides antigen to B cells, enhances antibody responses and provides cytokines which promote Th1 antibody isotypes. The specific function of Sialoadhesin in these cells is not known. As GBS is a rare event, it may be that Sialoadhesin functions to enhance tolerance by facilitating phagocytosis and promoting degradation to prevent this antigen reaching B cells. Alternatively, it may enhance or polarise immunity by delivering *C. jejuni* to endosomes where endosomal pathogen recognition receptors, such as TLR7 or TLR9, might signal to enhance interferon secretion, triggering B cell isotype switching. Interestingly, even in the absence of GBS, infection with *C. jejuni* expressing sialylated LOS is associated with more severe enteric disease³⁸⁵.

An additional ganglioside specific receptor, Siglec F, was shown to bind native gangliosides, ganglioside mimicking LOS and ganglioside mimicking *C. jejuni*, the latter two in a dose dependent manner. This again confirms my initial hypothesis. The closest human equivalent to Siglec F is Siglec 8 which is expressed on eosinophils and mast cells¹⁴⁶. Cross linking of Siglec 8 causes apoptosis of eosinophils and counteracts stimulatory signals in mast cells¹⁴⁶.

Mast cells and eosinophils lie at the front line of the immune system and are ideally placed to respond early and drive adaptive responses to mucosal pathogens. Human eosinophils are considered initiators of Th2 responses. However, eosinophils constitutively store an array of pre-formed cytokines associated with Th1, Th2 and immunoregulatory functions, including IL-4, IL-13, IL-6, IL-10, IL-12, IFN- γ and TNF- α ³⁸⁶. In addition, there is a differential release of these cytokines in response to different stimuli³⁸⁶. The presence of large quantities of pre-synthesised cytokines allows eosinophils to play a crucial role at the initiation of immune responses and an important

area of future research is to determine what effect Siglec F (or Siglec 8) signalling has both on the differential cytokine release and on subsequent antigen presentation by eosinophils³⁸⁷.

In addition to exploring cellular ganglioside receptors I also studied interactions with the humoral immune system, specifically looking at fH binding, complement activation and natural antibody binding. Factor H has been reported to bind to sialic acid on cells and pathogenic bacteria where it was thought to inhibit complement deposition^{241,242}. I could not demonstrate this with ganglioside mimicking *C. jejuni*. However, subsequent studies have shown sialic acid to be neither necessary nor sufficient for fH binding to bacteria^{242,245,271} so it is likely that my negative results are accurate.

All of my strains of *C. jejuni* were opsonised by complement. However, I showed that complement activates less efficiently on ganglioside mimicking *C. jejuni* than control strains. I believe that this is due to lower levels of natural antibodies in naïve human serum specific for the ganglioside mimicking LOS of the GBS associated strains. My experiments stopped short of showing a causative link between natural antibody levels and complement deposition, and these studies could have been improved by using purified human complement to establish if the differences were only present when antibody was present. It has been shown previously that *C. jejuni* are very sensitive to the bactericidal activity of human serum, in a complement and antibody dependent manner, when compared to *Campylobacter fetus*. It is therefore no surprise that *C. fetus* is frequently isolated from the bloodstream, whereas *C. jejuni* is very rarely isolated from the bloodstream³⁸⁸. Additional studies have also shown that sialylated strains of *C. jejuni* are more resistant to complement mediated killing than non-sialylated strains³⁸⁹, which is in keeping with my findings of less complement activation on ganglioside mimicking strains. Sialylation might be a strategy adopted by certain strains of *C. jejuni* to enhance their survival by compensating for their inherent complement sensitivity.

Complement and natural IgM function to clear self antigen and senescent cells from the circulation and complement deficiency is related to autoimmunity through defective clearance of self-antigens^{390,391,392}. Complement resistance in ganglioside mimicking strains could be considered analogous to an acquired complement deficiency, resulting in persistence of a self-antigen expressed in the context of an immunostimulatory molecule i.e. Lipid A. Natural IgM can enhance or inhibit subsequent IgG responses and does so in a complement dependent manner which involves antigen trapping and delivery to B cells^{393-395,396-398}. The role of natural IgM and complement in enhancing class switching to IgG is poorly understood, but is likely to be important in autoimmunity as switching from IgM to IgG correlates with the onset of autoimmune disease⁶⁵. IgM enhances IgG responses. Conversely, low levels or absence of IgM results in enhanced levels of auto-reactive IgG and increased severity of autoimmune disease in a number of mouse models^{395,399,400}. How natural IgM protects against IgG mediated autoimmunity while enhancing IgG responses is unclear and suggested mechanisms include facilitating rapid clearance of self antigen in collaboration with complement, protecting against chronic bacterial infections, delivering antigen to immature B cells to enhance central tolerance and antigen masking of self epitopes. Natural antibody and its collaboration with complement may be important in *C. jejuni* associated GBS where individual variations in natural antibodies could alter the outcome of infection.

7.1.3 Effect of ganglioside mimicry on LOS potency

By demonstrating *in vitro* binding of cellular receptors to LOS and whole *C. jejuni* I confirmed my first hypothesis. Next I decided to test my second hypothesis and establish if this ability to bind ganglioside specific receptors affects LOS potency. Many studies of siglec function have relied on antibody cross-linking of receptors or the use of knock out animals¹⁴⁶. To the best of my knowledge this is the first time a study has tried to demonstrate functional activity of siglecs ligands using a ganglioside mimicking LOS. The relative strength of each signal (TLR4 v siglec) and how they might interact was unknown and therefore I looked at a broad range of markers in a variety of cell types,

including B cell proliferation, CD138 positive cell differentiation, antibody secretion and cytokine secretion. The cytokines chosen were broad markers of immune activity: TNF- α as an acute phase inflammatory cytokine²⁷⁸, IL-10 as an inhibitory cytokine³²² and IL-12 as a pro-inflammatory, Th1 polarising, cytokine²⁸⁰.

Within the parameters measured, my studies failed to demonstrate any difference in potency between ganglioside mimicking and non-mimicking strains of LOS at stimulating B cells. Although I was measuring very general aspects of potency, the greater capacity of *E. coli* LPS at stimulating B cell proliferation and CD138 positive cell differentiation was very clear, which suggests my techniques would have detected differences associated with ganglioside mimicry, had they existed. In fact, the assays were sensitive enough to show inter-strain differences in immunoglobulin production between GB2 and GB19 derived *C. jejuni* strains, while the wild type and knock out variants within these strains gave remarkably similar results.

Very few studies have looked at direct stimulation of B cells with *C. jejuni* LOS so virtually all of my findings, from its ability to cause proliferation to its ability to mobilise MZ B cells *in vivo*, are new to the field. The discovery that its properties are qualitatively the same as *E. coli* LPS is not an unexpected finding, although it is surprising how low the potency of *C. jejuni* LOS is. Low potency had been reported before when macrophage stimulation was measured³¹⁶. However, when the size of LOS is considered (~4 kDa) relative to *E. coli* LPS (anywhere up to 100 kDa), the *C. jejuni* LOS molarity may have been as much as twenty times greater, and yet was substantially less potent. It may be that mice are very insensitive to *C. jejuni* LOS, as exposure tends to lead to asymptomatic colonisation and clearance rather than the inflammatory response seen in humans⁴⁰¹.

Myeloid cells express a wide array of ganglioside receptors and it was decided to stimulate dendritic cells and macrophages with *C. jejuni* LOS or whole, killed, bacteria.

A number of related studies have been done looking at live *C. jejuni* and LOS stimulation of human dendritic cells and macrophages, although these did not involve comparisons of ganglioside mimicking and non-mimicking strains^{92,352,402,403}. These studies concluded that LOS and whole *C. jejuni* stimulation of dendritic cells induce considerable production of IL-10, IL-12 and TNF- α as well as upregulation of costimulatory molecules such as CD40. They also concluded that LOS was a key contributor to cytokine production and that high levels of IL-12 production with lower IL-10 production suggested a Th1 polarising role. Monocyte stimulation gave similar results.

My studies on mouse dendritic cells found that LOS stimulation resulted in generally comparable IL-10 and IL-12 levels, although IL-12 was greater if whole bacteria were used. My dendritic cells produced large quantities of TNF- α in response to LOS, while the macrophages were less responsive. LOS and whole bacteria caused CD40 upregulation by dendritic cells and macrophages, respectively. Therefore, the general properties of whole *C. jejuni* and LOS were comparable to previous work. However, the IL-12 and TNF- α responses I achieved were quite variable and frequently had poor dose response curves. This makes it difficult to draw firm conclusions about the potency of wild type and knock out strains in inducing these cytokines. In contrast to IL-12 and TNF- α , IL-10 was a very reliable marker of potency, with levels which were reproducible and gave consistently good dose response curves.

A significant difference was noted in dendritic cell IL-10 production in response to ganglioside mimicking and non-mimicking LOS. The ganglioside mimicking strain induced half as much IL-10 as the non-mimicking strain, but this was only apparent at high concentrations of LOS. This difference was most marked with GB11 LOS but was also present with GB2 and GB19 strains. A number of possible mechanisms were explored to try and explain this difference. Firstly, exogenous gangliosides were added to the knock out strains to establish if this was a “ganglioside effect”. This strategy did not reproduce the reduced IL-10. Secondly, a panel of siglec blocking antibodies was used to block potential receptor signalling. Again, this did not reproduce the reduced IL-

10. Possible differences in cell death were also tested but this showed no statistical difference between strains. In addition, whole bacteria were used to stimulate dendritic cells, and the difference in IL-10 production between wild type and knock out strains was not seen.

In my final experiment designed to try and understand these results, dendritic cells from the LPS hyporesponsive C3H/HeJ mouse strain and from a TLR2^{-/-} mouse strain were used to establish if the difference in IL-10 could be accounted for by contamination by a TLR2 ligand such as capsular polysaccharide. The results of this assay were conflicting as, in the absence of TLR2 signalling, there was no difference in IL-10 production, while in the absence of TLR4 signalling (C3H/HeJ cells) no IL-10 was produced to either LOS strain. The former results indicated that a TLR2 agonist mediated the difference in IL-10 production while the latter result indicated that no TLR2 agonists were present. However, a review of the literature reveals conflicting reports on whether TLR2 signalling alone stimulates IL-10 from dendritic cells^{319,320,404} which calls into question the usefulness of the C3H/HeJ results. The one study which reports no IL-10 from TLR2 stimulated dendritic cells has a protocol which is most relevant to my study, however studies reporting IL-10 following TLR2 stimulation are more numerous.

In conclusion, this is an interesting and promising observation, but falls short of confirming the second part of my hypothesis, that is, that binding to ganglioside receptors will lead to altered signalling and responses by immune cells. Further work needs to be done to confirm that no contamination is present and this is a relatively simple set of experiments, for example, looking at TNF- α secretion from C3H/HeJ dendritic cells stimulated with wild type and knock out LOS.

If these results are taken at face value, they suggest that ganglioside mimicry mediates an inhibitory signal, by undetermined means, which is relatively specific for downregulating dendritic cell IL-10 (there was no difference in CD40 upregulation and TNF- α and IL-12

levels were highly variable). Such a scenario would fit well with my over-arching hypothesis, that altered signalling mediated by the ganglioside mimic can subvert tolerance. Dendritic cells are the most important antigen presenting cells in the immune system as they are capable of driving primary responses and of instructing the adaptive immune response⁴⁰⁵⁻⁴⁰⁸. Several bacterial products, including LPS, induce dendritic cell maturation⁴⁰⁹. Dendritic cells can skew T cell responses towards Th1 or Th2⁴¹⁰ and, through downstream effects, control the isotypes of antibodies in the ensuing humoral response (for example, eliciting IgG2a or IgG1)⁴¹¹. Dendritic cells can also directly activate naïve and memory B cells, are able to induce plasma cell differentiation and can trigger antibody isotype class switching in an IL-10 dependent manner⁴¹². Dendritic cells exhibit plasticity in function and Th1 polarising dendritic cells can be converted to Th2 polarising cells when treated with IL-10⁴¹².

IL-10 is model example of an anti-inflammatory and tolerogenic cytokine. Through inhibition of accessory cells⁴¹³ (e.g. macrophages), IL-10 can inhibit inflammatory cytokine production by T cells and NK cells^{414,415}, and it inhibits both the Th1 and Th2 arms of the immune response. IL-10^{-/-} mice develop inflammatory bowel disease as well as other inflammatory conditions⁴¹⁶⁻⁴¹⁸ and, interestingly, they are the only mouse model of inflammatory *C. jejuni* enteritis as normal strains are colonised asymptotically⁴¹⁹. The main biological action of IL-10 appears to be towards macrophages and dendritic cells where it inhibits antigen presentation, secretion of immune polarising cytokines and secretion of general inflammatory cytokines, such as TNF- α ³²²

A situation in which ganglioside mimicry inhibits production of this important anti-inflammatory cytokine from the primary cells driving an immune response could lead to a micro-environment where there is greater inflammation, greater antigen presentation and higher levels of co-stimulator molecule expression. A relative lack of IL-10 could lead to imbalances in the response and under such circumstances it is easy to imagine that auto-reactive B cell clones might be more likely to escape deletion and progress to antibody secreting plasma cells.

7.1.4 Uptake of ganglioside mimicking *C. jejuni*

My final hypothesis was that ganglioside mimicking strains of *C. jejuni* will show different immune trafficking than non-ganglioside mimicking strains. Having demonstrated differences in complement opsonisation and cellular receptor binding I conducted a number of *in vitro* studies to establish how this affected interactions with cells.

These studies required the development of a means of tracking my *C. jejuni*. Transformation of *C. jejuni* with *gfp* plasmid is difficult and I did not have the facilities to handle the live pathogens for prolonged periods. Instead I developed a protocol to durably label the bacteria with the cell tracking fluorophore CFSE. This has been used before for a number of bacterial species, but not *C. jejuni*³²⁵⁻³²⁸. In contrast to these previous studies, I wanted to compare two isogenic strains of bacteria and a protocol was developed that gave consistent levels of fluorescence regardless of the sialylation status.

Following on from my earlier complement opsonisation studies, I was able to demonstrate differences between wild type and knock out strains in their association with B cells, *in vitro*, following opsonisation with normal mouse serum. These experiments showed higher levels of B cell association of a non-ganglioside mimicking strain and were dependent on the presence of active complement. This confirmed my earlier results and supports my third hypothesis, that differences in humoral and cellular receptor interaction, which are dependent on ganglioside mimicry, will affect trafficking. It was possible to follow B cells within a mixed splenocyte population because they form a clearly delineated population when labelled for CD19. I expect that these differences are the same for other complement receptor bearing populations, such as macrophages and dendritic cells. However these proved difficult populations to clearly delineate because their markers, F4/80, CD11b and CD11c, show a spectrum in levels of expression, the

cells themselves become autofluorescent and the CFSE fluorescence bleeds into other channels in the FACS analysis.

Opsonisation by complement is important in enhancing antibody responses partly through increased delivery of antigen to antigen presenting cells and B cells^{262,420}. I would therefore predict that ganglioside mimicking strains induce weaker humoral responses, and this might be the case in the majority of people exposed to them. Alternatively, these results suggest that non-ganglioside mimicking strains will be cleared more readily through complement-receptor-mediated uptake which might ultimately lead to less overall inflammation due to less chronic antigen stimulation. Complement deficiency is strongly associated with autoimmunity^{390,391}, and low levels of opsonisation, due to ganglioside mimicry and low levels of natural antibody, might result in chronic antigen exposure.

In order to expand on my assays showing Sialoadhesin binding to *C. jejuni* I decided to test if this enhanced *in vitro* phagocytosis as has been shown with Sialoadhesin binding strains of meningococci²⁵⁵. My experiments showed early enhanced phagocytosis of a ganglioside mimicking *C. jejuni* strain compared to a non-ganglioside mimicking strain by bone marrow derived macrophages. Sialoadhesin was shown to be the receptor mediating this by the use of blocking antibodies to reduce phagocytosis of the wild type strain to the same rate as the knock out. Although the difference in phagocytosis was small, it remained significant in seven separate repeats (three in progressive time point experiments, and four at a single time point). In addition, the small difference between strains can be accounted for by the fact that bone marrow derived macrophages express low levels of Sialoadhesin^{209,248} and this experiment could have been improved by first priming the cells with interferons to upregulate Sialoadhesin²⁵⁰.

These *in vitro* observations again support my third hypothesis that ganglioside mimicry affects trafficking and there are a number of ways it can be related to my over-arching hypothesis about subverting tolerance. The populations of macrophages with the highest expression of Sialoadhesin are the metallophilic marginal zone macrophages and the sub-capsular sinus lymph node macrophages. They have been shown to be intimately involved in B cell activation and antibody production. Metallophilic macrophages are a major source of type I and type II interferons. These promote antibody isotype class switching to the Th1 isotypes (IgG1 and IgG3), which is one of the idiosyncratic features of the anti-ganglioside/LOS carbohydrate response often associated with GBS^{53,54}. TLR4 activation from inside endosomes (as oppose to the plasma membrane) triggers selective signalling through the TRIF/TRAM pathway which drives type I interferon production⁴²¹. Therefore efficient phagocytosis of ganglioside mimicking strains into these macrophage populations (which normally have low phagocytic activity) might enhance these cytokines within the B cell micro-environment. In contrast to the anti-ganglioside mimicking LOS response seen in GBS patients, anti-LOS antibodies to non-GBS associated *C. jejuni* enteritis strains are predominantly IgG2⁶⁰, as would be expected towards a glycolipid antigen.

The Th1 isotypes (IgG1 and IgG3) are the most efficient at fixing complement⁶⁴, which is thought to be a key part of GBS pathogenesis³⁵⁰. They are also more commonly associated with viral infections^{422,423}. It is possible that ganglioside mimicking *C. jejuni* induces a more viral-like, interferon driven, response than non-mimicking strains because of the way they are sensed by the immune system. The function of Sialoadhesin remains obscure, but one possible explanation for why the immune system expresses a receptor for a self molecule is because enveloped virus particles carry gangliosides with them when they bud from the host plasma membrane⁴²⁴ and Sialoadhesin may have evolved to detect these. Atypical isotype switching is not loss of tolerance per se (as it still requires an antigen specific component), and clearly cannot be the whole story, but class switching has been shown to be a crucial event in murine models of autoimmunity⁶⁵.

The final test of whether ganglioside mimicry affects trafficking was *in vivo* inoculation of mice. It was hoped that the ganglioside mimicking strains would engage Sialoadhesin on the metallophilic macrophages where I would be able to co-localise them using the metallophilic macrophage specific antibody MOMA1. The non-mimicking strains were expected to be rapidly removed by the reticuloendothelial system. Because the bacteria were rapidly destroyed or lost fluorescence, I was restricted to looking at early time points of 1 and 3 hours post-injection.

Analysis of splenic sections using co-localisation software revealed no difference between my strains in localisation to either metallophilic or marginal zone macrophages and both strains were found in association with both cell types. In addition, I used FACS analysis to study *C. jejuni* association with a number of cell types and was unable to demonstrate any difference between strains. This result was disappointing in the light of the positive results in my *in vitro* experiments leading up to the *in vivo* test. However, with hindsight, this result could have been predicted given that my complement binding tests had shown both strains to be opsonised efficiently, albeit it with inter-strain differences in levels. It is likely that both the ganglioside mimicking and non-mimicking strains were associating with both macrophage populations via complement mediated interactions making it impossible to determine a role for Sialoadhesin interactions.

A number of studies have looked at antigen localisation in subcapsular sinus macrophages, metallophilic macrophages and marginal zone macrophages. There appear to be subtle but distinct differences between these populations which require complex investigations to tease out. For example, while marginal zone macrophages and subcapsular sinus macrophages both capture vesicular stomatitis virus (VSV), the marginal zone macrophages require IgM and C3 to achieve this. These are not required by subcapsular sinus macrophages³⁷⁵ suggesting other receptors are involved. To the best of my knowledge this is the first time a ganglioside mimicking bacterial pathogen has been used to study these cells. More complex studies, eliminating complement using

cobra venom factor for example, might have shown the ganglioside mimicking bacteria localising to the metallophilic but not marginal zone population.

These results do not conclusively disprove my third hypothesis or the over-arching hypothesis. For example, the bacteria used were heat inactivated using a harsh protocol (the same one used for LOS extraction) which will have left them vulnerable to complement binding and lysis, which might have reduced differences between the strains and reduced the time window to analyse the spleens. An improvement would be to use an alternative method of inactivation such as U.V cross linking or sodium azide poisoning. As the initial experiments were very promising, it would be worthwhile transforming the bacteria to fluoresce, preferably using separate colours for each strain to allow simultaneous inoculation with live bacteria. In addition, I was hoping different receptor binding would have functional outcomes in terms of cytokine production. Serum was retained from these experiments to test this hypothesis.

In conclusion, the experiments presented in this thesis have successfully expanded our knowledge of how *C. jejuni* in general, and GBS associated ganglioside mimicking strains specifically, interact with the mammalian immune system at a number of levels. I have demonstrated basic properties of *C. jejuni* LOS which had not been formally shown before, for example B cell proliferation, antibody secretion and mobilisation of MZ B cells *in vivo*.

The experiments successfully addressed my three core hypotheses. I conclusively showed that the ganglioside mimic in LOS is able to interact with cellular receptors *in vitro*, and also that the mimic affects the interaction of the bacteria with innate humoral components of the immune system. While I did not conclusively show that the ganglioside mimic affected potency, I have gathered results which strongly support this hypothesis. Finally, I presented conclusive *in vitro* evidence that ganglioside mimicry affects trafficking of the bacteria. I was unable to show *in vivo* effects of ganglioside mimicry on bacterial

trafficking although I identified several technical reasons that might account for the discrepancy between the *in vitro* and *in vivo* results. My over-arching hypothesis is that additional signalling /interactions of the ganglioside mimicking epitopes on LOS might contribute to the breaking of tolerance in GBS. The results presented here neither confirm nor refute this, although they provide a foundation for the hypothesis, in that such interactions have now been shown to exist. Like much research, this ends with more questions than it started with, and the project can be carried forward addressing the precise effects of the ganglioside mimicking LOS receptor interactions.

7.1.5 Future experiments

Many of the findings in this project merit further investigation. Firstly, the effects of ganglioside-mimicking *C. jejuni* binding to Siglec F were not explored. This binding may result in apoptosis of eosinophils or basophils, and/or alterations of cytokine secretion. These could be important events in GBS. Secondly, although Sialoadhesin mediated phagocytosis was demonstrated, I did not measure many functional outcomes *in vivo* or *in vitro*. For example, it would be of interest to establish if IFN production was affected by the route of phagocytosis in metallophilic macrophages, or if the ganglioside mimicking and non-mimicking *C. jejuni* strains are trafficked into the same antigen processing pathways. Thirdly, the role of natural antibodies in determining the epitopes targeted by the adaptive immune response should also be explored further, for example by immunising mice with ganglioside antigens in the presence of blocking antibodies of known epitope specificity. Such studies could not only shed light on the evolution of GBS but also open potential avenues for therapeutic interventions.

8 Bibliography

1. Vucic, S., Kiernan, M.C. & Cornblath, D.R. Guillain-Barre syndrome: an update. *J Clin Neurosci* **16**, 733-741 (2009).
2. Asbury, A.K., Arnason, B.G. & Adams, R.D. The inflammatory lesion in idiopathic polyneuritis. Its role in pathogenesis. *Medicine (Baltimore)* **48**, 173-215 (1969).
3. Griffin, J.W., *et al.* Guillain-Barre syndrome in northern China. The spectrum of neuropathological changes in clinically defined cases. *Brain* **118 (Pt 3)**, 577-595 (1995).
4. McKhann, G.M., *et al.* Acute motor axonal neuropathy: a frequent cause of acute flaccid paralysis in China. *Ann Neurol* **33**, 333-342 (1993).
5. McKhann, G.M., *et al.* Clinical and electrophysiological aspects of acute paralytic disease of children and young adults in northern China. *Lancet* **338**, 593-597 (1991).
6. Griffin, J.W., *et al.* Pathology of the motor-sensory axonal Guillain-Barre syndrome. *Ann Neurol* **39**, 17-28 (1996).
7. Fisher, M. An unusual variant of acute idiopathic polyneuritis (syndrome of ophthalmoplegia, ataxia and areflexia). *N Engl J Med* **255**, 57-65 (1956).
8. Hughes, R.A. & Rees, J.H. Clinical and epidemiologic features of Guillain-Barre syndrome. *J Infect Dis* **176 Suppl 2**, S92-98 (1997).
9. Hiraga, A., *et al.* Recovery patterns and long term prognosis for axonal Guillain-Barre syndrome. *J Neurol Neurosurg Psychiatry* **76**, 719-722 (2005).
10. Chowdhury, D. & Arora, A. Axonal Guillain-Barre syndrome: a critical review. *Acta Neurol Scand* **103**, 267-277 (2001).
11. Hadden, R.D., *et al.* Electrophysiological classification of Guillain-Barre syndrome: clinical associations and outcome. Plasma Exchange/Sandoglobulin Guillain-Barre Syndrome Trial Group. *Ann Neurol* **44**, 780-788 (1998).
12. Paradiso, G., Tripoli, J., Galicchio, S. & Fejerman, N. Epidemiological, clinical, and electrodiagnostic findings in childhood Guillain-Barre syndrome: a reappraisal. *Ann Neurol* **46**, 701-707 (1999).
13. Cosi, V. & Versino, M. Guillain-Barre syndrome. *Neurol Sci* **27 Suppl 1**, S47-51 (2006).
14. Bernsen, R.A., de Jager, A.E., Schmitz, P.I. & van der Meche, F.G. Long-term impact on work and private life after Guillain-Barre syndrome. *J Neurol Sci* **201**, 13-17 (2002).
15. Rees, J.H., Thompson, R.D., Smeeton, N.C. & Hughes, R.A. Epidemiological study of Guillain-Barre syndrome in south east England. *J Neurol Neurosurg Psychiatry* **64**, 74-77 (1998).
16. Visser, L.H., Schmitz, P.I., Meulstee, J., van Doorn, P.A. & van der Meche, F.G. Prognostic factors of Guillain-Barre syndrome after intravenous immunoglobulin or plasma exchange. Dutch Guillain-Barre Study Group. *Neurology* **53**, 598-604 (1999).
17. van der Meche, F.G. & Schmitz, P.I. A randomized trial comparing intravenous immune globulin and plasma exchange in Guillain-Barre syndrome. Dutch Guillain-Barre Study Group. *N Engl J Med* **326**, 1123-1129 (1992).

18. Hughes, R., *et al.* Subacute idiopathic demyelinating polyradiculoneuropathy. *Arch Neurol* **49**, 612-616 (1992).
19. Prineas, J.W. Acute idiopathic polyneuritis. An electron microscope study. *Lab Invest* **26**, 133-147 (1972).
20. Hughes, R.A., Hadden, R.D., Gregson, N.A. & Smith, K.J. Pathogenesis of Guillain-Barre syndrome. *J Neuroimmunol* **100**, 74-97 (1999).
21. Prineas, J.W. Pathology of the Guillain-Barre syndrome. *Ann Neurol* **9 Suppl**, 6-19 (1981).
22. Lampert, P. Electron microscopic studies on ordinary and hyperacute experimental allergic encephalomyelitis. *Acta Neuropathol* **9**, 99-126 (1967).
23. Feasby, T.E., *et al.* An acute axonal form of Guillain-Barre polyneuropathy. *Brain* **109 (Pt 6)**, 1115-1126 (1986).
24. Griffin, J.W., *et al.* Early nodal changes in the acute motor axonal neuropathy pattern of the Guillain-Barre syndrome. *J Neurocytol* **25**, 33-51 (1996).
25. Hafer-Macko, C., *et al.* Acute motor axonal neuropathy: an antibody-mediated attack on axolemma. *Ann Neurol* **40**, 635-644 (1996).
26. Hafer-Macko, C.E., *et al.* Immune attack on the Schwann cell surface in acute inflammatory demyelinating polyneuropathy. *Ann Neurol* **39**, 625-635 (1996).
27. Willison, H.J. & Yuki, N. Peripheral neuropathies and anti-glycolipid antibodies. *Brain* **125**, 2591-2625 (2002).
28. Hughes, R.A. & Cornblath, D.R. Guillain-Barre syndrome. *Lancet* **366**, 1653-1666 (2005).
29. Ho, T.W., *et al.* Guillain-Barre syndrome in northern China. Relationship to *Campylobacter jejuni* infection and anti-glycolipid antibodies. *Brain* **118 (Pt 3)**, 597-605 (1995).
30. Press, R., *et al.* Temporal profile of anti-ganglioside antibodies and their relation to clinical parameters and treatment in Guillain-Barre syndrome. *J Neurol Sci* **190**, 41-47 (2001).
31. Ho, T.W., *et al.* Anti-GD1a antibody is associated with axonal but not demyelinating forms of Guillain-Barre syndrome. *Ann Neurol* **45**, 168-173 (1999).
32. Ogawara, K., *et al.* Axonal Guillain-Barre syndrome: relation to anti-ganglioside antibodies and *Campylobacter jejuni* infection in Japan. *Ann Neurol* **48**, 624-631 (2000).
33. Rees, J.H., Gregson, N.A. & Hughes, R.A. Anti-ganglioside GM1 antibodies in Guillain-Barre syndrome and their relationship to *Campylobacter jejuni* infection. *Ann Neurol* **38**, 809-816 (1995).
34. Gregson, N.A., Koblar, S. & Hughes, R.A. Antibodies to gangliosides in Guillain-Barre syndrome: specificity and relationship to clinical features. *Q J Med* **86**, 111-117 (1993).
35. Chiba, A., Kusunoki, S., Obata, H., Machinami, R. & Kanazawa, I. Serum anti-GQ1b IgG antibody is associated with ophthalmoplegia in Miller Fisher syndrome and Guillain-Barre syndrome: clinical and immunohistochemical studies. *Neurology* **43**, 1911-1917 (1993).
36. Kaida, K., *et al.* Ganglioside complexes as new target antigens in Guillain-Barre syndrome. *Ann Neurol* **56**, 567-571 (2004).

37. Jacobs, B.C., *et al.* The spectrum of antecedent infections in Guillain-Barre syndrome: a case-control study. *Neurology* **51**, 1110-1115 (1998).
38. Guillain-Barre syndrome: an Italian multicentre case-control study. Guillain-Barre Syndrome Study Group. *Neurol Sci* **21**, 229-234 (2000).
39. Aspinall, G.O., *et al.* Chemical structures of the core regions of *Campylobacter jejuni* serotypes O:1, O:4, O:23, and O:36 lipopolysaccharides. *Eur J Biochem* **216**, 880 (1993).
40. Jacobs, B.C., Hazenberg, M.P., van Doorn, P.A., Endtz, H.P. & van der Meche, F.G. Cross-reactive antibodies against gangliosides and *Campylobacter jejuni* lipopolysaccharides in patients with Guillain-Barre or Miller Fisher syndrome. *J Infect Dis* **175**, 729-733 (1997).
41. Yuki, N. & Odaka, M. Ganglioside mimicry as a cause of Guillain-Barre syndrome. *Curr Opin Neurol* **18**, 557-561 (2005).
42. Yuki, N., *et al.* A bacterium lipopolysaccharide that elicits Guillain-Barre syndrome has a GM1 ganglioside-like structure. *J Exp Med* **178**, 1771-1775 (1993).
43. Kusunoki, S., *et al.* Experimental sensory neuropathy induced by sensitization with ganglioside GD1b. *Ann Neurol* **39**, 424-431 (1996).
44. Susuki, K., *et al.* Acute motor axonal neuropathy rabbit model: immune attack on nerve root axons. *Ann Neurol* **54**, 383-388 (2003).
45. Yuki, N., *et al.* Animal model of axonal Guillain-Barre syndrome induced by sensitization with GM1 ganglioside. *Ann Neurol* **49**, 712-720 (2001).
46. Illa, I., *et al.* Acute axonal Guillain-Barre syndrome with IgG antibodies against motor axons following parenteral gangliosides. *Ann Neurol* **38**, 218-224 (1995).
47. Goodfellow, J.A., *et al.* Overexpression of GD1a ganglioside sensitizes motor nerve terminals to anti-GD1a antibody-mediated injury in a model of acute motor axonal neuropathy. *J Neurosci* **25**, 1620-1628 (2005).
48. Ang, C.W., *et al.* *Campylobacter jejuni* lipopolysaccharides from Guillain-Barre syndrome patients induce IgG anti-GM1 antibodies in rabbits. *J Neuroimmunol* **104**, 133-138 (2000).
49. Ang, C.W., *et al.* Guillain-Barre syndrome- and Miller Fisher syndrome-associated *Campylobacter jejuni* lipopolysaccharides induce anti-GM1 and anti-GQ1b Antibodies in rabbits. *Infect Immun* **69**, 2462-2469 (2001).
50. Ang, C.W., *et al.* Ganglioside mimicry of *Campylobacter jejuni* lipopolysaccharides determines antiganglioside specificity in rabbits. *Infect Immun* **70**, 5081-5085 (2002).
51. Takamiya, K., *et al.* Mice with disrupted GM2/GD2 synthase gene lack complex gangliosides but exhibit only subtle defects in their nervous system. *Proc Natl Acad Sci U S A* **93**, 10662-10667 (1996).
52. Bowes, T., *et al.* Tolerance to self gangliosides is the major factor restricting the antibody response to lipopolysaccharide core oligosaccharides in *Campylobacter jejuni* strains associated with Guillain-Barre syndrome. *Infect Immun* **70**, 5008-5018 (2002).
53. Willison, H.J. & Veitch, J. Immunoglobulin subclass distribution and binding characteristics of anti-GQ1b antibodies in Miller Fisher syndrome. *J Neuroimmunol* **50**, 159-165 (1994).

54. Garcia Guijo, C., *et al.* IgG anti-ganglioside antibodies and their subclass distribution in two patients with acute and chronic motor neuropathy. *J Neuroimmunol* **37**, 141-148 (1992).
55. Walsh, F.S., *et al.* Association between glycoconjugate antibodies and Campylobacter infection in patients with Guillain-Barre syndrome. *J Neuroimmunol* **34**, 43-51 (1991).
56. Koga, M., *et al.* Anti-GM1 antibody IgG subclass: a clinical recovery predictor in Guillain-Barre syndrome. *Neurology* **60**, 1514-1518 (2003).
57. Stavnezer, J. & Amemiya, C.T. Evolution of isotype switching. *Semin Immunol* **16**, 257-275 (2004).
58. Shackelford, P.G., *et al.* Subclass distribution of human antibodies to Haemophilus influenzae type b capsular polysaccharide. *J Immunol* **138**, 587-592 (1987).
59. Hammarstrom, L. & Smith, C.I. IgG2 deficiency in a healthy blood donor. Concomitant lack of IgG2, IgA and IgE immunoglobulins and specific anti-carbohydrate antibodies. *Clin Exp Immunol* **51**, 600-604 (1983).
60. Jacobs, B.C., *et al.* Humoral immune response against Campylobacter jejuni lipopolysaccharides in Guillain-Barre and Miller Fisher syndrome. *J Neuroimmunol* **79**, 62-68 (1997).
61. Alaniz, M.E., Lardone, R.D., Yudowski, S.L., Farace, M.I. & Nores, G.A. Normally occurring human anti-GM1 immunoglobulin M antibodies and the immune response to bacteria. *Infect Immun* **72**, 2148-2151 (2004).
62. Comin, R., Yuki, N., Lopez, P.H. & Nores, G.A. High affinity of anti-GM1 antibodies is associated with disease onset in experimental neuropathy. *J Neurosci Res* **84**, 1085-1090 (2006).
63. Lardone, R.D., Alaniz, M.E., Irazoqui, F.J. & Nores, G.A. Unusual presence of anti-GM1 IgG-antibodies in a healthy individual, and their possible involvement in the origin of disease-associated anti-GM1 antibodies. *J Neuroimmunol* **173**, 174-179 (2006).
64. Shakib, F. & Stanworth, D.R. Human IgG subclasses in health and disease. (A review). Part I. *Ric Clin Lab* **10**, 463-479 (1980).
65. Naparstek, Y. & Plotz, P.H. The role of autoantibodies in autoimmune disease. *Annu Rev Immunol* **11**, 79-104 (1993).
66. Azeredo da Silveira, S., *et al.* Complement activation selectively potentiates the pathogenicity of the IgG2b and IgG3 isotypes of a high affinity anti-erythrocyte autoantibody. *J Exp Med* **195**, 665-672 (2002).
67. Fossati-Jimack, L., *et al.* Markedly different pathogenicity of four immunoglobulin G isotype-switch variants of an antierythrocyte autoantibody is based on their capacity to interact in vivo with the low-affinity Fcγ receptor III. *J Exp Med* **191**, 1293-1302 (2000).
68. Nachamkin, I. Campylobacter Enteritis and the Guillain-Barre Syndrome. *Curr Infect Dis Rep* **3**, 116-122 (2001).
69. Geleijns, K., *et al.* The occurrence of Guillain-Barre syndrome within families. *Neurology* **63**, 1747-1750 (2004).
70. Ma, J.J., *et al.* Genetic contribution of the tumor necrosis factor region in Guillain-Barre syndrome. *Ann Neurol* **44**, 815-818 (1998).

71. Geleijns, K., *et al.* Functional polymorphisms in LPS receptors CD14 and TLR4 are not associated with disease susceptibility or *Campylobacter jejuni* infection in Guillain-Barre patients. *J Neuroimmunol* **150**, 132-138 (2004).
72. Geleijns, K., *et al.* HLA class II alleles are not a general susceptibility factor in Guillain-Barre syndrome. *Neurology* **64**, 44-49 (2005).
73. van Sorge, N.M., *et al.* Severity of Guillain-Barre syndrome is associated with Fc gamma Receptor III polymorphisms. *J Neuroimmunol* **162**, 157-164 (2005).
74. Yu, R.K., Usuki, S. & Ariga, T. Ganglioside molecular mimicry and its pathological roles in Guillain-Barre syndrome and related diseases. *Infect Immun* **74**, 6517-6527 (2006).
75. Kuijf, M.L., *et al.* Susceptibility to Guillain-Barre syndrome is not associated with CD1A and CD1E gene polymorphisms. *J Neuroimmunol* **205**, 110-112 (2008).
76. Konkel, M.E., Monteville, M.R., Rivera-Amill, V. & Joens, L.A. The pathogenesis of *Campylobacter jejuni*-mediated enteritis. *Curr Issues Intest Microbiol* **2**, 55-71 (2001).
77. Allos, B.M. & Blaser, M.J. *Campylobacter jejuni* and the expanding spectrum of related infections. *Clin Infect Dis* **20**, 1092-1099; quiz 1100-1091 (1995).
78. Patton, C.M., *et al.* Evaluation of 10 methods to distinguish epidemic-associated *Campylobacter* strains. *J Clin Microbiol* **29**, 680-688 (1991).
79. Yuki, N., *et al.* Serotype of *Campylobacter jejuni*, HLA, and the Guillain-Barre syndrome. *Muscle Nerve* **15**, 968-969 (1992).
80. Kuroki, S., *et al.* *Campylobacter jejuni* strains from patients with Guillain-Barre syndrome belong mostly to Penner serogroup 19 and contain beta-N-acetylglucosamine residues. *Ann Neurol* **33**, 243-247 (1993).
81. Nachamkin, I., *et al.* *Campylobacter jejuni* from patients with Guillain-Barre syndrome preferentially expresses a GD(1a)-like epitope. *Infect Immun* **70**, 5299-5303 (2002).
82. Hagensee, M.E., Benyunes, M., Miller, J.A. & Spach, D.H. *Campylobacter jejuni* bacteremia and Guillain-Barre syndrome in a patient with GVHD after allogeneic BMT. *Bone Marrow Transplant* **13**, 349-351 (1994).
83. Lastovica, A.J., Goddard, E.A. & Argent, A.C. Guillain-Barre syndrome in South Africa associated with *Campylobacter jejuni* O:41 strains. *J Infect Dis* **176 Suppl 2**, S139-143 (1997).
84. Koga, M., Yuki, N., Takahashi, M., Saito, K. & Hirata, K. Close association of IgA anti-ganglioside antibodies with antecedent *Campylobacter jejuni* infection in Guillain-Barre and Fisher's syndromes. *J Neuroimmunol* **81**, 138-143 (1998).
85. Black, R.E., Levine, M.M., Clements, M.L., Hughes, T.P. & Blaser, M.J. Experimental *Campylobacter jejuni* infection in humans. *J Infect Dis* **157**, 472-479 (1988).
86. Jin, S., Song, Y.C., Emili, A., Sherman, P.M. & Chan, V.L. JlpA of *Campylobacter jejuni* interacts with surface-exposed heat shock protein 90alpha and triggers signalling pathways leading to the activation of NF-kappaB and p38 MAP kinase in epithelial cells. *Cell Microbiol* **5**, 165-174 (2003).
87. Leon-Kempis Mdel, R., Guccione, E., Mulholland, F., Williamson, M.P. & Kelly, D.J. The *Campylobacter jejuni* PEB1a adhesin is an aspartate/glutamate-binding

- protein of an ABC transporter essential for microaerobic growth on dicarboxylic amino acids. *Mol Microbiol* **60**, 1262-1275 (2006).
88. Bras, A.M. & Ketley, J.M. Transcellular translocation of *Campylobacter jejuni* across human polarised epithelial monolayers. *FEMS Microbiol Lett* **179**, 209-215 (1999).
 89. MacCallum, A., Hardy, S.P. & Everest, P.H. *Campylobacter jejuni* inhibits the absorptive transport functions of Caco-2 cells and disrupts cellular tight junctions. *Microbiology* **151**, 2451-2458 (2005).
 90. Chen, M.L., Ge, Z., Fox, J.G. & Schauer, D.B. Disruption of tight junctions and induction of proinflammatory cytokine responses in colonic epithelial cells by *Campylobacter jejuni*. *Infect Immun* **74**, 6581-6589 (2006).
 91. Kopecko, D.J., Hu, L. & Zaal, K.J. *Campylobacter jejuni*--microtubule-dependent invasion. *Trends Microbiol* **9**, 389-396 (2001).
 92. Hickey, T.E., Majam, G. & Guerry, P. Intracellular survival of *Campylobacter jejuni* in human monocytic cells and induction of apoptotic death by cytholethal distending toxin. *Infect Immun* **73**, 5194-5197 (2005).
 93. Kiehlbauch, J.A., Albach, R.A., Baum, L.L. & Chang, K.P. Phagocytosis of *Campylobacter jejuni* and its intracellular survival in mononuclear phagocytes. *Infect Immun* **48**, 446-451 (1985).
 94. Mellits, K.H., *et al.* Activation of the transcription factor NF-kappaB by *Campylobacter jejuni*. *Microbiology* **148**, 2753-2763 (2002).
 95. MacCallum, A., Haddock, G. & Everest, P.H. *Campylobacter jejuni* activates mitogen-activated protein kinases in Caco-2 cell monolayers and in vitro infected primary human colonic tissue. *Microbiology* **151**, 2765-2772 (2005).
 96. Watson, R.O. & Galan, J.E. Signal transduction in *Campylobacter jejuni*-induced cytokine production. *Cell Microbiol* **7**, 655-665 (2005).
 97. Andersen-Nissen, E., *et al.* Evasion of Toll-like receptor 5 by flagellated bacteria. *Proc Natl Acad Sci U S A* **102**, 9247-9252 (2005).
 98. Dalpke, A., Frank, J., Peter, M. & Heeg, K. Activation of toll-like receptor 9 by DNA from different bacterial species. *Infect Immun* **74**, 940-946 (2006).
 99. Huber, M., *et al.* R-form LPS, the master key to the activation of TLR4/MD-2-positive cells. *Eur J Immunol* **36**, 701-711 (2006).
 100. Gilbert, M., *et al.* Biosynthesis of ganglioside mimics in *Campylobacter jejuni* OH4384. Identification of the glycosyltransferase genes, enzymatic synthesis of model compounds, and characterization of nanomole amounts by 600-mhz (1)h and (13)c NMR analysis. *J Biol Chem* **275**, 3896-3906 (2000).
 101. Godschalk, P.C., *et al.* The crucial role of *Campylobacter jejuni* genes in anti-ganglioside antibody induction in Guillain-Barre syndrome. *J Clin. Invest* **114** 5 1659-1665 (2004).
 102. Erridge, C., Bennett-Guerrero, E. & Poxton, I.R. Structure and function of lipopolysaccharides. *Microbes. Infect.* **4**, 837-851 (2002).
 103. Wicken, A.J. & Knox, K.W. Bacterial cell surface amphiphiles. *Biochim. Biophys. Acta* **604**, 1-26 (1980).
 104. Nikaido, H. & Nakae, T. The outer membrane of Gram-negative bacteria. *Adv. Microb. Physiol* **20**, 163-250 (1979).

105. Haziot, A., *et al.* The monocyte differentiation antigen, CD14, is anchored to the cell membrane by a phosphatidylinositol linkage. *J Immunol* **141**, 547-552 (1988).
106. Kitchens, R.L. Role of CD14 in cellular recognition of bacterial lipopolysaccharides. *Chem Immunol* **74**, 61-82 (2000).
107. Muzio, M., *et al.* Differential expression and regulation of toll-like receptors (TLR) in human leukocytes: selective expression of TLR3 in dendritic cells. *J Immunol* **164**, 5998-6004 (2000).
108. Muzio, M., Polentarutti, N., Bosisio, D., Prahlanan, M.K. & Mantovani, A. Toll-like receptors: a growing family of immune receptors that are differentially expressed and regulated by different leukocytes. *J Leukoc Biol* **67**, 450-456 (2000).
109. Genestier, L., *et al.* TLR agonists selectively promote terminal plasma cell differentiation of B cell subsets specialized in thymus-independent responses. *J Immunol* **178**, 7779-7786 (2007).
110. Van Kaer, L. NKT cells: T lymphocytes with innate effector functions. *Curr Opin Immunol* **19**, 354-364 (2007).
111. Tanamoto, K., *et al.* Biological activities of synthetic lipid A analogs: pyrogenicity, lethal toxicity, anticomplement activity, and induction of gelation of *Limulus* amoebocyte lysate. *Infect Immun* **44**, 421-426 (1984).
112. Moran, A.P. Structure and conserved characteristics of *Campylobacter jejuni* lipopolysaccharides. *J Infect Dis* **176 Suppl 2**, S115-121 (1997).
113. Janeway, C.A., Jr. & Medzhitov, R. Innate immune recognition. *Annu Rev Immunol* **20**, 197-216 (2002).
114. Akira, S., Uematsu, S. & Takeuchi, O. Pathogen recognition and innate immunity. *Cell* **124**, 783-801 (2006).
115. Lee, H.K. & Iwasaki, A. Innate control of adaptive immunity: dendritic cells and beyond. *Semin Immunol* **19**, 48-55 (2007).
116. Poltorak, A., *et al.* Defective LPS signaling in C3H/HeJ and C57BL/10ScCr mice: mutations in *Tlr4* gene. *Science* **282**, 2085-2088 (1998).
117. Tobias, P.S., Soldau, K. & Ulevitch, R.J. Isolation of a lipopolysaccharide-binding acute phase reactant from rabbit serum. *J Exp Med* **164**, 777-793 (1986).
118. Wright, S.D., Tobias, P.S., Ulevitch, R.J. & Ramos, R.A. Lipopolysaccharide (LPS) binding protein opsonizes LPS-bearing particles for recognition by a novel receptor on macrophages. *J Exp Med* **170**, 1231-1241 (1989).
119. Wright, S.D., Ramos, R.A., Tobias, P.S., Ulevitch, R.J. & Mathison, J.C. CD14, a receptor for complexes of lipopolysaccharide (LPS) and LPS binding protein. *Science* **249**, 1431-1433 (1990).
120. Fitzgerald, K.A., Rowe, D.C. & Golenbock, D.T. Endotoxin recognition and signal transduction by the TLR4/MD2-complex. *Microbes Infect* **6**, 1361-1367 (2004).
121. O'Neill, L.A. & Bowie, A.G. The family of five: TIR-domain-containing adaptors in Toll-like receptor signalling. *Nat Rev Immunol* **7**, 353-364 (2007).
122. Lu, Y.C., Yeh, W.C. & Ohashi, P.S. LPS/TLR4 signal transduction pathway. *Cytokine* **42**, 145-151 (2008).
123. Jiang, Z., *et al.* CD14 is required for MyD88-independent LPS signaling. *Nat Immunol* **6**, 565-570 (2005).

124. Divanovic, S., *et al.* Negative regulation of Toll-like receptor 4 signaling by the Toll-like receptor homolog RP105. *Nat Immunol* **6**, 571-578 (2005).
125. Chuang, T.H. & Ulevitch, R.J. Triad3A, an E3 ubiquitin-protein ligase regulating Toll-like receptors. *Nat Immunol* **5**, 495-502 (2004).
126. Mansell, A., *et al.* Suppressor of cytokine signaling 1 negatively regulates Toll-like receptor signaling by mediating Mal degradation. *Nat Immunol* **7**, 148-155 (2006).
127. Ogata, H., *et al.* The toll-like receptor protein RP105 regulates lipopolysaccharide signaling in B cells. *J Exp Med* **192**, 23-29 (2000).
128. Miyake, K., Ogata, H., Nagai, Y., Akashi, S. & Kimoto, M. Innate recognition of lipopolysaccharide by Toll-like receptor 4/MD-2 and RP105/MD-1. *J Endotoxin Res* **6**, 389-391 (2000).
129. Divanovic, S., *et al.* Regulation of TLR4 signaling and the host interface with pathogens and danger: the role of RP105. *J Leukoc Biol* **82**, 265-271 (2007).
130. Coutinho, A., Gronowicz, E., Bullock, W.W. & Moller, G. Mechanism of thymus-independent immunocyte triggering. Mitogenic activation of B cells results in specific immune responses. *J Exp Med* **139**, 74-92 (1974).
131. Martin, F. & Kearney, J.F. B-cell subsets and the mature preimmune repertoire. Marginal zone and B1 B cells as part of a "natural immune memory". *Immunol Rev* **175**, 70-79 (2000).
132. Brandtzaeg, P., *et al.* Plasma endotoxin as a predictor of multiple organ failure and death in systemic meningococcal disease. *J Infect Dis* **159**, 195-204 (1989).
133. Dye, J.R., Palvanov, A., Guo, B. & Rothstein, T.L. B cell receptor cross-talk: exposure to lipopolysaccharide induces an alternate pathway for B cell receptor-induced ERK phosphorylation and NF-kappa B activation. *J Immunol* **179**, 229-235 (2007).
134. Bergelson, L.D. Serum gangliosides as endogenous immunomodulators. *Immunol Today* **16**, 483-486 (1995).
135. Whisler, R.L. & Yates, A.J. Regulation of lymphocyte responses by human gangliosides. I. Characteristics of inhibitory effects and the induction of impaired activation. *J Immunol* **125**, 2106-2111 (1980).
136. Robb, R.J. The suppressive effect of gangliosides upon IL 2-dependent proliferation as a function of inhibition of IL 2-receptor association. *J Immunol* **136**, 971-976 (1986).
137. Berenson, C.S. & Ryan, J.L. Murine peritoneal macrophage gangliosides inhibit lymphocyte proliferation. *J Leukoc Biol* **50**, 393-401 (1991).
138. Cavaillon, J.M. & Fitting, C. Inhibition of lipopolysaccharide-induced monocyte interleukin 1 secretion by gangliosides. *Eur J Immunol* **16**, 1009-1012 (1986).
139. Ziegler-Heitbrock, H.W., *et al.* Gangliosides suppress tumor necrosis factor production in human monocytes. *J Immunol* **148**, 1753-1758 (1992).
140. Irani, D.N., Lin, K.I. & Griffin, D.E. Brain-derived gangliosides regulate the cytokine production and proliferation of activated T cells. *J Immunol* **157**, 4333-4340 (1996).
141. Shen, W., Stone, K., Jales, A., Leitenberg, D. & Ladisch, S. Inhibition of TLR activation and up-regulation of IL-1R-associated kinase-M expression by exogenous gangliosides. *J Immunol* **180**, 4425-4432 (2008).

142. Ladisch, S., Li, R. & Olson, E. Ceramide structure predicts tumor ganglioside immunosuppressive activity. *Proc Natl Acad Sci U S A* **91**, 1974-1978 (1994).
143. Crocker, P.R., *et al.* Siglecs: a family of sialic-acid binding lectins. *Glycobiology* **8**, v (1998).
144. Crocker, P.R., Paulson, J.C. & Varki, A. Siglecs and their roles in the immune system. *Nat Rev Immunol* **7**, 255-266 (2007).
145. Ravetch, J.V. & Lanier, L.L. Immune inhibitory receptors. *Science* **290**, 84-89 (2000).
146. von Gunten, S. & Bochner, B.S. Basic and clinical immunology of Siglecs. *Ann N Y Acad Sci* **1143**, 61-82 (2008).
147. Kirchberger, S., *et al.* Human rhinoviruses inhibit the accessory function of dendritic cells by inducing sialoadhesin and B7-H1 expression. *J Immunol* **175**, 1145-1152 (2005).
148. Avril, T., Wagner, E.R., Willison, H.J. & Crocker, P.R. Sialic acid-binding immunoglobulin-like lectin 7 mediates selective recognition of sialylated glycans expressed on *Campylobacter jejuni* lipooligosaccharides. *Infect Immun* **74**, 4133-4141 (2006).
149. Moody, D.B. The surprising diversity of lipid antigens for CD1-restricted T cells. *Adv Immunol* **89**, 87-139 (2006).
150. Kato, N., Kido, N., Ohta, M. & Naito, S. Comparative studies on adjuvanticity of *Klebsiella* O3 lipopolysaccharide and its lipid A and polysaccharide fractions. *Immunology* **54**, 317-324 (1985).
151. Kido, N., *et al.* Potent adjuvant action of lipopolysaccharides possessing the O-specific polysaccharide moieties consisting of mannans in antibody response against protein antigen. *Cell Immunol* **91**, 52-59 (1985).
152. Ohta, M., *et al.* Contribution of the mannan O side-chains to the adjuvant action of lipopolysaccharides. *Immunology* **60**, 503-507 (1987).
153. Amith, S.R., *et al.* Neu1 desialylation of sialyl alpha-2,3-linked beta-galactosyl residues of TOLL-like receptor 4 is essential for receptor activation and cellular signaling. *Cell Signal* **22**, 314-324.
154. Amith, S.R., *et al.* Dependence of pathogen molecule-induced toll-like receptor activation and cell function on Neu1 sialidase. *Glycoconj J* **26**, 1197-1212 (2009).
155. Mond, J.J., Lees, A. & Snapper, C.M. T cell-independent antigens type 2. *Annu Rev Immunol* **13**, 655-692 (1995).
156. Travers, J. *Immunobiology the immune system in health and disease*, (Churchill Livingstone, 1997).
157. Freimer, M.L., McIntosh, K., Adams, R.A., Alving, C.R. & Drachman, D.B. Gangliosides elicit a T-cell independent antibody response. *J Autoimmun* **6**, 281-289 (1993).
158. Martin, F. & Kearney, J.F. B1 cells: similarities and differences with other B cell subsets. *Curr Opin Immunol* **13**, 195-201 (2001).
159. Berland, R. & Wortis, H.H. Origins and functions of B-1 cells with notes on the role of CD5. *Annu Rev Immunol* **20**, 253-300 (2002).
160. Weill, J.C., Weller, S. & Reynaud, C.A. Human marginal zone B cells. *Annu Rev Immunol* **27**, 267-285 (2009).

161. Humphrey, J.H. & Grennan, D. Different macrophage populations distinguished by means of fluorescent polysaccharides. Recognition and properties of marginal-zone macrophages. *Eur J Immunol* **11**, 221-228 (1981).
162. Martin, F., Oliver, A.M. & Kearney, J.F. Marginal zone and B1 B cells unite in the early response against T-independent blood-borne particulate antigens. *Immunity* **14**, 617-629 (2001).
163. Gunn, K.E. & Brewer, J.W. Evidence that marginal zone B cells possess an enhanced secretory apparatus and exhibit superior secretory activity. *J Immunol* **177**, 3791-3798 (2006).
164. Snapper, C.M., *et al.* Comparative in vitro analysis of proliferation, Ig secretion, and Ig class switching by murine marginal zone and follicular B cells. *J Immunol* **150**, 2737-2745 (1993).
165. Pillai, S., Cariappa, A. & Moran, S.T. Marginal zone B cells. *Annu Rev Immunol* **23**, 161-196 (2005).
166. Song, H. & Cerny, J. Functional heterogeneity of marginal zone B cells revealed by their ability to generate both early antibody-forming cells and germinal centers with hypermutation and memory in response to a T-dependent antigen. *J Exp Med* **198**, 1923-1935 (2003).
167. MacLennan, I.C., *et al.* Extrafollicular antibody responses. *Immunol Rev* **194**, 8-18 (2003).
168. Attanavanich, K. & Kearney, J.F. Marginal zone, but not follicular B cells, are potent activators of naive CD4 T cells. *J Immunol* **172**, 803-811 (2004).
169. Amano, M., *et al.* CD1 expression defines subsets of follicular and marginal zone B cells in the spleen: beta 2-microglobulin-dependent and independent forms. *J Immunol* **161**, 1710-1717 (1998).
170. Mestas, J. & Hughes, C.C. Of mice and not men: differences between mouse and human immunology. *J Immunol* **172**, 2731-2738 (2004).
171. Weller, S., *et al.* Human blood IgM "memory" B cells are circulating splenic marginal zone B cells harboring a prediversified immunoglobulin repertoire. *Blood* **104**, 3647-3654 (2004).
172. Leclerc, C., Charbit, A., Martineau, P., Deriaud, E. & Hofnung, M. The cellular location of a foreign B cell epitope expressed by recombinant bacteria determines its T cell-independent or T cell-dependent characteristics. *J Immunol* **147**, 3545-3552 (1991).
173. Schreiber, J.R., Patawaran, M., Tosi, M., Lennon, J. & Pier, G.B. Anti-idiotypic-induced, lipopolysaccharide-specific antibody response to *Pseudomonas aeruginosa*. *J Immunol* **144**, 1023-1029 (1990).
174. Schreiber, J.R., Nixon, K.L., Tosi, M.F., Pier, G.B. & Patawaran, M.B. Anti-idiotypic-induced, lipopolysaccharide-specific antibody response to *Pseudomonas aeruginosa*. II. Isotype and functional activity of the anti-idiotypic-induced antibodies. *J Immunol* **146**, 188-193 (1991).
175. Schreiber, J.R. & Dahlhauser, P. Immunogenicity of tetanus toxoid conjugates of anti-idiotypes that mimic *Pseudomonas aeruginosa* surface polysaccharides. *Infect Immun* **62**, 308-312 (1994).
176. De Libero, G. & Mori, L. Recognition of lipid antigens by T cells. *Nat Rev Immunol* **5**, 485-496 (2005).

177. Matsumoto, Y., *et al.* Cutting edge: Guillain-Barre syndrome-associated IgG responses to gangliosides are generated independently of CD1 function in mice. *J Immunol* **180**, 39-43 (2008).
178. Hashimoto, K., Handa, H., Umehara, K. & Sasaki, S. Germfree mice reared on an "antigen-free" diet. *Lab Anim Sci* **28**, 38-45 (1978).
179. Kantor, A.B. & Herzenberg, L.A. Origin of murine B cell lineages. *Annu Rev Immunol* **11**, 501-538 (1993).
180. Hayakawa, K., *et al.* Positive selection of anti-thy-1 autoreactive B-1 cells and natural serum autoantibody production independent from bone marrow B cell development. *J Exp Med* **197**, 87-99 (2003).
181. Hayakawa, K., Hardy, R.R., Honda, M., Herzenberg, L.A. & Steinberg, A.D. Ly-1 B cells: functionally distinct lymphocytes that secrete IgM autoantibodies. *Proc Natl Acad Sci U S A* **81**, 2494-2498 (1984).
182. Benatuil, L., *et al.* Ig knock-in mice producing anti-carbohydrate antibodies: breakthrough of B cells producing low affinity anti-self antibodies. *J Immunol* **180**, 3839-3848 (2008).
183. Murakami, M., *et al.* Oral administration of lipopolysaccharides activates B-1 cells in the peritoneal cavity and lamina propria of the gut and induces autoimmune symptoms in an autoantibody transgenic mouse. *J Exp Med* **180**, 111-121 (1994).
184. Nisitani, S., Tsubata, T., Murakami, M. & Honjo, T. Administration of interleukin-5 or -10 activates peritoneal B-1 cells and induces autoimmune hemolytic anemia in anti-erythrocyte autoantibody-transgenic mice. *Eur J Immunol* **25**, 3047-3052 (1995).
185. Bondada, S., Bikah, G., Robertson, D.A. & Sen, G. Role of CD5 in growth regulation of B-1 cells. *Curr Top Microbiol Immunol* **252**, 141-149 (2000).
186. Kawahara, T., Ohdan, H., Zhao, G., Yang, Y.G. & Sykes, M. Peritoneal cavity B cells are precursors of splenic IgM natural antibody-producing cells. *J Immunol* **171**, 5406-5414 (2003).
187. Claflin, J.L. & Berry, J. Genetics of the phosphocholine-specific antibody response to *Streptococcus pneumoniae*. Germ-line but not mutated T15 antibodies are dominantly selected. *J Immunol* **141**, 4012-4019 (1988).
188. Pecquet, S.S., Ehrat, C. & Ernst, P.B. Enhancement of mucosal antibody responses to *Salmonella typhimurium* and the microbial hapten phosphorylcholine in mice with X-linked immunodeficiency by B-cell precursors from the peritoneal cavity. *Infect Immun* **60**, 503-509 (1992).
189. Wicker, L.S., Guelde, G., Scher, I. & Kenny, J.J. The asymmetry in idiotype-isotype expression in the response to phosphocholine is due to divergence in the expressed repertoires of Lyb-5+ and Lyb-5- B cells. *J Immunol* **131**, 2468-2476 (1983).
190. Claflin, J.L., Lieberman, R. & Davie, J.M. Clonal nature of the immune response to phosphorylcholine. I. Specificity, class, and idiotype of phosphorylcholine-binding receptors on lymphoid cells. *J Exp Med* **139**, 58-73 (1974).
191. Ogawa-Goto, K. & Abe, T. Gangliosides and glycosphingolipids of peripheral nervous system myelins--a minireview. *Neurochem Res* **23**, 305-310 (1998).

192. Chiba, A., Kusunoki, S., Obata, H., Machinami, R. & Kanazawa, I. Ganglioside composition of the human cranial nerves, with special reference to pathophysiology of Miller Fisher syndrome. *Brain Res* **745**, 32-36 (1997).
193. Hayakawa, K., Hardy, R.R. & Herzenberg, L.A. Peritoneal Ly-1 B cells: genetic control, autoantibody production, increased lambda light chain expression. *Eur J Immunol* **16**, 450-456 (1986).
194. Hayakawa, K., Hardy, R.R., Parks, D.R. & Herzenberg, L.A. The "Ly-1 B" cell subpopulation in normal immunodefective, and autoimmune mice. *J Exp Med* **157**, 202-218 (1983).
195. Kroese, F.G., Butcher, E.C., Stall, A.M. & Herzenberg, L.A. A major peritoneal reservoir of precursors for intestinal IgA plasma cells. *Immunol Invest* **18**, 47-58 (1989).
196. Donze, H.H., *et al.* Human peritoneal B-1 cells and the influence of continuous ambulatory peritoneal dialysis on peritoneal and peripheral blood mononuclear cell (PBMC) composition and immunoglobulin levels. *Clin Exp Immunol* **109**, 356-361 (1997).
197. Fugier-Vivier, I., *et al.* Molecular cloning of human RP105. *Eur J Immunol* **27**, 1824-1827 (1997).
198. Dono, M., *et al.* The human marginal zone B cell. *Ann N Y Acad Sci* **987**, 117-124 (2003).
199. Ferreira, V.P., Herbert, A.P., Hocking, H.G., Barlow, P.N. & Pangburn, M.K. Critical role of the C-terminal domains of factor H in regulating complement activation at cell surfaces. *J Immunol* **177**, 6308-6316 (2006).
200. Jozsi, M., Oppermann, M., Lambiris, J.D. & Zipfel, P.F. The C-terminus of complement factor H is essential for host cell protection. *Mol Immunol* **44**, 2697-2706 (2007).
201. Jozsi, M. & Zipfel, P.F. Factor H family proteins and human diseases. *Trends Immunol* **29**, 380-387 (2008).
202. Aspinall, G.O., McDonald, A.G., Pang, H., Kurjanczyk, L.A. & Penner, J.L. Lipopolysaccharides of *Campylobacter jejuni* serotype O:19: structures of core oligosaccharide regions from the serostrain and two bacterial isolates from patients with the Guillain-Barre syndrome. *Biochemistry* **33** **5** 241-249 (1994).
203. Aspinall, G.O., Lynch, C.M., Pang, H., Shaver, R.T. & Moran, A.P. Chemical structures of the core region of *Campylobacter jejuni* O:3 lipopolysaccharide and an associated polysaccharide. *Eur.J Biochem.* **231** **5** 570-578 (1995).
204. Goodfellow, J.A., *et al.* Overexpression of GD1a ganglioside sensitizes motor nerve terminals to anti-GD1a antibody-mediated injury in a model of acute motor axonal neuropathy. *J Neurosci.* **25** **5** 1620-1628 (2005).
205. Tomida, M., Yamamoto-Yamaguchi, Y. & Hozumi, M. Purification of a factor inducing differentiation of mouse myeloid leukemic M1 cells from conditioned medium of mouse fibroblast L929 cells. *J Biol Chem* **259**, 10978-10982 (1984).
206. COPE. -Cytokines and Cells Online Pathfinder Encyclopedia
207. Lutz, M.B., *et al.* An advanced culture method for generating large quantities of highly pure dendritic cells from mouse bone marrow. *J Immunol Methods* **223**, 77-92 (1999).

208. Neidhardt, F.C., Ingraham, J.L. & Schaechter, M. *Physiology of the bacterial cell : a molecular approach*, (Sinauer Associates, Sunderland, Mass., U.S.A., 1990).
209. Crocker, P.R. & Gordon, S. Mouse macrophage hemagglutinin (sheep erythrocyte receptor) with specificity for sialylated glycoconjugates characterized by a monoclonal antibody. *J Exp.Med.* **169** 5 1333-1346 (1989).
210. Brade, L., *et al.* The immunogenicity and antigenicity of lipid A are influenced by its physicochemical state and environment. *Infect Immun* **55**, 2636-2644 (1987).
211. Luderitz, T., *et al.* Structural and physicochemical requirements of endotoxins for the activation of arachidonic acid metabolism in mouse peritoneal macrophages in vitro. *Eur J Biochem* **179**, 11-16 (1989).
212. Galanos, C., Luderitz, O. & Westphal, O. A new method for the extraction of R lipopolysaccharides. *Eur.J Biochem.* **9**, 245-249 (1969).
213. Muck, A., Ramm, M. & Hamburger, M. Efficient method for preparation of highly purified lipopolysaccharides by hydrophobic interaction chromatography. *J Chromatogr B Biomed Sci Appl* **732**, 39-46 (1999).
214. Gottschalk, G. *Methods in Microbiology*.
215. Darveau, R.P. & Hancock, R.E. Procedure for isolation of bacterial lipopolysaccharides from both smooth and rough *Pseudomonas aeruginosa* and *Salmonella typhimurium* strains. *J Bacteriol.* **155**, 831-838 (1983).
216. Aderem, A. & Ulevitch, R.J. Toll-like receptors in the induction of the innate immune response. *Nature* **406**, 782-787 (2000).
217. Karlyshev, A.V. & Wren, B.W. Detection and initial characterization of novel capsular polysaccharide among diverse *Campylobacter jejuni* strains using alcian blue dye. *J Clin Microbiol* **39**, 279-284 (2001).
218. Westphal, O. & Jann, K. Bacterial lipopolysaccharides: Extraction by phenol water and further applications of the procedure. in *Methods in carbohydrate chemistry*, Vol. 5 83-91 (1965).
219. Mills, S.D., Bradbury, W.C. & Penner, J.L. Basis for serological heterogeneity of thermostable antigens of *Campylobacter jejuni*. *Infection and immunity* **50**, 284-291 (1985).
220. Brandenburg, K., Koch, M.H. & Seydel, U. Biophysical characterisation of lysozyme binding to LPS Re and lipid A. *Eur J Biochem* **258**, 686-695 (1998).
221. Galen, J.E., *et al.* Role of *Vibrio cholerae* neuraminidase in the function of cholera toxin. *Infect Immun* **60**, 406-415 (1992).
222. Svennerholm, L. Chromatographic Separation of Human Brain Gangliosides. *J Neurochem* **10**, 613-623 (1963).
223. Saito, M., Sugano, K. & Nagai, Y. Action of *Arthrobacter ureafaciens* sialidase on sialoglycolipid substrates. Mode of action and highly specific recognition of the oligosaccharide moiety of ganglioside GM1. *J Biol Chem* **254**, 7845-7854 (1979).
224. Schromm, A.B., *et al.* Lipopolysaccharide-binding protein mediates CD14-independent intercalation of lipopolysaccharide into phospholipid membranes. *FEBS Lett* **399**, 267-271 (1996).
225. Aurell, C.A. & Wistrom, A.O. Critical aggregation concentrations of gram-negative bacterial lipopolysaccharides (LPS). *Biochem Biophys Res Commun* **253**, 119-123 (1998).

226. Shands, J.W., Jr., Graham, J.A. & Nath, K. The morphologic structure of isolated bacterial lipopolysaccharide. *J Mol Biol* **25**, 15-21 (1967).
227. Kunitz, M. Crystalline desoxyribonuclease; isolation and general properties; spectrophotometric method for the measurement of desoxyribonuclease activity. *J Gen Physiol* **33**, 349-362 (1950).
228. Schomberg, D.S., M. *Enzyme Handbook*, (1990).
229. Bajorath, J., Hinrichs, W. & Saenger, W. The enzymatic activity of proteinase K is controlled by calcium. *Eur J Biochem* **176**, 441-447 (1988).
230. Ribi, E., *et al.* Reaction of endotoxin and surfactants I. Physical and biological properties of endotoxin treated with sodium deoxycholate. *Journal of Bacteriology* **92**, 1493-1509-1493-1509 (1966).
231. Tarmina, D.F., Milner, K.C., Ribi, E. & Rudbach, J.A. Modification of selected host-reactive properties of endotoxin by treatment with sodium deoxycholate. *Journal of Bacteriology* **96**, 1611-1616-1611-1616 (1968).
232. Shnyra, A., Hultenby, K. & Lindberg, A.A. Role of the physical state of Salmonella lipopolysaccharide in expression of biological and endotoxic properties. *Infect Immun* **61**, 5351-5360 (1993).
233. Greenshields, K.N., *et al.* The neuropathic potential of anti-GM1 autoantibodies is regulated by the local glycolipid environment in mice. *J Clin Invest* **119**, 595-610 (2009).
234. Corzo, J., Perez-Galdona, R., Leon-Barrios, M. & Gutierrez-Navarro, A.M. Alcian blue fixation allows silver staining of the isolated polysaccharide component of bacterial lipopolysaccharides in polyacrylamide gels. *Electrophoresis* **12**, 439-441 (1991).
235. Tsai, C.M. & Frasch, C.E. A sensitive silver stain for detecting lipopolysaccharides in polyacrylamide gels. *Anal Biochem* **119**, 115-119 (1982).
236. Warren, L. The thiobarbituric acid assay of sialic acids. *J Biol Chem* **234**, 1971-1975 (1959).
237. Kusunoki, S., *et al.* N-acetylgalactosaminyl GD1a is a target molecule for serum antibody in Guillain-Barre syndrome. *Ann Neurol* **35**, 570-576 (1994).
238. Yuki, N., *et al.* Molecular mimicry between GQ1b ganglioside and lipopolysaccharides of Campylobacter jejuni isolated from patients with Fisher's syndrome. *Ann Neurol* **36**, 791-793 (1994).
239. Jacobs, B.C., *et al.* Serum anti-GQ1b IgG antibodies recognize surface epitopes on Campylobacter jejuni from patients with Miller Fisher syndrome. *Ann Neurol* **37**, 260-264 (1995).
240. Crocker, P.R. & Redelinghuys, P. Siglecs as positive and negative regulators of the immune system. *Biochem Soc Trans* **36**, 1467-1471 (2008).
241. Meri, S. & Pangburn, M.K. Discrimination between activators and nonactivators of the alternative pathway of complement: regulation via a sialic acid/polyanion binding site on factor H. *Proc Natl Acad Sci U S A* **87**, 3982-3986 (1990).
242. Ram, S., *et al.* A novel sialic acid binding site on factor H mediates serum resistance of sialylated Neisseria gonorrhoeae. *J Exp Med* **187**, 743-752 (1998).
243. Vogel, U., *et al.* Complement factor C3 deposition and serum resistance in isogenic capsule and lipooligosaccharide sialic acid mutants of serogroup B Neisseria meningitidis. *Infect Immun* **65**, 4022-4029 (1997).

244. Jarvis, G.A. & Vedros, N.A. Sialic acid of group B Neisseria meningitidis regulates alternative complement pathway activation. *Infect Immun* **55**, 174-180 (1987).
245. Madico, G., *et al.* Factor H binding and function in sialylated pathogenic neisseriae is influenced by gonococcal, but not meningococcal, porin. *J Immunol* **178**, 4489-4497 (2007).
246. Crocker, P.R., *et al.* Sialoadhesin, a macrophage sialic acid binding receptor for haemopoietic cells with 17 immunoglobulin-like domains. *EMBO J* **13**, 4490-4503 (1994).
247. Crocker, P.R., *et al.* Purification and properties of sialoadhesin, a sialic acid-binding receptor of murine tissue macrophages. *EMBO J* **10**, 1661-1669 (1991).
248. Hartnell, A., *et al.* Characterization of human sialoadhesin, a sialic acid binding receptor expressed by resident and inflammatory macrophage populations. *Blood* **97**, 288-296 (2001).
249. McWilliam, A.S., Tree, P. & Gordon, S. Interleukin 4 regulates induction of sialoadhesin, the macrophage sialic acid-specific receptor. *Proc Natl Acad Sci U S A* **89**, 10522-10526 (1992).
250. York, M.R., *et al.* A macrophage marker, Siglec-1, is increased on circulating monocytes in patients with systemic sclerosis and induced by type I interferons and toll-like receptor agonists. *Arthritis Rheum* **56**, 1010-1020 (2007).
251. van den Berg, T.K., *et al.* Sialoadhesin on macrophages: its identification as a lymphocyte adhesion molecule. *J Exp Med* **176**, 647-655 (1992).
252. Wu, C., *et al.* Sialoadhesin-positive macrophages bind regulatory T cells, negatively controlling their expansion and autoimmune disease progression. *J Immunol* **182**, 6508-6516 (2009).
253. Jiang, H.R., *et al.* Sialoadhesin promotes the inflammatory response in experimental autoimmune uveoretinitis. *J Immunol* **177**, 2258-2264 (2006).
254. Oetke, C., Vinson, M.C., Jones, C. & Crocker, P.R. Sialoadhesin-deficient mice exhibit subtle changes in B- and T-cell populations and reduced immunoglobulin M levels. *Mol Cell Biol* **26**, 1549-1557 (2006).
255. Jones, C., Virji, M. & Crocker, P.R. Recognition of sialylated meningococcal lipopolysaccharide by siglecs expressed on myeloid cells leads to enhanced bacterial uptake. *Mol Microbiol* **49**, 1213-1225 (2003).
256. Karlyshev, A.V., McCrossan, M.V. & Wren, B.W. Demonstration of polysaccharide capsule in *Campylobacter jejuni* using electron microscopy. *Infect Immun* **69**, 5921-5924 (2001).
257. Angata, T., Hingorani, R., Varki, N.M. & Varki, A. Cloning and characterization of a novel mouse Siglec, mSiglec-F: differential evolution of the mouse and human (CD33) Siglec-3-related gene clusters. *J Biol Chem* **276**, 45128-45136 (2001).
258. Zhang, J.Q., Biedermann, B., Nitschke, L. & Crocker, P.R. The murine inhibitory receptor mSiglec-E is expressed broadly on cells of the innate immune system whereas mSiglec-F is restricted to eosinophils. *Eur J Immunol* **34**, 1175-1184 (2004).
259. Zhang, M., *et al.* Defining the in vivo function of Siglec-F, a CD33-related Siglec expressed on mouse eosinophils. *Blood* **109**, 4280-4287 (2007).

260. Tateno, H., *et al.* Distinct endocytic mechanisms of CD22 (Siglec-2) and Siglec-F reflect roles in cell signaling and innate immunity. *Mol Cell Biol* **27**, 5699-5710 (2007).
261. Ulyanova, T., Shah, D.D. & Thomas, M.L. Molecular cloning of MIS, a myeloid inhibitory siglec, that binds protein-tyrosine phosphatases SHP-1 and SHP-2. *J Biol Chem* **276**, 14451-14458 (2001).
262. Walport, M.J. Complement. First of two parts. *N Engl J Med* **344**, 1058-1066 (2001).
263. Ripoché, J., Day, A.J., Harris, T.J. & Sim, R.B. The complete amino acid sequence of human complement factor H. *Biochem J* **249**, 593-602 (1988).
264. Farries, T.C., Seya, T., Harrison, R.A. & Atkinson, J.P. Competition for binding sites on C3b by CR1, CR2, MCP, factor B and Factor H. *Complement Inflamm* **7**, 30-41 (1990).
265. Weiler, J.M., Daha, M.R., Austen, K.F. & Fearon, D.T. Control of the amplification convertase of complement by the plasma protein beta1H. *Proc Natl Acad Sci U S A* **73**, 3268-3272 (1976).
266. Oppermann, M., *et al.* The C-terminus of complement regulator Factor H mediates target recognition: evidence for a compact conformation of the native protein. *Clin Exp Immunol* **144**, 342-352 (2006).
267. Manuelian, T., *et al.* Mutations in factor H reduce binding affinity to C3b and heparin and surface attachment to endothelial cells in hemolytic uremic syndrome. *J Clin Invest* **111**, 1181-1190 (2003).
268. Fearon, D.T. Regulation by membrane sialic acid of beta1H-dependent decay-dissociation of amplification C3 convertase of the alternative complement pathway. *Proc Natl Acad Sci U S A* **75**, 1971-1975 (1978).
269. Pangburn, M.K. & Muller-Eberhard, H.J. Complement C3 convertase: cell surface restriction of beta1H control and generation of restriction on neuraminidase-treated cells. *Proc Natl Acad Sci U S A* **75**, 2416-2420 (1978).
270. Michalek, M.T., Bremer, E.G. & Mold, C. Effect of gangliosides on activation of the alternative pathway of human complement. *J Immunol* **140**, 1581-1587 (1988).
271. Schneider, M.C., *et al.* Neisseria meningitidis recruits factor H using protein mimicry of host carbohydrates. *Nature* **458**, 890-893 (2009).
272. Galanos, C. Physical state and biological activity of lipopolysaccharides. Toxicity and immunogenicity of the lipid A component. *Z Immunitätsforsch Exp Klin Immunol* **149**, 214-229 (1975).
273. Roshak, A.K., *et al.* Anti-human RP105 sera induces lymphocyte proliferation. *J Leukoc Biol* **65**, 43-49 (1999).
274. Chan, V.W., *et al.* The molecular mechanism of B cell activation by toll-like receptor protein RP-105. *J Exp Med* **188**, 93-101 (1998).
275. Nagai, Y., *et al.* Requirement for MD-1 in cell surface expression of RP105/CD180 and B-cell responsiveness to lipopolysaccharide. *Blood* **99**, 1699-1705 (2002).
276. Miyake, K., Yamashita, Y., Hitoshi, Y., Takatsu, K. & Kimoto, M. Murine B cell proliferation and protection from apoptosis with an antibody against a 105-kD

- molecule: unresponsiveness of X-linked immunodeficient B cells. *J Exp Med* **180**, 1217-1224 (1994).
277. Beutler, B. & Cerami, A. The biology of cachectin/TNF--a primary mediator of the host response. *Annu Rev Immunol* **7**, 625-655 (1989).
278. Vassalli, P. The pathophysiology of tumor necrosis factors. *Annu Rev Immunol* **10**, 411-452 (1992).
279. Akira, S. & Kishimoto, T. IL-6 and NF-IL6 in acute-phase response and viral infection. *Immunol Rev* **127**, 25-50 (1992).
280. Trinchieri, G. Interleukin-12: a proinflammatory cytokine with immunoregulatory functions that bridge innate resistance and antigen-specific adaptive immunity. *Annu Rev Immunol* **13**, 251-276 (1995).
281. Moore, K.W., O'Garra, A., de Waal Malefyt, R., Vieira, P. & Mosmann, T.R. Interleukin-10. *Annu Rev Immunol* **11**, 165-190 (1993).
282. Sweet, M.J. & Hume, D.A. Endotoxin signal transduction in macrophages. *J Leukoc Biol* **60**, 8-26 (1996).
283. Condie, R.M., Zak, S.J. & Good, R.A. Effect of meningococcal endotoxin on the immune response. *Proc Soc Exp Biol Med* **90**, 355-360 (1955).
284. Skidmore, B.J., Chiller, J.M., Weigle, W.O., Riblet, R. & Watson, J. Immunologic properties of bacterial lipopolysaccharide (LPS). III. Genetic linkage between the in vitro mitogenic and in vivo adjuvant properties of LPS. *J Exp Med* **143**, 143-150 (1976).
285. Skidmore, B.J., Chiller, J.M., Morrison, D.C. & Weigle, W.O. Immunologic properties of bacterial lipopolysaccharide (LPS): correlation between the mitogenic, adjuvant, and immunogenic activities. *J Immunol* **114**, 770-775 (1975).
286. Hoebe, K., *et al.* Upregulation of costimulatory molecules induced by lipopolysaccharide and double-stranded RNA occurs by Trif-dependent and Trif-independent pathways. *Nat Immunol* **4**, 1223-1229 (2003).
287. Gray, D., Kumararatne, D.S., Lortan, J., Khan, M. & MacLennan, I.C. Relation of intra-splenic migration of marginal zone B cells to antigen localization on follicular dendritic cells. *Immunology* **52**, 659-669 (1984).
288. Groeneveld, P.H., Erich, T. & Kraal, G. The differential effects of bacterial lipopolysaccharide (LPS) on splenic non-lymphoid cells demonstrated by monoclonal antibodies. *Immunology* **58**, 285-290 (1986).
289. Ferguson, A.R., Youd, M.E. & Corley, R.B. Marginal zone B cells transport and deposit IgM-containing immune complexes onto follicular dendritic cells. *Int Immunol* **16**, 1411-1422 (2004).
290. Cinamon, G., Zachariah, M.A., Lam, O.M., Foss, F.W., Jr. & Cyster, J.G. Follicular shuttling of marginal zone B cells facilitates antigen transport. *Nat Immunol* **9**, 54-62 (2008).
291. Barr, T.A., Brown, S., Ryan, G., Zhao, J. & Gray, D. TLR-mediated stimulation of APC: Distinct cytokine responses of B cells and dendritic cells. *Eur J Immunol* **37**, 3040-3053 (2007).
292. Kenneth M. Murphy, K.P.M., Paul Travers, Mark Walport, Charles Janeway. *Janeways Immunobiology*, (Garland Science; 7 edition (November 27, 2007), 2008).

293. Hirschfeld, M., *et al.* Signaling by toll-like receptor 2 and 4 agonists results in differential gene expression in murine macrophages. *Infect Immun* **69**, 1477-1482 (2001).
294. Werts, C., *et al.* Leptospiral lipopolysaccharide activates cells through a TLR2-dependent mechanism. *Nat Immunol* **2**, 346-352 (2001).
295. Netea, M.G., van Deuren, M., Kullberg, B.J., Cavaillon, J.M. & Van der Meer, J.W. Does the shape of lipid A determine the interaction of LPS with Toll-like receptors? *Trends Immunol* **23**, 135-139 (2002).
296. Triantafilou, M., *et al.* Combinational clustering of receptors following stimulation by bacterial products determines lipopolysaccharide responses. *Biochem J* **381**, 527-536 (2004).
297. Freudenberg, M.A., *et al.* Lipopolysaccharide sensing an important factor in the innate immune response to Gram-negative bacterial infections: benefits and hazards of LPS hypersensitivity. *Immunobiology* **213**, 193-203 (2008).
298. Shen, W., Falahati, R., Stark, R., Leitenberg, D. & Ladisch, S. Modulation of CD4 Th cell differentiation by ganglioside GD1a in vitro. *J Immunol* **175**, 4927-4934 (2005).
299. Shen, W. & Ladisch, S. Ganglioside GD1a impedes lipopolysaccharide-induced maturation of human dendritic cells. *Cell Immunol* **220**, 125-133 (2002).
300. Kanda, N. & Watanabe, S. Gangliosides GD1b, GT1b, and GQ1b enhance IL-2 and IFN-gamma production and suppress IL-4 and IL-5 production in phytohemagglutinin-stimulated human T cells. *J Immunol* **166**, 72-80 (2001).
301. Kimata, H. & Yoshida, A. Differential effects of gangliosides on Ig production and proliferation by human B cells. *Blood* **84**, 1193-1200 (1994).
302. Shamshiev, A., *et al.* Self glycolipids as T-cell autoantigens. *Eur J Immunol* **29**, 1667-1675 (1999).
303. Shamshiev, A., *et al.* The alphabeta T cell response to self-glycolipids shows a novel mechanism of CD1b loading and a requirement for complex oligosaccharides. *Immunity* **13**, 255-264 (2000).
304. Wu, D.Y., Segal, N.H., Sidobre, S., Kronenberg, M. & Chapman, P.B. Cross-presentation of disialoganglioside GD3 to natural killer T cells. *J Exp Med* **198**, 173-181 (2003).
305. Sorice, M., *et al.* Role of GM3-enriched microdomains in signal transduction regulation in T lymphocytes. *Glycoconj J* **20**, 63-70 (2004).
306. Garofalo, T., *et al.* Association of GM3 with Zap-70 induced by T cell activation in plasma membrane microdomains: GM3 as a marker of microdomains in human lymphocytes. *J Biol Chem* **277**, 11233-11238 (2002).
307. Engering, A.J., *et al.* Mannose receptor mediated antigen uptake and presentation in human dendritic cells. *Adv Exp Med Biol* **417**, 183-187 (1997).
308. Tan, M.C., *et al.* Mannose receptor-mediated uptake of antigens strongly enhances HLA class II-restricted antigen presentation by cultured dendritic cells. *Eur J Immunol* **27**, 2426-2435 (1997).
309. Stahl, P.D. & Ezekowitz, R.A. The mannose receptor is a pattern recognition receptor involved in host defense. *Curr Opin Immunol* **10**, 50-55 (1998).

310. Parish, C.R., Glidden, M.H., Quah, B.J. & Warren, H.S. Use of the intracellular fluorescent dye CFSE to monitor lymphocyte migration and proliferation. *Curr Protoc Immunol* **Chapter 4**, Unit4 9 (2009).
311. Lyons, A.B. & Parish, C.R. Determination of lymphocyte division by flow cytometry. *J Immunol Methods* **171**, 131-137 (1994).
312. Bernfield, M., *et al.* Biology of the syndecans: a family of transmembrane heparan sulfate proteoglycans. *Annu Rev Cell Biol* **8**, 365-393 (1992).
313. Garcia De Vinuesa, C., *et al.* Dendritic cells associated with plasmablast survival. *Eur J Immunol* **29**, 3712-3721 (1999).
314. Ma, D.Y. & Clark, E.A. The role of CD40 and CD154/CD40L in dendritic cells. *Semin Immunol* **21**, 265-272 (2009).
315. Suttles, J. & Stout, R.D. Macrophage CD40 signaling: a pivotal regulator of disease protection and pathogenesis. *Semin Immunol* **21**, 257-264 (2009).
316. Moran, A.P. Biological and serological characterization of *Campylobacter jejuni* lipopolysaccharides with deviating core and lipid A structures. *FEMS Immunol Med Microbiol* **11**, 121-130 (1995).
317. Beutler, B., Tkacenko, V., Milsark, I., Krochin, N. & Cerami, A. Effect of gamma interferon on cachectin expression by mononuclear phagocytes. Reversal of the lpsd (endotoxin resistance) phenotype. *J Exp Med* **164**, 1791-1796 (1986).
318. Flebbe, L., Vukajlovich, S.W. & Morrison, D.C. Immunostimulation of C3H/HeJ lymphoid cells by R-chemotype lipopolysaccharide preparations. *J Immunol* **142**, 642-652 (1989).
319. Hirata, N., *et al.* Selective synergy in anti-inflammatory cytokine production upon cooperated signaling via TLR4 and TLR2 in murine conventional dendritic cells. *Mol Immunol* **45**, 2734-2742 (2008).
320. Dillon, S., *et al.* A Toll-like receptor 2 ligand stimulates Th2 responses in vivo, via induction of extracellular signal-regulated kinase mitogen-activated protein kinase and c-Fos in dendritic cells. *J Immunol* **172**, 4733-4743 (2004).
321. Liang, S., *et al.* Ganglioside GD1a is an essential coreceptor for Toll-like receptor 2 signaling in response to the B subunit of type IIb enterotoxin. *J Biol Chem* **282**, 7532-7542 (2007).
322. Mosser, D.M. & Zhang, X. Interleukin-10: new perspectives on an old cytokine. *Immunol Rev* **226**, 205-218 (2008).
323. Miller, W.G., *et al.* Detection on surfaces and in Caco-2 cells of *Campylobacter jejuni* cells transformed with new gfp, yfp, and cfp marker plasmids. *Appl Environ Microbiol* **66**, 5426-5436 (2000).
324. Breeuwer, P., Drocourt, J., Rombouts, F.M. & Abee, T. A Novel Method for Continuous Determination of the Intracellular pH in Bacteria with the Internally Conjugated Fluorescent Probe 5 (and 6-)-Carboxyfluorescein Succinimidyl Ester. *Appl Environ Microbiol* **62**, 178-183 (1996).
325. Schnitger, K., *et al.* Staining of *Chlamydia trachomatis* elementary bodies: a suitable method for identifying infected human monocytes by flow cytometry. *J Microbiol Methods* **69**, 116-121 (2007).
326. Tuominen-Gustafsson, H., Penttinen, M., Hytonen, J. & Viljanen, M.K. Use of CFSE staining of borreliae in studies on the interaction between borreliae and human neutrophils. *BMC Microbiol* **6**, 92 (2006).

327. Logan, R.P., *et al.* A novel flow cytometric assay for quantitating adherence of *Helicobacter pylori* to gastric epithelial cells. *J Immunol Methods* **213**, 19-30 (1998).
328. Vander Top, E.A., Perry, G.A. & Gentry-Nielsen, M.J. A novel flow cytometric assay for measurement of in vivo pulmonary neutrophil phagocytosis. *BMC Microbiol* **6**, 61 (2006).
329. Lay, W.H. & Nussenzweig, V. Receptors for complement of leukocytes. *J Exp Med* **128**, 991-1009 (1968).
330. Bianco, C., Patrick, R. & Nussenzweig, V. A population of lymphocytes bearing a membrane receptor for antigen-antibody-complement complexes. I. Separation and characterization. *J Exp Med* **132**, 702-720 (1970).
331. Nussenzweig, V. Receptors for immune complexes on lymphocytes. *Adv Immunol* **19**, 217-258 (1974).
332. Pepys, M.B. Role of complement in induction of the allergic response. *Nat New Biol* **237**, 157-159 (1972).
333. Ellman, L., Green, I., Judge, F. & Frank, M.M. In vivo studies in C4-deficient guinea pigs. *J Exp Med* **134**, 162-175 (1971).
334. Jackson, C.G., Ochs, H.D. & Wedgwood, R.J. Immune response of a patient with deficiency of the fourth component of complement and systemic lupus erythematosus. *N Engl J Med* **300**, 1124-1129 (1979).
335. Ochs, H.D., Wedgwood, R.J., Frank, M.M., Heller, S.R. & Hosea, S.W. The role of complement in the induction of antibody responses. *Clin Exp Immunol* **53**, 208-216 (1983).
336. Tuveson, D.A., Ahearn, J.M., Matsumoto, A.K. & Fearon, D.T. Molecular interactions of complement receptors on B lymphocytes: a CR1/CR2 complex distinct from the CR2/CD19 complex. *J Exp Med* **173**, 1083-1089 (1991).
337. Matsumoto, A.K., *et al.* Intersection of the complement and immune systems: a signal transduction complex of the B lymphocyte-containing complement receptor type 2 and CD19. *J Exp Med* **173**, 55-64 (1991).
338. Bradbury, L.E., Kansas, G.S., Levy, S., Evans, R.L. & Tedder, T.F. The CD19/CD21 signal transducing complex of human B lymphocytes includes the target of antiproliferative antibody-1 and Leu-13 molecules. *J Immunol* **149**, 2841-2850 (1992).
339. Krop, I., Shaffer, A.L., Fearon, D.T. & Schlissel, M.S. The signaling activity of murine CD19 is regulated during cell development. *J Immunol* **157**, 48-56 (1996).
340. Carter, R.H., Spycher, M.O., Ng, Y.C., Hoffman, R. & Fearon, D.T. Synergistic interaction between complement receptor type 2 and membrane IgM on B lymphocytes. *J Immunol* **141**, 457-463 (1988).
341. Hivroz, C., Fischer, E., Kazatchkine, M.D. & Grillo-Courvalin, C. Differential effects of the stimulation of complement receptors CR1 (CD35) and CR2 (CD21) on cell proliferation and intracellular Ca²⁺ mobilization of chronic lymphocytic leukemia B cells. *J Immunol* **146**, 1766-1772 (1991).
342. Aichele, P., *et al.* Macrophages of the splenic marginal zone are essential for trapping of blood-borne particulate antigen but dispensable for induction of specific T cell responses. *J Immunol* **171**, 1148-1155 (2003).

343. Harms, G., Hardonk, M.J. & Timens, W. In vitro complement-dependent binding and in vivo kinetics of pneumococcal polysaccharide TI-2 antigens in the rat spleen marginal zone and follicle. *Infect Immun* **64**, 4220-4225 (1996).
344. Groeneveld, P.H. & van Rooijen, N. Localization of intravenously injected lipopolysaccharide (LPS) in the spleen of the mouse. An immunoperoxidase and histochemical study. *Virchows Arch B Cell Pathol Incl Mol Pathol* **48**, 237-245 (1985).
345. Conlan, J.W. Early pathogenesis of *Listeria monocytogenes* infection in the mouse spleen. *J Med Microbiol* **44**, 295-302 (1996).
346. Kraal, G. Cells in the marginal zone of the spleen. *Int Rev Cytol* **132**, 31-74 (1992).
347. Kraal, G. & Janse, M. Marginal metallophilic cells of the mouse spleen identified by a monoclonal antibody. *Immunology* **58**, 665-669 (1986).
348. Eloranta, M.L. & Alm, G.V. Splenic marginal metallophilic macrophages and marginal zone macrophages are the major interferon-alpha/beta producers in mice upon intravenous challenge with herpes simplex virus. *Scand J Immunol* **49**, 391-394 (1999).
349. Goodyear, C.S., *et al.* Monoclonal antibodies raised against Guillain-Barre syndrome-associated *Campylobacter jejuni* lipopolysaccharides react with neuronal gangliosides and paralyze muscle-nerve preparations. *J Clin Invest* **104**, 697-708 (1999).
350. Willison, H.J., *et al.* The role of complement and complement regulators in mediating motor nerve terminal injury in murine models of Guillain-Barre syndrome. *J Neuroimmunol* **201-202**, 172-182 (2008).
351. Karlyshev, A.V., Ketley, J.M. & Wren, B.W. The *Campylobacter jejuni* glycome. *FEMS Microbiol Rev* **29**, 377-390 (2005).
352. Rathinam, V.A., Hoag, K.A. & Mansfield, L.S. Dendritic cells from C57BL/6 mice undergo activation and induce Th1-effector cell responses against *Campylobacter jejuni*. *Microbes Infect* **10**, 1316-1324 (2008).
353. Kopitz, J., von Reitzenstein, C., Burchert, M., Cantz, M. & Gabius, H.J. Galectin-1 is a major receptor for ganglioside GM1, a product of the growth-controlling activity of a cell surface ganglioside sialidase, on human neuroblastoma cells in culture. *J Biol Chem* **273**, 11205-11211 (1998).
354. Shands, J.W., Jr. & Chun, P.W. The dispersion of gram-negative lipopolysaccharide by deoxycholate. Subunit molecular weight. *J Biol Chem* **255**, 1221-1226 (1980).
355. Rinaldi, S., Brennan, K.M. & Willison, H.J. Heteromeric glycolipid complexes as modulators of autoantibody and lectin binding. *Prog Lipid Res* (2009).
356. Rinaldi, S., *et al.* Analysis of lectin binding to glycolipid complexes using combinatorial glycoarrays. *Glycobiology* **19**, 789-796 (2009).
357. Vreugdenhil, A.C., *et al.* Lipopolysaccharide (LPS)-binding protein mediates LPS detoxification by chylomicrons. *J Immunol* **170**, 1399-1405 (2003).
358. Harris, H.W., Grunfeld, C., Feingold, K.R. & Rapp, J.H. Human very low density lipoproteins and chylomicrons can protect against endotoxin-induced death in mice. *J Clin Invest* **86**, 696-702 (1990).

359. Harris, H.W., *et al.* Chylomicrons alter the fate of endotoxin, decreasing tumor necrosis factor release and preventing death. *J Clin Invest* **91**, 1028-1034 (1993).
360. Munford, R.S., Andersen, J.M. & Dietschy, J.M. Sites of tissue binding and uptake in vivo of bacterial lipopolysaccharide-high density lipoprotein complexes: studies in the rat and squirrel monkey. *J Clin Invest* **68**, 1503-1513 (1981).
361. Munford, R.S., Hall, C.L., Lipton, J.M. & Dietschy, J.M. Biological activity, lipoprotein-binding behavior, and in vivo disposition of extracted and native forms of Salmonella typhimurium lipopolysaccharides. *J Clin Invest* **70**, 877-888 (1982).
362. Olins, A.L. & Warner, R.C. Physicochemical studies on a lipopolysaccharide from the cell wall of Azotobacter vinelandii. *J Biol Chem* **242**, 4994-5001 (1967).
363. Galanos, C. & Luderitz, O. The role of the physical state of lipopolysaccharides in the interaction with complement. High molecular weight as prerequisite for the expression of anti-complementary activity. *Eur J Biochem* **65**, 403-408 (1976).
364. Hellman, J., Tehan, M.M. & Warren, H.S. Murein lipoprotein, peptidoglycan-associated lipoprotein, and outer membrane protein A are present in purified rough and smooth lipopolysaccharides. *J Infect Dis* **188**, 286-289 (2003).
365. Hirschfeld, M., Ma, Y., Weis, J.H., Vogel, S.N. & Weis, J.J. Cutting edge: repurification of lipopolysaccharide eliminates signaling through both human and murine toll-like receptor 2. *J Immunol* **165**, 618-622 (2000).
366. Tapping, R.I., Akashi, S., Miyake, K., Godowski, P.J. & Tobias, P.S. Toll-like receptor 4, but not toll-like receptor 2, is a signaling receptor for Escherichia and Salmonella lipopolysaccharides. *J Immunol* **165**, 5780-5787 (2000).
367. Qi, H., Egen, J.G., Huang, A.Y. & Germain, R.N. Extrafollicular activation of lymph node B cells by antigen-bearing dendritic cells. *Science* **312**, 1672-1676 (2006).
368. Martinez-Pomares, L. & Gordon, S. Antigen presentation the macrophage way. *Cell* **131**, 641-643 (2007).
369. Heikema, A.P., *et al.* Characterization of the specific interaction between sialoadhesin and sialylated Campylobacter jejuni lipooligosaccharides. *Infect Immun* **78**, 3237-3246.
370. Plomp, J.J. & Willison, H.J. Pathophysiological actions of neuropathy-related anti-ganglioside antibodies at the neuromuscular junction. *J Physiol* **587**, 3979-3999 (2009).
371. Ariga, T., Miyatake, T. & Yu, R.K. Recent studies on the roles of antiglycosphingolipids in the pathogenesis of neurological disorders. *J Neurosci Res* **65**, 363-370 (2001).
372. Ariga, T., *et al.* Characterization of sulfated glucuronic acid containing glycolipids reacting with IgM M-proteins in patients with neuropathy. *J Biol Chem* **262**, 848-853 (1987).
373. Ariga, T. & Yu, R.K. Antiglycolipid antibodies in Guillain-Barre syndrome and related diseases: review of clinical features and antibody specificities. *J Neurosci Res* **80**, 1-17 (2005).
374. Ogino, M., Orazio, N. & Latov, N. IgG anti-GM1 antibodies from patients with acute motor neuropathy are predominantly of the IgG1 and IgG3 subclasses. *J Neuroimmunol* **58**, 77-80 (1995).

375. Junt, T., *et al.* Subcapsular sinus macrophages in lymph nodes clear lymph-borne viruses and present them to antiviral B cells. *Nature* **450**, 110-114 (2007).
376. Carrasco, Y.R. & Batista, F.D. B cells acquire particulate antigen in a macrophage-rich area at the boundary between the follicle and the subcapsular sinus of the lymph node. *Immunity* **27**, 160-171 (2007).
377. Phan, T.G., Green, J.A., Gray, E.E., Xu, Y. & Cyster, J.G. Immune complex relay by subcapsular sinus macrophages and noncognate B cells drives antibody affinity maturation. *Nat Immunol* **10**, 786-793 (2009).
378. Taylor, P.R., *et al.* Macrophage receptors and immune recognition. *Annu Rev Immunol* **23**, 901-944 (2005).
379. Steiniger, B., Barth, P., Herbst, B., Hartnell, A. & Crocker, P.R. The species-specific structure of microanatomical compartments in the human spleen: strongly sialoadhesin-positive macrophages occur in the perifollicular zone, but not in the marginal zone. *Immunology* **92**, 307-316 (1997).
380. Buiting, A.M., De Rover, Z., Kraal, G. & Van Rooijen, N. Humoral immune responses against particulate bacterial antigens are dependent on marginal metallophilic macrophages in the spleen. *Scand J Immunol* **43**, 398-405 (1996).
381. Snapper, C.M. & Paul, W.E. Interferon-gamma and B cell stimulatory factor-1 reciprocally regulate Ig isotype production. *Science* **236**, 944-947 (1987).
382. Tovey, M.G., Lallemand, C. & Thyphronitis, G. Adjuvant activity of type I interferons. *Biol Chem* **389**, 541-545 (2008).
383. Zhu, J., Huang, X. & Yang, Y. Type I IFN signaling on both B and CD4 T cells is required for protective antibody response to adenovirus. *J Immunol* **178**, 3505-3510 (2007).
384. Finkelman, F.D., *et al.* Lymphokine control of in vivo immunoglobulin isotype selection. *Annu Rev Immunol* **8**, 303-333 (1990).
385. Mortensen, N.P., *et al.* Sialylation of *Campylobacter jejuni* lipo-oligosaccharides is associated with severe gastro-enteritis and reactive arthritis. *Microbes Infect* **11**, 988-994 (2009).
386. Spencer, L.A., *et al.* Human eosinophils constitutively express multiple Th1, Th2, and immunoregulatory cytokines that are secreted rapidly and differentially. *J Leukoc Biol* **85**, 117-123 (2009).
387. Wang, H.B., Ghiran, I., Matthaei, K. & Weller, P.F. Airway eosinophils: allergic inflammation recruited professional antigen-presenting cells. *J Immunol* **179**, 7585-7592 (2007).
388. Blaser, M.J., Smith, P.F. & Kohler, P.F. Susceptibility of *Campylobacter* isolates to the bactericidal activity of human serum. *J Infect Dis* **151**, 227-235 (1985).
389. Guerry, P., Ewing, C.P., Hickey, T.E., Prendergast, M.M. & Moran, A.P. Sialylation of lipooligosaccharide cores affects immunogenicity and serum resistance of *Campylobacter jejuni*. *Infect Immun* **68**, 6656-6662 (2000).
390. Truedsson, L., Bengtsson, A.A. & Sturfelt, G. Complement deficiencies and systemic lupus erythematosus. *Autoimmunity* **40**, 560-566 (2007).
391. Lewis, M.J. & Botto, M. Complement deficiencies in humans and animals: links to autoimmunity. *Autoimmunity* **39**, 367-378 (2006).

392. Baumgarth, N., Tung, J.W. & Herzenberg, L.A. Inherent specificities in natural antibodies: a key to immune defense against pathogen invasion. *Springer Semin Immunopathol* **26**, 347-362 (2005).
393. Boes, M., *et al.* Enhanced B-1 cell development, but impaired IgG antibody responses in mice deficient in secreted IgM. *J Immunol* **160**, 4776-4787 (1998).
394. Ehrenstein, M.R., O'Keefe, T.L., Davies, S.L. & Neuberger, M.S. Targeted gene disruption reveals a role for natural secretory IgM in the maturation of the primary immune response. *Proc Natl Acad Sci U S A* **95**, 10089-10093 (1998).
395. Boes, M. Role of natural and immune IgM antibodies in immune responses. *Mol Immunol* **37**, 1141-1149 (2000).
396. Fang, Y., Xu, C., Fu, Y.X., Holers, V.M. & Molina, H. Expression of complement receptors 1 and 2 on follicular dendritic cells is necessary for the generation of a strong antigen-specific IgG response. *J Immunol* **160**, 5273-5279 (1998).
397. Croix, D.A., *et al.* Antibody response to a T-dependent antigen requires B cell expression of complement receptors. *J Exp Med* **183**, 1857-1864 (1996).
398. Ahearn, J.M., *et al.* Disruption of the Cr2 locus results in a reduction in B-1a cells and in an impaired B cell response to T-dependent antigen. *Immunity* **4**, 251-262 (1996).
399. Cavallo, T. & Granholm, N.A. Lipopolysaccharide from gram-negative bacteria enhances polyclonal B cell activation and exacerbates nephritis in MRL/lpr mice. *Clin Exp Immunol* **82**, 515-521 (1990).
400. Ehrenstein, M.R., Cook, H.T. & Neuberger, M.S. Deficiency in serum immunoglobulin (Ig)M predisposes to development of IgG autoantibodies. *J Exp Med* **191**, 1253-1258 (2000).
401. Young, K.T., Davis, L.M. & Dirita, V.J. Campylobacter jejuni: molecular biology and pathogenesis. *Nat Rev Microbiol* **5**, 665-679 (2007).
402. Hu, L. & Hickey, T.E. Campylobacter jejuni induces secretion of proinflammatory chemokines from human intestinal epithelial cells. *Infect Immun* **73**, 4437-4440 (2005).
403. Jones, M.A., Totemeyer, S., Maskell, D.J., Bryant, C.E. & Barrow, P.A. Induction of proinflammatory responses in the human monocytic cell line THP-1 by Campylobacter jejuni. *Infect Immun* **71**, 2626-2633 (2003).
404. Dillon, S., *et al.* Yeast zymosan, a stimulus for TLR2 and dectin-1, induces regulatory antigen-presenting cells and immunological tolerance. *J Clin Invest* **116**, 916-928 (2006).
405. Banchereau, J. & Steinman, R.M. Dendritic cells and the control of immunity. *Nature* **392**, 245-252 (1998).
406. Bell, D., Young, J.W. & Banchereau, J. Dendritic cells. *Adv Immunol* **72**, 255-324 (1999).
407. Hart, D.N. Dendritic cells: unique leukocyte populations which control the primary immune response. *Blood* **90**, 3245-3287 (1997).
408. Steinman, R.M. The dendritic cell system and its role in immunogenicity. *Annu Rev Immunol* **9**, 271-296 (1991).
409. Rescigno, M., Granucci, F., Citterio, S., Foti, M. & Ricciardi-Castagnoli, P. Coordinated events during bacteria-induced DC maturation. *Immunol Today* **20**, 200-203 (1999).

410. Rissoan, M.C., *et al.* Reciprocal control of T helper cell and dendritic cell differentiation. *Science* **283**, 1183-1186 (1999).
411. Pulendran, B., *et al.* Distinct dendritic cell subsets differentially regulate the class of immune response in vivo. *Proc Natl Acad Sci U S A* **96**, 1036-1041 (1999).
412. Banchereau, J., *et al.* Immunobiology of dendritic cells. *Annu Rev Immunol* **18**, 767-811 (2000).
413. Bogdan, C., Vodovotz, Y. & Nathan, C. Macrophage deactivation by interleukin 10. *J Exp Med* **174**, 1549-1555 (1991).
414. de Waal Malefyt, R., *et al.* Interleukin 10 (IL-10) and viral IL-10 strongly reduce antigen-specific human T cell proliferation by diminishing the antigen-presenting capacity of monocytes via downregulation of class II major histocompatibility complex expression. *J Exp Med* **174**, 915-924 (1991).
415. Fiorentino, D.F., *et al.* IL-10 acts on the antigen-presenting cell to inhibit cytokine production by Th1 cells. *J Immunol* **146**, 3444-3451 (1991).
416. Kuhn, R., Lohler, J., Rennick, D., Rajewsky, K. & Muller, W. Interleukin-10-deficient mice develop chronic enterocolitis. *Cell* **75**, 263-274 (1993).
417. Berg, D.J., *et al.* Interleukin-10 is a central regulator of the response to LPS in murine models of endotoxic shock and the Shwartzman reaction but not endotoxin tolerance. *J Clin Invest* **96**, 2339-2347 (1995).
418. Berg, D.J., *et al.* Interleukin 10 but not interleukin 4 is a natural suppressant of cutaneous inflammatory responses. *J Exp Med* **182**, 99-108 (1995).
419. Mansfield, L.S., *et al.* C57BL/6 and congenic interleukin-10-deficient mice can serve as models of *Campylobacter jejuni* colonization and enteritis. *Infect Immun* **75**, 1099-1115 (2007).
420. Youd, M.E., Ferguson, A.R. & Corley, R.B. Synergistic roles of IgM and complement in antigen trapping and follicular localization. *Eur J Immunol* **32**, 2328-2337 (2002).
421. Kagan, J.C., *et al.* TRAM couples endocytosis of Toll-like receptor 4 to the induction of interferon-beta. *Nat Immunol* **9**, 361-368 (2008).
422. Coleman, R.M., *et al.* IgG subclass antibodies to herpes simplex virus. *J Infect Dis* **151**, 929-936 (1985).
423. Linde, G.A. Subclass distribution of rubella virus-specific immunoglobulin G. *J Clin Microbiol* **21**, 117-121 (1985).
424. Pickl, W.F., Pimentel-Muinos, F.X. & Seed, B. Lipid rafts and pseudotyping. *J Virol* **75**, 7175-7183 (2001).
425. Angata, T., Tabuchi, Y., Nakamura, K. & Nakamura, M. Siglec-15: an immune system Siglec conserved throughout vertebrate evolution. *Glycobiology* **17**, 838-846 (2007).
426. Yamanaka, M., Kato, Y., Angata, T. & Narimatsu, H. Deletion polymorphism of SIGLEC14 and its functional implications. *Glycobiology* **19**, 841-846 (2009).
427. Rapoport, E., Mikhalyov, I., Zhang, J., Crocker, P. & Bovin, N. Ganglioside binding pattern of CD33-related siglecs. *Bioorg Med Chem Lett* **13**, 675-678 (2003).
428. Tateno, H., Crocker, P.R. & Paulson, J.C. Mouse Siglec-F and human Siglec-8 are functionally convergent paralogs that are selectively expressed on eosinophils

and recognize 6'-sulfo-sialyl Lewis X as a preferred glycan ligand. *Glycobiology* **15**, 1125-1135 (2005).

Appendix 1 – Buffers and media

Complete RPMI (cRPMI)

RPMI 1640 media (Gibco, UK) with 10% Foetal Bovine Serum (FBS) (Sigma, UK), 100µg/ml Penicillin, 100µg/ml Streptomycin and 2mM L-glutamine (all Gibco, UK).

Supplemented cRPMI

RPMI 1640 media with 10% Foetal Bovine Serum, 100µg/ml Penicillin, 100µg/ml Streptomycin and 2mM L-glutamine supplemented with 500µl 2-mercaptoethanol and 5ml non-essential amino acids (both Gibco, UK) per 500ml of media.

FACS Buffer

3% Bovine Serum Albumin (BSA) in PBS (phosphate buffered saline) with 0.05% sodium azide (NaN₃).

Complete RPMI for phagocytosis experiments

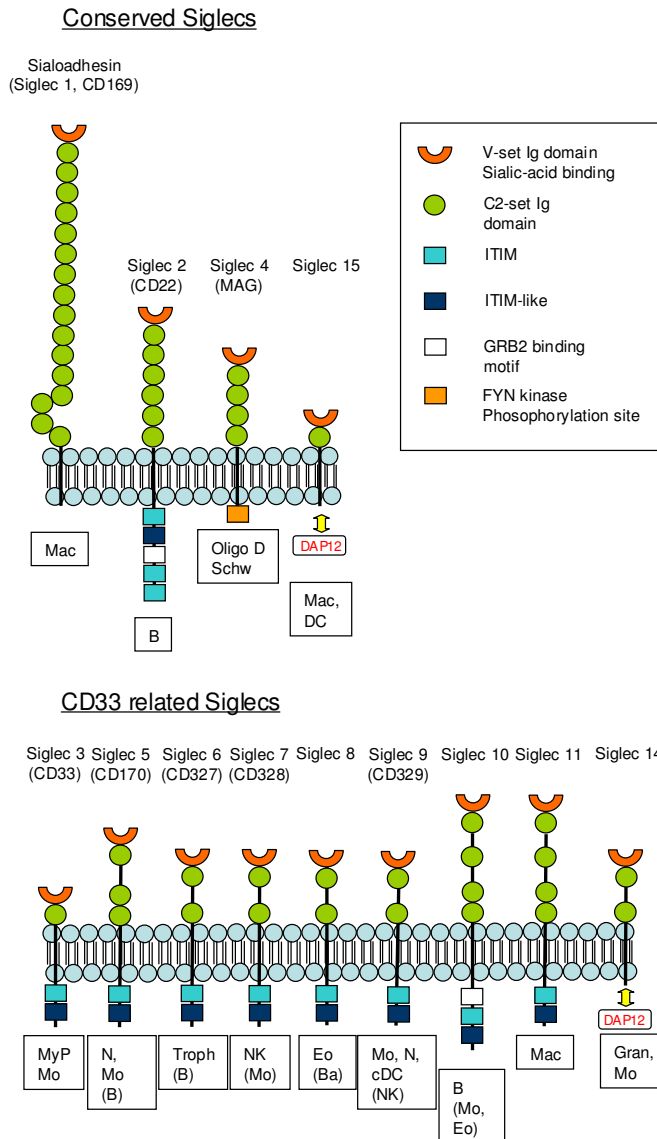
RPMI 1640 media (Gibco, UK) with 10% Ultra-low IgG Foetal Bovine Serum (Invitrogen, UK), 100µg/ml Penicillin, 100µg/ml Streptomycin and 2mM L-glutamine (all Gibco, UK).

0.1 M Sodium Carbonate buffer for Ig ELISAs

8.40 g NaHCO₃, 3.56 g Na₂CO₃; dilute to 1.0 L in distilled water; pH to 9.5.

Appendix 2 – Structure and expression of siglecs

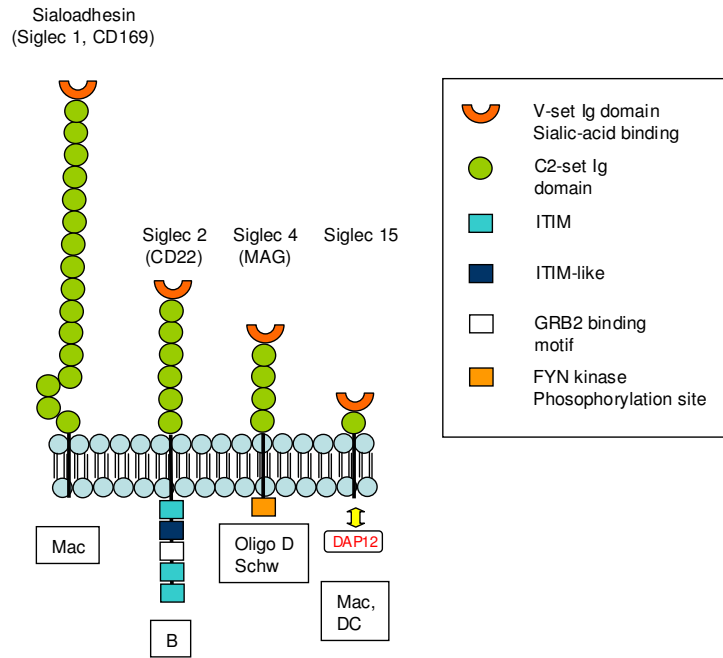
Human siglecs



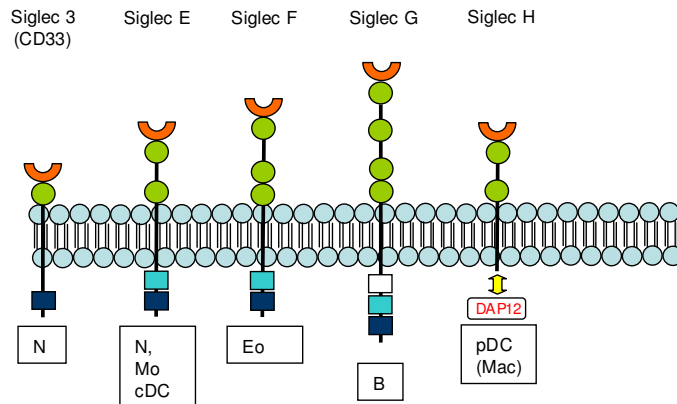
Human siglecs and their cellular expression^{144,425,426}. Siglecs are type 1 membrane proteins with an amino-terminal V-set immunoglobulin domain that mediates sialic acid recognition and varying numbers of C2-set immunoglobulin domains. Siglecs can be divided into two groups – those which show conservation between species (Sialoadhesin, CD22, MAG and Siglec 15) and those which differ between species (the CD33 related siglecs). Cell expression has been determined by antibodies (brackets indicate low levels of expression). B–B cells, Mac–macrophages, Mo–monocytes, Oligo–oligodendrocytes, Schw–schwann cells, DC–dendritic cells, MyP–myeloid progenitors, N–neutrophils, Troph–trophoblasts, NK–natural killer cells, Eo–eosinophils, Ba–basophils, cDC–conventional dendritic cells, Gran–granulocytes, ITIM–immunoreceptor tyrosine-based inhibitory motif, GRB2–growth-factor-receptor-bound protein 2. DAP12 interacts with siglec 14 and 15 through charged residues. Figure adapted with permission¹⁴⁴.

Murine siglecs

Conserved Siglecs



CD33 related Siglecs



Murine siglecs and their cellular expression^{144,425,426}. Cell expression has been determined by antibodies (brackets indicate low levels of expression). B–B cells, Mac–macrophages, Mo–monocytes, Oligo–oligodendrocytes, Schw–schwann cells, DC–dendritic cells, N–neutrophils, Eo–eosinophils, cDC–conventional dendritic cells, ITIM–immunoreceptor tyrosine-based inhibitory motif, GRB2–growth-factor-receptor-bound protein 2. DAP12 interacts with siglec H and 15 through charged residues. Figure adapted with permission¹⁴⁴.

Appendix 3 – Binding specificities of siglecs

Sialic Acid Configurations

Sequence	Human					Murine		
	CD22	Siglec 7	Siglec 8	Siglec 9	Siglec 10	CD22	Siglec E	Siglec F
	0	+	+	+	+	0	++	++
	+++	+	+	+	++	+	++	+/-
	+++	+	+	+	+++	+++	+	0
	0	+++	+	0	0	0	++	0
	ND	++	+++	0	0	0	++	+++
	ND	+	0	+++	0	0	+	0

Siglec sialoside binding specificities determined by glycan array analysis. Sequences are present in glycoproteins or glycolipids. +++ strong binding. ++ moderate binding. + low binding. +/- detectable binding. 0 no binding. ND not determined. GlcNac N-acetylglucosamine. Neu5Gc N-glycolylneuraminic acid. Neu5Ac N-acetylneuraminic acid. (Neuraminic acid = sialic acid) Figure adapted with permission ¹⁴⁴.

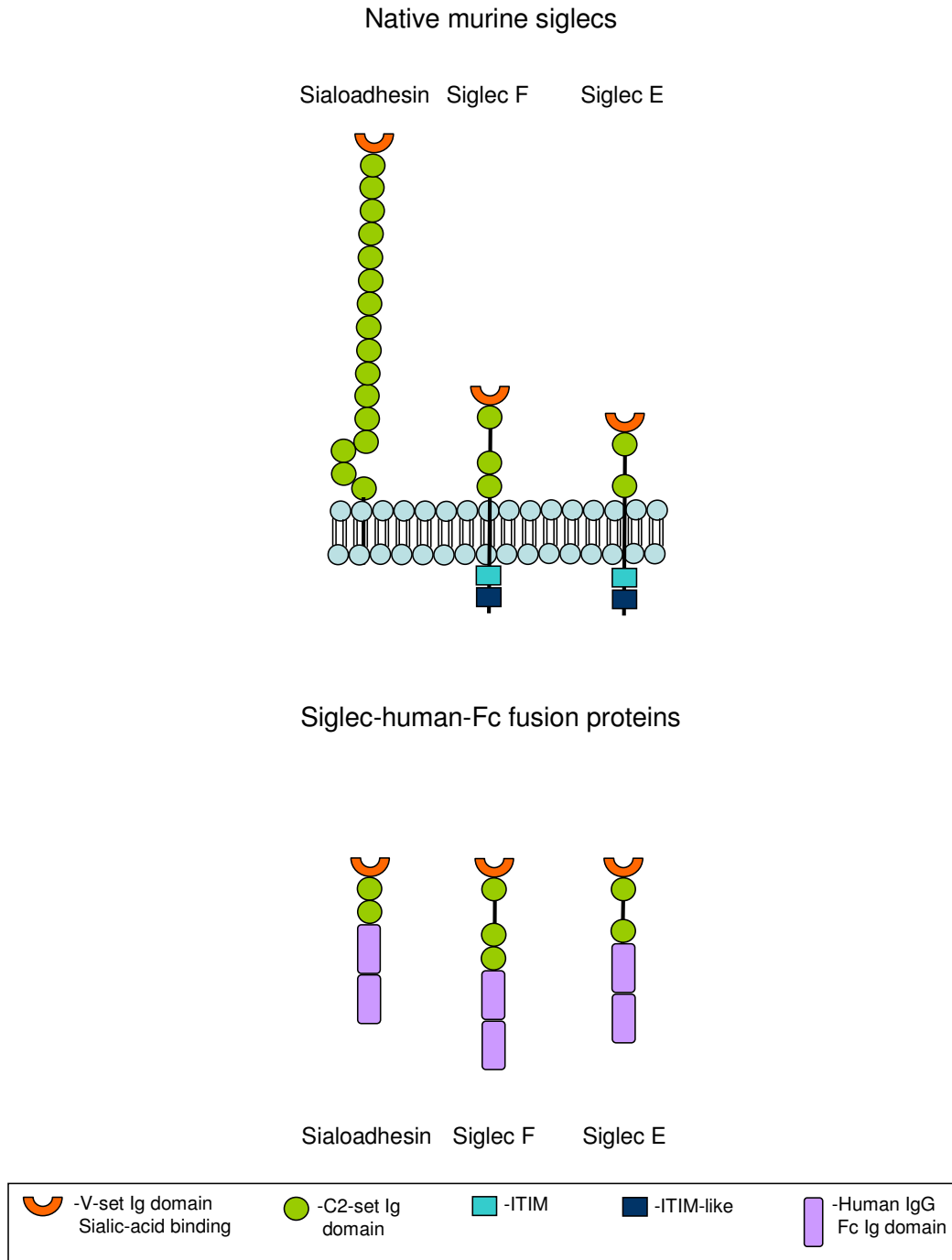
Siglec binding to native gangliosides

	GT1b	GQ1b	GD3	GM2	GM3	GD1a
Siglec 5	+	++				
Siglec 7	++	++	++			
Siglec 8						
Siglec 9	++	++	++		++	
Siglec 10	++					
Sialoadhesin						++
Siglec F	++					++
Siglec E	+					++

Siglec binding to gangliosides^{369,427}. (blue is human siglecs, green is murine siglecs). Sialoadhesin, Siglec F and Siglec E binding to gangliosides had not been demonstrated prior to this thesis. (+ weaker binding, ++ stronger binding).

Siglecs do not have specificities for gangliosides per se. Siglecs have specificity for sialic acid and the binding affinity is determined by the sialic acid linkages to the surrounding molecules. A siglec can bind to sialic acid with the correct configuration whether on gangliosides, other glycolipids or glycoproteins.

Appendix 4 – Structures of siglec-human-Fc fusion proteins



Murine siglecs and the structures of siglec-human-Fc fusion protein reagents^{255,258,428}. Ig, Immunoglobulin. Fc, fraction crystallisable. ITIM, immunoreceptor tyrosine-based inhibitory motif.